Identification and pharmacological characterization of nucleotide pyrophosphatase/phosphodiesterase-1 (NPP1) and -4 (NPP4) inhibitors

Dissertation

zur

Erlangung des Doktorgrades (Dr. rer. nat.)

der

Mathematisch-Naturwissenschaftlichen Fakultät

der

Rheinischen Friedrich-Wilhelms-Universität Bonn

vorgelegt von

Vittoria Lopez

Aus San Giovanni in Fiore, Italien

Bonn, 2022

Angefertigt mit Genehmigung der Mathematisch-Naturwissenschaftlichen Fakultät
der Rheinischen Friedrich-Wilhelms-Universität Bonn.

1. Gutachterin: Prof. Dr. Christa E. Müller

2. Gutachter: Prof. Dr. Ivar von Kügelgen

Tag der Promotion: 30/06/2022

Erscheinungsjahr: 2022

Contents

ABSTRACT 6

1. PURINERGIC SIGNALING AND ECTO-NUCLEOSIDASES 9

1.1 NPP1 15

1.1.1 Tissue distribution and structure 15

1.1.2 Kinetic property and substrates of NPP1 18

1.1.3 Pathological role of NPP1 20

1.1.4 NPP1 inhibitors 26

1.2 NPP4 32

1.2.1 Tissue distribution and structure 32

1.2.2 Kinetic properties and substrates 33

1.2.3 Pathological role of NPP4 34

1.2.4 NPP4 inhibitors 36

2. SULFATED POLYSACCHARIDES FROM MACROALGAE ARE POTENT DUAL INHIBITORS OF HUMAN ATP-HYDROLYZING ECTONUCLEOTIDASES NPP1 AND CD39 46

2.1 INTRODUCTION 46

2.2 PUBLICATION 48

2.3 SUMMARY AND OUTLOOK 61

3. HEPARINS ARE POTENT INHIBITORS OF ECTONUCLEOTIDE PYROPHOSPHATASE/PHOSPHODIESTERASE-1 (NPP1) – A PROMISING TARGET FOR THE IMMUNOTHERAPY OF CANCER AND INFECTIONS 64

3.1 INTRODUCTION 64

3.2 PRELIMINARY MANUSCRIPT 66

3.3 SUMMARY AND OUTLOOK 99

4. RECOMBINANT EXPRESSION OF ECTO-NUCLEOTIDE PYROPHOSPHATASE/ 102

PHOSPHODIESTERASE 4 (NPP4) AND DEVELOPMENT OF A LUMINESCENCE-BASED ASSAY TO IDENTIFY INHIBITORS 102

4.1 INTRODUCTION 102
4.2 PUBLICATION 103
4.3 SUMMARY AND OUTLOOK 116

5. SEARCH FOR NOVEL NPP4 INHIBITORS BY HIGH-THROUGHPUT SCREENING 118

5.1 COMPOUND LIBRARY SCREENING TO IDENTIFY NOVEL NPP4 INHIBITORS 119
5.2 SELECTIVITY STUDIES OF NPP4 INHIBITORS 131
5.3 SCREENING OF HIT ANALOGUES AND AN ADDITIONAL TAILORED LIBRARY 135
5.4 ORTHOGONAL ASSAY SYSTEM FOR MONITORING NPP4 ACTIVITY 158
5.5 SUMMARY AND OUTLOOK 161

6. CHARACTERIZATION OF NPP4: SUBSTRATE PREFERENCES AND ENZYME KINETICS 164

6.1 SCREENING OF NUCLEOTIDES AS POTENTIAL NPP4 SUBSTRATES 164
6.2 BIOCHEMICAL CHARACTERIZATION OF NPP4 KINETICS 173
6.3 QUALITATIVE AND QUANTITATIVE SUBSTRATE ANALYSIS CE-UV 179
6.4 SUMMARY AND OUTLOOK 185

7. SUMMARY AND CONCLUSIONS 188

8. ACKNOWLEDGMENT 196

9. PUBLICATIONS 198

10. DECLARATION 200

Abstract

Ectonucleotidases are enzymes involved in different physiological functions and mainly in the regulation of purinergic signaling; in fact, they regulate the duration of purinergic receptor activation by catalyzing the hydrolysis of nucleotides (mainly ATP) producing the nucleoside adenosine. As a result, they are involved in a broad range of physiological process, and have emerged as promising drug targets.

Ectonucleotidases are allocated into four subfamilies: ecto-nucleoside triphosphates diphosphohydrolases (NTPDases), alkaline phosphatases (APs), ecto-5′-nucleotidase (CD73), and ecto-nucleotide pyrophosphatases/phosphodiesterases (NPPs). The NPP family consists of seven structurally related subtypes, NPP1-7, and despite their enormous therapeutic potential, the availability of powerful and selective modulators remains still limited. As a matter of fact, molecules acting as activators or inhibitors of their enzymatic activity are useful tool for pharmacological investigations to advance the basic research of these enzymes, their physiological functions as well as their participation in diseases. Additionally, tool compounds may be used as lead structures for drug development. The objective of this project was to advance the field of drug development for two NPP isoenzymes, human NPP1 and NPP4. The results were published in three original research articles presented in Sections 2-4. Sections 5 and 6 describe experimental results that have not been published yet.

Section 1 provides an overview of hNPP1 and -4, with an emphasis on the current level of knowledge concerning enzyme structures and kinetics, as well as the state of the art regarding modulators and their activity, in particular inhibitors including tool compounds, and therapeutic candidates.

In order to identify new, potent, and selective hNPP1 inhibitors, we studied the potential inhibitor activity of sulfated polysaccharides derived from sea algae, which were reported to have anti-cancer effects, and to be nontoxic and well tolerated by humans (**Section 2**). We identified and comprehensively characterized them *in vitro*

with respect to potency, selectivity versus related enzymes and mechanism of inhibition. These sulfated polysaccharides, natural constituent of some marine algae, are the most potent NPP1 inhibitors known to date, with nano- to sub-nanomolar potencies. A sulfated polysaccharide isolated from *Saccharina latissima* was identified as a dual inhibitor of NPP1 and CD39. Due to their involvement in ATP-hydrolysis, this dual activity may be beneficial in cancer immunotherapy. Further advancement in the identification of new hNPP1 inhibitors is described in **Section 3**. Heparin and its derivatives including marked antithrombotic as well as newly synthetized analogs, were found to negatively modulate hNPP1 activity and thus inhibit the breakdown of ATP. Moreover, using heparins we observed reduction of adenosine formation in a cell-based assay using tumor cells with native NPP1 expression. Adenosine is an immunosuppressive and tumor-promoting compound and, although still speculative, the reported hNPP1 inhibition by heparin and its derivatives may be crucial to explain the clinical evidence of heparinized cancer patients showing improved survival rates.

In order to discover novel enzyme inhibitors, we developed reliable analytical methods for the monitoring of NPP4 enzymatic reactions. **Chapter 4** describes the development of an HTS (High-throughput screening) assay, using Ap_4A (diadenosine tetraphosphate) as substrate and bio-luminescence as detection method. The assay was fully optimized and validated following FDA (Food and Drug Administration) and ICH (International Council for Harmonisation) guidelines for bio-analytical assays. It was subsequentially used for the screening of a compound library from which two new hNPP4 inhibitors were discovered, further characterized, and validated with a second analytical method based on capillary electrophoresis (CE) with Diode-Array Detection (DAD). The compounds PSB-POM145 and PSB-POM146 are the first hNPP4 inhibitors reported in the literature showing IC_{50} values of 0.298 and 3.36 μM, respectively. These compounds represent essential tools for further studies on NPP4. In order to discover new chemical scaffold, with potential as lead compounds, for drug development, additional screening of compound libraries was performed. The obtained data are

presented in **Chapter 5**. We identified new hit molecules with (moderate) inhibitory potency and selectivity for hNPP4, which may serve as lead structures for future optimization.

Section 6 describes an extensive study on NPP4 enzyme kinetics for a wide range of (potential) substrates. Novel natural substrates of hNPP4 were discovered and characterized.

In conclusion, this work advances the field of ligand discovery for a therapeutically important class of ecto-enzymes. The discovered and reported powerful NPP1 and NPP4 inhibitors will be useful tools for *in vitro* and *in vivo* studies aiming to elucidate the enzymes' roles in physiology and pathology. The new tool compounds may contribute to the validation of NPP1 and NPP4 as novel therapeutic targets, e.g., in cancer (immune)therapy and antithrombotic therapy, respectively.

1. Purinergic signaling and ecto-nucleosidases

Nucleotides and nucleosides located extracellularly are signaling molecules which regulate short- and long-term cellular functions, acting as autocrine and paracrine molecules. They serve as extracellular signaling molecules that activate P1 receptors for the nucleoside adenosine and P2 receptors for nucleotides (e.g., ADP, ATP, UDP, and UTP) [1–5]. P1 adenosine receptors are G protein-coupled receptors (GPCRs), and based on pharmacology, function, and sequence, those receptors are subdivided into four subtypes: A_1, A_{2A}, A_{2B}, and A_3. P2 receptors are further subdivided into P2Y (GPCRs) and P2X (ligand-coupled ion channel) receptors. Seven mammalian P2X receptors (P2X1-7) and eight mammalian P2Y receptors ($P2Y_1$, $P2Y_2$, $P2Y_4$, $P2Y_6$, $P2Y_{11}$, $P2Y_{12}$, $P2Y_{13}$, $P2Y_{14}$) have been cloned, characterized, and accepted as valid members of the P2 receptor family (see Fig. 1). Purinergic signaling is involved in a variety of biological processes, including neurotransmission, neuroprotection in hypoxia and ischemia, cardiovascular function regulation, platelet aggregation, smooth muscle contraction, hormone secretion, immune response modulation, and cell proliferation, differentiation, and apoptosis control [6]. Many tumor cells overexpress ectonucleotidases which metabolize proinflammatory, anti-proliferative ATP to adenosine, thus actively promoting immunosuppressive, angiogenic, pro-metastatic effect and tumor growth [5]. Due to the extracellular role of nucleosides and nucleotides in cell signaling, their hydrolysis is tightly regulated by cell surface-bound ecto-nucleosidases family.

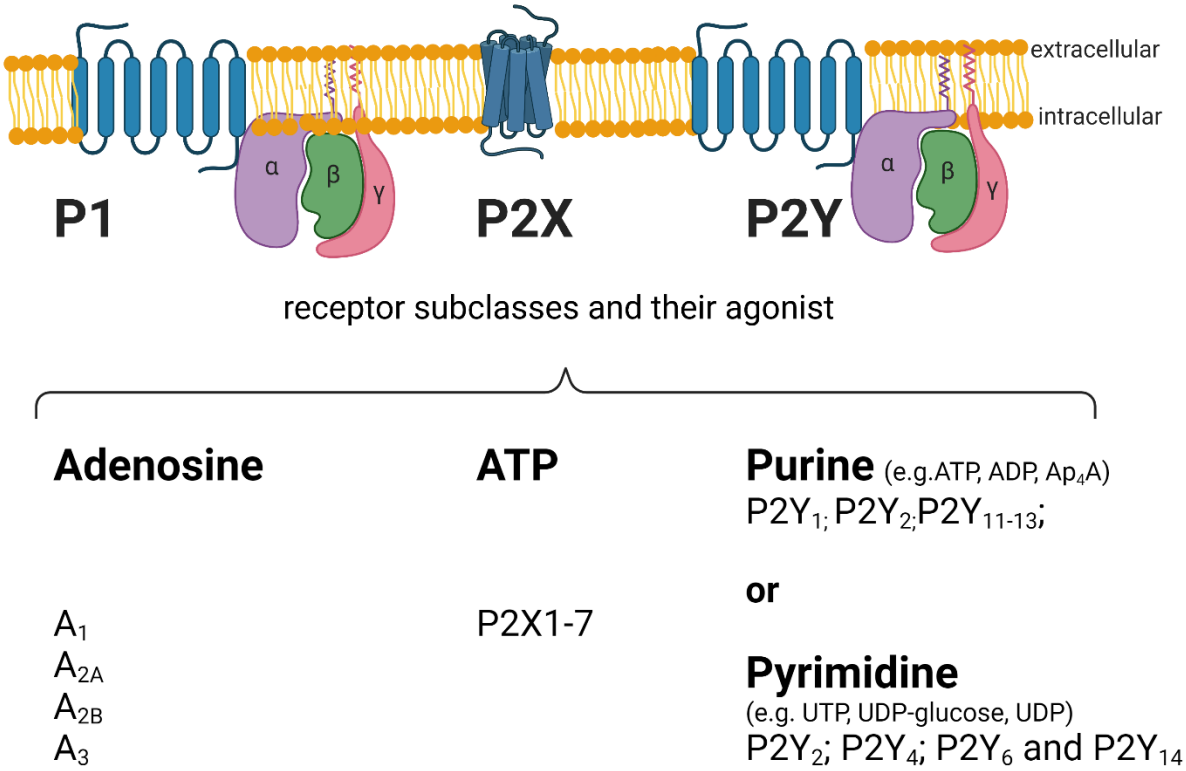

Fig. 1 Purinergic receptors with their activators and subclasses. Illustration created with BioRender.com

The ectonucleotidase family comprises four subfamilies of enzymes, i.e. ecto-nucleoside triphosphates diphosphohydrolases (NTPDases, EC 3.6.1.5), alkaline phosphatases (APs, EC 3.1.3.1), ecto-5′-nucleotidase (CD73, EC 3.1.3.5) [7][8] and ecto-nucleotide pyrophosphatases/phosphodiesterases (NPPs, EC 3.1.4.1 and EC 3.6.1.9). NTPDases hydrolyze nucleoside 5′-triphosphates (NTPs) to nucleoside 5′-diphosphates (NDPs), as well as nucleoside (NDPs) to nucleoside 5′-monophosphates (NMPs), releasing inorganic phosphate [9]. Alkaline phosphatases can hydrolyze a wide range of phosphoric acid ester bonds, e.g. NTPs to NDPs, NDPs to NMPs, and NMPs to nucleosides [10]. The subfamily of NPPs degrades NTPs to NMPs in a single step to releasing diphosphate (PP_i) [11]. The extracellular nucleoside 5′-monophosphates (NMPs) are subsequently hydrolyzed by CD73 (e.g. AMP to adenosine) [12] (see Figure 2).

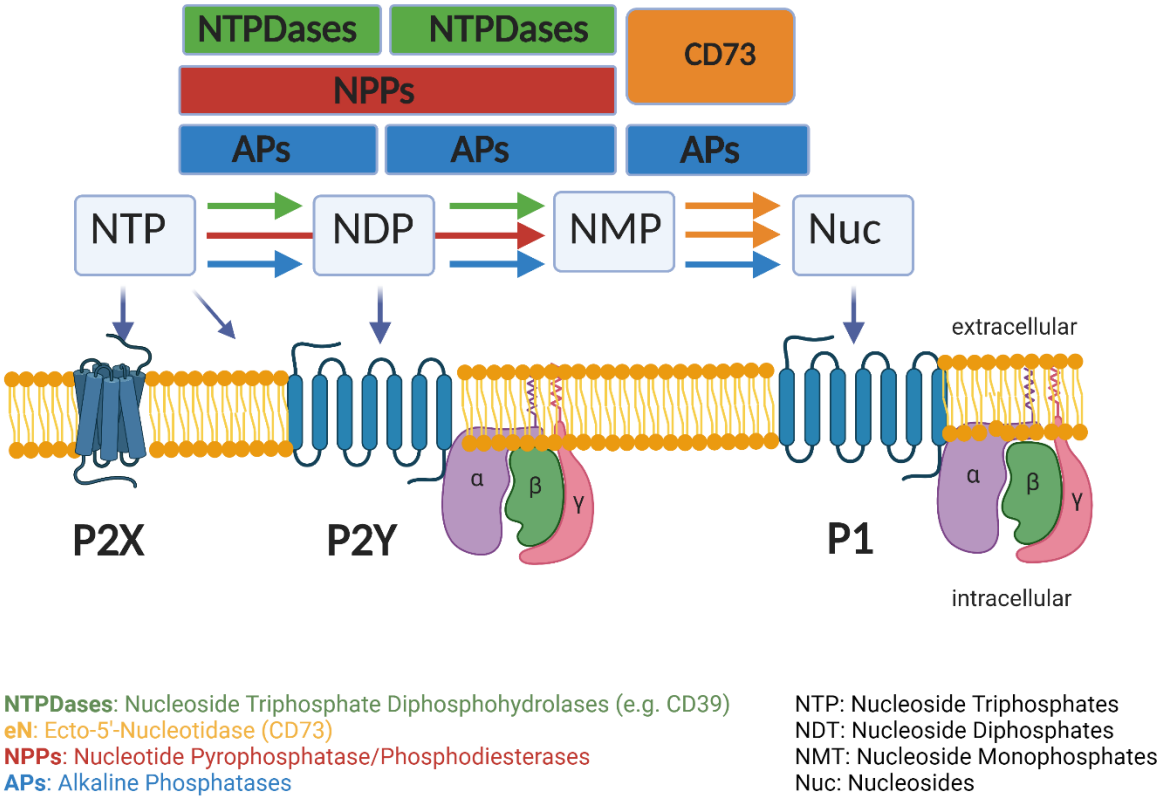

Fig. 2 Ectonucleotidase family and substrates. Illustration created with BioRender.com

Nucleotide pyrophosphatases/phosphodiesterases (NPPs) constitute a family of seven conserved eukaryotic glycoproteins that are expressed as transmembrane ecto-enzymes as well as soluble proteins in body fluids. [8] They are composed of seven structurally related ecto-enzymes that are ordered by date of discovery. Ecto-NPPases are found in a variety of tissues [13] and display a variety of substrate specificities. In the 1950s, enzymes which hydrolyze nucleotide phosphodiester bonds including diphosphates were discovered in the plasma membrane of the liver and other tissues [14,15]. Nevertheless, the isoform specificity was not defined in the earlier literature. Their catalytic activity is divalent cation-dependent and exhibits an alkaline pH preference [8]. NPP1 was first identified as a differentiation alloantigen (Plasma Cell 1, PC-1) in liver, kidney, brain, lymph nodes, and myelomas in 1970 [16]. NPP1 is, for example,

expressed by osteoblasts and chondrocytes, where it produces PP_i and functions by a mechanism that is not dependent on purinergic signaling. PP_i serves as a physiological regulator of bone and soft tissue mineralization by inhibiting the absorption of inorganic phosphate into hydroxyapatite crystals [16]. The peri-articular tissues and ligaments of mice lacking functional NPP1, or mice in which the Enpp1 gene is deleted, have substantial calcification [17]. In humans, mutations that cause loss of function are linked to a variety of tissue mineralization diseases, including idiopathic infantile arterial calcification. NPP1 is found in lymphoid organs and certain tumors, among other places. It has recently been discovered to be part of a pathway that activates the innate immune system through STING (stimulator of interferon genes). NPP1 inhibits cyclic GMP–AMP synthase (cGAS)–stimulator of interferon genes (STING) immune activation pathway by hydrolyzing the STING agonist cyclic 2′,3″-cGAMP (cyclic guanosine monophosphate–adenosine monophosphate) [18]. Antagonists of mouse STING cause shrinking and sometimes even complete resolution of solid tumors. Furthermore, the formation of AMP and GMP as hydrolysis products of 2′,3″-cGAMP lead to the formation of nucleosides, including the immunosuppressive adenosine. NPP1 inhibitors and cGAMP analogs have therefore potential uses in immunotherapy [7,19]. NPP1 has also been implicated in insulin receptor signalling by binding to the insulin receptor [7]. The pathophysiological role of NPP1 will be discussed in more detail in the next paragraph.

NPP2 (EC 3.1.4.39) is a unique enzyme of the NPP family, since it is capable of hydrolyzing phosphodiester bonds of phospholipids and has only a weak activity in hydrolyzing nucleotides, its major substrate is lysophosphatidylcholine. It contains 863 aa (ammino acid) and it has a molecular weight of ~98 kDa. It is involved in several motility-related processes such as angiogenesis and neurite outgrowth and acts as an angiogenic factor by stimulating migration of smooth muscle cells and microtubule formation. Predominantly expressed in brain, placenta, ovary, and small intestine [7].

NPP3 (EC 3.6.1.9) is expressed abundantly in a variety of organs and is particularly abundant in activated basophils and mast cells. By activating basophils and mast cells, ATP causes allergic inflammation. NPP3 decreases ATP levels and thus basophil and mast cell activity [20]. Its activation thus reduces chronic allergic inflammation. As a result, Enpp3 knockout mice are extremely susceptible to chronic allergic pathologies. The protein is frequently used to diagnose allergen sensitivity in patients' basophils [21]. It is a type II protein, contains 875 aa and its molecular weight is ca. 100 kDa.

NPP4, a diadenosine polyphosphate-cleaving enzyme, was discovered on the surface of the vascular endothelium in 2012 [22,23]. According to published findings, NPP4 is a prothrombotic enzyme that promotes platelet aggregation at the site of a nascent thrombus by sustained hydrolysis of platelet-released Ap_3A into prothrombotic ADP. NPP4 was thus proposed as a novel target for antithrombotic therapy [24] and it will be the focus of this PhD thesis together with multiple novel research projects related to NPP1.

NPP5, a type I membrane protein contains 477 aa with a molecular weight of 57 kDa, and only recently it was functionally described as an NAD^+-hydrolyzing enzyme. It has previously been shown to be highly expressed in the human brain, on the respiratory epithelium, the epididymis, and a variety of murine tissues. The primary phenotype of NPP5 knockout mice is characterized by decreased serum insulin levels [25]. Since NAD^+ is an agonist of the $P2Y_1$ and $P2Y_{11}$ receptors, NPP5 plays a role in neural functions, among other effects.

NPP6 and NPP7 can hydrolyze only phospholipids, both with an average of 445 aa and about 50 kDa of molecular weight. Specifically, NPP6 is predominantly expressed in kidney and brain [26] whose function is hydrolyzing glycerophosphocholine (GPC) and lysophosphatidylcholine (LPC) and contributes to supplying choline to the cells. NPP7 is a choline-specific phosphodiesterase that hydrolyzes sphingomyelin releasing the ceramide and phosphocholine and therefore is involved in sphingomyelin digestion, ceramide formation, and fatty acid (FA) absorption in the gastrointestinal tract. NPP7 is

expressed in the duodenum, jejunum, and liver and at low levels in the ileum. Expression was very low in the esophagus, stomach and colon [27,28].

NPP1, NPP3, NPP4, and NPP5 are involved in purinergic signaling due to their hydrolysis activity at physiological substrates, e.g., ATP, diadenosine polyphosphate, NAD^+ and ADP-ribose, AMP is always one of the products of their hydrolysis. Thus, the enzymes regulate nucleoside triphosphate receptor signaling and provide AMP for subsequent adenosine hydrolysis by ecto-5′-nucleotidase or alkaline phosphatase (Figure 2). UDP-glucose, which is also substrate of some NPPs, is a $P2Y_{14}$ receptor agonist, whereas NAD^+ is a $P2Y_1$ and $P2Y_{11}$ receptor agonist [29,30]. NAD^+ also acts as a substrate for ecto-ADP-ribosyl transferases (ARTs) [31]. ADP-ribose (ADPR) activates the TRPM2 (Transient Receptor Potential Cation Channel Subfamily Member 2) cation channel with a transient receptor potential [31]. Diadenosine polyphosphates interact with a variety of P2X and P2Y receptors [31], and their hydrolysis products, ATP or ADP, can further activate P2 receptors before being hydrolyzed to adenosine.

In the last decade, the crystal structures of NPP1, NPP2, NPP3, NPP4, NPP5, NPP6, and NPP7 have aided in the synthesis of E-NPP inhibitors [31]. NPP1 was the first crystal structure of an ecto-NPPase that hydrolyzes nucleotides, to be determined in 2012 [32,33], and recently, in 2020, also the human NPP1 crystal structure was resolved [34]. The structures of the ecto-nucleotidase family elucidated the conserved arrangement of the domains of the nuclease and phosphodiesterase. The conserved core catalytic center contains two zinc ions and an asparagine residue that interacts with the zinc-coordinated phosphate group. However, the architecture of the substrate binding pockets for nucleotide and phospholipid substrates is significantly different. Furthermore, the structures elucidated the relationship between ecto-NPPases and APs. Co-crystals with nucleotide ligands aided in elucidating the structural factors governing substrate binding and hydrolysis [25,35,36].

1.1 NPP1

1.1.1 Tissue distribution and structure

Takahashi et al., initially identified ecto-nucleotide pyrophosphatase/phosphodiesterase 1 (NPP1) on the surface of mouse lymphocytes as plasma cell differentiation antigen 1 (PC-1) [37]. It prevents apoptosis of plasma cells via nicotinamide adenine dinucleotide (NAD^+) induced activation of P2X7 receptors [13,38,39]. This enzyme is found in abundance throughout the human body. NPP1 is expressed predominantly in bone, cartilage, and adipose tissue in humans [40], but also in the heart, liver, placenta, and testis [41,42]. NPP1 is as well expressed in the kidney's distal tubules, pancreatic islets, vas deferens, chondrocytes, lymphocytes, dermal fibroblasts, epithelium of salivary gland ducts, brain, capillary endothelium, and epididymis [41,43–45]. Additionally, soluble NPP1 was detected in human serum and plasma at concentrations ranging from 15 to 600 pM (2 to 80 ng/ml) [46]. Although no expression has been detected in human neurons or glial cells, increased expression in human astrocytoma and glioblastoma cells has been reported [46]. Increasing aggressiveness of astrocytic brain tumours (Aerts et al., 2011) is correlated with the expression of NPP1. A high level of NPP1 is also associated with increased of bone metastasis formation from breast cancer (Lau et al., 2013). NPP1, notable for its modular structure, is a type II transmembrane glycoprotein with an N-terminal transmembrane domain, two somatomedin-B-like domains, a catalytic domain, and a nuclease-like domain at the C-terminus (see Figure 3) [8,13]. Additionally, it is well established that while NPP1 is expressed as a homodimer in the plasma membrane, it is secreted as a monomer into the extracellular space [8,47–49]. The monomer of NPP1 has an apparent molecular mass of 115–130 kDa, while the dimer has a molecular mass of 230–260 kDa, depending on the cell type [50,51]. NPP1 in humans contains 925 amino acids [47] and it has been shown to be N-glycosylated [32,33,47]. Crystal structures of human NPP1 in apo- and bound forms were crystallized by Dennis et al. in 2020, and five structures are available in the Protein Data Bank (PDB): 6WET, 6WEV, 6WEW,6WEU and 6WFJ [34].

The hNPP1 protein has nine potential glycosylation sites listed in UniProt (ID P22413), and Dennis et al. observed electron density for glycosylation at several of them (Asn285, Asn341, Asn477, Asn585, and Asn731), but two of them (Asn700 and Asn748) showed low density, implying that these sites are unlikely to be glycosylated. Asn179 and Asn643 do not exhibit any additional density that would suggest glycosylation. Mass spectrometric analysis reveals glycosylation at all nine potential hNPP1 sites, although the extent of glycosylation varies from 10% to 95%, with Asn179 and Asn748 having low levels of glycosylation (10–27%), Asn285 being almost completely modified, and the remaining residues having between 36% and 100% glycosylation. Several cysteine residues are present, in particular three cysteine residues (Cys67, Cys75, and Cys83) have been proposed to be required for dimerization between monomers via multiple disulfide bonds [32]. Additionally, it has been demonstrated that the transmembrane region of murine NPP1 is cleaved by intracellular peptidases in the endoplasmic reticulum, resulting in the enzyme's secretion [32]. NPP1 contains two somatomedin-like domains, designated SMB1 and SMB2, respectively [13,32,39]. Indeed, somatomedin-B (SMB) is a serum peptide with mitogenic activity that is believed to be an epidermal growth factor [52]. Additionally, it is derived via proteolysis from vitronectin, a serum and extracellular matrix protein involved in cell adhesion [52]. While the SMB domain of vitronectin has been shown to interact with both the urokinase receptor and plasminogen activator inhibitor-1 (PAI-1), the two SMB domains of NPP1 do not [52]. NPP1's somatomedin-B-like domains are largely uncharacterized in terms of function. Nonetheless, it has been proposed that these domains aid in the stabilization of the transmembrane-catalytic domain interface. Additionally, the K173Q polymorphism in human NPP1 has been associated with increased insulin resistance due to an increase in binding affinity for the insulin receptor [53]. Thus, it has been proposed that the SMB2 domain of NPP1 is involved in the interaction with the insulin receptor [8,33]. The phosphodiesterase (PDE) catalytic domain of NPP1 contains approximately 400 amino acid residues and shares 24-60% of the amino acid sequence between the various human isoforms [53,54]. This catalytic

domain is related to the alkaline phosphatase family (APs) [53]. NPPs are members of the phospho-/sulfo-coordinating metalloenzyme superfamily [54]. As with the APs, a set of six conserved Asp/His residues tightly binds two Zn^{2+} ions in the active site [32][33]. Additionally, a "lasso loop" connects this domain to the nuclease-like domain (NUC domain) [33]. This linker forms hydrophobic interactions, hydrogen bonds, and two cysteine bonds between the PDE and NUC domains [33]. Mutation of this linker region in NPP1 abolishes catalytic activity, indicating that the lasso-loop interaction between the catalytic and nuclease-like domains is required for its activity [33][32]. The nuclease-like domain shares structural similarities with non-specific DNA/RNA endoribonucleases, both in terms of its primary structure and predicted folding [55]. Although this domain lacks catalytic activity, it is required for proper NPP folding and translocation from the endoplasmic reticulum to the Golgi apparatus [8]. Additionally, the NUC domain contains a putative 'EF-hand' Ca^{2+} binding motif, which is required for NPP1 catalysis [56,57].

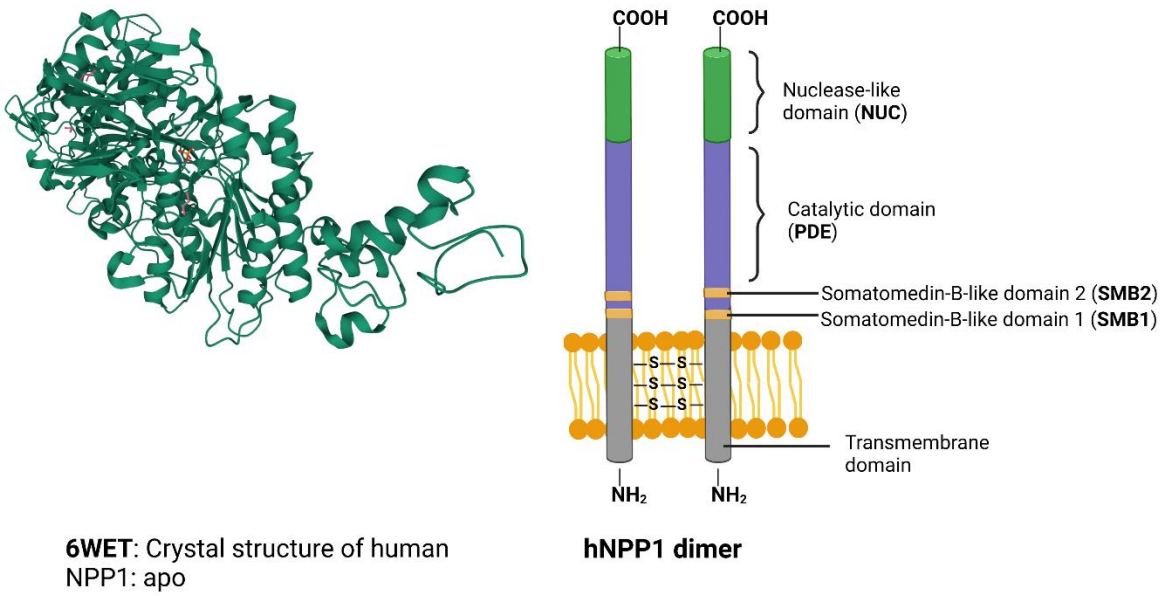

Fig. 3 NPP1 crystal structure (source Protein data bank) and schematic representation of dimer domains. Illustration created with BioRender.com

1.1.2 **Kinetic property and substrates of NPP1**

NPP1 exhibits an astonishingly broad substrate specificity. It catalyzes the hydrolysis of a variety of nucleotides, including ATP, nicotinamide adenine dinucleotide (NAD^+), 3'-phosphoadenosine-5'-phosphosulfate (PAPS), flavin adenosine dinucleotide (FAD), diadenosine polyphosphates, and UDP-glucose [8][58]. Also, purine and pyrimidine nucleotides function as substrates of NPP1. Additionally, it has been reported that 3',5'-cyclic AMP is either not a substrate or a poor substrate [14,59]. Furthermore, NPP1 can hydrolyze cyclic dinucleotides such as 2′,3′′-cGAMP, which is an important immunomodulator with possible applications in immunotherapy. Even though nucleoside monophosphates, such as AMP or UMP, are not hydrolyzed by NPP1, they can moderately inhibit NPP reactions competitively (product inhibition) [60]. NPP1 can generate nucleoside 5'-monophosphate during the hydrolysis of (di)nucleotides. Additionally, NPP1 activity can convert PAPS (3′-phosphoadenosine-5′-phosphosulfate) and UDP-glucose to adenosine 3',5'-diphosphate and uridine 5'-monosphate (UMP), respectively (Figure 4) [8][58]. *p*-Nitrophenyl 5'-thymidine monophosphate (*p*-Nph-5'-TMP) and *p*-nitrophenyl phenyl phosphate (p-NPPP) have been used as synthetic substrates for monitoring NPP1 reactions [7]. Both of the aforementioned synthetic substrates produce the intensely yellow *p*-nitrophenolate during the enzymatic reactions, enabling simple colorimetric detection in the visible region (400 nm) and thus high-throughput screening of compound libraries [7].

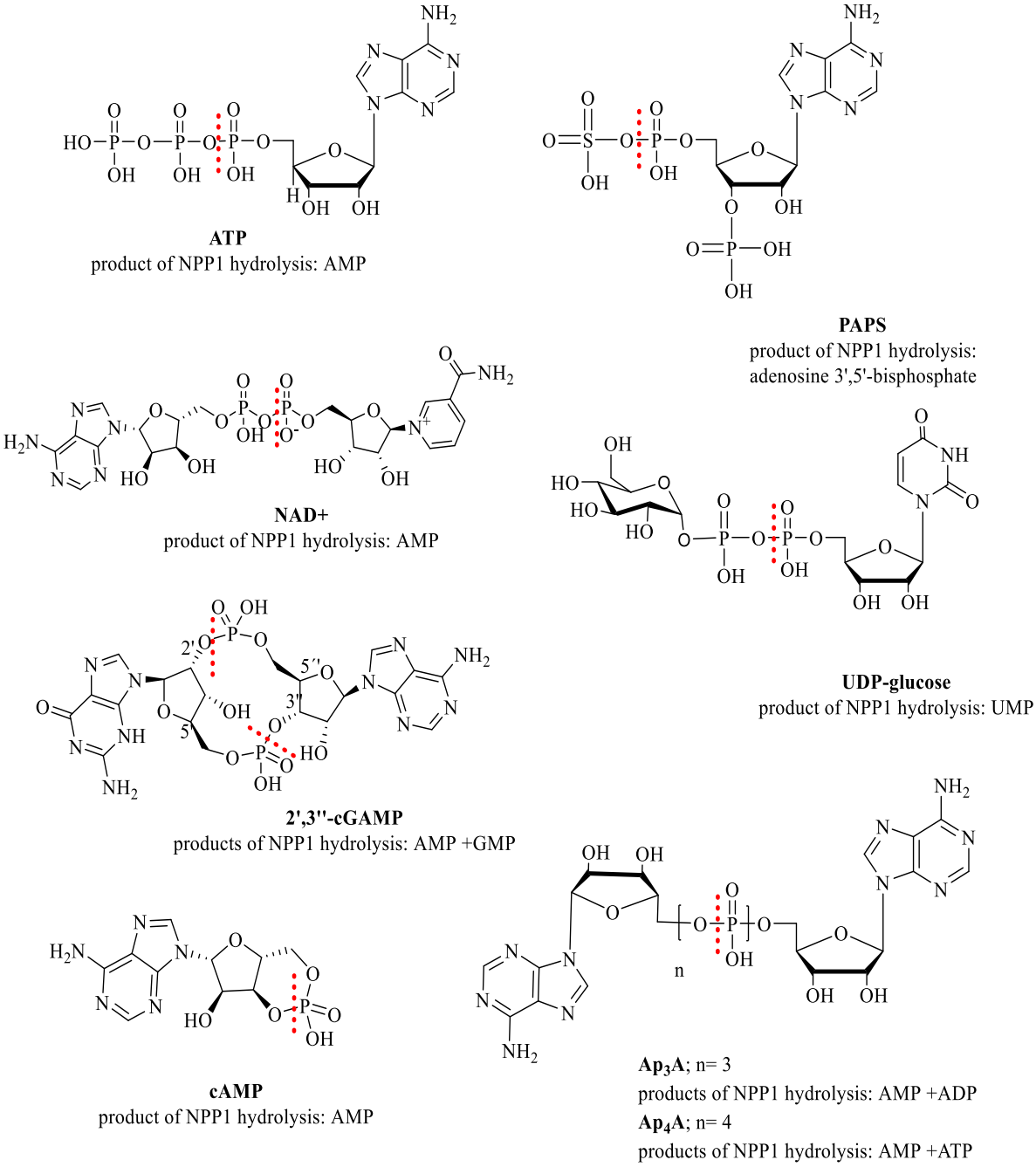

Fig. 4 Structures of natural NPP1 substrates. The site of hydrolysis is marked with a dashed red line.

1.1.3 Pathological role of NPP1

Immuno-oncology

Cyclic dinucleotides, such as cyclic guanosine-(2′,5′)-monophosphate-adenosine-(3′,5′′)-monophosphate (2′,3′′- cGAMP**),** have been reported as substrates of NPP1 [19,61]. cGAMP is a STING agonist (stimulator of the interferon gene), which is crucial for the induction of interferon type I (IFN) in the development of the innate immunity response [19,35,61]. As strong immunomodulators with possible applications in immunotherapy, cGAMP or its analogues have emerged to play a pivotal role in the immunotherapy of cancer, and therefore the interest in the modulation of NPP1 activity through small molecule inhibitors has increased tremendously in the past years.

STING pathway activation can stimulate anti-inflammatory T-cell responses by increasing IDO (indoleamine-2,3-dioxygenase), which leads to immune suppression in the tumour microenvironment [62–65]. IDO1 is an interferon-stimulated gene (ISG) that is activated by IFNs via IFN-responsive elements found in the mammalian IDO1 gene promoters. IDO, an enzyme that catabolizes tryptophan, increases the activation of $CD4^+$ regulatory T- cells and suppresses effector and helper T-cell functions [63].

IDO promotes immune tolerance in dendritic cells by inducing transforming growth factor beta (TGF) [64,66]. Lemos et al. demonstrated that silencing STING enhanced cancer cell killing in a Lewis lung carcinoma mouse model by increasing $CD8^+$ T-cell activity, decreasing myeloid suppressor cell infiltration, and increasing IL10 production in the tumor microenvironment [64]. However, induction of IDO did not have the same effect in EL4 thymoma, B16 melanoma, or neo-antigen-expressing lung carcinoma that were STING-deficient [64]. IDO's immunosuppressive effect promotes tumorigenesis in tumors with low antigenicity [64]. Thus, when tumor antigenicity is low, STING activation primarily induces immune-regulatory responses via IDO, whereas immune-stimulatory responses are enhanced in tumors with a high antigenicity [64].

Moreover, adenosine produced by the adenosinergic pathway has immunosuppressive effects in the tumor microenvironment and contributes to tumor progression. The ecto-nucleotidases CD39, NPP1 and CD73 rapidly dephosphorylate ATP in the extracellular milieu. CD39 normally converts ATP to ADP and ADP to AMP, while NPP1 converts ATP directly to AMP, then CD73 dephosphorylates AMP to adenosine. In addition, tumor hypoxia increases CD39 and CD73-mediated adenosine production [67,68]. Additionally, hypoxia inhibits adenosine breakdown and potentiates adenosine release by inhibiting adenosine kinase [69,70]. Adenosine production increases, and the breakdown of adenosine is inhibited, resulting in greatly increased levels of adenosine in tumors [71]. G-protein-coupled A_{2A} and A_{2B} adenosine receptors that stimulate cyclic AMP production ultimately increase anti-inflammatory cytokine production while inhibiting the production of proinflammatory cytokines [69]. In a study by Lourdes Mora-Garcia et al. the authors demonstrated that in mesenchymal stromal cells (MSCs) derived from cervical cancer, the T-cell cytotoxic activity, including proliferation and production of IFN-γ, was inhibited by adenosine in a dose-dependent manner [69]. Previous studies have shown that MSCs derived from cervical cancer secrete anti-inflammatory cytokines, such as TGF-β1 and IL-10, which help the cells to resist T-cell cytotoxicity [72]. The hydrolysis of cGAMP by NPP1 yields AMP, which leads to more immunosuppression due to its dephosphorylation to adenosine by CD73 [73]. The function of NPP1 in cancer is exemplified by the observation that overexpression of NPP1 enhances tumor metastasis to bone in breast cancer [74]. The significance of NPP1 and CD73-mediated adenosine synthesis is further demonstrated by several reports of mice deficient in either CD73 or NPP1 being resistant to carcinogenesis or metastasis [68,74–76].

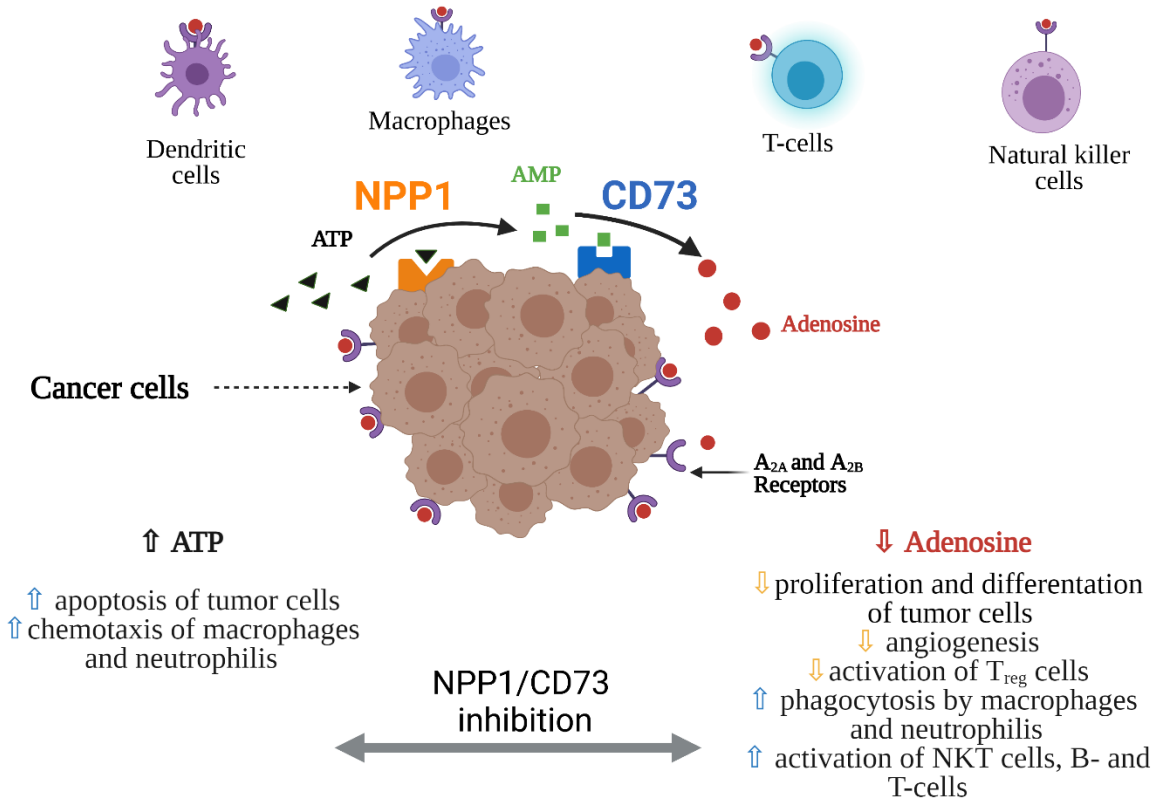

Fig. 5 Role of ectonucleotidases in immuno-oncology. Illustration created with BioRender.com.

Bone mineralization, soft-tissue calcification, and calcium pyrophosphate dihydrate deposition (CPPD)disease

NPP1 is directly involved in bone mineralization and also in the calcification of vascular smooth muscle cells [40]. As illustrated in Figure 6, NPP1 synthesizes diphosphate (PP_i) from ATP, which is then converted to inorganic monophosphate (P_i) by the tissue non-specific alkaline phosphatase (TNAP). P_i then binds to extracellular calcium to form hydroxyapatite (HA, $Ca_{10}(PO_4)_6(OH)_2$), a tissue mineralization matrix which promotes both bone mineralization and soft-tissue calcification [77]. Additional feedback mechanisms exist to prevent ectopic mineralization; PP_i acts as an inhibitor of HA formation by increasing the expression of osteopontin (OPN), a suppressor of tissue mineralization, while simultaneously decreasing the expression of osteocalcin (OCN)

and TNAP, both of which promote tissue mineralization, thereby suppressing HA crystal precipitation and growth [77,78]. NPP1 expression is elevated in chondrocytes, which causes an increase in diphosphate. Since the enzymatic activity of TNAP is limited, the excessive amounts of diphosphate formed can bind to the extracellular calcium, forming nearly insoluble calcium diphosphate (see Fig. 7). CPPD (calcium pyrophosphate dihydrate deposition) disease is a buildup of this calcium salt in joints and cartilage, which causes arthritis and joint pain [79]. NPP1 inhibitors thus show promise as new medications for CPPD diseases.

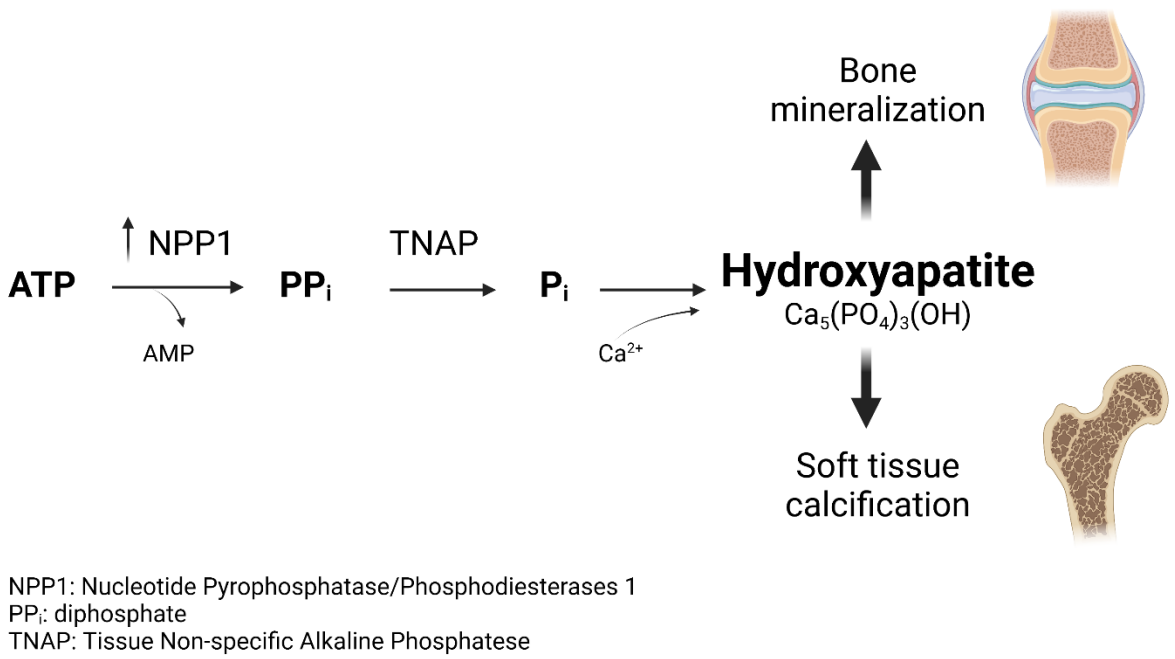

Fig. 6 Role of NPP1 in bone mineralization and soft tissue calcification. Illustration created with BioRender.com.

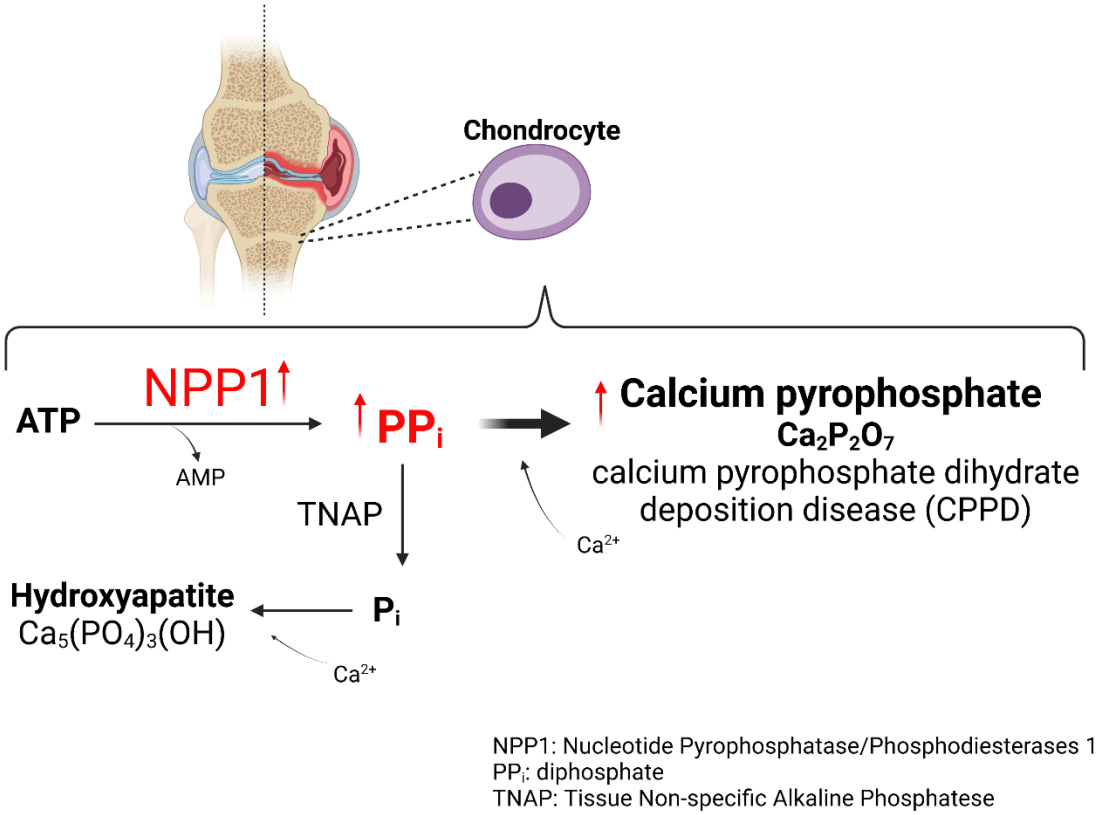

Fig. 7 Pathological calcification by increased expression of NPP1 in the chondrocytes. This disease is known as calcium pyrophosphate dihydrate deposition (CPPD) disease. Illustration created with BioRender.com.

Insulin receptor signaling

It has been reported that NPP1 plays a role in insulin receptor signaling [43,46,80,81]. Firstly, it was determined that dermal fibroblast cultures from patients with non-insulin-dependent type 2 diabetes mellitus and extreme insulin resistance had an increased NPP1 content [82]. Secondly, it was discovered that an overexpression of NPP1 results in impaired insulin-stimulated insulin receptor (IR) autophosphorylation in patients with type 2 diabetes [43]. Thirdly, insulin resistance and diabetes were observed in transgenic mice overexpressing PC-1 (NPP1) in various tissues [80]. NPP1 was reported to bind directly to the insulin receptor subunit, specifically to residues 485-599 (see Fig. 8). Subsequently, this association prevents further signaling by

decreasing the autophosphorylation of the insulin receptor subunit, which ultimately results in its desensitization [43,53]. NPP1 inhibition of the insulin receptor is independent of its phosphodiesterase activity; its control of the insulin receptor is mediated by simple protein-protein interactions [43,53,83]. The NPP1 polymorphism K173Q has been associated with insulin resistance in a number of human populations [84–86]. These results, however, were not replicated in many other populations [87]. The uncommon NPP1 variant Q173 was found to have a greater physical association with the insulin receptor in vitro than the more prevalent NPP1 variant K173 [87]. Since this K173 residue is in NPP1's SMB2 domain, this domain most likely represents the binding residue for the insulin receptor interaction.

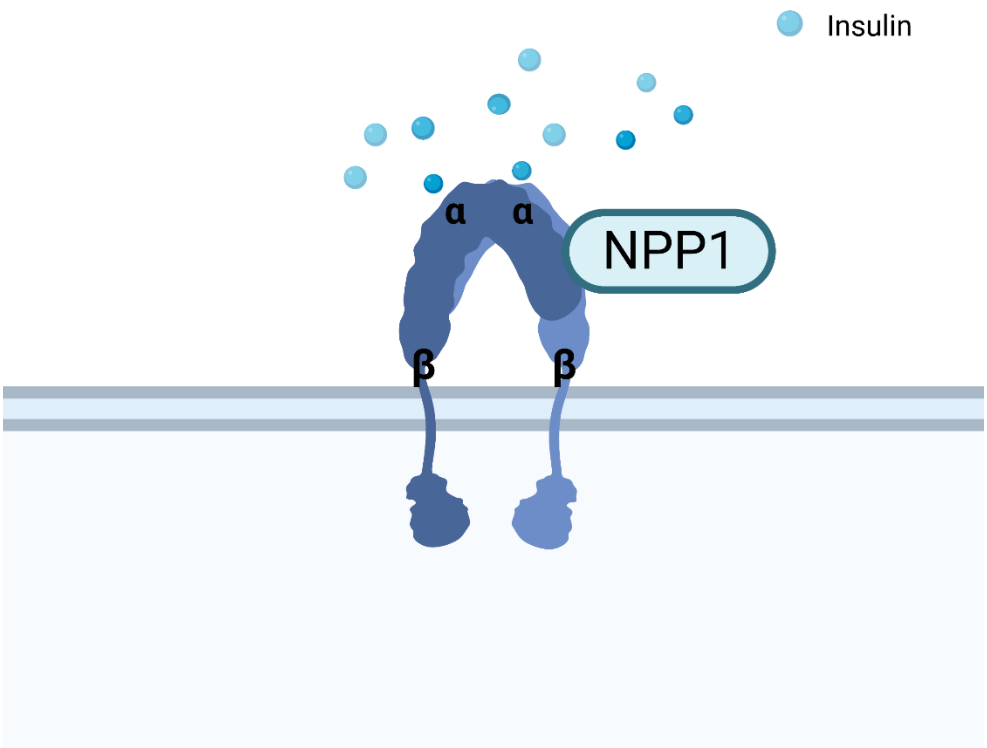

Fig. 8 Interaction between the insulin receptor and NPP1. Illustration created with BioRender.com.

Brain cancer

NPP1 expression was found to be increased in neural brain tumors, and its level of expression was found to be closely linked to the tumor grade [85,86]. NPP1 expression is increased in the membranes of rat C6 glioma cells [84]. Furthermore, it was demonstrated that NPP1 expression is increased in human astrocytic brain tumors (glioblastoma), and that NPP1 expression increases with tumor grade [51]. Also, increased NPP1 expression was observed in human glioblastoma stem-like cells [86]. Finally, it has been shown that NPP1 is expressed in N2a mouse neuroblastoma cells, with its expression level significantly changing as cells differentiate into a neuronal-like phenotype [85]. As a result, NPP1 inhibitors may prove to be effective as novel anticancer agents in neural brain cancers.

1.1.4 NPP1 inhibitors

So far, a limited number of NPP1 inhibitors has been discovered and described in the literature. Those inhibitors have mainly a nucleotide-like structure, however also non-nucleotide scaffolds have been reported. For example, the purinoceptor antagonists Reactive Blue 2 (**1**) and Suramin (**3**) have been characterized as strong NPP1 inhibitors versus ATP as a substrate, displaying K_i values of 0.52 and 0.26 μM, respectively [88]. They appeared to inhibit the NPP1 activity non-competitively (RB2, **1**) or un-competitively (Suramin, **3**) [7]. The selectivity of Reactive Blue 2 and Suramin for NPP1 is poor, since both compounds also inhibit NPP3 strongly as well as various P2 receptors (RB2 additionally inhibits CD73). A series of quinazoline-4-piperidine-4-methylsulfamide (**4**) were shown to be strong NPP1 inhibitors against *p*-Nph-5′-TMP as an artificial substrate with a K_i value of the best compound of 0.58 μM [89]. Recently, new quinazoline derivatives have been synthetized having a K_i of 2 nM using cGAMP as substrate (**12**). Furthermore, negatively charged compounds like polyoxometalates and sulfated polysaccharides strongly inhibit the NPP1 activity. The polyoxometalates are an inorganic cluster of molecules with negative charges, containing tungsten (W), molybdenum (Mo) or vanadium (V) as central atoms, surrounded by oxygen atoms. A

polyoxotungstate compound $[TiW_{11}CoO_{40}]^{8-}$ (PSB-POM141, **2**) is among the most potent inhibitors of human soluble NPP1 with a K_i value of 1.46 nM vs. ATP as a substrate. PSB-POM141 revealed a non-competitive mechanism of inhibition. This inorganic cluster compound was shown to be highly selective vs. other human ecto-nucleotidases, including NTPDase1–3, NPP2–3, CD73 and TNAP (tissue non-specific alkaline phosphatase) [90]. However, oral administration of such polyanionic cluster compounds is limited because of their negative charge and their high molecular weight. A series of sulfated polysaccharides extracted from sea algae represent, up to date, the most potent hNPP1 inhibitors, displaying a good selectivity profile and a non-competitive mechanism of inhibition. The second chapter of the present thesis includes the publication where this novelty is described in more detail. A compound extracted from *Delesseria sanguinea* has a K_i value, using ATP as substrate, of 0.0517 nM [91]. Also, heparin and its derivatives strongly inhibit the NPP1 activity, and this will be described in detail in the third chapter of the present dissertation. Among the nucleotide derived scaffolds, to which most of the known NPP1 inhibitors belong, are adenine nucleotide analogs and derivatives such as adenosine 5′-(α,β-methylene)diphosphate (α,β-metADP, **5**) and its analog (α,β-metATP, **6**), (2-MeSADP, **7**) and (2-MeSATP, **8**) with reported K_i values in the range of 21-24 μM determined versus ATP as a substrate (see Table 1 for details).

Moreover, when tested against *p*-Nph-5'-TMP as a substrate, the NTPDase1 inhibitor N^6,*N*-diethyl- dibromomethylene-ATP (ARL 67156, **10**) was found to be a moderately potent NPP1 inhibitor with a K_i value of 12 μM [92]. A series of diadenosine 5',5''-(boranato)-polyphosphonate analogs (diadenosine boranosphosphate derivatives, e.g., **9**) were found to be inhibitors of human NPP1 versus *p*-Nph-5'-TMP as a substrate. The most active molecule in this series had a K_i value of 9 μM, showing selectivity against other NPPs such as NPP2 and 3. Another class of compounds with an adenine nucleotide scaffold is the adenine bisphosphonate, **12** with the best compound having a K_i in the low micromolar range [93]. Recently, new classes of hNPP1 inhibitors, having

uracil in their scaffolds (compounds **11** and **13** in Table 1), have been also described. The uridine dithiophosphate analogues and uracil scaffolds analogues have a K_i lower than 1 μM when tested with *p*-Nph-5'-TMP [94,95]. Pyrrolo [2,3]pyridine derivative was reported to have IC_{50} of 0.80 μM (**15**) with *p*-Nph-5'-TMP as substrates, while thioguanine derivatives are reported to have Ki around 2 nM (**16**).

Table 1. NPP1 inhibitors

	Inhibitor	**Substrate**	**Enzyme (human NPP1)**	**Ki value**	**Ref.**
1	Reactive blue	ATP [a]	Membrane-bound	0.52 μM	Iqbal et al., 2008 [88]
2	PSB-POM141	ATP [b]	Soluble	1.46 **nM**	Lee et al., 2015 [90]
3	Suramin	ATP [a]	Membrane-bound	0.26 μM	Iqbal et al., 2008 [88]
4	Quinazoline derivative	p-Nph-5′-TMP [c]	Membrane-bound	0.58 μM	Forcellini et al., 2018 [89]
5	α,β-metADP	ATP [b]	Soluble	24 μM	Lee et al., 2014 [96]
6	α,β-metATP	ATP [b]	Soluble	27 μM	Lee et al., 2014 [96]
7	2-MeSADP	ATP [b]	Soluble	24 μM	Lee et al., 2014 [96]
8	2-MeSATP	ATP [b]	Soluble	21 μM	Lee et al., 2014 [96]
9	Diadenosine boranosphophate	p-Nph-5′-TMP [c]	Membrane-bound	9 μM	Eliahu et al., 2010 [97]

10	ARL67156	p-Nph-5′-TMP [c]	Membrane-bound	12 μM	Levesque et al., 20007 [92]
11	Uridine Dithiophosphate Analogues	p-Nph-5′-TMP [c]	Membrane-bound	0.27 μM	Zelikman et al., 2018 [94]
12	Quinazoline derivative	cGAMP [d]	Soluble **mouse**	2 **nM**	Carrozza et al., 2020 [98]
13	Uracil scaffold	p-Nph-5′-TMP [c]	Membrane-bound	0.73 μM	Nassir et al., 2019 [95]
14	Sulfated polysaccharide	ATP [b]	Soluble	0.0517 **nM**	Lopez et al., 2021 [91]
15	Pyrrolo [2,3-b] pyridine derivative	p-Nph-5′-TMP [e]	Membrane-bound	0.80 μM (**IC_{50}**)	Ullah et al., 2021 [99]
16	Thioguanine derivatives	cGAMP [f]	Soluble	2.88 **nM**	Gangar et al., 2021 [103]

a CE-based assay; buffer: 10 mM HEPES, 2 $CaCl_2$, 1 $MgCl_2$ pH 7.4

b CE-based assay; buffer: 10 mM CHES, 2 $CaCl_2$, 1 $MgCl_2$ pH 9.0

c Absorbance-based assay; buffer: 50 mM TRIS, 140 mM NaCl, 5 mM KCl, 1 $CaCl_2$, pH 8.5

d Radio assay; buffer: 50 mM TRIS, 25 mM NaCl, 0.001 mM $ZnCl_2$, 0.5 mM $CaCl_2$ pH 7.4

e Absorbance-based assay; buffer: 50 mM TRIS, 5 mM $MgCl_2$, 0.1 $ZnCl_2$ pH 9.5

f AMP-Glo assay; 50 mM Tris, 250 mM NaCl, 0.5 mM $CaCl_2$, 1 mM $ZnCl_2$, pH 9.5

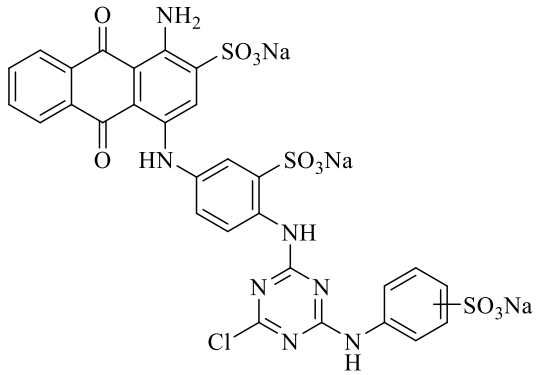

Reactive blue (**1**)

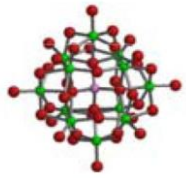

PSB-POM141 (**2**)
$[TiW_{11}CoO_{40}]^{8-}$

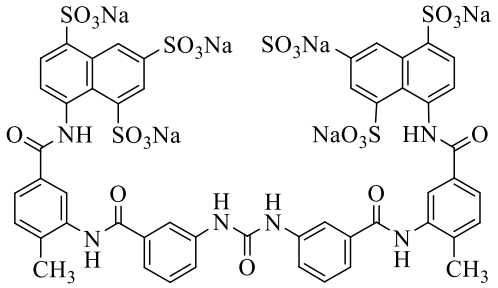

Suramin (**3**)

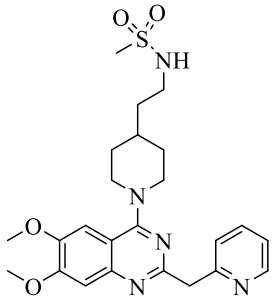

Quinazoline-4-piperidinesulfamide (QPS) derivative (**4**)

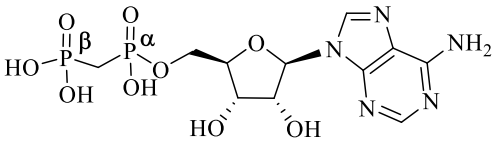

α,β methylene-ADP (**5**)

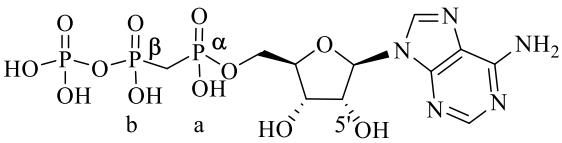

α,β methylene-ATP (**6**)

Fig. 9A Know inhibitors of NPP1

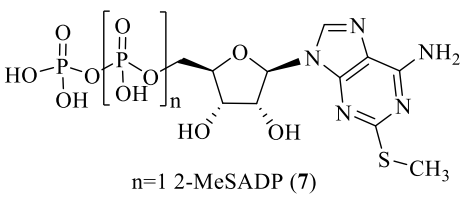

n=1 2-MeSADP (**7**)
n=2 2-MeSATP (**8**)

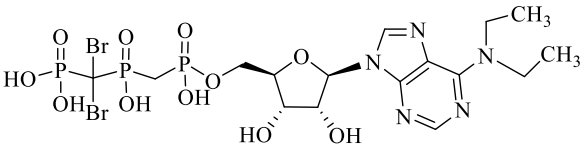

ARL 67156 (**10**)

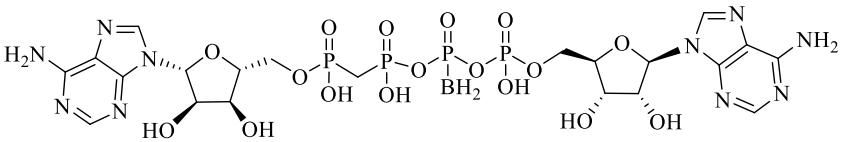

diadenosine boranophosphate derivative (**9**)

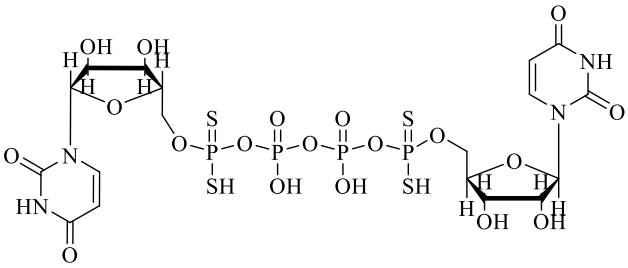

uridine 5'-P-$_{\alpha,\alpha}$dithiophosphate analogues (**11**)

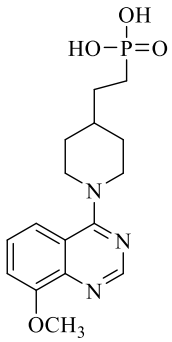

8- Methoxy Quinazoline derivative(**12**)

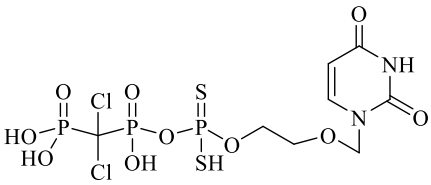

uracil-nucleotides derivative (**13**)

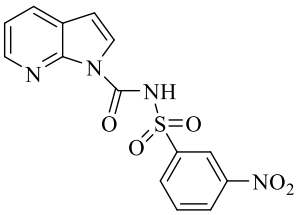

pyrrolo [2,3-b]pyridine derivative (**15**)

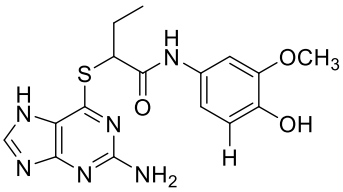

Thioguanine derivative (**16**)

Fig. 9B NPP1 know inhibitors

1.2 NPP4

1.2.1 Tissue distribution and structure

NPP4 (EC 3.6.1.29) is widely and highly expressed in many organs, tissues, and cells in the brain (on brain vascular endothelial cells) as well as in the periphery (on platelets). High expression at the protein level is found in the cerebral cortex, hippocampal formation, and basal ganglia. Furthermore, high protein level is also present in the GI tract, in the stomach, small intestine and duodenum. High protein levels are also present in the heart muscle, in lungs and thyroid. Human NPP4 is a type I transmembrane protein, with 463 aa residues with a topological domain (position 16 – 407), a small transmembrane domain (position 408 – 428) and another cytoplasmatic topological domain (position 429 – 463). The protein has two disulfide bonds and four glycosylation sites in position 155, 166, 276 and 386. The crystal structure of hNPP4 is available in the apo-form and with AMP bound (PDB code 4LR2 and 4LQY) at 1.5 Å resolution [22].

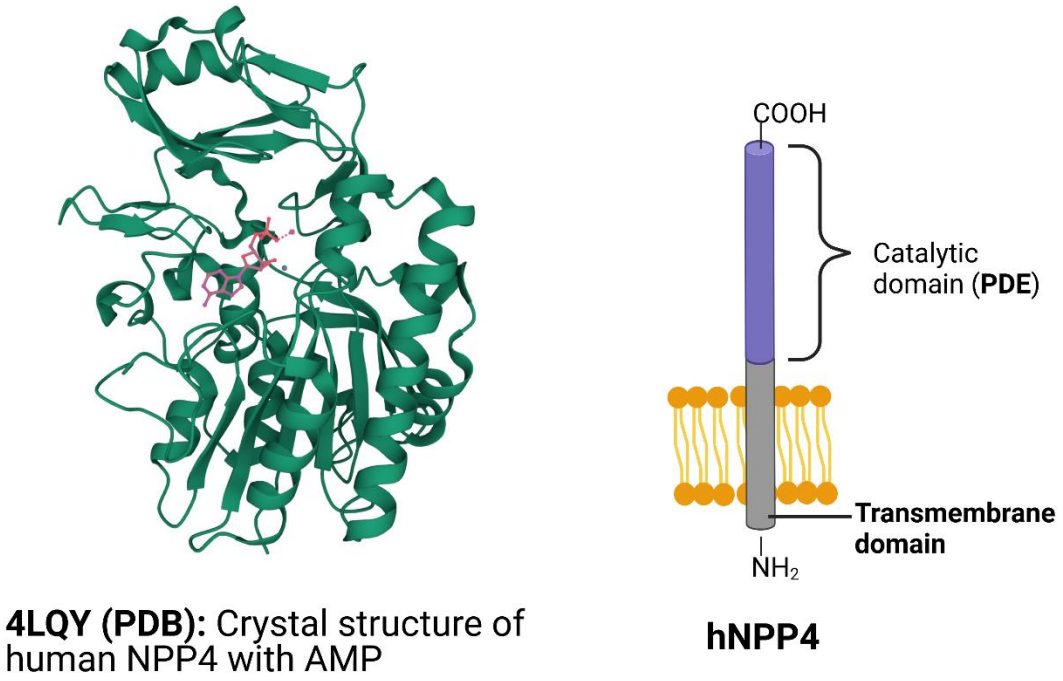

Fig. 10 NPP4 crystal structure (source Protein data bank) and schematic representation of domains. Illustration created with BioRender.com

1.2.2 Kinetic properties and substrates

NPP4 is known to hydrolyze diadenosine polyphosphates, Ap_3A and Ap_4A, into AMP and ADP or ATP, respectively. According to the literature, the K_m values for these substrates are ~200 μM for Ap_4A with a k_{cat} of ~ 0.78 s^{-1} and a K_{cat}/K_m of 3.7 x 10^3, and a K_m of ~840 μM for Ap_3A with k_{cat} a of ~ 4.2 s^{-1} and a K_{cat}/K_m of 5 x 10^3 [23]. Despite the similarity of all members of the NPP family, NPP4 only weakly hydrolyzes ATP, but it can hydrolyze the artificial substrate *p*NP-TMP. No other substrates have been described in the literature up to date, and for these reasons, a full characterization of substrates kinetics has been performed. Data will be presented in Chapter 6 of this dissertation, which represent novel data, that are planned to be published.

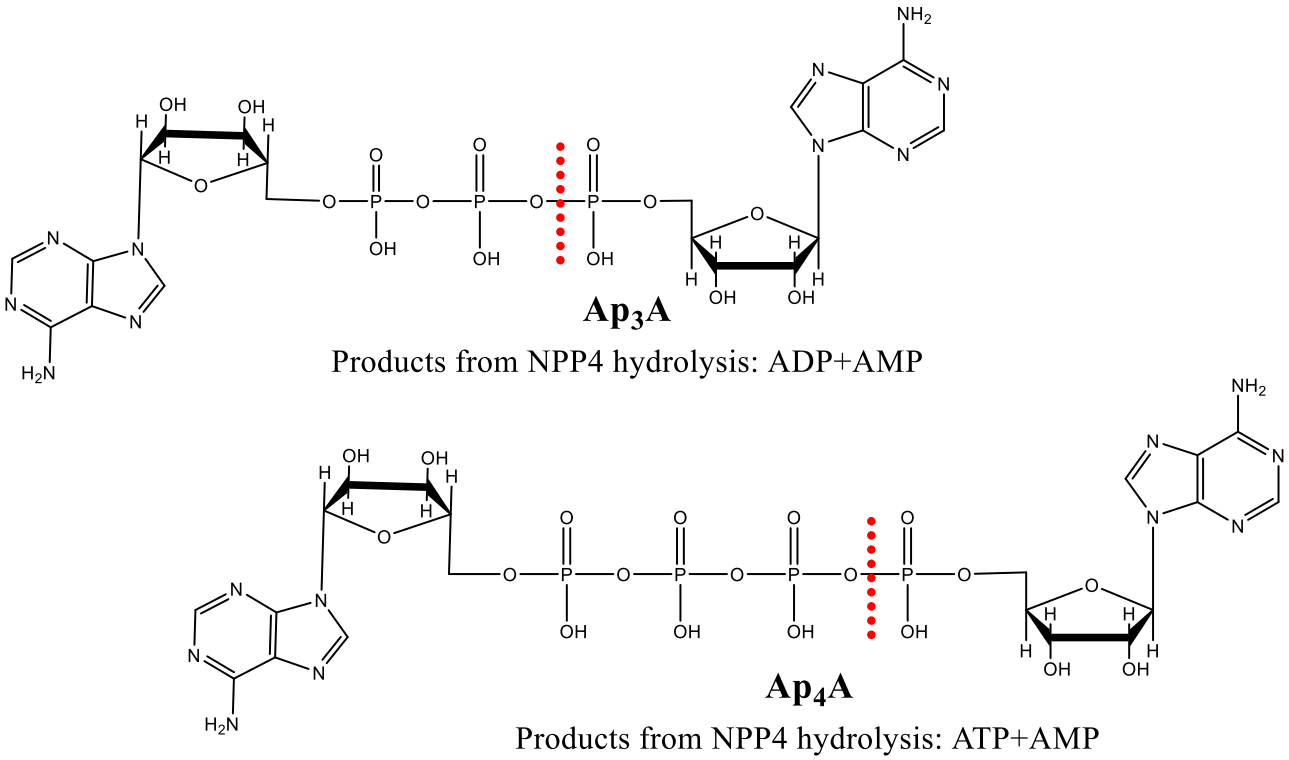

Fig. 11 Known physiological hNPP4 substrates. Red dots represent the cleaving site.

1.2.3 Pathological role of NPP4

The function of NPP4 was for many years unknown. In 2012, Albright *et al.* demonstrated its role as a procoagulant enzyme due to the hydrolysis of Ap_3A to ADP and AMP during the coagulation process. Between 1983-1989, Lüthje and Ogilvie discovered and described the presence of Ap_3A in human platelets for the first time [100], and elucidated its role in human platelet aggregation by liberation of ADP due to the action of a hydrolyzing glycoprotein that was neither stored in nor released by platelets, with optimum enzymatic activity at pH 8.5 to 9.0 and a divalent cation dependency [101,102]. Whereas a subset of the NPP family (NPP1-3) was previously reported to hydrolyze diadenosine polyphosphates, including Ap_3A and Ap_4A, to AMP and related products, their enzymatic activity implied that these isoforms may be candidates for intravascular diadenosine polyphosphate hydrolysis. A review of the literature indicated that NPP2, NPP4, and NPP5 have the strongest evidence for an intravascular location. In order to elucidate this role, Albright et al., expressed and purified soluble recombinant extracellular domains of human NPP2 and NPP4, characterized their enzymatic activities using the substrates Ap_3A and Ap_4A (also released by dense granules), and were able to confirm the intravascular location of NPP4 using immunofluorescence. Additionally, they used turbidimetric analysis to determine the effects of NPPs on PRP (platelet-rich plasma) aggregation directly. Their results revealed that NPP4 is a prothrombotic intravascular enzyme that stimulates platelet aggregation at the nascent thrombus location via continuous Ap_3A hydrolysis to ADP [23]. Thrombus formation, which is the final step in blood coagulation, also produces a first wave of the nucleotide ADP which in turn activates $P2Y_1$ and $P2Y_{12}$ receptors on thrombocytes whose function is to stop bleeding by clumping and clotting blood vessel. CD39 and NPP4 are present on endothelial cells. In fact, ADP is rapidly degraded to AMP by CD39, thereby limiting thrombus formation. In a second wave, while CD39 is saturated with the ADP produced from the first wave, Ap_3A is secreted and hydrolyzed to ADP and AMP by NPP4 which is associated to the surface of

endothelial cells, thus inducing prolonged platelet aggregation due to the production of ADP. The inhibition of the NPP4 activity would lead in reduced ADP production and less activation of the thrombocytes. Moreover, Ap_4A accumulation due to NPP4 inhibition may lead to a blockade of the prothrombotic $P2Y_1$ and $P2Y_{12}$ receptors thereby exerting anti-thrombotic effects, in addition to indirect inhibitory effects on $P2X_1$ receptor, another platelet-activating receptor [15–17]. Thus, NPP4 inhibitors may be useful as antithrombotic drugs.

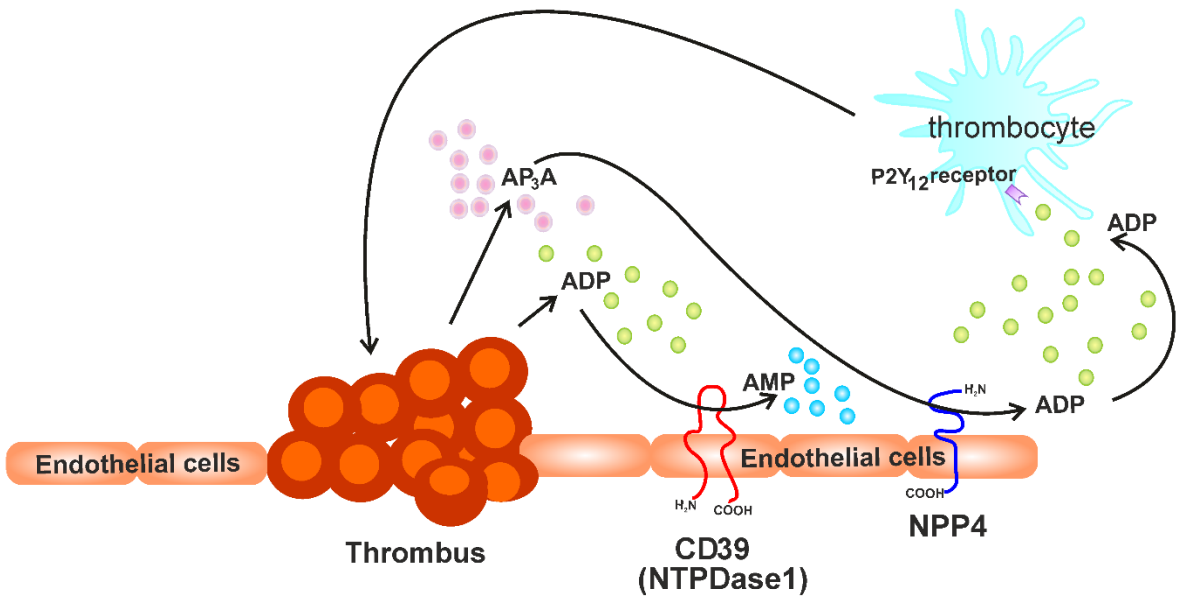

Fig. 12 Thrombocytes (platelets) are localized at the site of injury when a vascular injury occurs, such as a cholesterol plaque fracture. ADP and Ap_3A are secreted into the immediate area when platelets bind to subendothelial collagen. ADP is reduced in the thrombotic microenvironment by ectoenzymes (CD39) and soluble phosphohydrolases. Endothelial cell surface NPP4 metabolizes Ap_3A produced by platelets during the second wave of aggregation into ADP, raising ADP levels at the injury site. Prolonged low-level ADP release causes platelet activation, via $P2Y_{12}$ receptors and aggregation, culminating in a platelet clog on which additional hemostasias events occur to create a solid thrombus. Illustration created with CorelDraw.

1.2.4 NPP4 inhibitors

NPP4 is a member of the NPP family that only lately has attracted interest because its role has been unknown for a long time. Despite some mononucleotides like AMP, CMP and GMP which have been reported as extremely weak inhibitors of the enzymatic activity of NPP4 (IC_{50} ~ 130 μM for AMP, ~ 320 μM for CMP and 2110 μM for UTP) [22], no other NPP4 inhibitors are described in the literature. Novel compounds are described in Chapter 4 and 5 of this PhD dissertation.

References

1. G. Burnstock, Pathophysiology and therapeutic potential of purinergic signalling, *Pharmacol. Rev.* **2006**, *58*, 58–86, https://doi.org/10.1124/pr.58.1.5.
2. Abbracchio, M.P.; Burnstock, G.; Boeynaems, J.-M.; Barnard, E.A.; Boyer, J.L.; Kennedy, C.; Knight, G.E.; Fumagalli, M.; Gachet, C.; Jacobson, K.A.; et al. International union of pharmacology LVIII: update on the P2Y G protein-coupled nucleotide receptors: from molecular mechanisms and pathophysiology to therapy. *Pharmacol. Rev.* **2006**, *58*, 281–341, doi:10.1124/pr.58.3.3.
3. Coddou, C.; Yan, Z.; Obsil, T.; Pablo Huidobro-Toro, J.; Stojilkovic, S.S. Activation and regulation of purinergic P2X receptor channels. *Pharmacol. Rev.* **2011**, *63*, 641–683, doi:10.1124/pr.110.003129.
4. Antonioli, L.; Blandizzi, C.; Pacher, P.; Haskó, G. The purinergic system as a pharmacological target for the treatment of immune-mediated inflammatory diseases. *Pharmacol. Rev.* **2019**, *71*, 345–382, doi:10.1124/pr.117.014878.
5. Vitiello, L.; Gorini, S.; Rosano, G.; La Sala, A. Immunoregulation through extracellular nucleotides. *Blood* **2012**, *120*, 511–518, doi:10.1182/blood-2012-01-406496.
6. Zimmermann, H. History of ectonucleotidases and their role in purinergic signaling. *Biochem. Pharmacol.* **2021**, *187*, 114322, doi:10.1016/j.bcp.2020.114322.
7. Lee, S.-Y.; Müller, C.E. Nucleotide pyrophosphatase/phosphodiesterase 1 (NPP1) and its inhibitors. *MedChemComm* **2017**, *8*, 823–840, doi:10.1039/C7MD00015D.
8. Zimmermann, H.; Zebisch, M.; Sträter, N. Cellular function and molecular structure of ecto-nucleotidases. *Purinergic Signal.* **2012**, *8*, 437–502, doi:10.1007/s11302-012-9309-4.
9. Kukulski, F.; Lévesque, S.A.; Sévigny, J. *Impact of Ectoenzymes on P2 and P1 Receptor Signaling*; **2011**; Vol. 61; ISBN 9780123855268.
10. Rashida, M.; Iqbal, J. Inhibition of alkaline phosphatase: An emerging new drug target. *Mini-Reviews Med. Chem.* **2015**, *15*, 41–51, doi:10.2174/1389557515666150219113205.

11. Zimmermann, H.; Zebisch, M.; Sträter, N. Cellular function and molecular structure of ecto-nucleotidases. *Purinergic Signal.* **2012**, *8*, 437–502, doi:10.1007/s11302-012-9309-4.

12. Yegutkin, G.G. Enzymes involved in metabolism of extracellular nucleotides and nucleosides: functional implications and measurement of activities. *Crit. Rev. Biochem. Mol. Biol.* **2014**, *49*, 473–97, doi:10.3109/10409238.2014.953627.

13. Stefan, C.; Jansen, S.; Bollen, M. Modulation of purinergic signaling by NPP-type ectophosphodiesterases. *Purinergic Signal.* **2006**, *2*, 361–370, doi:10.1007/s11302-005-5303-4.

14. Evans, W.H.; Hood, D.O.; Gurd, J.W. Purification and properties of a mouse liver plasma-membrane glycoprotein hydrolysing nucleotide pyrophosphate and phosphodiester bonds. *Biochem. J.* **1973**, *135*, 819–826, doi:10.1042/bj1350819.

15. Jacobson, K.B.; Kaplan, N.O. Distribution of enzymes cleaving pyridine nucleotides in animal tissues. *J. Biophys. Biochem. Cytol.* **1957**, *3*, 31–43, doi:10.1083/jcb.3.1.31.

16. Takahashi, T.; Old, L.J.; Boyse, E.A. Surface alloantigens of plasma cells. *J. Exp. Med.* **1970**, *131*, 1325–1341, doi:10.1084/jem.131.6.1325.

17. Sali, Adnan; Favaloro, Joanne L; Terkeltaub, Robert; Goding, J.W. Germline deletion of the nucleoside triphosphate pyrophosphohydrolase (NTPPPH) plasma cell membrane glycoprotein (PC-1) produces abnormal calcification of periarticular tissues. *Ecto-ATPases Relat. ectonucleotidases* **2000**, 267–282.

18. Li, L.; Yin, Q.; Kuss, P.; Maliga, Z.; Millán, J.L.; Wu, H.; Mitchison, T.J. Hydrolysis of 2′3′-cGAMP by ENPP1 and design of nonhydrolyzable analogs. *Nat. Chem. Biol.* **2014**, *10*, 1043–1048, doi:10.1038/nchembio.1661.

19. Onyedibe, K.I.; Wang, M.; Sintim, H.O. ENPP1, an old enzyme with new functions, and small molecule inhibitors—A STING in the tale of ENPP1. *Molecules* **2019**, *24*, 4192, doi:10.3390/molecules24224192.

20. Stefan, C.; Jansen, S.; Bollen, M. NPP-type ectophosphodiesterases: unity in diversity. *Trends Biochem. Sci.* **2005**, *30*, 542–550, doi:10.1016/j.tibs.2005.08.005.

21. Gorelik, A.; Randriamihaja, A.; Illes, K.; Nagar, B. Structural basis for nucleotide recognition by the ectoenzyme CD203c. *FEBS J.* **2018**, *285*, 2481–2494, doi:10.1111/febs.14489.

22. Albright, R.A.; Ornstein, D.L.; Cao, W.; Chang, W.C.; Robert, D.; Tehan, M.; Hoyer, D.; Liu, L.; Stabach, P.; Yang, G.; et al. Molecular basis of purinergic signal metabolism by ectonucleotide pyrophosphatase/phosphodiesterases 4 and 1 and implications in stroke. *J. Biol. Chem.* **2014**, *289*, 3294–3306, doi:10.1074/jbc.M113.505867.

23. Albright, R.A.; Chang, W.C.; Robert, D.; Ornstein, D.L.; Cao, W.; Liu, L.; Redick, M.E.; Young, J.I.; De La Cruz, E.M.; Braddock, D.T. NPP4 is a procoagulant enzyme on the surface of vascular endothelium. *Blood* **2012**, *120*, 4432–4440, doi:10.1182/blood-2012-04-425215.

24. Lopez, V.; Lee, S.-Y.; Stephan, H.; Müller, C.E. Recombinant expression of ecto-nucleotide pyrophosphatase/phosphodiesterase 4 (NPP4) and development of a luminescence-based assay to identify inhibitors. *Anal. Biochem.* **2020**, *603*, 113774, doi:10.1016/j.ab.2020.113774.

25. Gorelik, A.; Randriamihaja, A.; Illes, K.; Nagar, B. A key tyrosine substitution restricts nucleotide hydrolysis by the ectoenzyme NPP5. *FEBS J.* **2017**, *284*, 3718–3726, doi:10.1111/febs.14266.

26. Sakagami, H.; Aoki, J.; Natori, Y.; Nishikawa, K.; Kakehi, Y.; Natori, Y.; Arai, H. Biochemical and molecular characterization of a novel choline-specific glycerophosphodiester phosphodiesterase

belonging to the nucleotide pyrophosphatase/phosphodiesterase family. *J. Biol. Chem.* **2005**, *280*, 23084–93, doi:10.1074/jbc.M413438200.

27. Duan, R.-D.; Cheng, Y.; Hansen, G.; Hertervig, E.; Liu, J.-J.; Syk, I.; Sjostrom, H.; Nilsson, A. Purification, localization, and expression of human intestinal alkaline sphingomyelinase. *J. Lipid Res.* **2003**, *44*, 1241–50, doi:10.1194/jlr.M300037-JLR200.

28. Duan, R.-D.; Bergman, T.; Xu, N.; Wu, J.; Cheng, Y.; Duan, J.; Nelander, S.; Palmberg, C.; Nilsson, A. Identification of human intestinal alkaline sphingomyelinase as a novel ecto-enzyme related to the nucleotide phosphodiesterase family. *J. Biol. Chem.* **2003**, *278*, 38528–36, doi:10.1074/jbc.M305437200.

29. Von Kügelgen, I. Pharmacology of P2Y receptors. *Brain Res. Bull.* **2019**, *151*, 12–24, doi:10.1016/j.brainresbull.2019.03.010.

30. Mutafova-Yambolieva, V.N.; Durnin, L. The purinergic neurotransmitter revisited: A single substance or multiple players? *Pharmacol. Ther.* **2014**, *144*, 162–191, doi:10.1016/j.pharmthera.2014.05.012.

31. Koch-Nolte, F.; Adriouch, S.; Bannas, P.; Krebs, C.; Scheuplein, F.; Seman, M.; Haag, F. ADP-ribosylation of membrane proteins: Unveiling the secrets of a crucial regulatory mechanism in mammalian cells. *Ann. Med.* **2006**, *38*, 188–199, doi:10.1080/07853890600655499.

32. Jansen, S.; Perrakis, A.; Ulens, C.; Winkler, C.; Andries, M.; Joosten, R.P.; Van Acker, M.; Luyten, F.P.; Moolenaar, W.H.; Bollen, M. Structure of npp1, an ectonucleotide pyrophosphatase/phosphodiesterase involved in tissue calcification. *Structure* **2012**, *20*, 1948–1959, doi:10.1016/j.str.2012.09.001.

33. Kato, K.; Nishimasu, H.; Okudaira, S.; Mihara, E.; Ishitani, R.; Takagi, J.; Aoki, J.; Nureki, O. Crystal structure of Enpp1, an extracellular glycoprotein involved in bone mineralization and insulin signaling. *Proc. Natl. Acad. Sci.* **2012**, *109*, 16876–16881, doi:10.1073/pnas.1208017109.

34. Dennis, M.L.; Newman, J.; Dolezal, O.; Hattarki, M.; Surjadi, R.N.; Nuttall, S.D.; Pham, T.; Nebl, T.; Camerino, M.; Khoo, P.S.; et al. Crystal structures of human ENPP1 in apo and bound forms. *Acta Crystallogr. Sect. D, Struct. Biol.* **2020**, *76*, 889–898, doi:10.1107/S2059798320010505.

35. Kato, K.; Nishimasu, H.; Oikawa, D.; Hirano, S.; Hirano, H.; Kasuya, G.; Ishitani, R.; Tokunaga, F.; Nureki, O. Structural insights into cGAMP degradation by Ecto-nucleotide pyrophosphatase phosphodiesterase 1. *Nat. Commun.* **2018**, *9*, 4424, doi:10.1038/s41467-018-06922-7.

36. Döhler, C.; Zebisch, M.; Sträter, N. Crystal structure and substrate binding mode of ectonucleotide phosphodiesterase/pyrophosphatase-3 (NPP3). *Sci. Rep.* **2018**, *8*, 10874, doi:10.1038/s41598-018-28814-y.

37. Takahashi, T.; Old, L.J.; McIntire, K.R.; Boyse, E.A. Immunoglobulin and other surface antigens of cells of the immune system. *J. Exp. Med.* **1971**, *134*, 815–832, doi:10.1084/jem.134.4.815.

38. Seman, M.; Adriouch, S.; Scheuplein, F.; Krebs, C.; Freese, D.; Glowacki, G.; Deterre, P.; Haag, F.; Koch-Nolte, F. NAD-Induced T Cell Death. *Immunity* **2003**, *19*, 571–582, doi:10.1016/S1074-7613(03)00266-8.

39. Cimpean, A.; Stefan, C.; Gijsbers, R.; Stalmans, W.; Bollen, M. Substrate-specifying determinants of the nucleotide pyrophosphatases/phosphodiesterases NPP1 and NPP2. *Biochem. J.* **2004**, *381*, 71–77, doi:10.1042/BJ20040465.

40. Mackenzie, N.C.W.; Huesa, C.; Rutsch, F.; MacRae, V.E. New insights into NPP1 function: Lessons from clinical and animal studies. *Bone* **2012**, *51*, 961–968, doi:10.1016/j.bone.2012.07.014.

41. A R Harahap, J.W.G. Distribution of the murine plasma cell antigen PC-1 in non-lymphoid tissues. *J. Immunol.* **1988**, *141*, 2317–2320.

42. Piao-Jin Hua, James W Goding, Hajime Nakamura, K.S. Molecular cloning and chromosomal localization of PD-1beta (PNDP3), a new member of the human phosphodiesterase I genes. *Genomics* **1997**, 412–415.

43. Goldfine, I.D.; Maddux, B.A.; Youngren, J.F.; Reaven, G.; Accili, D.; Trischitta, V.; Vigneri, R.; Frittitta, L. The role of membrane glycoprotein plasma cell antigen 1/ectonucleotide pyrophosphatase phosphodiesterase 1 in the pathogenesis of insulin resistance and related abnormalities. *Endocr. Rev.* **2008**, *29*, 62–75, doi:10.1210/er.2007-0004.

44. RAZZELL, W.E. Tissue and intracellular distribution of two phosphodiesterases. *J. Biol. Chem.* **1961**, *236*, 3028–30.

45. Morley, D.J.; Hawley, D.M.; Ulbright, T.M.; Butler, L.G.; Culp, J.S.; Hodes, M.E. Distribution of phosphodiesterase I in normal human tissues. *J. Histochem. Cytochem.* **1987**, *35*, 75–82, doi:10.1177/35.1.3025290.

46. Frittitta, L.; Camastra, S.; Baratta, R.; Costanzo, B. V; D'Adamo, M.; Graci, S.; Spampinato, D.; Maddux, B. A.; Vigneri, R.; Ferrannini, E.; Trischitta, V.A. A. Soluble PC-1 circulates in human plasma: relationship with insulin resistance and associated abnormalities. *J. Clin. Endocrinol. Metab* **1999**, *84*, 3620– 3625.

47. Belli, S.I.; Goding, J.W. Biochemical characterization of human pc-1, an enzyme possessing alkaline phosphodiesterase i and nucleotide pyrophosphatase activities. *Eur. J. Biochem.* **1994**, *226*, 433–443, doi:10.1111/j.1432-1033.1994.tb20068.x.

48. Hosoda, N.; Hoshino, S.; Kanda, Y.; Katada, T. Inhibition of phosphodiesterase/pyrophosphatase activity of PC-1 by its association with glycosaminoglycans. *Eur. J. Biochem.* **1999**, *265*, 763–770, doi:10.1046/j.1432-1327.1999.00779.x.

49. Jansen, S.; Perrakis, A.; Ulens, C.; Winkler, C.; Andries, M.; Joosten, R.P.; Van Acker, M.; Luyten, F.P.; Moolenaar, W.H.; Bollen, M. Structure of NPP1, an ectonucleotide pyrophosphatase/phosphodiesterase involved in tissue calcification. *Structure* **2012**, *20*, 1948–59, doi:10.1016/j.str.2012.09.001.

50. Funakoshi, I.; Kato, H.; Horie, K.; Yano, T.; Hori, Y.; Kobayashi, H.; Inoue, T.; Suzuki, H.; Fukui, S.; Tsukahara, M.; et al. Molecular cloning of cDNAs for human fibroblast nucleotide pyrophosphatase. *Arch. Biochem. Biophys.* **1992**, *295*, 180–187, doi:10.1016/0003-9861(92)90504-P.

51. Aerts, I.; Martin, J.-J.; Deyn, P.P. De; Van Ginniken, C.; Van Ostade, X.; Kockx, M.; Dua, G.; Slegers, H. The expression of ecto-nucleotide pyrophosphatase/phosphodiesterase 1 (E-NPP1) is correlated with astrocytic tumor grade. *Clin. Neurol. Neurosurg.* **2011**, *113*, 224–229, doi:10.1016/j.clineuro.2010.11.018.

52. Heldin, C.; Wasteson, A.; Fryklund, L.; Westermark, B. Somatomedin B: mitogenic activity derived from contaminant epidermal growth factor. *Science.* **1981**, *213*, 1122–1123, doi:10.1126/science.6973821.

53. Abate, N.; Chandalia, M.; Di Paola, R.; Foster, D.W.; Grundy, S.M.; Trischitta, V. Mechanisms of Disease: ectonucleotide pyrophosphatase phosphodiesterase 1 as a "gatekeeper" of insulin receptors. *Nat. Clin. Pract. Endocrinol. Metab.* **2006**, *2*, 694–701, doi:10.1038/ncpendmet0367.

54. Zalatan, J.G.; Fenn, T.D.; Brunger, A.T.; Herschlag, D. Structural and functional comparisons of nucleotide pyrophosphatase/phosphodiesterase and alkaline phosphatase: implications for mechanism and evolution. *Biochemistry* **2006**, *45*, 9788–9803, doi:10.1021/bi060847t.

55. Gijsbers, R.; Ceulemans, H.; Stalmans, W.; Bollen, M. Structural and catalytic similarities between nucleotide pyrophosphatases/phosphodiesterases and alkaline phosphatases. *J. Biol. Chem.* **2001**, *276*, 1361–8, doi:10.1074/jbc.M007552200.

56. Petersen, C.B.; Nygård, A.-B.; Viuff, B.; Fredholm, M.; Aasted, B.; Salomonsen, J. Porcine ecto-nucleotide pyrophosphatase/phosphodiesterase 1 (NPP1/CD203a): Cloning, transcription, expression, mapping, and identification of an NPP1/CD203a epitope for swine workshop cluster 9 (SWC9) monoclonal antibodies. *Dev. Comp. Immunol.* **2007**, *31*, 618–631, doi:10.1016/j.dci.2006.08.012.

57. Johnson, K.; Moffa, A.; Chen, Y.; Pritzker, K.; Goding, J.; Terkeltaub, R. Matrix vesicle plasma cell membrane glycoprotein-1 regulates mineralization by murine osteoblastic MC3T3 cells. *J. Bone Miner. Res.* **1999**, *14*, 883–892, doi:10.1359/jbmr.1999.14.6.883.

58. Bollen, M.; Gijsbers, R.; Ceulemans, H.; Stalmans, W.; Stefan, C. Nucleotide pyrophosphatases/phosphodiesterases on the move. *Crit. Rev. Biochem. Mol. Biol.* **2000**, *35*, 393–432, doi:10.1080/10409230091169249.

59. Stefan, C.; Gijsbers, R.; Stalmans, W.; Bollen, M. Differential regulation of the expression of nucleotide pyrophosphatases/phosphodiesterases in rat liver. *Biochim. Biophys. Acta - Mol. Cell Res.* **1999**, *1450*, 45–52, doi:10.1016/S0167-4889(99)00031-2.

60. Vollmayer, P.; Clair, T.; Goding, J.W.; Sano, K.; Servos, J.; Zimmermann, H. Hydrolysis of diadenosine polyphosphates by nucleotide pyrophosphatases/phosphodiesterases. *Eur. J. Biochem.* **2003**, *270*, 2971–8, doi:10.1046/j.1432-1033.2003.03674.x.

61. Namasivayam, V.; Lee, S.-Y.; Müller, C.E. The promiscuous ectonucleotidase NPP1: molecular insights into substrate binding and hydrolysis. *Biochim. Biophys. Acta - Gen. Subj.* **2017**, *1861*, 603–614, doi:10.1016/j.bbagen.2016.12.019.

62. Liu, M.; Wang, X.; Wang, L.; Ma, X.; Gong, Z.; Zhang, S.; Li, Y. Targeting the IDO1 pathway in cancer: from bench to bedside. *J. Hematol. Oncol.* **2018**, *11*, 100, doi:10.1186/s13045-018-0644-y.

63. Lemos, H.; Huang, L.; McGaha, T.L.; Mellor, A.L. Cytosolic DNA sensing via the stimulator of interferon genes adaptor: Yin and Yang of immune responses to DNA. *Eur. J. Immunol.* **2014**, *44*, 2847–2853, doi:10.1002/eji.201344407.

64. Lemos, H.; Mohamed, E.; Huang, L.; Ou, R.; Pacholczyk, G.; Arbab, A.S.; Munn, D.; Mellor, A.L. STING promotes the growth of tumors characterized by low antigenicity via ido activation. *Cancer Res.* **2016**, *76*, 2076–2081, doi:10.1158/0008-5472.CAN-15-1456.

65. Corrales, L.; McWhirter, S.M.; Dubensky, T.W.; Gajewski, T.F. The host STING pathway at the interface of cancer and immunity. *J. Clin. Invest.* **2016**, *126*, 2404–2411, doi:10.1172/JCI86892.

66. Huang, L.; Li, L.; Lemos, H.; Chandler, P.R.; Pacholczyk, G.; Baban, B.; Barber, G.N.; Hayakawa, Y.; McGaha, T.L.; Ravishankar, B.; et al. Cutting Edge: DNA Sensing via the STING adaptor in myeloid dendritic cells induces potent tolerogenic responses. *J. Immunol.* **2013**, *191*, 3509–3513, doi:10.4049/jimmunol.1301419.

67. Rao, S.R.; Snaith, A.E.; Marino, D.; Cheng, X.; Lwin, S.T.; Orriss, I.R.; Hamdy, F.C.; Edwards, C.M. Tumour-derived alkaline phosphatase regulates tumour growth, epithelial plasticity and disease-free survival in metastatic prostate cancer. *Br. J. Cancer* **2017**, *116*, 227–236, doi:10.1038/bjc.2016.402.

68. Allard, B.; Longhi, M.S.; Robson, S.C.; Stagg, J. The ectonucleotidases CD39 and CD73: Novel checkpoint inhibitor targets. *Immunol. Rev.* **2017**, *276*, 121–144, doi:10.1111/imr.12528.

69. De Lourdes Mora-García, M.; García-Rocha, R.; Morales-Ramírez, O.; Montesinos, J.J.; Weiss-

Steider, B.; Hernández-Montes, J.; Ávila-Ibarra, L.R.; Don-López, C.A.; Velasco-Velázquez, M.A.; Gutiérrez-Serrano, V.; et al. Mesenchymal stromal cells derived from cervical cancer produce high amounts of adenosine to suppress cytotoxic T lymphocyte functions. *J. Transl. Med.* **2016**, *14*, 302, doi:10.1186/s12967-016-1057-8.

70. Vigano, S.; Alatzoglou, D.; Irving, M.; Ménétrier-Caux, C.; Caux, C.; Romero, P.; Coukos, G. Targeting adenosine in cancer immunotherapy to enhance t-cell function. *Front. Immunol.* **2019**, *10*, doi:10.3389/fimmu.2019.00925.

71. Montalbán del Barrio, I.; Penski, C.; Schlahsa, L.; Stein, R.G.; Diessner, J.; Wöckel, A.; Dietl, J.; Lutz, M.B.; Mittelbronn, M.; Wischhusen, J.; et al. Adenosine-generating ovarian cancer cells attract myeloid cells which differentiate into adenosine-generating tumor associated macrophages – a self-amplifying, CD39- and CD73-dependent mechanism for tumor immune escape. *J. Immunother. Cancer* **2016**, *4*, 49, doi:10.1186/s40425-016-0154-9.

72. García-Rocha, R.; Moreno-Lafont, M.; Mora-García, M.L.; Weiss-Steider, B.; Montesinos, J.J.; Piña-Sánchez, P.; Monroy-García, A. Mesenchymal stromal cells derived from cervical cancer tumors induce TGF-β1 expression and IL-10 expression and secretion in the cervical cancer cells, resulting in protection from cytotoxic T cell activity. *Cytokine* **2015**, *76*, 382–390, doi:10.1016/j.cyto.2015.09.001.

73. Horenstein, A.L.; Chillemi, A.; Zaccarello, G.; Bruzzone, S.; Quarona, V.; Zito, A.; Serra, S.; Malavasi, F. A CD38/CD203a/CD73 ectoenzymatic pathway independent of CD39 drives a novel adenosinergic loop in human T lymphocytes. *Oncoimmunology* **2013**, *2*, e26246, doi:10.4161/onci.26246.

74. Lau, W.M.; Doucet, M.; Stadel, R.; Huang, D.; Weber, K.L.; Kominsky, S.L. Enpp1: a potential facilitator of breast cancer bone metastasis. *PLoS One* **2013**, *8*, 666-752, doi:10.1371/journal.pone.0066752.

75. Stagg, J.; Divisekera, U.; Duret, H.; Sparwasser, T.; Teng, M.W.L.; Darcy, P.K.; Smyth, M.J. CD73-deficient mice have increased antitumor immunity and are resistant to experimental metastasis. *Cancer Res.* **2011**, *71*, 2892–2900, doi:10.1158/0008-5472.CAN-10-4246.

76. Stagg, J.; Beavis, P.A.; Divisekera, U.; Liu, M.C.P.; Möller, A.; Darcy, P.K.; Smyth, M.J. CD73-deficient mice are resistant to carcinogenesis. *Cancer Res.* **2012**, *72*, 2190–2196, doi:10.1158/0008-5472.CAN-12-0420.

77. Nam, H.K.; Liu, J.; Li, Y.; Kragor, A.; Hatch, N.E. Ectonucleotide pyrophosphatase/phosphodiesterase-1 (enpp1) protein regulates osteoblast differentiation. *J. Biol. Chem.* **2011**, *286*, 39059–39071, doi:10.1074/jbc.M111.221689.

78. Nitschke, Y.; Weissen-Plenz, G.; Terkeltaub, R.; Rutsch, F. Npp1 promotes atherosclerosis in ApoE knockout mice. *J. Cell. Mol. Med.* **2011**, *15*, 2273–2283, doi:10.1111/j.1582-4934.2011.01327.x.

79. Mackenzie, N.C.W.; Zhu, D.; Milne, E.M.; van 't Hof, R.; Martin, A.; Quarles, D.L.; Millán, J.L.; Farquharson, C.; MacRae, V.E. Altered bone development and an increase in fgf-23 expression in Enpp1−/− Mice. *PLoS One* **2012**, *7*, e32177, doi:10.1371/journal.pone.0032177.

80. Grupe, A.; Alleman, J.; Goldfine, I.D.; Sadick, M.; Stewart, T.A. Inhibition of insulin receptor phosphorylation by PC-1 is not mediated by the hydrolysis of adenosine triphosphate or the generation of adenosine. *J. Biol. Chem.* **1995**, *270*, 22085–8, doi:10.1074/jbc.270.38.22085.

81. Maddux, B.A.; Chang, Y.-N.; Accili, D.; McGuinness, O.P.; Youngren, J.F.; Goldfine, I.D. Overexpression of the insulin receptor inhibitor PC-1/ENPP1 induces insulin resistance and hyperglycemia. *Am. J. Physiol. Metab.* **2006**, *290*, 746–749, doi:10.1152/ajpendo.00298.2005.

82. Lee, J.; Pilch, P.F. The insulin receptor: structure, function, and signaling. *Am. J. Physiol.* **1994**, *266*, C319-34, doi:10.1152/ajpcell.1994.266.2.C319.

83. McAteer, J.B.; Prudente, S.; Bacci, S.; Lyon, H.N.; Hirschhorn, J.N.; Trischitta, V.; Florez, J.C.; ENPP1 Consortium The ENPP1 K121Q polymorphism is associated with type 2 diabetes in European populations: evidence from an updated meta-analysis in 42,042 subjects. *Diabetes* **2008**, *57*, 1125–30, doi:10.2337/db07-1336.

84. Grobben, B.; De Deyn, P.P.; Slegers, H. Rat C6 glioma as experimental model system for the study of glioblastoma growth and invasion. *Cell Tissue Res.* **2002**, *310*, 257–70, doi:10.1007/s00441-002-0651-7.

85. Gómez-Villafuertes, R.; Pintor, J.; Miras-Portugal, M.T.; Gualix, J. Ectonucleotide pyrophosphatase/phosphodiesterase activity in Neuro-2a neuroblastoma cells: changes in expression associated with neuronal differentiation. *J. Neurochem.* **2014**, *131*, 290–302, doi:10.1111/jnc.12794.

86. Bageritz, J.; Puccio, L.; Piro, R.M.; Hovestadt, V.; Phillips, E.; Pankert, T.; Lohr, J.; Herold-Mende, C.; Lichter, P.; Goidts, V. Stem cell characteristics in glioblastoma are maintained by the ecto-nucleotidase E-NPP1. *Cell Death Differ.* **2014**, *21*, 929–940, doi:10.1038/cdd.2014.12.

87. González-Sánchez, J.L.; Martínez-Larrad, M.T.; Fernández-Pérez, C.; Kubaszek, A.; Laakso, M.; Serrano-Ríos, M. K121Q PC-1 gene polymorphism is not associated with insulin resistance in a spanish population. *Obes. Res.* **2003**, *11*, 603–605, doi:10.1038/oby.2003.86.

88. Iqbal, J.; Lévesque, S.A.; Sévigny, J.; Müller, C.E. A highly sensitive CE-UV method with dynamic coating of silica-fused capillaries for monitoring of nucleotide pyrophosphatase/ phosphodiesterase reactions. *Electrophoresis* **2008**, *29*, 3685–3693, doi:10.1002/elps.200800013.

89. Forcellini, E.; Boutin, S.; Lefebvre, C.A.; Shayhidin, E.E.; Boulanger, M.C.; Rhéaume, G.; Barbeau, X.; Lagüe, P.; Mathieu, P.; Paquin, J.F. Synthesis and biological evaluation of novel quinazoline-4-piperidinesulfamide derivatives as inhibitors of NPP1. *Eur. J. Med. Chem.* **2018**, *147*, 130–149, doi:10.1016/j.ejmech.2018.01.094.

90. Lee, S.Y.; Fiene, A.; Li, W.; Hanck, T.; Brylev, K.A.; Fedorov, V.E.; Lecka, J.; Haider, A.; Pietzsch, H.J.; Zimmermann, H.; et al. Polyoxometalates - Potent and selective ecto-nucleotidase inhibitors. *Biochem. Pharmacol.* **2015**, *93*, 171–181, doi:10.1016/j.bcp.2014.11.002.

91. Lopez, V.; Schäkel, L.; Schuh, H.J.M.; Schmidt, M.S.; Mirza, S.; Renn, C.; Pelletier, J.; Lee, S.-Y.; Sévigny, J.; Alban, S.; et al. Sulfated polysaccharides from macroalgae are potent dual inhibitors of human ATP-hydrolyzing ectonucleotidases NPP1 and CD39. *Mar. Drugs* **2021**, *19*, 51, doi:10.3390/md19020051.

92. Lévesque, S.A.; Lavoie, É.G.; Lecka, J.; Bigonnesse, F.; Sévigny, J. Specificity of the ecto-ATPase inhibitor ARL 67156 on human and mouse ectonucleotidases. *Br. J. Pharmacol.* **2007**, *152*, 141–150, doi:10.1038/sj.bjp.0707361.

93. Nassir, M.; Arad, U.; Lee, S.Y.; Journo, S.; Mirza, S.; Renn, C.; Zimmermann, H.; Pelletier, J.; Sévigny, J.; Müller, C.E.; et al. Identification of adenine-N9-(methoxy)ethyl-β-bisphosphonate as NPP1 inhibitor attenuates NPPase activity in human osteoarthritic chondrocytes. *Purinergic Signal.* **2019**, *15*, 247–263, doi:10.1007/s11302-019-09649-2.

94. Zelikman, V.; Pelletier, J.; Simhaev, L.; Sela, A.; Gendron, F.P.; Arguin, G.; Senderowitz, H.; Sévigny, J.; Fischer, B. Highly selective and potent ectonucleotide pyrophosphatase-1 (NPP1) inhibitors based on uridine 5′-P α,α -dithiophosphate analogues. *J. Med. Chem.* **2018**, *61*, 3939–3951, doi:10.1021/acs.jmedchem.7b01906.

95. Nassir, M.; Pelletier, J.; Arad, U.; Arguin, G.; Khazanov, N.; Gendron, F.P.; Sévigny, J.; Senderowitz, H.; Fischer, B. Structure-activity relationship study of NPP1 inhibitors based on uracil-N1-(methoxy)ethyl-β-phosphate scaffold. *Eur. J. Med. Chem.* **2019**, *184*, 111754, doi:10.1016/j.ejmech.2019.111754.

96. Lee, S.Y.; Müller, C.E. Large-volume sample stacking with polarity switching for monitoring of nucleotide pyrophosphatase/phosphodiesterase 1 (NPP1) reactions by capillary electrophoresis. *Electrophoresis* **2014**, *35*, 855–863, doi:10.1002/elps.201300453.

97. Eliahu, S.; Lecka, J.; Reiser, G.; Haas, M.; Bigonnesse, F.; Lévesque, S.A.; Pelletier, J.; Sévigny, J.; Fischer, B. Diadenosine 5′,5′-(Boranated)polyphosphonate analogues as selective nucleotide pyrophosphatase/phosphodiesterase inhibitors ⊥. *J. Med. Chem.* **2010**, *53*, 8485–8497, doi:10.1021/jm100597c.

98. Carozza, J.A.; Brown, J.A.; Böhnert, V.; Fernandez, D.; AlSaif, Y.; Mardjuki, R.E.; Smith, M.; Li, L. Structure-Aided Development of Small-Molecule Inhibitors of ENPP1, the Extracellular Phosphodiesterase of the Immunotransmitter cGAMP. *Cell Chem. Biol.* **2020**, *27*, 1347-1358.e5, doi:10.1016/j.chembiol.2020.07.007.

99. Ullah, S.; El-Gamal, M.I.; El-Gamal, R.; Pelletier, J.; Sévigny, J.; Shehata, M.K.; Anbar, H.S.; Iqbal, J. Synthesis, biological evaluation, and docking studies of novel pyrrolo[2,3-b]pyridine derivatives as both ectonucleotide pyrophosphatase/phosphodiesterase inhibitors and antiproliferative agents. *Eur. J. Med. Chem.* **2021**, *217*, 113339, doi:10.1016/j.ejmech.2021.113339.

100. Lüthje, J.; Ogilvie, A. The presence of diadenosine 5′,5‴-P 1 ,P 3 -triphosphate (Ap3A) in human platelets. *Biochem. Biophys. Res. Commun.* **1983**, *115*, 253–260, doi:10.1016/0006-291X(83)90997-X.

101. Lüthje, J.; Ogilvie, A. Diadenosine triphosphate (Ap3A) mediates human platelet aggregation by liberation of ADP. *Biochem. Biophys. Res. Commun.* **1984**, *118*, 704–709, doi:10.1016/0006-291X(84)91451-7.

102. Lüthje, J.; Ogilvie, A. Catabolism of Ap3A and Ap4A in human plasma: Purification and characterization of a glycoprotein complex with 5′-nucleotide phosphodiesterase activity. *Eur. J. Biochem.* **1985**, *149*, 119–127, doi:10.1111/j.1432-1033.1985.tb08901.x.

103. Gangar, M.; Goyal, S.; Raykar, D.; Khurana, P.; Martis, A.M.; Goswami, A.; Ghoshal, I.; Patel, K. V.; Nagare, Y.; Raikar, S.; et al. Design, Synthesis and Biological evaluation studies of Novel Small Molecule ENPP1 Inhibitors for Cancer Immunotherapy. Bioorg. Chem. 2021, 119, 105549, doi:10.1016/j.bioorg.2021.105549.

2. Sulfated Polysaccharides from Macroalgae Are Potent Dual Inhibitors of Human ATP-Hydrolyzing Ectonucleotidases NPP1 and CD39

2.1 Introduction

In recent years there has been a surge of interest in finding and developing ectonucleotidase inhibitors, antibodies, and small compounds as potential cancer immunotherapeutics. Among the NPPs and NTPDases, hNPP1 and hCD9 are the most promising drug targets. Sulfated polysaccharides derived from sea algae, fucoidans found in brown algae, such as *Sargassum polycystum* [1], have been shown to exhibit anticancer activity *in vitro* and *in vivo* [2–5]. These natural compounds have been demonstrated to directly suppress cell development, for example by triggering apoptosis, as well as to engage the immune system in its fight against cancer [6–8]. Their molecular modes of action are currently unknown, as well as their molecular targets [6–8]. This motivated us to investigate the inhibitory effects of sulfated polysaccharides from red and brown algae that are negatively charged, similar to previously known ectonucleotidase inhibitors. In the following publication we describe our findings on the modulation of hNPP1 and hCD39 activity by sulfated polysaccharides.

References

1. Fernando, I.P.S.; Sanjeewa, K.K.A.; Lee, H.G.; Kim, H.S.; Vaas, A.P.J.P.; De Silva, H.I.C.; Nanayakkara, C.M.; Abeytunga, D.T.U,M Lee, D.S.; Lee, J.S.; Jeon, Y.J. Fucoidan purified from *Sargassum polycystum* induces apoptosis through mitochondria-mediated pathway in HL-60 and MCF-7 cells. *Mar. Drugs* **2020**, 18, 196, Doi: 10.3390/md18040196.
2. Oliveira, C.; Neves, N.M.; Reis, R.L.; Martins, A.; Silva, T.H. A review on fucoidan antitumor strategies: From a biological active agent to a structural component of fucoidan-based systems. *Carbohydr. Polym.* **2020** 239, 116131, doi: 10.1016/j.carbpol.2020.116131. Epub 2020 Mar 9.

3. Peñalver, R.; Lorenzo, J.M.; Ros, G.; Amarowicz, R.; Pateiro, M.; Nieto, G. Seaweeds as a functional ingredient for a healthy diet. *Mar. Drugs* **2020**, 18, 301, doi: 10.3390/md18060301.

4. Bittkau, K.S.; Dörschmann, P.; Blümel, M; Tasdemir, D.; Roider, J.; Klettner, A.; Alban, S. Comparison of the effects of fucoidans on the cell viability of tumor and non-tumor cell lines. *Mar. Drugs* **2019**, 17, 441, doi: 10.3390/md17080441.

5. Martínez Andrade, K.A.; Lauritano, C.; Romano, G.; Ianora, A. Marine microalgae with anti-cancer properties. *Mar. Drugs* **2018**, 16, 165; doi: 10.3390/md16050165.

6. van Weelden, G.; Bobiński, M.; Okła, K.; van Weelden, W.J.; Romano, A.; Pijnenborg, J.M.A. Fucoidan structure and activity in relation to anti-cancer mechanisms. *Mar. Drugs* **2019**, 17,32, doi: 10.3390/md17010032.

7. Kiddane, A.T.; Kim, G.D. Anticancer and immunomodulatory effects of polysaccharides. *Nutr. Cancer* **2020**, doi: 10.1080/01635581.2020.1861310.

8. Lin, Y.; Qi, X.; Liu, H.; Xue, K.; Xu, S.; Tian, Z. The anti-cancer effects of fucoidan: a review of both in vivo and in vitro investigations. Cancer Cell Int. **2020**, 20,154, doi: 10.1186/s12935-020-01233-8.

2.2 Publication

marine drugs

MDPI

Article

Sulfated Polysaccharides from Macroalgae Are Potent Dual Inhibitors of Human ATP-Hydrolyzing Ectonucleotidases NPP1 and CD39

Vittoria Lopez [1,2], Laura Schäkel [1,2], H. J. Maximilian Schuh [3], Michael S. Schmidt [3], Salahuddin Mirza [1,2], Christian Renn [1,2], Julie Pelletier [4], Sang-Yong Lee [1,2], Jean Sévigny [4,5], Susanne Alban [6], Gerd Bendas [3] and Christa E. Müller [1,2,*]

1 Pharmaceutical & Medicinal Chemistry, Pharmaceutical Institute, University of Bonn, An der Immenburg 4, 53121 Bonn, Germany; vlopez@uni-bonn.de (V.L.); laura.schaekel@uni-bonn.de (L.S.); salahuddinmirza@gmail.com (S.M.); christian.renn@posteo.de (C.R.); s6saleee@uni-bonn.de (S.-Y.L.)
2 PharmaCenter Bonn, University of Bonn, An der Immenburg 4, 53121 Bonn, Germany
3 Pharmaceutical & Cell Biological Chemistry, Pharmaceutical Institute, University of Bonn, An der Immenburg 4, 53121 Bonn, Germany; maxschuh@uni-bonn.de (H.J.M.S.); michael.sebastian.schmidt@uni-bonn.de (M.S.S.); gbendas@uni-bonn.de (G.B.)
4 Centre de Recherche du CHU de Québec—Université Laval, Québec City, QC G1V 4G2, Canada; julie.pelletier@crchudequebec.ulaval.ca (J.P.); jean.Sevigny@crchudequebec.ulaval.ca (J.S.)
5 Départment de Microbiologie-Infectiologie et d'Immunologie, Faculté de Médecine, Université Laval, Quebec City, QC G1V 0A6, Canada
6 Pharmaceutical Institute, Christian-Albrechts-University of Kiel, Gutenbergstraße 76, 24118 Kiel, Germany; salban@pharmazie.uni-kiel.de
* Correspondence: christa.mueller@uni-bonn.de; Tel.: +49-228-73-2301; Fax: +49-228-73-2567

check for updates

Citation: Lopez, V.; Schäkel, L.; Schuh, H.J.M.; Schmidt, M.S.; Mirza, S.; Renn, C.; Pelletier, J.; Lee, S.-Y.; Sévigny, J.; Alban, S.; et al. Sulfated Polysaccharides from Macroalgae Are Potent Dual Inhibitors of Human ATP-Hydrolyzing Ectonucleotidases NPP1 and CD39. *Mar. Drugs* **2021**, *19*, 51. https://doi.org/10.3390/md19020051

Received: 29 December 2020
Accepted: 15 January 2021
Published: 22 January 2021

Publisher's Note: MDPI stays neutral with regard to jurisdictional claims in published maps and institutional affiliations.

Copyright: © 2021 by the authors. Licensee MDPI, Basel, Switzerland. This article is an open access article distributed under the terms and conditions of the Creative Commons Attribution (CC BY) license (https://creativecommons.org/licenses/by/4.0/).

Abstract: Extracellular ATP mediates proinflammatory and antiproliferative effects via activation of P2 nucleotide receptors. In contrast, its metabolite, the nucleoside adenosine, is strongly immunosuppressive and enhances tumor proliferation and metastasis. The conversion of ATP to adenosine is catalyzed by ectonucleotidases, which are expressed on immune cells and typically upregulated on tumor cells. In the present study, we identified sulfopolysaccharides from brown and red sea algae to act as potent dual inhibitors of the main ATP-hydrolyzing ectoenzymes, ectonucleotide pyrophosphatase/phosphodiesterase-1 (NPP1) and ecto-nucleoside triphosphate diphosphohydrolase-1 (NTPDase1, CD39), showing nano- to picomolar potency and displaying a non-competitive mechanism of inhibition. We showed that one of the sulfopolysaccharides tested as a representative example reduced adenosine formation at the surface of the human glioblastoma cell line U87 in a concentration-dependent manner. These natural products represent the most potent inhibitors of extracellular ATP hydrolysis known to date and have potential as novel therapeutics for the immunotherapy of cancer.

Keywords: adenosine; CD39; ectonucleotidase inhibitors; fucoidan; immuno-oncology; NPP1; NTPDase1; macroalgae constituents; sulfated polysaccharides

1. Introduction

Nucleosides and nucleotides, e.g., adenosine, ATP and ADP, act as extracellular signaling molecules activating P1 (adenosine) or P2 (nucleotide) receptors [1–5]. Adenosine receptors are G protein-coupled receptors (GPCRs), while P2 receptors are further subdivided into P2Y (GPCRs) and P2X (ligand-gated ion channel) receptor subtypes. Nucleotides can be converted by a cascade of ectonucleotidases to adenosine (see Figure 1). Many tumor cells overexpress ectonucleotidases that metabolize proinflammatory ATP to adenosine, which exerts immunosuppressive, angiogenic, prometastatic and tumor growth promoting activities [5]. Ectonucleotidase inhibition has therefore been proposed as a novel approach for cancer immunotherapy [6,7]. Different classes of ectonucleotidases exist including

nucleotide pyrophosphatase/phosphodiesterases (NPPs), nucleoside triphosphate diphosphohydrolases (NTPDases), alkaline phosphatases (AP) and ecto-5′-nucleotidase (cluster of differentiation 73 (CD73)). The NPP family consists of seven structurally related ectoenzymes (NPP1-NPP7), four of which are known to hydrolyze extracellular nucleotides [1,2,8]. NPP1 (CD203a, also known as PC-1 (plasma cell antigen-1), EC 3.1.4.1) and NPP3 catalyze the hydrolysis of a variety of nucleotides including nucleoside triphosphates (e.g., ATP and UTP), dinucleotide polyphosphates (e.g., Ap_3A and Ap_4A), cyclic dinucleotides (e.g., 2′,3″-cGAMP) and nucleotide sugars (e.g., UDP-glucose and ADP-ribose) [9–12], NPP1 preferentially hydrolyzes ATP into AMP and PPi. NPP4 was reported to hydrolyze the physiological dinucleotides Ap_3A and Ap_4A, while ATP hydrolysis by this enzyme is negligible [11]. NPP5 has recently been reported to hydrolyze nicotinamide adenine dinucleotide (NAD^+) [13]. Other members of the NPP family, i.e., NPP2 (autotaxin), NPP6 and NPP7 (alkaline sphingomyelinase) act as phospholipases [8]. The NTPDase family comprises eight members (NTPDase 1-8), NTPDase1 (CD39, EC 3.6.1.5) being the most prominent member of this family in blood vessels and at the surface of leukocytes. They catalyze the hydrolysis of extracellular nucleoside tri- and diphosphates by cleaving off phosphate [8]. Ecto-5′-nucleotidase (CD73) hydrolyzes nucleoside monophosphates, e.g., AMP, to the corresponding nucleoside, e.g., adenosine. Thus, proinflammatory, antiproliferative ATP can be converted by subsequent action of NPP1 or CD39 and CD73 to immunosuppressive adenosine (Figure 1), which then accumulates in the tumor environment leading to immune escape of the tumor.

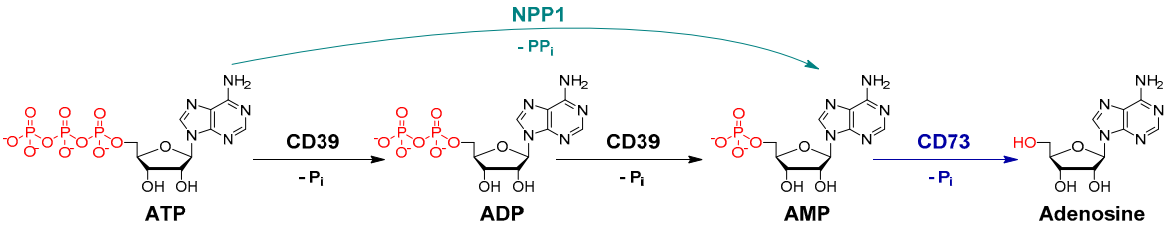

Figure 1. Hydrolysis of ATP to adenosine catalyzed by the key ectonucleotidases NPP1, CD39 and CD73 (P_i, inorganic phosphate).

Recently, there has been an enormous interest in identifying and developing ectonucleotidase inhibitors, antibodies and small molecules, as novel cancer immunotherapeutics [4,6,7].

Several antibodies and small molecules have been developed for blocking the AMP-hydrolyzing, adenosine-producing ectoenzyme CD73, and the first drugs are currently evaluated in clinical trials for the immunotherapy of cancer to prevent the formation of immunosuppressive adenosine [14]. The blockade of enzymes that hydrolyze extracellular ATP to AMP could be even more efficient since it would lead to the accumulation of antiproliferative ATP in addition to preventing the formation of immunosuppressive adenosine due to the depletion of AMP as a CD73 substrate.

On the other hand, ATP, which acts on different subtypes of P2Y (G protein-coupled) and P2X (ligand-gated ion channel) receptors that are activated by different ATP concentrations depending on the receptor subtype, can also display proinflammatory effects since they belong to the danger-associated molecular patterns (DAMPs) [15]. In these cases, inhibition of ATP hydrolysis may result in proinflammatory effects.

So far, only moderately potent and/or non-selective NPP1 and CD39 inhibitors have been described, which can be divided into nucleotides and non-nucleotides. N^6-Diethyl-β,γ-dibromomethylene-ATP (ARL 67156, **1**) is a weak dual CD39/CD73 inhibitor with low metabolic stability [16,17]. Several other negatively charged compound classes including (poly)sulfonates such as suramin (**2**) and sulfoanthraquinones [18–20], and polyoxometalates (POMs), e.g., $[TiW_{11}CoO_{40}]^{8-}$ (**3**) and $[Co_4(H_2O)_2(PW_9O_{34})_2]^{10-}$ (**4**) [21,22], were found to inhibit CD39 and/or NPP1. A selection of the most potent NPP1 and CD39 inhibitors is depicted in Figure 2.

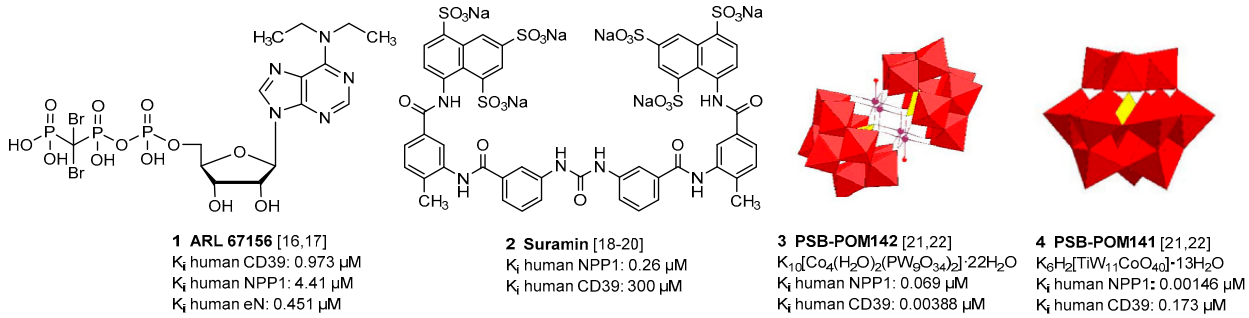

Figure 2. Selected inhibitors of ectonucleotidases NPP1 and CD39.

Sulfated polysaccharides from sea algae, in particular fucoidans present in brown algae, e.g., from *Sargassum polycystum* [23], have been reported to possess antitumor activity in vitro and in vivo [24–27]. These natural products were shown to inhibit cell growth directly, e.g., by inducing apoptosis, and, in addition, to activate the immune system in its fight against cancer [28–30]. Their molecular mechanism of action is not fully understood at present, and the molecular targets are largely unknown [31]. This prompted us to study exemplary polysaccharides from red and brown algae, which are negatively charged like reported ectonucleotidase inhibitors (Figure 2), for inhibitory effects on these enzymes.

2. Results and Discussion

Four sulfated polysaccharides **5**–**8** (Table 1), extracted from different algae species, were investigated in the present study as potential inhibitors of ectonucleotidases. Compounds **5** and **8** represent sulfated xylogalactans from red algae, compounds **6** and **7** are brown algae-derived fucoidans. They were extracted, purified and chemically characterized as previously described [32–34]. The chemical characteristics of the used batches are shown in Tables 1 and 2.

Table 1. Basic characteristics of investigated sulfated algae polysaccharides.

Compound	Type of Sulfated Polysaccharide	Extracted Alga Species	Degree of Sulfation [a]	Molar Mass (kDa) [b]	Proteins (%) [c]	Uronic Acids (%) [d]
5	Xylogalactan	*Delesseria sanguinea*	0.65 ± 0.02	214 ± 28	7.24 ±0.07	3.96 ± 0.54
6	Fucoidan	*Saccharina latissima*	0.52 ± 0.01	534 ± 11	8.08 ±0.09	7.42 ± 0.18
7	Fucoidan	*Fucus vesiculosus*	0.59 ± 0.01	38 ± 1	7.07 ± 1.59	0.27 ± 0.27
8	Xylogalactan	*Coccotylus truncatus*	0.52 ± 0.01	128 ± 4	3.74 ±1.29	9.50 ± 0.23

[a] Average number of sulfate groups per monosaccharide related to the total glycan content; it was calculated by means of the SO_3Na, which was derived from % sulfur content determined by elemental analysis (mean ± SD, n = 2). [b] Mean weight average molar mass, determined by SEC-MALS-RI, mean ± SD (mean ± SD, n = 3). [c] The content of protein was calculated by elemental analysis (% nitrogen) (mean ± SD, n = 2). [d] Determined according to the method of Blumenkrantz et al. [35] and Filisetti-Cozzi et al. [36] (mean ± SD, n = 2 × 2).

Table 2. Composition of investigated sulfated algae polysaccharides.[a]

Compound	Type of Sulfated Polysaccharide	Fucose (mol%)	Galactose (mol%)	Xylose (mol%)	Mannose (mol%)	Glucose (mol%)	Rhamnose (mol%)
5	Xylogalactan	0.0	75.3	16.1	2.5	6.1	0.0
6	Fucoidan	53.4	13.6	6.7	5.4	19.8	1.3
7	Fucoidan	83.1	7.3	6.5	2.0	0.4	0.7
8	Xylogalactan	0.0	87.6	3.8	6.7	2.0	0.0

[a] Determined according to the method of Blakeney et al. [37].

We initially tested the effects of the compounds at a concentration of 20,000 ng/mL on the most prominent ectonucleotidase families, NPPs (NPP1, 3, 4 and 5), NTPDases (NTPDase1, 2, 3 and 8) and CD73 (see Figure 3).

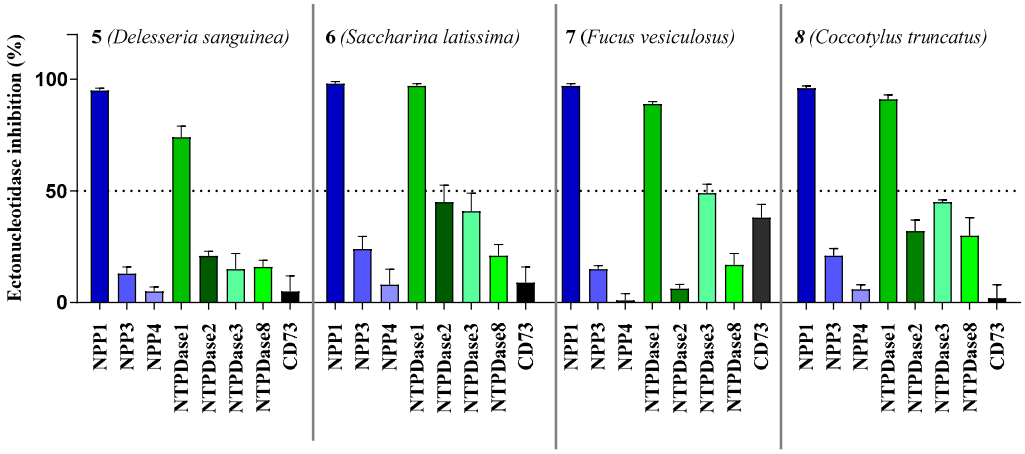

Figure 3. Ectonucleotidase inhibition by sulfopolysaccharides **5**–**8** extracted from sea algae. Compounds were tested at a concentration of 20,000 ng/mL. NPP1 and NTPDase2, 3 and 8 activities were analyzed using a CE-based assay employing ATP as a substrate as described in the experimental section; NPP3 was investigated using *p*-Nph-5′-TMP as a substrate (see Section 3.2 for details); NPP4 was tested with Ap_4A as a substrate using a luciferase assay (for details see Section 3.3); NTPDase1 (CD39) activity was determined with a malachite green assay, or a CE-based assay, respectively (see Section 3.4 for details). The data is normalized with respect to positive (100%) and negative (0%) controls.

All compounds showed the highest inhibition of NPP1, which was completely inhibited at the test concentration, combined with high selectivity versus the other NPP subtypes. The second highest inhibition was observed at NTPDase1 (CD39) while inhibition of all other enzymes was below 50%. As a next step, we investigated concentration-dependent inhibition by determining full concentration–inhibition curves for all four compounds at NPP1 and CD39, and determined the compounds' K_i values (see Table 3). Curves for compound **7** as a representative inhibitor are depicted in Figure 4. Compound **7** was selected because it showed the lowest molecular weight of all tested sulfated polysaccharides and was available in high quantity.

Table 3. Potencies of investigated compounds at ectonucleotidases NPP1 and CD39 in comparison to standard inhibitors.

Compound	Compound Name or Algal Species	Human NPP1 Ki ± SEM (nM)	Human CD39 Ki ± SEM (nM)
	Standard ectonucleotidase inhibitors		
1	ARL 67156	973 ± 239 [14] [a]	4410 ± 3,530 [14] [b]
2	Suramin	780 ± 81 [38] [b]	300,000 ± 100 [18] [b]
3	PSB-POM142	690 ± 4 [22] [b]	3.88 ± 1.40 [22] [c]
4	PSB-POM141	1.46 ± 0.01 [22] [b]	173 ± 4 [22] [c]
	Sulfated algae polysaccharides		
5	*Delesseria sanguinea*	0.0517 ± 0.0016 [b] (11.1 ng/mL)	1.72 ± 0.00 [d] (366 ng/mL)
6	*Saccharina latissimi*	0.136 ± 0.001 [b] (72.8 ng/mL)	0.408 ± 0.001 [d] (218 ng/mL)
7	*Fucus vesiculosus*	1.19 ± 0.00 [b] (45.2 ng/mL)	12.3 ± 0.0 [d] (469 ng/mL)
8	*Coccotylus truncatus*	5.33 ± 0.00 [b] (682 ng/mL)	16.0 ± 0.0 [b] (2045 ng/mL)

[a] absorbance-based assay; [b] CE-based assay; [c] fluorescence polarization (FP) assay; [d] malachite-green assay.

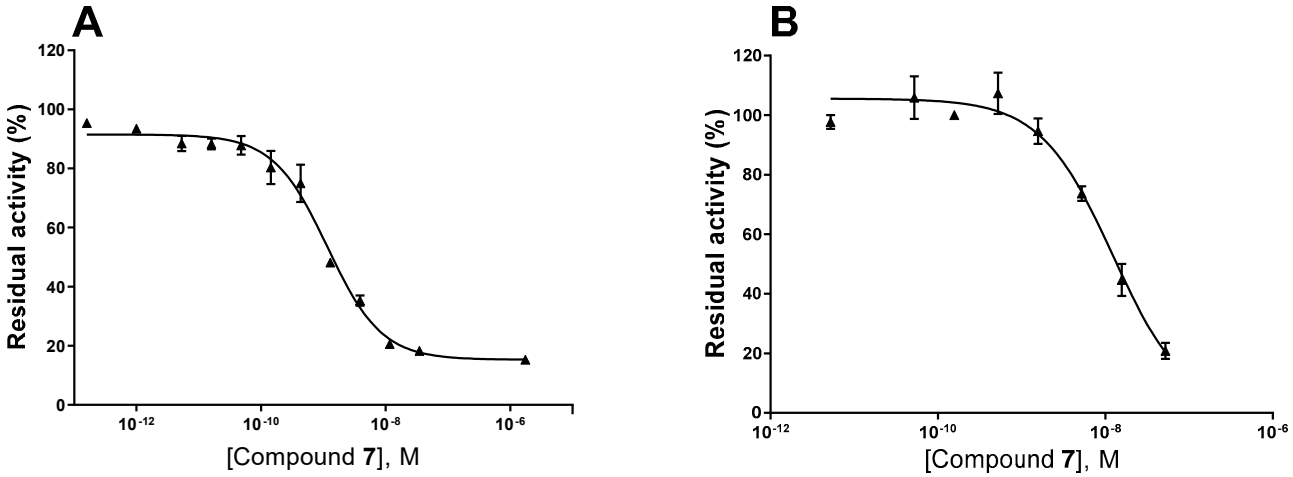

Figure 4. Concentration–inhibition curves of compound **7** at human NPP1 (**A**) and human CD39 (**B**). For details see Experimental Section.

Some of the investigated sulfated polysaccharides from sea algae were discovered to be the most potent NPP1 and CD39 inhibitors described to date displaying nano- to subnanomolar potencies. The potency calculated in nmol/L (nM) did not depend on the molecular weight. Sulfated polysaccharide **5** (MW 214 kDa) was almost 3-fold more potent at NPP1 as compared to compound **6** (MW 534 kDa). Compound **5** showed 33-fold selectivity for NPP1 over CD39, while **6** was about equipotent. Compounds **7** and **8** displayed somewhat lower potency combined with moderate selectivity for NPP1 versus CD39 (see Figure 5). Compound **5** is an extremely potent NPP1 inhibitor with picomolar inhibitory potency at NPP1 (K_i 0.0517 nM) showing ancillary CD39 inhibition (K_i 1.72 nM), but being highly selective versus all other investigated ectonucleotidases. Sulfated polysaccharide **6** is about equipotent at both NPP1 and CD39, and can be envisaged as a dual NPP1/CD39 inhibitor. Such dual activity could be a big advantage in cancer therapy since both ATP-hydrolyzing enzymes may be upregulated and constitute redundant pathways for nucleotide degradation.

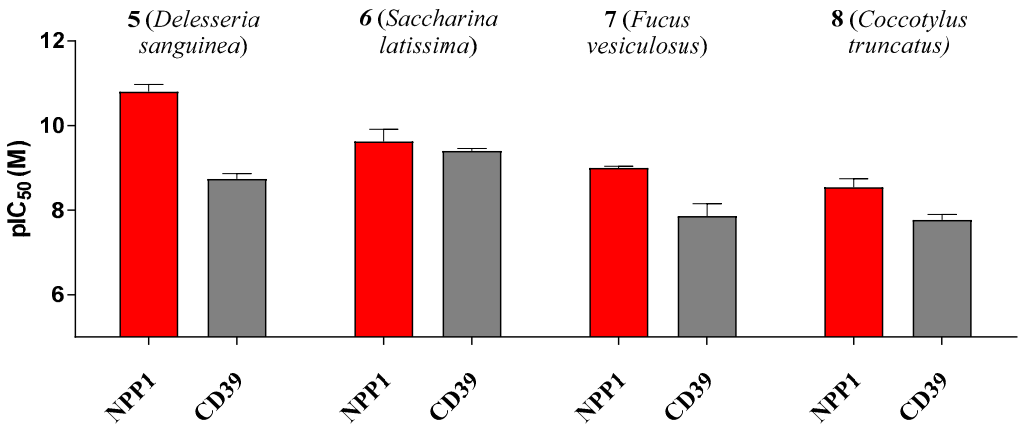

Figure 5. pIC_{50} ($-\log IC_{50}$) values of compounds **5**–**8** at the ectonucleotidases NPP1 and CD39 are shown. Error bars represent SD values. For IC_{50} values see Table 3.

Next, we studied the inhibition type for compound **7**, the compound with the lowest molecular weight, as a representative for this new class of ectonucleotidase inhibitors using ATP as a substrate. Considering the size of the compounds (with molecular masses ranging from 38 to 534 kDa) and based on their structures, we presumed an allosteric mechanism of inhibition. The effect of inhibitor **7** on the kinetics of NPP1 and CD39 was investigated. In both cases, the Michaelis–Menten plots (Figure 6A,C) clearly showed a decrease in

V_{max} in the presence of the inhibitor, which is indicative of a non-competitive or mixed type of inhibition. Moreover, the apparent K_m values are increased at higher inhibitor concentrations. The Lineweaver–Burk plot [39] confirmed a non-competitive/mixed type of inhibition (Figure 6B,D) at both enzymes, NPP1 and CD39.

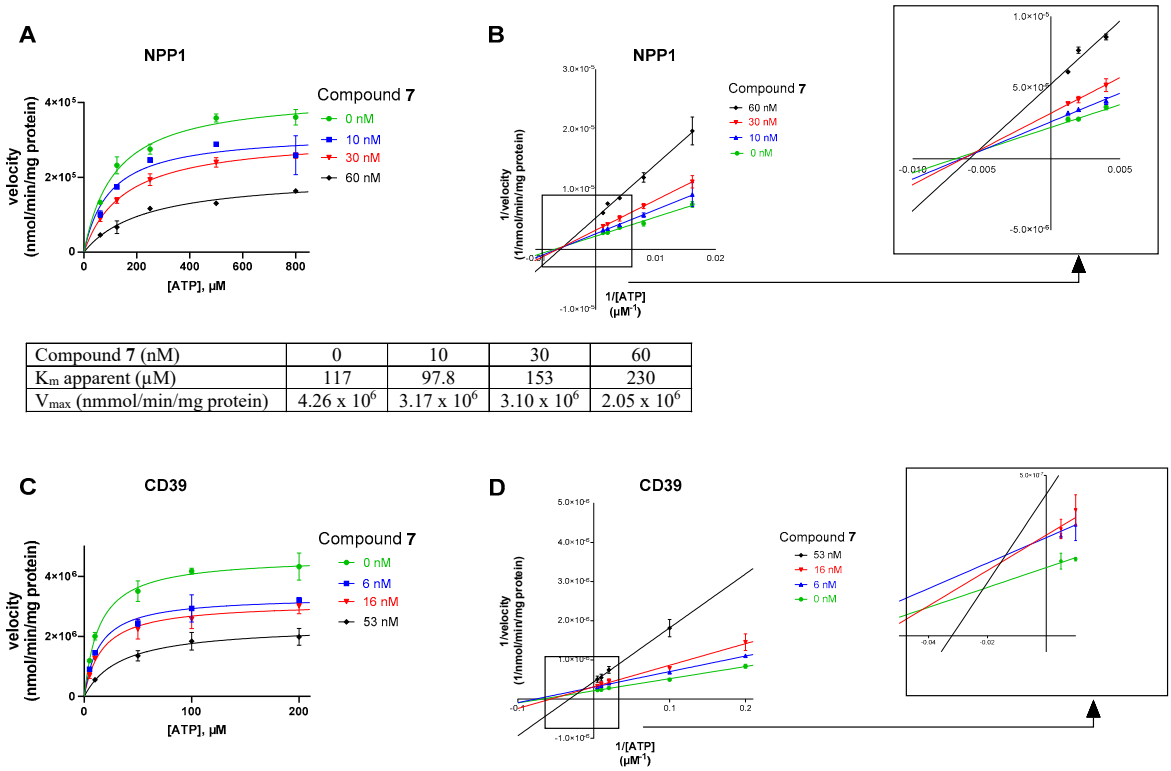

Compound **7** (nM)	0	10	30	60
K_m apparent (µM)	117	97.8	153	230
V_{max} (nmmol/min/mg protein)	4.26 x 10^6	3.17 x 10^6	3.10 x 10^6	2.05 x 10^6

Compound **7** (nM)	0	6	16	53
K_m apparent (µM)	13.9	13.9	16.7	34.1
V_{max} (nmmol/min/mg protein)	4.64 x 10^6	3.33 x 10^6	3.12 x 10^6	2.36 x 10^6

Figure 6. Investigation of the enzyme inhibition type for inhibitor **7** at NPP1 (**A**,**B**) and CD39 (**C**,**D**). In (**A**,**C**) the Michaelis–Menten curves are shown without and in the presence of different concentrations of inhibitor **7**. For the determination of the inhibition type, Lineweaver–Burk plots are shown in (**B**,**D**) (see Sections 3.1 and 3.4 for experimental details). The results indicate a non-competitive/mixed type of inhibition. The kinetic parameters of ATP hydrolysis by CD39 and NPP1, respectively, in the absence and presence of inhibitor **7** are provided.

Finally, we investigated compound **7** in a more complex cellular system. The human glioblastoma cell line U87 had previously been shown to express NPP1 and CD73 [40–43], but only negligible amounts of CD39 [44]. These enzymes are known to convert ATP to adenosine in a sequential reaction cascade (see Figure 1). Therefore, we used this cancer cell line to determine the hydrolysis of extracellular ATP, added to the cells, resulting in the formation of adenosine, which is known to produce antiproliferative, antiangiogenic, metastasis-promoting and immunosuppressive effects when released into the tumor microenvironment. Dipyridamole was added to block the cellular uptake of adenosine via the SLC29 transporter family [45], and erythro-9-(2-hydroxy-3-nonyl)adenine (EHNA) was present to inhibit metabolism of adenosine to inosine [46]. Cells treated with ATP, dipyridamole and EHNA were studied in the absence and in the presence of sulfopolysaccharide **7**, and extracellular adenosine accumulation was quantified by capillary electrophoresis coupled to UV detection. The results clearly showed a concentration-dependent inhibition of adenosine formation by sulfopolysaccharide **7** in U87 glioma cells, which is assumed to be due to the blockade of NPP1 by inhibitor **7**. These data confirmed the strong inhibitory activity of ectonucleotidase inhibitor **7** (as a representative of the chemical class of

sulfopolysaccharides) on the formation of extracellular adenosine from ATP by a human glioblastoma cell line (Figure 7).

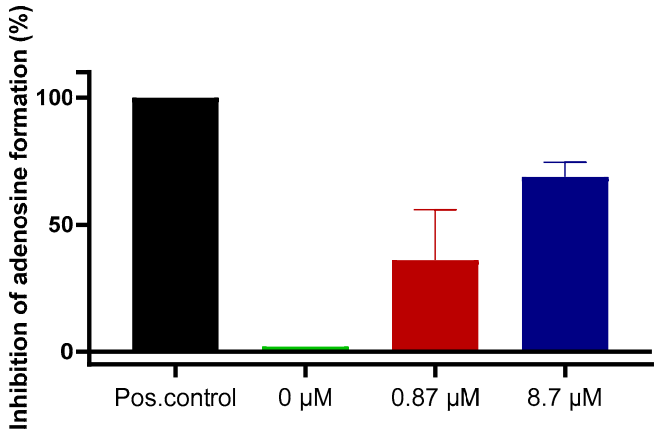

Figure 7. Blockade of extracellular adenosine formation from ATP by compound **7** on human U87 glioblastoma cells. The cells were treated with ATP (ectonucleotidase substrate) and incubated for 3 h in the presence of dipyridamole to prevent cellular uptake of adenosine, and EHNA to prevent adenosine deamination. Adenosine was quantified by CE-UV. Results represent means of two independent experiments each performed in quadruplicate measurements. Positive (Pos.) control: the potent NPP1 inhibitor PSB-POM141 (**4**, 10 µM) or the potent CD73 inhibitor PSB-19316 (0.1 µM) were added both of which led to a full blockade of NPP1 and CD73 activity thereby preventing the formation of adenosine. For details see Experimental Section 3.6.

3. Materials and Methods

The sulfated polysaccharides **5**–**8** were isolated from the two brown algae *Saccharina latissima* (Laminariales, Laminariaceae) (North Atlantic Faroe Island) and *Fucus vesiculosus* (Fucales, Fucaceae) and the two red algae *Delesseria sanguinea* (Ceramiales, Delesseriaceae) and *Coccotylus truncatus* (Gigartinales, Phyllophoraceae) (both collected in the sublittoral habitat of the large artificial reef near Nienhagen (Baltic Sea, Germany). They were extracted, purified and chemically characterized as previously described [32–34], whereby compound **7**, fucoidan from *Fucus vesiculosus* was purchased from Sigma-Aldrich, catalog No. F5631, Lot No SLBC4004 V). In short: the pulverized algal material was defatted with Soxhlet extraction (99% *v/v* ethanol). The main extraction was performed with demineralized water at 85 °C for 8 h (compound **5**) and aqueous 2% $CaCl_2$ at 85 °C for 2 h (compounds **6** and **8**) (reflux condition). The supernatant was evaporated and precipitated with ethanol (final concentration 60% *v*/*v*) at 4 °C. Further steps involved centrifugation, dissolving in demineralized water, dialysis and lyophilization. The analyzed chemical parameters included sulfate content and degree of sulfation, weight average molar mass, monosaccharide composition, contents of protein and uronic acids.

3.1. Chemicals

Nucleotides (AMP, ADP, ATP and cAMP), nucleosides (adenosine, inosine and uridine), dipyridamole, erythro-9-(2-hydroxy-3-nonyl)adenine (EHNA), disodium hydrogenphosphate and sodium dodecyl sulfate were purchased from Merck KGaA (Darmstadt, Germany). Sodium chloride, potassium chloride, potassium dihydrogen phosphate, sodium hydrogencarbonate, D-glucose, *N*-[2-hydroxyethyl]piperazine-*N*′-[2-ethanesulfonic acid] (HEPES), calcium chloride and magnesium sulfate were purchased from PAN Biotech GmbH (Aidenbach, Germany). Dulbecco's modified Eagle medium, fetal calf serum (FCS), penicillin/streptomycin (P/S) and L-glutamine were also from PAN Biotech GmbH.

3.2. NPP1 Assay

Recombinant soluble human NPP1 was obtained as previously described [22]. Compounds **5**–**8** were tested as inhibitors of human NPP1 at a concentration of 20,000 ng/mL vs. ATP (400 μM) as a substrate. Subsequent concentration–inhibition curves were performed using several dilutions of the test compounds prepared in assay buffer (10 mM *N*-cyclohexyl-2-aminoethanesulfonic acid (CHES), 2 mM $CaCl_2$ and 1 mM $MgCl_2$, pH 9.00). The human NPP1, prepared as previously described [22], was diluted in the assay buffer, and 0.224 μg of the enzyme were employed per vial. The mixture was incubated for 30 min at 37 °C, and the reaction was terminated by heating at 90 °C for 5 min. After cooling down on ice, analysis was carried out using capillary electrophoresis (CE). Positive and negative controls were studied in parallel. Data collection and peak area analysis were performed by the P/ACE MDQ software 32 KARAT obtained from Beckman Coulter (Fullerton, CA, USA). A polyacrylamide-coated capillary was used (30 cm (20 cm effective length) × 50 μm (id) × 360 μm (od) purchased from Chromatographie Service GmbH (Langerwehe, Germany)). Samples were injected electrokinetically by applying a voltage of −6 kV for 30 s. Finally, analytes were separated by applying a separation voltage of −20 kV, and detected by UV at 260 nm. The IC_{50} values were determined by nonlinear curve fitting using the GraphPad Prism software 7.0. The mechanism of inhibition of human NPP1 was determined by employing different concentrations of the inhibitor (0, 10, 30 and 60 nM) vs. five different substrate concentrations ranging from 62 to 800 μM ATP. The assay procedure and operation conditions were the same as described above. The experiments were conducted two times, each in triplicates. A Lineweaver–Burk was calculated using GraphPad Prism 7.0 for predicting the inhibition type of the inhibitor.

3.3. NPP3 Assay

Recombinant soluble human NPP3 was obtained as previously described [47]. Compounds **5**–**8** were screened at a concentration of 20,000 ng/mL vs. 400 μM *p*-Nph-5′-TMP to study a potential inhibition of NPP3, using a colorimetric assay as previously described [38]. Soluble, purified human NPP3 was diluted in the assay buffer (50 mM TRIS HCl, 2 mM $CaCl_2$ and 0.2 mM $ZnCl_2$ pH 9.00), and 0.45 μg of enzyme per vial was used. The mixture was incubated for 30 min at 37 °C, and the reactions were subsequently terminated by adding 20 μL of 1.0 N NaOH. The assay is based on the enzymatic ester hydrolysis of *p*-Nph-5′-TMP that results in the formation of *p*-nitrophenolate. The absorption maximum was measured at 400 nm using a BMG PheraStar FS plate reader (BMG Labtech GmbH, Ortenberg, Germany). Each analysis was repeated three times in triplicate measurements.

3.4. NPP4 Assay

Recombinant human soluble NPP4 was obtained as previously described [48]. Screening of the test compounds **5**–**8** was performed at a concentration of 20,000 ng/mL versus 20 μM of Ap_4A as a substrate employing a previously described luminescence-based assay [48]. The assay buffer consisted of 10 mM HEPES, 1 mM $MgCl_2$ and 2 mM $CaCl_2$ (pH 8.0). The enzyme reaction was started by adding 0.14 μg of human purified NPP4 to the reaction mixture which was incubated at 37 °C for 60 min. The released product, ATP, was quantified using the luciferin–luciferase reaction. The firefly luciferase reacts with D-luciferin in the presence of the formed ATP and Mg^{2+}, which act as cofactors. The resulting luminescence correlates to the enzyme activity. It was measured at 560 nm using a microplate reader (BMG PheraStar, Labtech GmbH, Ortenberg, Baden-Württemberg, Germany). Three independent experiments were performed, each in duplicates with positive and negative controls studied in parallel.

3.5. NTPDase Assays

Human NTPDases (subtypes 1, 2, 3 and 8) were recombinantly expressed as previously described and cell membrane preparations overexpressing one of the NTPDase subtypes were used for the experiments according to described procedures [46]. For monitoring

the inhibitory activity of the compounds at the NTPDases two different assay system were utilized. The malachite green assay was used for the determination of NTPDase1 (CD39) concentration–inhibition curves with compound **5**–**7** and for the determination of the inhibition type of compound **7**. The CE-based assay was utilized for selectivity studies of compound **5**–**8** at NTPDase2, NTPDase3 and NTPDase8, and for the determination of concentration–inhibition curves for compound **8** at human CD39. The test compounds were investigated at 20,000 ng/mL for initial screening, and subsequently at different concentrations for obtaining concentration–inhibition curves. The enzyme amounts were selected after enzymatic titration and adjusted to ensure a conversion rate of 10–20%; for NTPDase1 assays, 0.1 μg of human umbilical cord membrane preparation [49,50] was employed per vial, for NTPDase2 assays, 0.07 μg of recombinant enzyme was used, for NTPDase3 assays, 0.45 μg of enzyme was employed and for NTPDase8 assays, 0.52 μg of enzyme was utilized. Human NTPDase1, -2, -3 and -8 were expressed as previously described [49,50]. When the malachite assay was used, the reaction was initiated by the addition of 50 μM ATP (K_m (NTPDase1) = 17 μM) [50]. The reaction buffer consisted of 10 mM HEPES, 2 mM $CaCl_2$ and 1 mM $MgCl_2$, pH 7.4. The enzyme reaction mixture was incubated at 37 °C for 15 min. The released phosphate was quantified by adding malachite-green and molybdate reagents, incubating for 20 min at room temperature, and measuring the UV-absorption at 600 nm [51]. The prediction of the mechanism of inhibition at human NTPDase1 was determined for compound **7** as a representative example employing different concentrations of the investigated inhibitor (0, 6, 16 and 53 nM of **7**) vs. five different substrate concentrations of ATP (from 5 to 200 μM). The assay procedure and operation conditions were the same as described above. A Lineweaver–Burk plot was calculated using GraphPad Prism 7.0 for predicting the inhibition type of the compound. In the CE assay, the selected substrate concentration of ATP was 100 μM for human NTPDase2, -3 and -8. The reaction buffer was the same as for NTPDase1 described above. The mixtures of enzyme with the substrate and test compound were incubated at 37 °C for 30 min, and the enzymatic reaction was stopped by heating it for 10 min at 95 °C. The released products were separated by capillary electrophoresis and quantified by their UV-absorption at 260 nm in the presence of ADP and AMP as external standards as previously described [48]. Positive and negative controls were studied in parallel.

3.6. CD73 Assay

Soluble human CD73 was recombinantly expressed and purified as described [52], and the assays were performed according to a described procedure [53]. The enzymatic reaction was performed by mixing 0.36 ng of human CD73 [52], with the test compound (20,000 ng/mL) in the assay buffer (25 mM Tris, 140 mM sodium chloride and 25 mM sodium dihydrogenphosphate, pH 7.4), and 5 μM of [2,8-^{3}H]AMP (specific activity 7.4 × 10^8 Bq/mmol, 20 mCi/mmol, American Radio-labeled Chemicals, MO, USA, distributed by Hartmann Analytic, Germany) was added. The enzymatic reaction was performed for 25 min at 37 °C in a shaking water bath. Then, 500 μL of cold precipitation buffer (100 mM lanthanum chloride and 100 mM sodium acetate, pH 4.00) was added to stop the reaction and to facilitate precipitation of free phosphate and unconverted [2,8-^{3}H]AMP. After the precipitation was completed (after at least 30 min on ice), the mixture was separated by filtration through GF/B glass fiber filters using a cell harvester (M-48, Brandel, MD, USA). After washing each reaction vial three times with 400 μL of cold (4 °C) demineralized water, 5 mL of the scintillation cocktail (ULTIMA Gold XR, PerkinElmer, MA, USA) was added, and the radioactivity was measured by scintillation counting (TRICARB 2900 TR, Packard/PerkinElmer; counting efficacy: 49–52%). Positive and negative controls were tested in parallel.

3.7. Experiments on U87 Glioblastoma Cells

U87 glioblastoma cells were grown in cell culture flasks until reaching a confluent cell layer. Cells were cultivated at 37 °C and 5% CO_2 in Dulbecco's modified Eagle medium

(DMEM) with additions of 10% FCS, 1% penicillin/streptomycin and 1% L-glutamine. The cells were rinsed with phosphate-buffered saline (PBS) and detached with ethylenediaminetetraacetic acid (EDTA). Thereafter, they were counted in a cell counter (CASY® 1 Model TT, Schärfe System GmbH, Reutlingen, Germany), then rinsed three times with PBS before they were resuspended in Krebs-HEPES buffer at a concentration of 1×10^6 cells/mL per well [54]. Cells (1 mL of a cell suspension containing 10^6 cells) were then pipetted into each well of a 24-well plate (Sarstedt AG, Nümbrecht, Germany). Subsequently, the cells were pretreated with dipyridamole (20 μM) for 30 min to block nucleoside transport. Adenosine deaminase (ADA) activity was inhibited by the addition of 1 μM of the inhibitor EHNA, which was added to each sample, and controls [4]. Thereafter, inhibitor **7** was added, and the samples were incubated with 300 μM of ATP for 3 h. Then, an aliquot of 230 μL of solution from each vial was transferred to 1.5 mL Eppendorf tubes, and heated at 95 °C for 10 min to inactivate the enzymes in order to avoid further nucleotide degradation. Before performing capillary electrophoresis (CE) measurements, the samples were centrifuged at 600 × *g* to remove insoluble material like cell debris from the supernatant. Until CE measurement, the supernatants were stored at −20 °C. Nucleotides (ATP, ADP, AMP and cAMP) and nucleosides (adenosine, inosine and uridine), which were also used as standards to monitor efficient separation by CE, were dissolved in Krebs-HEPES buffer at a concentration of 10 μM [54] and stored at −20 °C as well. For analysis of the formed products, CE measurements were performed according to published procedures [55].

4. Conclusions

In conclusion, we identified sulfopolysaccharides isolated from sea algae to act as extremely potent, noncompetitive inhibitors of the ectonucleotidases NPP1 and CD39 with somewhat higher inhibitory potency against NPP1. Both of these enzymes catalyze the hydrolysis of proinflammatory, antiproliferative ATP yielding, in concert with the AMP-hydrolyzing ectoenzyme CD73, adenosine, which displays immunosuppressive and tumor-promoting activities. In fact, we observed reduced formation of adenosine in human glioblastoma U87 cells treated with a representative example of the investigated sulfopolysaccharides. These effects might explain or at least contribute to the previously observed anticancer effects of sulfated algae polysaccharides from sea weeds, which were shown to be non-toxic and well tolerated by humans. The sulfate groups are believed to be essential for their ectonucleotidase-inhibitory effects because other negatively charged compounds, e.g., some polyoxometalates, can also inhibit these ATP-hydrolyzing enzymes with high potency. The substrate ATP itself is also a negatively charged compound, and the enzymes may therefore preferably recognize negatively charged molecules. While ATP would subsequently be guided to the substrate binding pocket, the large anionic polymers and cluster compounds likely remain attached to the initial recognition site at the surface of the enzymes showing allosteric inhibition. In future studies, we plan to investigate the role of the sulfate groups on the seaweed polysaccharides for their enzyme-inhibitory potency by investigating derivatives without or with lower degrees of sulfation.

Author Contributions: C.E.M. designed the study; V.L. performed the experiments on NPP1, NPP4, NTPDase2, 3 and NTPDase8; L.S. performed the experiments on NTPDase 1; H.J.M.S. and M.S.S. performed and analyzed the data of the cell based-assay under the supervision of G.B.; S.M. performed the experiments on NPP3; C.R. performed the experiments on CD73; V.L., S.-Y.L., L.S., S.M., C.R. analyzed the data under the supervision of C.E.M.; S.A. provided the compounds; J.S. and J.P. provided NTPDase preparations; V.L. and C.E.M. wrote the manuscript with contributions by all coauthors. All authors have read and agreed to the published version of the manuscript.

Funding: This study was funded by the Federal Ministry of Education and Research (BMBF, BIGS DrugS project) and by the Deutsche Forschungsgemeinschaft (DFG, German Research Foundation)—Project-ID: 335447717-SFB 1328. J.S. received support from the Natural Sciences and Engineering Research Council of Canada (NSERC; RGPIN-2016-05867).

Institutional Review Board Statement: Human umbilical cords as a source of CD39 were obtained under approved institutional review board protocol (Comité d'Éthique de la Recherche du CHU de Québec—Université Laval) following written consent.

Informed Consent Statement: Not applicable.

Data Availability Statement: The data presented in this study are available on request from the corresponding author. The data are not publicly available due to privacy reasons.

Acknowledgments: We are grateful to Holger Stephan, Helmholtz-Zentrum Dresden-Rossendorf (HZDR), for the gift of PSB-POM141.

Conflicts of Interest: The authors declare no conflict of interest. The funders had no role in the design of the study; in the collection, analyses, or interpretation of data; in the writing of the manuscript, or in the decision to publish the results.

Abbreviations

Ap_4A	diadenosine tetraphosphate
CD	cluster of differentiation
CE	capillary electrophoresis
CHES	*N*-cyclohexyl-2-aminoethanesulfonic acid
CD39	nucleoside triphosphate diphosphohydrolase-1
CD73	ecto-5′-nucleotidase
DAD	diode array detector
DMEM	Dulbecco's Modified Eagle Medium
EDTA	ethylenediaminetetraacetic acid
EHNA	erythro-9-(2-hydroxy-3-nonyl)-adenine
HEPES	4-(2-hydroxyethyl)piperazine-1-ethanesulfonic acid
NTPDase1	nucleoside triphosphate diphosphohydrolase-1
NPP1	nucleotide pyrophosphatase/phosphodiesterase-1 (CD203a)
pIC_{50}	negative log of the half-maximal inhibitory concentration
PBS	phosphate-buffered saline
*p*NP-TMP	*p*-nitrophenyl thymidine 5-monophosphate
PSB	Pharmaceutical Sciences Bonn
SDS	sodium dodecylsulfate

References

1. Hara, H.; Takeda, N.; Komuro, I. Pathophysiology and therapeutic potential of cardiac fibrosis. *Inflamm. Regen.* **2017**, *37*, 13. [CrossRef] [PubMed]
2. Abbracchio, M.P.; Burnstock, G.; Boeynaems, J.-M.; Barnard, E.A.; Boyer, J.L.; Kennedy, C.; Knight, G.E.; Fumagalli, M.; Gachet, C.; Jacobson, K.A.; et al. International Union of Pharmacology LVIII: Update on the P2Y G protein-coupled nucleotide receptors: From molecular mechanisms and pathophysiology to therapy. *Pharmacol. Rev.* **2006**, *58*, 281–341. [CrossRef] [PubMed]
3. Coddou, C.; Yan, Z.; Obsil, T.; Pablo Huidobro-Toro, J.; Stojilkovic, S.S. Activation and regulation of purinergic P2X receptor channels. *Pharmacol. Rev.* **2011**, *63*, 641–683. [CrossRef] [PubMed]
4. Antonioli, L.; Blandizzi, C.; Pacher, P.; Haskó, G. The purinergic system as a pharmacological target for the treatment of immune-mediated inflammatory diseases. *Pharmacol. Rev.* **2019**, *71*, 345–382. [CrossRef]
5. Vitiello, L.; Gorini, S.; Rosano, G.; La Sala, A. Immunoregulation through extracellular nucleotides. *Blood* **2012**, *120*, 511–518. [CrossRef]
6. Allard, B.; Longhi, M.S.; Robson, S.C.; Stagg, J. The ectonucleotidases CD39 and CD73: Novel checkpoint inhibitor targets. *Immunol. Rev.* **2017**, *276*, 121–144. [CrossRef]
7. Onyedibe, K.I.; Wang, M.; Sintim, H.O. ENPP1, an old enzyme with new functions, and small molecule inhibitors—A STING in the tale of ENPP1. *Molecules* **2019**, *24*, 4192. [CrossRef]
8. Zimmermann, H.; Zebisch, M.; Sträter, N. Cellular function and molecular structure of ecto-nucleotidases. *Purinergic Signal.* **2012**, *8*, 437–502. [CrossRef]
9. Lee, S.-Y.; Müller, C.E. Nucleotide pyrophosphatase/phosphodiesterase 1 (NPP1) and its inhibitors. *MedChemComm* **2017**, *8*, 823–840. [CrossRef]
10. Namasivayam, V.; Lee, S.Y.; Müller, C.E. The promiscuous ectonucleotidase NPP1: Molecular insights into substrate binding and hydrolysis. *Biochim. Biophys. Acta Gen. Subj.* **2017**, *1861*, 603–614. [CrossRef]

11. Albright, R.A.; Ornstein, D.L.; Cao, W.; Chang, W.C.; Robert, D.; Tehan, M.; Hoyer, D.; Liu, L.; Stabach, P.; Yang, G.; et al. Molecular basis of purinergic signal metabolism by ectonucleotide pyrophosphatase/phosphodiesterases 4 and 1 and implications in stroke. *J. Biol. Chem.* **2014**, *289*, 3294–3306. [CrossRef] [PubMed]
12. Kato, K.; Nishimasu, H.; Oikawa, D.; Hirano, S.; Hirano, H.; Kasuya, G.; Ishitani, R.; Tokunaga, F.; Nureki, O. Structural insights into cGAMP degradation by Ecto-nucleotide pyrophosphatase phosphodiesterase 1. *Nat. Commun.* **2018**, *9*, 4424. [CrossRef] [PubMed]
13. Gorelik, A.; Randriamihaja, A.; Illes, K.; Nagar, B. A key tyrosine substitution restricts nucleotide hydrolysis by the ectoenzyme NPP5. *FEBS J.* **2017**, *5*, 1–9. [CrossRef] [PubMed]
14. Hay, C.M.; Sult, E.; Huang, Q.; Mulgrew, K.; Fuhrmann, S.R.; McGlinchey, K.A.; Hammond, S.A.; Rothstein, R.; Rios-Doria, J.; Poon, E.; et al. Targeting CD73 in the tumor microenvironment with MEDI9447. *Oncoimmunology* **2016**, *5*, 1–10. [CrossRef] [PubMed]
15. Di Virgilio, F.; Sarti, A.C.; Coutinho-Silva, R. Purinergic signaling, DAMPs, and inflammation. *Am. J. Physiol. Cell Physiol.* **2020**, *318*, C832–C835. [CrossRef]
16. Crack, B.E.; Pollard, C.E.; Beukers, M.W.; Roberts, S.M.; Hunt, S.F.; Ingall, A.H.; McKechnie, K.C.; IJzerman, A.P.; Leff, P. Pharmacological and biochemical analysis of FPL 67156, a novel, selective inhibitor of ecto-ATPase. *Br. J. Pharmacol.* **1995**, *114*, 475–481. [CrossRef]
17. Schäkel, L.; Schmies, C.C.; Idris, R.M.; Luo, X.; Lee, S.-Y.; Lopez, V.; Mirza, S.; Vu, T.H.; Pelletier, J.; Sévigny, J.; et al. Nucleotide analog ARL67156 as a lead structure for the development of CD39 and Dual CD39/CD73 ectonucleotidase inhibitors. *Front. Pharmacol.* **2020**, *11*. [CrossRef]
18. Iqbal, J.; Vollmayer, P.; Braun, N.; Zimmermann, H.; Müller, C.E. A capillary electrophoresis method for the characterization of ecto-nucleoside triphosphate diphosphohydrolases (NTPDases) and the analysis of inhibitors by in-capillary enzymatic microreaction. *Purinergic Signal.* **2005**, *1*, 349–358. [CrossRef]
19. Baqi, Y.; Weyler, S.; Iqbal, J.; Zimmermann, H.; Müller, C.E. Structure-Activity relationships of anthraquinone derivatives derived from bromaminic acid as inhibitors of ectonucleoside triphosphate diphosphohydrolases (E-NTPDases). *Purinergic Signal.* **2009**, *5*, 91–106. [CrossRef]
20. Iqbal, J.; Lévesque, S.A.; Sévigny, J.; Müller, C.E. A highly sensitive CE-UV method with dynamic coating of silica-fused capillaries for monitoring of nucleotide pyrophosphatase/phosphodiesterase reactions. *Electrophoresis* **2008**, *29*, 3685–3693. [CrossRef]
21. Müller, C.E.; Iqbal, J.; Baqi, Y.; Zimmermann, H.; Röllich, A.; Stephan, H. Polyoxometalates—A new class of potent ecto-nucleoside triphosphate diphosphohydrolase (NTPDase) inhibitors. *Bioorg. Med. Chem. Lett.* **2006**, *16*, 5943–5947. [CrossRef] [PubMed]
22. Lee, S.Y.; Fiene, A.; Li, W.; Hanck, T.; Brylev, K.A.; Fedorov, V.E.; Lecka, J.; Haider, A.; Pietzsch, H.J.; Zimmermann, H.; et al. Polyoxometalates—Potent and selective ecto-nucleotidase inhibitors. *Biochem. Pharmacol.* **2015**, *93*, 171–181. [CrossRef] [PubMed]
23. Fernando, I.P.S.; Sanjeewa, K.K.A.; Lee, H.G.; Kim, H.S.; Vaas, A.P.J.P.; De Silva, H.I.C.; Nanayakkara, C.M.; Abeytunga, D.T.U.M.; Lee, D.S.; Lee, J.S.; et al. Fucoidan purified from *Sargassum polycystum* induces apoptosis through mitochondria-mediated pathway in HL-60 and MCF-7 cells. *Mar. Drugs* **2020**, *18*, 196. [CrossRef] [PubMed]
24. Oliveira, C.; Neves, N.M.; Reis, R.L.; Martins, A.; Silva, T.H. A review on fucoidan antitumor strategies: From a biological active agent to a structural component of fucoidan-based systems. *Carbohydr. Polym.* **2020**, *239*, 116131. [CrossRef]
25. Peñalver, R.; Lorenzo, J.M.; Ros, G.; Amarowicz, R.; Pateiro, M.; Nieto, G. Seaweeds as a functional ingredient for a healthy diet. *Mar. Drugs* **2020**, *18*, 301. [CrossRef]
26. Bittkau, K.S.; Dörschmann, P.; Blümel, M.; Tasdemir, D.; Roider, J.; Klettner, A.; Alban, S. Comparison of the effects of fucoidans on the cell viability of tumor and non-tumor cell lines. *Mar. Drugs* **2019**, *17*, 441. [CrossRef]
27. Martínez Andrade, K.A.; Lauritano, C.; Romano, G.; Ianora, A. Marine microalgae with anti-cancer properties. *Mar. Drugs* **2018**, *16*, 165. [CrossRef]
28. van Weelden, G.; Bobiński, M.; Okła, K.; van Weelden, W.J.; Romano, A.; Pijnenborg, J.M.A. Fucoidan structure and activity in relation to anti-cancer mechanisms. *Mar. Drugs* **2019**, *17*, 32. [CrossRef]
29. Kiddane, A.T.; Kim, G.D. Anticancer and immunomodulatory effects of polysaccharides. *Nutr. Cancer* **2020**. [CrossRef]
30. Lin, Y.; Qi, X.; Liu, H.; Xue, K.; Xu, S.; Tian, Z. The anti-cancer effects of fucoidan: A review of both in vivo and in vitro investigations. *Cancer Cell Int.* **2020**, *20*, 154. [CrossRef]
31. Techel, I.; Lahrsen, E.; Alban, S. Degraded fucoidan fractions and β-1,3-glucan sulfates inhibit CXCL12-induced Erk1/2 activation and chemotaxis in Burkitt lymphoma cells. *Int. J. Biol. Macromol.* **2020**, *143*, 968–976. [CrossRef] [PubMed]
32. Grünewald, N.; Alban, S. Optimized and standardized isolation and structural characterization of anti-inflammatory sulfated polysaccharides from the red alga *Delesseria sanguinea* (Hudson) Lamouroux (Ceramiales, Delesseriaceae). *Biomacromolecules* **2009**, *10*, 2998–3008. [CrossRef] [PubMed]
33. Ehrig, K.; Alban, S. Sulfated galactofucan from the brown alga *Saccharina latissimi*—Variability of yield, structural composition and bioactivity. *Mar. Drugs* **2014**, *13*, 76–101. [CrossRef] [PubMed]
34. Lahrsen, E.; Schoenfeld, A.-K.; Alban, S. Degradation of eight sulfated polysaccharides extracted from red and brown algae and its impact on structure and pharmacological activities. *ACS Biomater. Sci. Eng.* **2019**, *5*, 1200–1214. [CrossRef]
35. Allen, J.; Brock, S.A. Tailoring the message. *Minn. Med.* **2000**, *83*, 45–48.
36. Filisetti-Cozzi, T.M.C.C.; Carpita, N.C. Measurement of uronic acids without interference from neutral sugars. *Anal. Biochem.* **1991**, *197*, 157–162. [CrossRef]

37. Blakeney, A.B.; Harris, P.J.; Henry, R.J.; Stone, B.A. A simple and rapid preparation of alditol acetates for monosaccharide analysis. *Carbohydr. Res.* **1983**, *113*, 291–299. [CrossRef]
38. Lee, S.Y.; Sarkar, S.; Bhattarai, S.; Namasivayam, V.; De Jonghe, S.; Stephan, H.; Herdewijn, P.; El-Tayeb, A.; Müller, C.E. Substrate-Dependence of competitive nucleotide pyrophosphatase/phosphodiesterase1 (NPP1) inhibitors. *Front. Pharmacol.* **2017**, *8*, 1–7. [CrossRef]
39. Lineweaver, H.; Burk, D. The Determination of enzyme dissociation constants. *J. Am. Chem. Soc.* **1934**, *56*, 658–666. [CrossRef]
40. Grobben, B.; De Deyn, P.; Slegers, H. Rat C6 glioma as experimental model system for the study of glioblastoma growth and invasion. *Cell Tissue Res.* **2002**, *310*, 257–270. [CrossRef]
41. Aerts, I.; Martin, J.J.; De Deyn, P.P.; Van Ginniken, C.; Van Ostade, X.; Kockx, M.; Dua, G.; Slegers, H. The expression of ecto-nucleotide pyrophosphatase/phosphodiesterase 1 (E-NPP1) is correlated with astrocytic tumor grade. *Clin. Neurol. Neurosurg.* **2011**, *113*, 224–229. [CrossRef] [PubMed]
42. Gõmez-Villafuertes, R.; Pintor, J.; Miras-Portugal, M.T.; Gualix, J. Ectonucleotide pyrophosphatase/phosphodiesterase activity in neuro-2a neuroblastoma cells: Changes in expression associated with neuronal differentiation. *J. Neurochem.* **2014**, *131*, 290–302. [CrossRef]
43. Bageritz, J.; Puccio, L.; Piro, R.M.; Hovestadt, V.; Phillips, E.; Pankert, T.; Lohr, J.; Herold-Mende, C.; Lichter, P.; Goidts, V. Stem cell characteristics in glioblastoma are maintained by the ecto-nucleotidase E-NPP1. *Cell Death Differ.* **2014**, *21*, 929–940. [CrossRef] [PubMed]
44. Xu, S.; Shao, Q.Q.; Sun, J.T.; Yang, N.; Xie, Q.; Wang, D.H.; Huang, Q.B.; Huang, B.; Wang, X.Y.; Li, X.G.; et al. Synergy between the ectoenzymes CD39 and CD73 contributes to adenosinergic immunosuppression in human malignant gliomas. *Neuro Oncol.* **2013**, *15*, 1160–1172. [CrossRef]
45. Pastor-Anglada, M.; Pérez-Torras, S. Who is who in adenosine transport. *Front. Pharmacol.* **2018**, *9*, 1–10. [CrossRef]
46. Poppe, D.; Doerr, J.; Schneider, M.; Wilkens, R.; Steinbeck, J.A.; Ladewig, J.; Tam, A.; Paschon, D.E.; Gregory, P.D.; Reik, A.; et al. Genome editing in neuroepithelial stem cells to generate human neurons with high adenosine-releasing capacity. *Stem Cells Transl. Med.* **2018**, *7*, 477–486. [CrossRef] [PubMed]
47. Gorelik, A.; Randriamihaja, A.; Illes, K.; Nagar, B. Structural basis for nucleotide recognition by the ectoenzyme CD203c. *FEBS J.* **2018**, *285*, 2481–2494. [CrossRef] [PubMed]
48. Lopez, V.; Lee, S.-Y.; Stephan, H.; Müller, C.E. Recombinant expression of ecto-nucleotide pyrophosphatase/phosphodiesterase 4 (NPP4) and development of a luminescence-based assay to identify inhibitors. *Anal. Biochem.* **2020**, *603*, 113774. [CrossRef] [PubMed]
49. Lévesque, S.A.; Lavoie, É.G.; Lecka, J.; Bigonnesse, F.; Sévigny, J. Specificity of the ecto-ATPase inhibitor ARL 67156 on human and mouse ectonucleotidases. *Br. J. Pharmacol.* **2007**, *152*, 141–150. [CrossRef]
50. Kukulski, F.; Lévesque, S.A.; Lavoie, E.G.; Lecka, J.; Bigonnesse, F.; Knowles, A.F.; Robson, S.C.; Kirley, T.L.; Sévigny, J. Comparative hydrolysis of P2 receptor agonists by NTPDases 1, 2, 3 and 8. *Purinergic Signal.* **2005**, *1*, 193–204. [CrossRef]
51. Cogan, E.B.; Birrell, G.B.; Griffith, O.H. A robotics-Based automated assay for inorganic and organic phosphates. *Anal. Biochem.* **1999**, *271*, 29–35. [CrossRef] [PubMed]
52. Junker, A.; Renn, C.; Dobelmann, C.; Namasivayam, V.; Jain, S.; Losenkova, K.; Irjala, H.; Duca, S.; Balasubramanian, R.; Chakraborty, S.; et al. Structure-Activity relationship of purine and pyrimidine nucleotides as ecto-5′-nucleotidase (CD73) inhibitors. *J. Med. Chem.* **2019**, *62*, 3677–3695. [CrossRef] [PubMed]
53. Freundlieb, M.; Zimmermann, H.; Müller, C.E. A new, sensitive ecto-5-nucleotidase assay for compound screening. *Anal. Biochem.* **2014**, *446*, 53–58. [CrossRef] [PubMed]
54. Qurishi, R.; Kaulich, M.; Müller, C.E. Fast, efficient capillary electrophoresis method for measuring nucleotide degradation and metabolism. *J. Chromatogr. A* **2002**, *952*, 275–281. [CrossRef]
55. Kaulich, M.; Qurishi, R.; Müller, C.E. Extracellular metabolism of nucleotides in neuroblastoma x glioma NG108-15 cells determined by capillary electrophoresis. *Cell. Mol. Neurobiol.* **2003**, *23*, 349–364. [CrossRef]

2.3 Summary and outlook

Four sulfonated polysaccharides, extracted from brown and red sea algae, were explored in this work as possible inhibitors of ectonucleotidases. We first examined the compounds' effects on the most prevalent ectonucleotidase families: NPPs (NPP1, 3, 4, 5), NTPDases (NTPDase1, 2, 3, 8) and CD73. NPP1 and CD39 were the most strongly inhibited enzymes by all candidates. Subsequently, we explored concentration-dependent inhibition by establishing complete concentration-inhibition curves for all four compounds at NPP1 and CD39 and calculating their K_i values. These sulfonated polysaccharides isolated from marine algae were found to be the most effective NPP1 inhibitors known to date, with nano- to sub-nanomolar potencies, showing ancillary CD39 inhibition. Compound 5 (from *Delesseria sanguinea*) is a highly selective inhibitor of hNPP1 with picomolar inhibitory potency (K_i 0.0517 nM) and ancillary CD39 inhibition (K_i 1.72 nM), and high selectivity against all other studied ectonucleotidases. Sulfated polysaccharide 6 (from *Saccharina latissima*) is equally potent at NPP1 and CD39, and hence can be considered a dual inhibitor of NPP1 and CD39. This dual activity may be a significant advantage in cancer therapy, as both ATP-hydrolyzing enzymes may be increased and serve as redundant nucleotide degradation routes. We investigated the mode of inhibition for compound 7, as a representative of this novel class of ectonucleotidase inhibitors, utilizing ATP as a substrate. We studied the effect of inhibitor 7 on the kinetics of NPP1 and CD39. Michaelis-Menten plots and Lineweaver-Burk plots both show a non-competitive/mixed type of inhibition in both cases. Finally, we examined compound 7 derived from *Fucus vesiculosus* in a cellular environment. NPP1 and CD73 expression was reported in the human glioma cell line U-87. In a sequential chemical cascade, these enzymes convert ATP to adenosine. As a result, we used this cancer cell line to determine how extracellular ATP is hydrolyzed in the cells, resulting in the formation of adenosine, which is known to induce proliferative, angiogenic, metastasis-promoting, and immunosuppressive properties when released into the tumor microenvironment.

The results clearly demonstrated that the sulfopolysaccharide inhibited adenosine production in U87 glioma cells in a concentration-dependent manner, which is attributable to blocking NPP1 activity. In conclusion, we discovered that sulfopolysaccharides derived from marine algae are extremely powerful, non-competitive inhibitors of the ectonucleotidases NPP1 and CD39, with somewhat greater inhibitory potency against NPP1. Both enzymes catalyze the hydrolysis of antiproliferative ATP to produce, in conjunction with the AMP-hydrolyzing ectoenzyme CD73, adenosine, a compound with immunosuppressive and tumor-promoting properties. Indeed, we observed decreased adenosine synthesis in human glioma U87 cells treated with a representative example of the examined sulfopolysaccharides. These effects could account for or contribute to the previously documented anti-cancer properties of sulfated algal polysaccharides from sea weeds, which have been demonstrated to be non-toxic and well tolerated by humans. The presented novel data represent a solid and promising basis for further investigations in the field of anticancer treatment using nature-derived drugs.

3. **Heparins are potent inhibitors of ectonucleotide pyrophosphatase/phosphodiesterase-1 (NPP1) – a promising target for the immunotherapy of cancer and infections**

3.1 Introduction

Due to its potent anticoagulant effect heparin is used to prevent and treat venous thromboembolism in cancer patients. Different clinical investigations indicate that anticoagulant therapy with heparin, improves the prognosis and survival of patients with diversiform tumors. These data indicate that heparin is not only an excellent anticoagulant, but potentially a unique anticancer drug that has yet to be discovered. Heparin may slow the progression of cancer and metastases, according to a growing body of research. Apart from its anticoagulant function, heparin possesses several biological activities that may influence cancer growth, including the inhibition of heparanase, the suppression of P-and L-selectin-mediated cell adhesion, and the prevention of angiogenesis [1-5]. Heparin and its derivatives interact with different proteins in the body but it is yet unclear if other proteins may also be a suitable pharmacological target, for this reason and due to the role of hNPP1 in immuno-oncology we have been motivated to investigate the inhibitory effects of heparin on ectonucleotidase family, furthermore those heparins are negatively charged, similar to previously known potent ectonucleotidase inhibitors (such as sulfated polysaccharides and polyoxometalates complex). In the following manuscript we present the results of this interesting study.

References

1. Borsig, L. Antimetastatic activities of heparins and modified heparins. Experimental evidence. *Thromb. Res.* **2010**, *125*, S66–S71, doi:10.1016/S0049-3848(10)70017-7.

2. Bendas, G.; Borsig, L. Cancer cell adhesion and metastasis: Selectins, integrins, and the inhibitory potential of heparins. *Int. J. Cell Biol.* **2012**, *2012*, doi:10.1155/2012/676731.

3. Ma, S.N.; Mao, Z.X.; Wu, Y.; Liang, M.X.; Wang, D.D.; Chen, X.; Chang, P. an; Zhang, W.; Tang, J.H. The anti-cancer properties of heparin and its derivatives: a review and prospect. *Cell Adhes. Migr.* **2020**, *14*, 118–128, doi:10.1080/19336918.2020.1767489.

4. Smorenburg, S.M.; Van Noorden, C.J.F. The complex effects of heparins on cancer progression and metastasis in experimental studies. *Pharmacol. Rev.* **2001**, *53*, 93–105.

5. Kuderer, N.M.; Khorana, A.A.; Lyman, G.H.; Francis, C.W. A meta-analysis and systematic review of the efficacy and safety of anticoagulants as cancer treatment: Impact on survival and bleeding complications. *Cancer* **2007**, *110*, 1149–1161, doi:10.1002/cncr.22892

3.2 Preliminary manuscript

Heparins are potent inhibitors of ectonucleotide pyrophosphatase/phosphodiesterase-1 (NPP1) – a promising target for the immunotherapy of cancer and infections

Vittoria Lopez, [a, b] H.J. Maximilian Schuh, [c] Salahuddin Mirza, [a, b] Michael S. Schmidt,[c] Katharina Sylvester , [a, b] Riham Mohammed Idris, [a, b] Christian Renn, [a, b] Laura Schäkel, [a, b] Julie Pelletier, [d, e] Jean Sévigny, [d, e] Annamaria Naggi, [f] Sang-Yong Lee, [a, b] Björn Scheffler,[g] Gerd Bendas,[c] and Christa E. Müller [a, b]*[1]

[1] The author sequence after the first author is provisional and may change in the final published version

[a] Pharmaceutical Institute, Pharmaceutical & Medicinal Chemistry, University of Bonn, Bonn, Germany

[b] PharmaCenter Bonn, University of Bonn, An der Immenburg 4, 53121 Bonn, Germany

[c] Pharmaceutical Institute, Pharmaceutical and Cell Biology Chemistry, University of Bonn, Bonn, Germany

[d] Centre de Recherche du CHU de Québec – Université Laval, Québec City, QC, Canada

[e] Départment de Microbiologie-Infectiologie et d'Immunologie, Faculté de Médecine, Université Laval, Quebec City, QC, Canada

[f] Institute for Chemical and Biochemical Research "G. Ronzoni", Milan, Italy

[g] Division of Translational Oncology / Neurooncology at the West German Cancer Canter (WTZ) University Hospital Essen, Germany

*Address correspondence to:

Prof. Dr. Christa E. Müller
Pharmaceutical Institute, Pharmaceutical & Medicinal Chemistry
An der Immenburg 4, D-53121 Bonn, Germany
Phone: +49-228-73-2301
Fax: +49-228-73-2567
E-Mail : christa.mueller@uni-bonn.de

Abstract

Heparins, including unfractionated, low-molecular-weight, and synthetic heparins, that are routinely used for the prevention of venous thromboembolism, have been found to improve the survival rate of cancer patients in several studies. Heparin was reported to affect cancer cell proliferation, adhesion, angiogenesis, migration, and invasion. Extracellular ATP is known to exert antiproliferative and immunostimulatory effects by activating nucleotide P2 receptors expressed in cell membranes. Its metabolite, the nucleoside adenosine, is strongly immunosuppressive and promotes tumor proliferation, metastasis, and angiogenesis. Ectonucleotidases, which are expressed on immune cells and are often upregulated on tumor cells, catalyze the conversion of ATP to adenosine providing a cancer-promoting microenvironment. The prominent ATP-hydrolyzing ectonucleotidase nucleotide pyrophosphatase/phosphodiesterase-1 (NPP1) was recently discovered to additionally catalyze the degradation of another potent activator of immune responses, namely guanosine-(2′,5′)-monophosphate-adenosine-(3′,5″)-monophosphate (2′,3″-cGAMP), an activator of STING (stimulator of interferon genes). In the present study, we discovered that heparin and its derivatives act as potent and selective allosteric inhibitors of NPP1 in vitro and in vivo, at the surface of the human NPP1-expressing glioma cell line U87, inhibiting adenosine production in a concentration-dependent manner. Inhibition was observed at therapeutically relevant concentrations. Structure-activity relationship analysis indicated that the NPP1-inhibitory activity can be separated from the antithrombotic effect. Heparin-derived biomacromolecules have the potential for further optimization as NPP1 inhibitors that are promising therapeutics for the immunotherapy of cancer and infections.

Abbreviations: **ADO**, adenosine; **cGAMP**, cyclic guanosine-(2′,5′)-monophosphate-adenosine-(3′,5″)-monophosphate; **CD,** cluster of differentiation; **CE**, capillary electrophoresis; **CHES,** *N*-cyclohexyl-2-aminoethanesulfonic acid; **CD39**, nucleoside triphosphate diphosphohydrolase-1 (NTPDase1); **CD73**, ecto-5’-nucleotidase; **DAD**, diode array detector; **DMEM**, Dulbecco’s Modified Eagle Medium; **EDTA**, Ethylenediaminetetraacetic acid; **HEPES**, 4-(2-hydroxyethyl)piperazine-1-ethanesulfonic acid; **INO**, inosine; **LMWH**, low molecular weight heparin; **NTPDase1**, nucleoside triphosphate diphosphohydrolase-1; **NPP1**, nucleotide pyrophosphatase/phosphodiesterase-1; **NKT**, natural killer T-cell; **PC**-1, plasma cell membrane glycoprotein-1; **p*IC*$_{50}$**, negative log of the half-maximal inhibitory concentration;

***p*NP-TMP,** *p*-nitrophenyl thymidine 5-monophosphate; **PBS,** phosphate-buffered saline; **SDS,** sodium dodecyl sulfate; **UDO**, uridine; **UFH**, unfractionated heparin.

Keywords: adenosine; ectonucleotidase inhibitors; NPP1 inhibitors; immuno-oncology; U87 cells; heparin derivatives; UFH; LMWH.

Graphical abstract

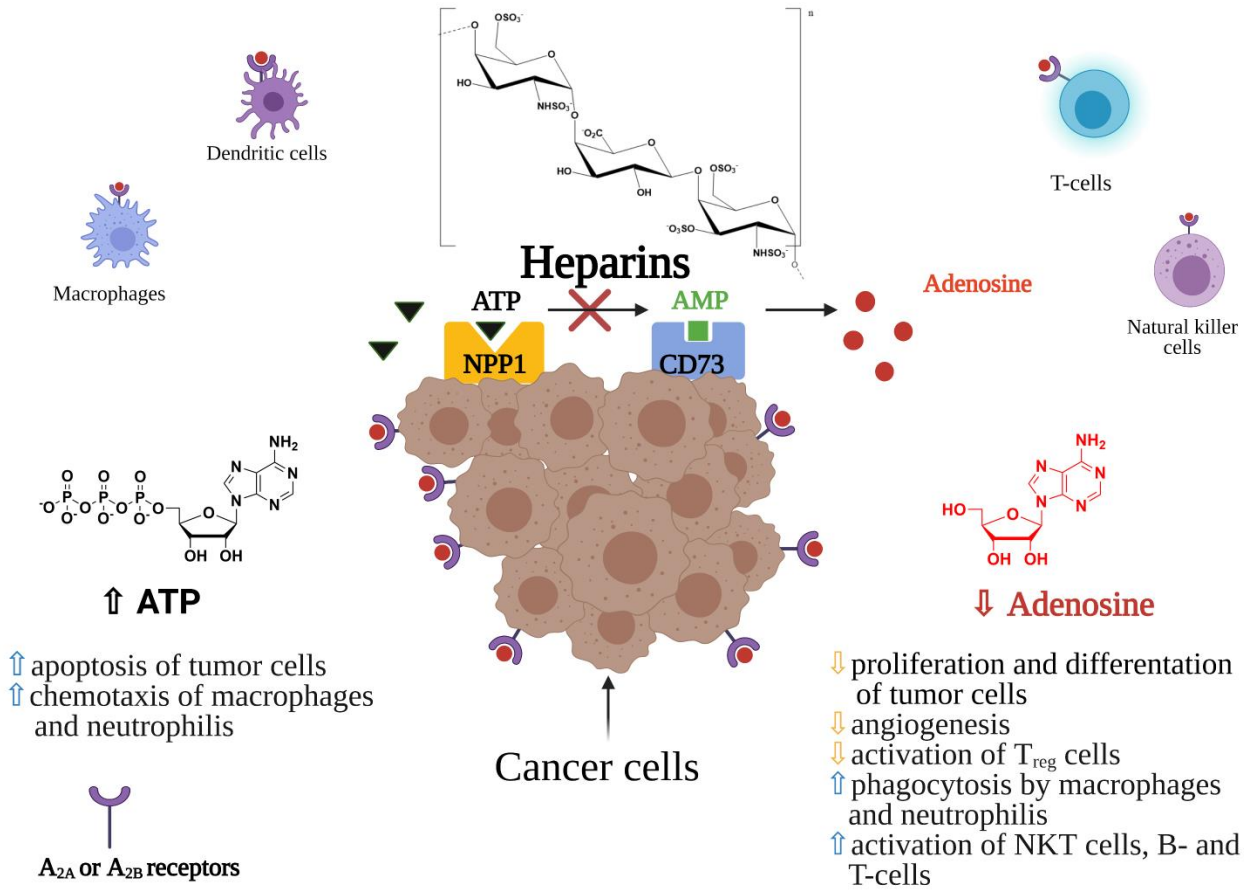

INTRODUCTION

Heparin is a heterogeneous mixture of linear sulfated glycosaminoglycan polymers ranging in molecular weight between 3000 and 30,000 Da with an average of 15 kDa [1]. It is a naturally occurring anticoagulant that is secreted by mast cells and binds reversibly to antithrombin III. Thereby, it enhances the rate at which antithrombin III inactivates the pro-coagulatory enzymes thrombin (factor IIa) and factor Xa resulting in an antithrombotic effect [1]. Anticoagulant therapy with heparin is frequently used to prevent or treat thromboembolism associated with cancer. Clinical evidence suggests that heparin and its low-molecular-weight fractions enhance cancer patient survival [2-5]. Heparin's potential to inhibit metastasis has been demonstrated experimentally in a variety of animal models [3,5]. Apart from its anticoagulant activity, heparin possesses several biological activities that might contribute to its anti-cancer effects, e.g., inhibition of heparanase and the suppression of P- and L-selectin-mediated cell adhesion [4]. However, the precise mechanism by which heparins exert anti-cancer effects and enhance cancer patient survival is still unknown.

We recently observed that sulfopolysaccharides isolated from sea algae [6] can inhibit ATP-hydrolyzing ectonucleotidases NPP1 (CD203a; CD, cluster of differentiation) and CD39, enzymes whose important role in cancer proliferation, angiogenesis, metastasis, and immune escape is increasingly recognized [7]. Ectonucleotidases are expressed on cancer cells, catalyzing the hydrolysis of ATP released by the cells due to hypoxic conditions and cell death, producing cancer-promoting, immunosuppressive adenosine (see Figure 1) [7-9].

These surface-bound ecto-nucleosidases include ecto-nucleoside triphosphate diphosphohydrolases (NTPDases, EC 3.6.1.5), ecto-nucleotide pyrophosphatases/phospho-diesterases (NPPs, EC 3.6.1.9), and ecto-5′-nucleotidase (CD73, EC 3.1.3.5) [7]. NTPDases convert nucleoside 5′-triphosphates (NTPs) to nucleoside 5′-diphosphates (NDPs) and further to nucleoside 5′-monophosphates (NMPs) [9]. The NPP subfamily of ectonucleotidases degrades NTPs directly to NMPs, releasing diphosphate (pyrophosphate, PP_i) [9]. CD73 further hydrolyzes NMPs to nucleosides, primarily AMP to adenosine [7,9].

The main substrate of human NPP1, or CD203a, previously known as PC-1 (plasma cell membrane glycoprotein-1), is ATP [10]. In addition, it hydrolyzes further nucleotides, e.g., nicotinamide adenine dinucleotide (NAD^+), diadenosine polyphosphates and cyclic dinucleotides such as cyclic guanosine-(2′,5′)-monophosphate-adenosine-(3′,5″)-monophosphate (2′,3″-cGAMP) (see **Figure 1**). This cyclic dinucleotide is the natural agonist of

the stimulator of interferon genes (STING), which is crucial for the induction of a type I interferon response by the innate immune system [10-12]. Inhibiting the hydrolysis of immunostimulatory ATP and cGAMP and the subsequent production of immunosuppressive, cancer-promoting adenosine has been proposed as a novel strategy to treat cancer and infections [13].

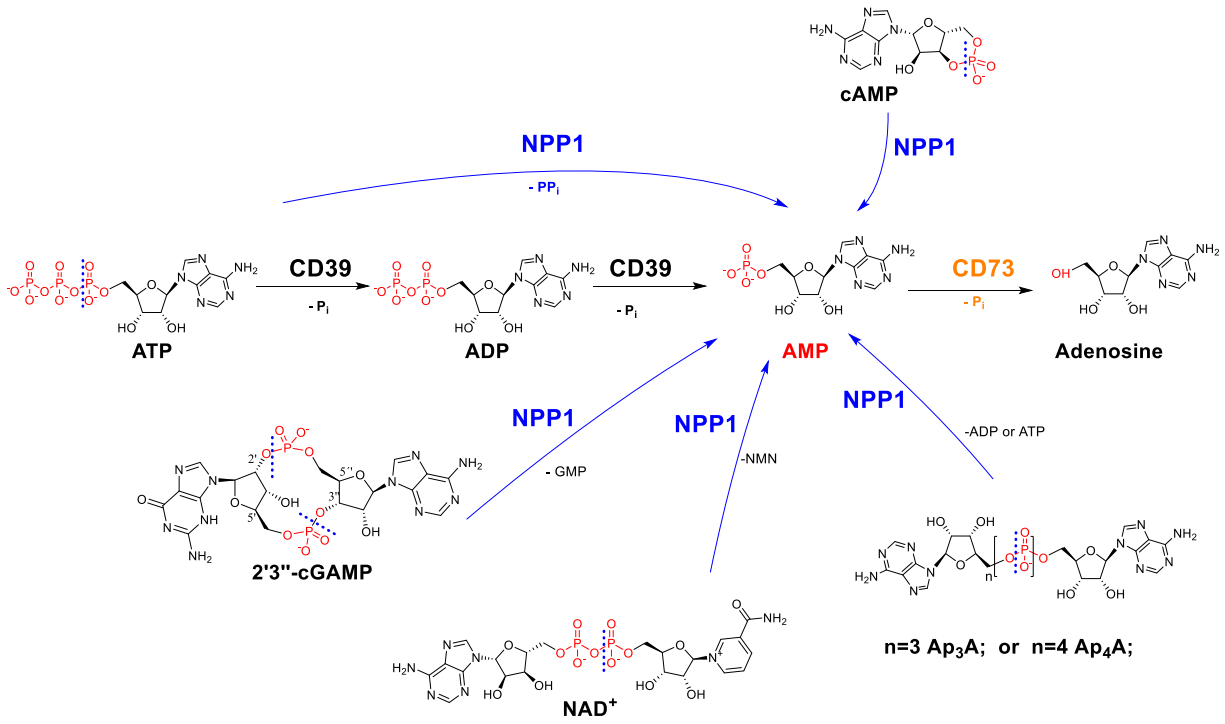

Figure 1. Ectonucleotidases present in cell membranes catalyze the hydrolysis of extracellular nucleotides finally yielding cancer-promoting, immunosuppressive adenosine. NPP1 (CD203a): ecto-nucleotide pyrophosphatase/phosphodiesterase-1; CD39: ecto-nucleoside triphosphate diphosphohydrolase-1 (NTPDase1); CD73: ecto-5'-nucleotidase. CD, cluster of differentiation; NMP, nucleoside monophosphate; P_i, inorganic phosphate.

In the present study, we investigated the potential of heparin and heparin-derived sulfopolysaccharides to inhibit ectonucleotidases. In fact, we discovered that heparin and its derivatives are potent and selective allosteric inhibitors of NPP1. This mechanism of action may contribute to the anti-cancer effects observed for some heparins. The present results and the observed structure-activity relationships provide the basis for the future development of more potent NPP1 inhibitors lacking the associated anti-thrombotic activity.

MATERIALS AND METHODS

Chemicals

Nucleotides (AMP, ADP, ATP, cAMP), nucleosides (adenosine, ADO; inosine, INO; uridine; UDO), dipyridamole, EHNA (erythro-9-(2-hydroxy-3-nonyl)adenine), disodium hydrogen phosphate, and sodium dodecyl sulfate were purchased from Sigma-Aldrich Chemie GmbH by Merck (Darmstadt, Germany). Sodium chloride, potassium chloride, potassium dihydrogen phosphate, sodium hydrogencarbonate, D-glucose, HEPES (*N*-[2-hydroxyethyl]piperazine-*N*'-[2-ethanesulfonic acid]), calcium chloride, and magnesium sulfate were purchased from PAN Biotech GmbH (Aidenbach, Germany). Dulbecco's Modified Eagle Medium, fetal calf serum (FCS), penicillin/streptomycin (P/S) mixture, and L-glutamine were also from PAN Biotech GmbH. The commercially available heparin and derivatives were purchased from the following sources: unfractionated (UFH) heparin-sodium (**1**), Heparin-25000-ratiopharm; LMWH, tinzaparin (**2**), Innohep®, dalteparin (**3**) under the brand name of Fragmin®, nadroparin (**4**) as Fraxiparin®, enoxaparin (**5**) as Clexane®, fondaparinux (**6**) as Arixtra®. The non-commercially available compounds **7-15** were synthetized as described [14] (see **Table 1** and **Figure 2** for details).

Table 1. Investigated heparins

No.	Compound	MW (KDa)	SD[a]	Structural Information[b]	Targets (Activity)[c]
1	Heparin sodium	8-25	2.7	25-40 m.u.	- Antithrombin III (potentiator) - Factor Xa and IIa (inhibitor) - P-selectin (inhibitor) - Heparanase (inhibitor)
2	Tinzaparin	6.5		~ 20 m.u.	
3	Dalteparin	5.0	2.6	~ 17 m.u.	
4	Nadroparin	4.5	2.5	< 17 m.u.	- Antithrombin III (potentiator) - Factor Xa (inhibitor) - P-selectin (inhibitor) - Heparanase (inhibitor)
5	Enoxaparin	4.5	2.3		
6	Fondaparinux	1.7	8	pentasaccaride	- Antithrombin III (potentiator) - Factor Xa (inhibitor)
7	G9694	16.6	2.2	RO heparin (reduced oxyheparin) repetitive disaccharide unit MW 600	
8	G5945	16.6	1.1	2-O-des-heparin (desulphated) repetitive disaccharide unit	

				Mw 530	
9	G6658	15.4	0.7	6-O-des-heparin (85% 6-OH; 52% non-sulfated uronic acid) repetitive disaccharide unit of MW 490 Da	
10	A3875-G6	3.6	2.6	dodesaccharide fraction of dalteparin (dalte)	
11	A3875-H6	3.0	2.6	dalte-ecasaccharide	
12	A3875-I6	2.4	2.7	dalte-octasaccharide	
13	G4271A	3.0	nd[d]	depolymerization product of RO-heparin and 2-O-des heparin	
14	G4271B	3.0	nd	depolymerization product of RO-heparin and 2-O-des heparin	
15	G4185	ca. 3.0	nd	G4271A + G4271B	

[a] Sulfation degree (average number of sulfate groups per disaccharide repeating unit; for fondaparinux the total number of sulfate group is given).

[b] **Factor Xa**: produced by both extrinsic tenase and intrinsic tenase complexes, represents the point of convergence of the extrinsic and intrinsic pathways of the coagulation cascade and converts prothrombin into thrombin; **Factor IIa**: thrombin

[c] **m.u.**: monosaccharide unit

[d] nd, not determined

Experimental details

2.1 NPP1 assay

Concentration-inhibition curves of the test compounds at human NPP1 were performed with ATP as substrate at a final concentration of 400 µM. Several different dilutions of the test compounds were prepared in assay buffer (10 mM *N*-cyclohexyl-2-aminoethanesulfonic acid (CHES), 2 mM $CaCl_2$, 1 mM $MgCl_2$, pH 9.00) and incubated with 20 ng of human recombinant soluble NPP1 (Val191 - Leu591) expressed in murine myeloma NS0 cells obtained from R&D Systems GmbH (Wiesbaden, Germany, purity 95%, purified by using an *N*-terminal His-tag). For initial screening and selectivity analysis, NPP1 prepared as previously described [15], diluted in assay buffer, was used. The mixture of enzyme, substrate and test compound or buffer without test compound was incubated for 30 min at 37 °C, and the reaction was terminated by heating at 90 °C for 5 min. Capillary electrophoresis (CE) analysis was carried out to analyze the formation of the product. Data collection and peak area analysis were performed by the P/ACE MDQ software

32 KARAT obtained from Beckman Coulter (Fullerton, CA, USA). A polyacrylamide-coated capillary was used [30 cm (20 cm effective length) × 50 µm (id) × 360 µm (od) purchased from Chromatographie Service GmbH (Langerwehe, Germany)]. Samples were injected electro-kinetically by applying a voltage of -6 kV for 30 s. Finally, analytes were separated by applying a separation voltage of -20 kV, and detected by UV at 260 nm. The IC_{50} values were determined by nonlinear curve fitting using the GraphPad Prism Software 7.0. The mechanism of inhibition at human NPP1 was determined employing different concentrations of the investigated compounds **6** (at 0, 0.4, 4.0 µM), and **7** (at 0.4 and 40 µM) versus four different substrate concentrations ranging from 20 to 500 µM of ATP. The assay procedure and operation conditions were the same as described above. The experiment was conducted twice, each in triplicates. A Lineweaver-Burk was calculated using GraphPad Prism 7.0 for predicting the inhibition type of the compound.

2.2 NPP3 and NPP5 assay

Compounds **1**, **2**, **5**, **6**, and **7** were screened at different concentrations using 400 µM of *p*-nitrophenyl thymidine monophosphate (*p*-Nph-5´-TMP) as substrate to study potential inhibition of NPP3 and NPP5 using a colorimetric assay as previously described [16]. Soluble and purified human NPP3, prepared as previously described [17], and human NPP5 [18] were diluted in the assay buffer (50 mM TRIS HCl, 2 mM $CaCl_2$, and 0.2 mM $ZnCl_2$ pH 9.00), and 0.09 µg of enzyme NPP3, or 0.4 µg of NPP5 were employed. The mixtures were incubated for 30 min at 37 °C in case of NPP3, and for 100 min at 37 °C in case of NPP5, and the reactions were subsequently terminated by adding 20 µL of 1.0 N aq. NaOH solution. The assay is based on the enzymatic ester hydrolysis of *p*-Nph-5'-TMP which results in the formation of the yellow *p*-nitrophenolate anion. The absorption maximum was measured at 400 nm using a BMG PheraStar FS plate reader (BMG Labtech GmbH, Ortenberg, Germany). Each analysis was repeated three times with triplicate measurements.

2.3 NPP4 assay

Selectivity studies on NPP4 were performed using the published luminescence-based assay [19] versus 20 µM of diadenosine tetraphosphate (Ap_4A) as a substrate and human soluble NPP4 [19]. The assay buffer consisted of 10 mM HEPES, 1 mM $MgCl_2$, and 2 mM $CaCl_2$ (pH 8.00). The enzyme reaction was started by adding 0.14 µg of purified human NPP4 to the reaction mixture, which was incubated at 37 °C for 90 min. The released product ATP was quantified using the luciferin-luciferase reaction. The firefly luciferase reacts with D-luciferin in the presence of the

formed ATP and Mg^{2+}, which act as a co-factor. The resulting luminescence is a measure of the enzymatic activity, and the luminescence was read at 560 nm using a microplate reader (BMG PheraStar). Three independent experiments were performed, each in duplicate measurements.

2.4 NTPDase assays

For monitoring the activity of human NTPDases (subtypes 1, 2, 3 and 8) in the presence of test compounds a CE-based assay system was used, according to a published procedure [6]. The following concentrations of test compounds were investigated in initial screening studies: 63 IU/ml of compounds **1** and **2**, 30 µM of compound **6**. For selectivity studies, the following concentration were employed: 50 IU/mL of **1**, 12 µM of **6**, and 48 µM of **7**. The amount of enzyme was selected according to previously performed enzymatic titration, and adjusted to ensure a 10–20 % conversion rates. Enzymes were expressed and purified as previously described [20,21]. The reaction buffer consisted of 10 mM HEPES, 2 mM $CaCl_2$, and 1 mM $MgCl_2$, pH 7.4. In the CE assay, the selected substrate concentration (ATP) was 100 µM for all human NTPDases (1, 2, 3 and 8). Mixtures of enzymes with substrate and test compounds were incubated at 37 °C for 30 min, and the enzymatic reaction was stopped by heating for 10 min at 95 °C. The released products were separated by capillary electrophoresis and quantified by their UV-absorption at 260 nm with ADP and AMP as external standards, as previously described [6]; positive and negative control were included.

2.5 CD73 assay

The assay was performed essentially as previously described [22]. The enzymatic reaction was performed by mixing 0.36 ng of human CD73 [23] with test compound in assay buffer (25 mM Tris, 140 mM sodium chloride, 25 mM sodium dihydrogen phosphate, pH 7.4) and 5 µM of [2,8-^{3}H]AMP [(specific activity 7.4x10^8 Bq/mmol (20 mCi/mmol)), American Radio-labeled Chemicals, MO, USA, distributed by Hartmann Analytic, Germany]. Compound **7** was used at 800 µg/mL and compound **6** at 20 µg/mL for the selectivity test, while for initial screening compound **5** was tested at a concentration of 55 µM and **6** at 30 µM, while **1** and **2** were tested at 50 IU/mL (**Figure S1** of Supporting Information). The enzymatic reaction was performed for 25 min at 37°C in a shaking water bath. Then, 500 µl of cold precipitation buffer (100 mM lanthanum chloride, 100 mM sodium acetate, pH 4.00) was added to stop the reaction and to facilitate precipitation of free phosphate and unconverted [2,8-^{3}H]AMP. After the precipitation was completed (after at least 30 min on ice), the mixture was separated by filtration through GF/B glass fiber filters using a cell harvester (M-48, Brandel, MD, USA). After washing each

reaction vial three times with 400 µl of cold (4°C) demineralized water, 5 ml of the scintillation cocktail (ULTIMA Gold XR, PerkinElmer, MA, USA) was added and the radioactivity was measured by scintillation counting (TRICARB 2900 TR, Packard/PerkinElmer; counting efficacy: 49-52%). Positive and negative controls were included.

2.6 mRNA gene expression of ectonucleotidases in primary and secondary human glioblastoma cell lines

The mRNA isolated from several primary human glioblastoma cell lines, namely 46Z, 78Z, 106Z, 138Z, from adults' human brain-derived neural progenitors, 155Z and 167Z, and mRNA isolated from human glioblastoma cell lines T98G, LN229, U138, and U87, were studied with respect to gene expression of ectonucleotidases. A two-step RT-qPCR (quantitative reverse transcription polymerase chain reaction) technique was used. The reverse transcription and PCR amplification steps were performed in two separate reactions. mRNA samples from the cell lines (1 µg) were treated with 1 µl of DNase (NEB; Cat. No. M0303S) for the removal of contaminating genomic DNA, incubated at room temperature, followed by addition of 25 mM of EDTA (ethylenediaminetetraacetic acid) and incubated at 65°C for 10 min. Then, the reverse transcription was achieved with the iScript cDNA Synthesis Kit (Bio-Rad; Cat. Num: 170-8891) using 0.5 µg of reaction mix available from the manufacturer, 1 µl of reverse transcriptase and RNA templates. Subsequently, 1 µl (5000 U/µl) of Rnase H digest (NEB; Cat. No. M0297S) was added to each cDNA sample and incubated for 20 min at 37 °C. Finally, the cDNA samples were diluted to a final concentration of 2.5 ng/µl, and qPCR was performed using SYBR Green (Bio-Rad iQ SYBR Green Supermix; Cat. No. 170-8887); the cDNA (5 ng) was mixed with 250 nM of the respective sequence-specific primers of the different investigated ectonucleotidases, which have been checked for their efficiency, and positive and negative controls together with reference genes were tested in parallel. The qPCR cycle started with polymerase activation and DNA denaturation at 95°C for 3 min, followed by 49 cycles of amplification at 95 °C for 20 s, 60°C for 20 s and 40 s at 68 °C, finishing with 95°C for 30 s and 30 s at 65°C; melt curve: 60 °C to 95 °C, increments of 0.5°C and finally the plate was read (hard shell, thin wall white 96-well plates from Bio-Rad Cat. No. HSP9655). The data were collected and analysed using CFX manager 2.0 software provided by Bio-Rad using their system C1000Thermal Cycler + CFX96 Real-Time System.

2.7 Membrane preparation of U87 cells

U87 glioblastoma cells were grown in cell culture dishes until reaching a fully covered confluent cell layer. Cells were cultivated at 37 °C and 5 % CO_2 in DMEM with additions of 10 % FCS, 1 % penicillin/streptomycin (P/S) mixture and 1 % L-glutamine. When confluent, the cell culture media was carefully removed and cells were frozen at -20 °C overnight. The cells were then scraped off with a cell scraper using 2-3 mL of buffer (5 mM Tris, 2 mM EDTA, pH 7.4), homogenized and centrifuged for 10 min at 1000*g*. The supernatant was collected and centrifuged for 60 min at 48000*g* at 4°C. The pellet was then resuspended twice with Tris buffer, pH 7.4, followed by vortexing and centrifugation. The whole procedure was performed on ice. Finally, the pellet was resuspended and homogenized. A protein concentration of 1.5 mg/ml was determined with the Bradford method [24], and the protein was kept at -20°C until used. The enzymatic assay was performed by incubating the membrane preparation and the substrate at 37°C and 500 rpm for 30 min, followed by heat inactivation at 95°C for 5 min. For the determination of kinetic parameters (**Figure 7** section **A** and **B**), several substrate concentrations (from 6 to 500 µM of ATP or AMP) were utilized and incubated with 10 µg of membrane preparation for 30 min at 37°C, followed by heat inactivation. Capillary electrophoresis (CE) was used for analysis and quantification of the enzymatic product according to published procedures [6,25]. For the determination of the enzymatic activity (**Figure 7C**) 400 µM of ATP were employed, and three different amount of membrane preparation (6, 10 and 30 µg of protein) were utilized. A positive control using the known NPP1 inhibitor PSB-POM-141 (20 µM) was performed [15]. Data were obtained from three independent experiments each in duplicate measurements. Subsequently, compounds **6** and **7** were studied for their potency to reduce adenosine formation, at 3 and 30 µM (Compound **6,** Fondaparinux), and at 35 µM (Compound **7**, G9694). Controls were run in parallel.

2.8 Cell culture, preparation, and cell-based assay

U87 human glioblastoma cells were grown in cell culture flasks until reaching a fully covered confluent cell layer. Cells were cultivated at 37 °C and 5% CO_2 in DMEM with additions of 10 % FCS, 1 % penicillin/streptomycin and 1 % L-glutamine. The cells were rinsed with phosphate-buffered saline (PBS) and detached with EDTA. Thereafter, they were counted by a Cell Counter CASY® 1 Model TT (Schärfe System GmbH, Reutlingen, Germany) to retrieve the number of viable cells, and washed three times with PBS before they were resuspended in Krebs-HEPES

buffer at a concentration of 10^6 cells/mL [26]. Then, 1 mL of cell suspension was transferred into a 24-well plate. The cells were pretreated with the nucleoside transport inhibitor dipyridamole (20 µM) for 30 min [27]. Adenosine deaminase (ADA) activity was inhibited by the addition of 1 µM of the inhibitor EHNA (erythro-9-amino-β-hexyl-α-methyl-9*H*-purine-9-ethanol hydrochloride [28]. Heparins, their non-anticoagulative analogs, and the known ectonucleotidase inhibitor PSB-POM-141 [15] were added. The samples were incubated with 300 µM of ATP for 3 h at 37 °C and 5 % CO_2. Then, an aliquot of 300 µL of solution from each vial was transferred to 1.5 mL Eppendorf tubes, and heated at 95 °C for 10 min to inactivate enzymes in order to avoid further nucleotide degradation. Before performing capillary electrophoresis (CE) measurements, the samples were centrifuged at 600*g* to remove insoluble material like cell debris from the supernatant. Until measurement, the samples were stored at -20 °C. Nucleotides (ATP, ADP, AMP, cAMP) and nucleosides (adenosine, inosine, uridine), which were used as standard compounds to monitor efficient separation by CE, were dissolved in Krebs-HEPES buffer at a concentration of 10 µM and stored at -20 °C [26]. All CE measurements were performed on a P/ACE capillary electrophoresis system MDQ glycoprotein (Beckman Coulter Instruments, Fullerton, CA, USA) using an uncharged fused silica capillary without coating, according to a published method [29]. The capillary dimensions were 40 cm in length (30 cm effective length to detection window) and 75 µm in diameter. Preliminary to the measurement, the capillary was rinsed with 0.1 N aq. NaOH solution, Millipore water and running buffer to establish consistent conditions. The running buffer consisted of sodium dodecyl sulfate (SDS, 100 mM) and disodium hydrogen phosphate (10 mM) at pH 8.0. SDS creates a pseudo-stationary phase, which enables the migration of the uncharged nucleosides. The hydrodynamic injection lasted 30 s with a pressure of 0.1 psi. A constant current of -90 µA and a pressure of 0.1 psi were required for the separation. The detection was performed by a UV diode array detector which allows to identify the UV spectra of the nucleosides and nucleotides at a wavelength of $\lambda = 260$ nm.

RESULTS AND DISCUSSION

Four commercially available heparins, heparin-Na (**1**), tinzaparin (**2**), enoxaparin (**5**) and fondaparinux (**6**) (for structures see **Figure 2**), were initially evaluated as potential inhibitors of prominent members of the ectonucleotidase family, namely NTPDase1 (CD39) and its isoenzymes NTPDase2, -3, and -8, NPP1 and its isoenzymes NPP2 and -3, and ecto-5'-nucleotidase (CD73). We observed almost complete inhibition of human NPP1 by all four compounds at a concentration of 63 IU/mL for heparin-Na (**1**) and tinzaparin (**2**), and 250 µg/mL and 50 µg/mL of enoxaparin (**5**) and fondaparinux (**6**), respectively, while low or very low inhibition was observed for the other investigated ectonucleotidases under the same conditions (**Figure S1,** Supporting Information (**SI**)). Due to the observed selectivity, we decided to test a broader range of heparin derivatives, as potential inhibitors of NPP1.

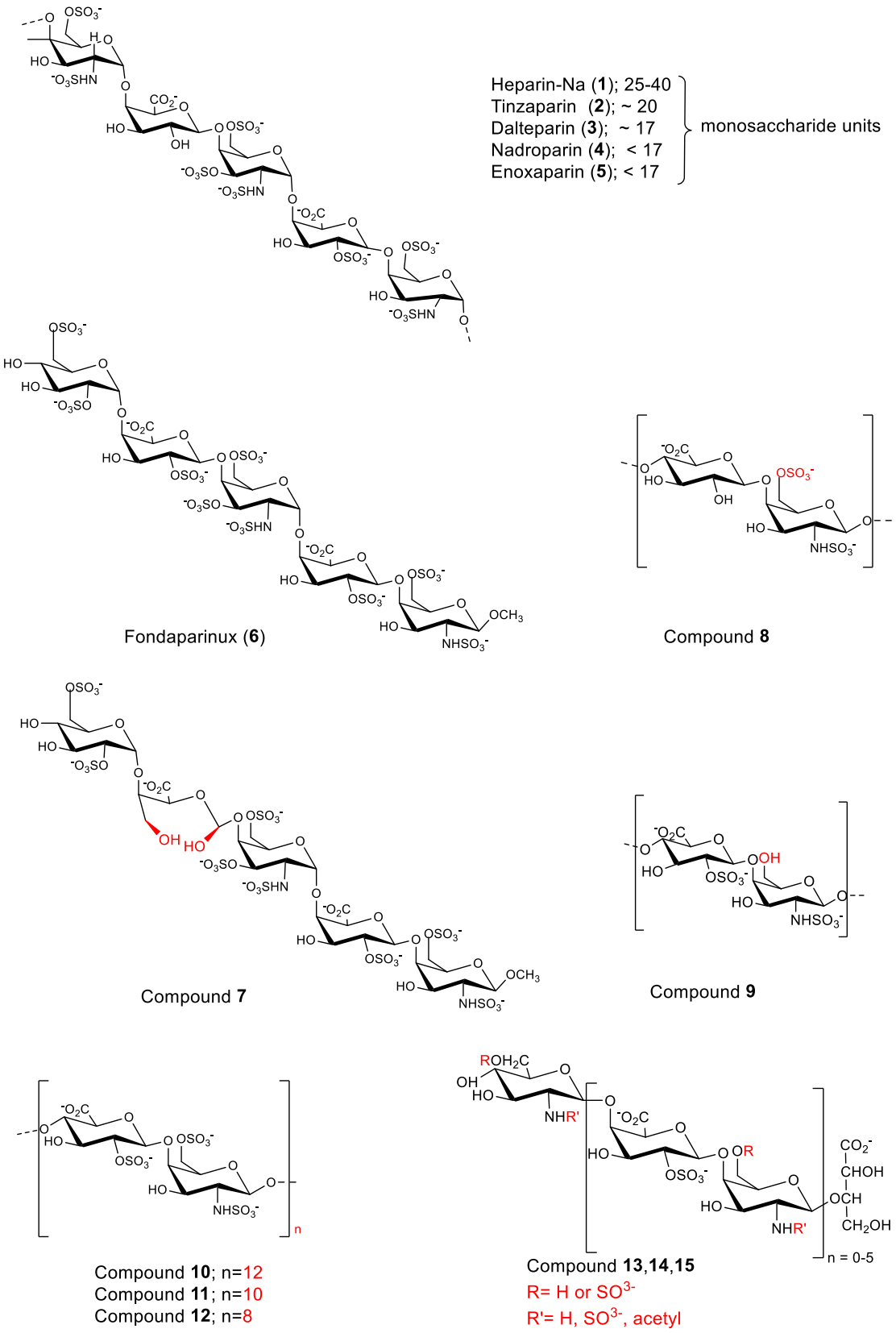

Figure 2. Structures of investigated sulfopolysaccharides. For details see Table 1 and Table 2.

NPP1-inhibitory potency

Heparin is a complex mixture of naturally occurring glycoproteins extracted from pig gut, provided as sodium salts. Unfractionated heparin (UFH, **1**) is distinguished from low molecular weight heparin (LMWH). The latter is obtained from UFH by chemical and enzymatic depolymerization resulting in polysaccharide fragments of smaller size. UFH (**1**) whose MW is ranging from 8-25 KDa, is a linear polymer made up of 1→4 linked disaccharide repeating units, consisting of a α-D-glucosamine and a hexuronic acid, α-L-iduronic or β-D-glucuronic acid. LMWHs differ from the parent heparin only by their lower average molecular weight, which are approximately one third of that of UFH. A variety of LMWHs have been produced including tinzaparin (compound **2**), sodium deltaparin (compound **3**), calcium nadroparin (compound **4**) and enoxaparin (compound **5**). In the last decade, many new kinds of heparin derivatives have been developed such as fondaparinux (compound **6**). In contrast to UFH and LMWH that have a natural biological source, fondaparinux is a fully synthetic anticoagulant which is based on the pentasaccharides sequence that represents the antithrombin binding region of heparin. In addition to commercially available drugs, we tested the non-commercial heparin derivatives **7-15** (see **Figure 2**) with MWs ranging from 2.4 to 16.6 kDa, including non-anticoagulant compound G9646 (**7**), and derivatives obtained as depolymerization product of RO-heparin (non-anticoagulant reduced oxyheparin) and 2-O-des-heparin (desulphated in position 2 of glucosamine) such as compounds G4271A (**13**), G4271B (**14**) and G4185 (**15**). G5945 (**8**) is a 2-O des-heparin, while compound **9** is desulphated in position 6 of glucosamine with a similar MW as the RO heparin G9694 (**7**) of around 16 KDa, with 1.1, 0.7 and 2.2 degrees of sulfation, respectively. Compound **11** is dalte-decasaccharide (fraction of dalteparin), compound 1**2** is dalte-octasaccharide fraction while compound **10** a dalte-dodesaccharide.

Altogether, 15 heparin derivatives were pharmacologically characterized, and their potencies in inhibiting ATP hydrolysis by human NPP1 were determined using a capillary electrophoresis(CE)-based assay (see **Table 2**, **Figure 3,** and **Figure S2**).

Table 2. Investigated heparins and their inhibitory potency at human NPP1

No.	Compound	MW (Da)	IC_{50} ± SD (µM)	IC_{50} ± SD (µg/ml) or (IU/mL)
1	Heparin sodium	8000-25000	ca. 0.50 ± 0.10 [a]	8.29 ± 1.74 4.15 ± 0.87 **IU/mL**
2	Tinzaparin	6500	ca. 2.8 ± 0.6 [a]	18.4 ± 4.2[b] 9.21 ± 2.1 **IU/mL**
3	Dalteparin	5000	29.6 ± 10.5	148 ± 52
4	Nadroparin	4500	42.7 ± 12.7	192 ± 57
5	Enoxaparin	4500	8.86 ± 1.40	52.1 ± 6.3
6	Fondaparinux	1700	2.94 ± 0.61	4.99 ± 0.98
7	G9694	16600	15.4 ± 2.13	256 ± 35.5
8	G5945	16600	29.7 ± 0.005[b]	487 ± 0.01[b]
9	G6658	15400	0.79 ± 1.05	12.1 ± 16.1
10	A3875-G6	3600	3.31 ± 2.30	11.9 ± 8.1
11	A3875-H6	3000	16.7 ± 4.8	50.0 ± 14.3
12	A3875-I6	2400	4.48 ± 0.89	10.7 ± 2.1
13	G4271A	3000	19.7 ± 3.2	59.1 ± 9.5
14	G4271B	3000	73.5 ± 22.9	220 ± 69
15	G4785	~3000	3.46 ± 4.14	5.33 ± 12.41

[a] Estimated; 1IU equal. to 0.002 mg of heparin; a mean value of 16.5 KDa for heparin-sodium was considered for calculation

[b]IC_{50} value estimated from % inhibition

The IC_{50} values ranged from 0.503 µM for heparin-sodium (compound **1**) to 73 µM for G4271B (compound **11**). Among the clinically used heparins, compound **1** (heparin-Na) and fondaparinux (**6**) appeared to be the most potent in inhibiting NPP1 activity, followed by tinzaparin (**2**). These highly sulfated compounds have 2.7, 3.2 and 2.5 sulfate groups per disaccharide repeating unit on average. LMWHs possess a lower number of sulfate groups compared to UFH (IC_{50} 8.29 µg/mL) and fondaparinux (IC_{50} 4.99 µg/mL); their IC_{50} values range from 20 to 190 µg/mL. Among the LMWHs, deltaparin (**3**), nadroparin (**4**) and enoxaparin (**5**) have a similar MW (4500-5000 Da); compound **5** is almost 5 times more potent than compounds **3** and **4**. Desulfation of position 6 (in G6658, **9**), instead of position 2 (G5945, **8**), improved the potency dramatically by about 35-fold. Compounds **10**, **11**, and **12**, which differentiate between each other by two units in length, displayed IC_{50} values in a similar range, however a dodesaccharide of 3.6 kDa

(compound **10**) showed stronger inhibition of NPP1 activity compared with 8 or 10 units. G9694 (**7**), the RO non-anticoagulant heparin has an IC_{50} value of 30 µM, thus, the ring-opening modification does not seem to interfere with the compound's inhibitory activity at NPP1. For direct comparison, the pIC_{50} values are depicted in Figure 3. Due to the large differences in the molecular weights of the compounds, a comparison based on g/L (**Figure 3B**) appears to be more meaningful than a comparison of molar concentrations (**Figure 3A**). These data confirm that different heparin derivatives are suitable to block NPP1 activity; the size of the oligo/polyglycolides does not seem to be the only determining factor for inhibitory activity. The potency of the heparin derivatives depends significantly on charge density, and is unrelated to anticoagulant activity.

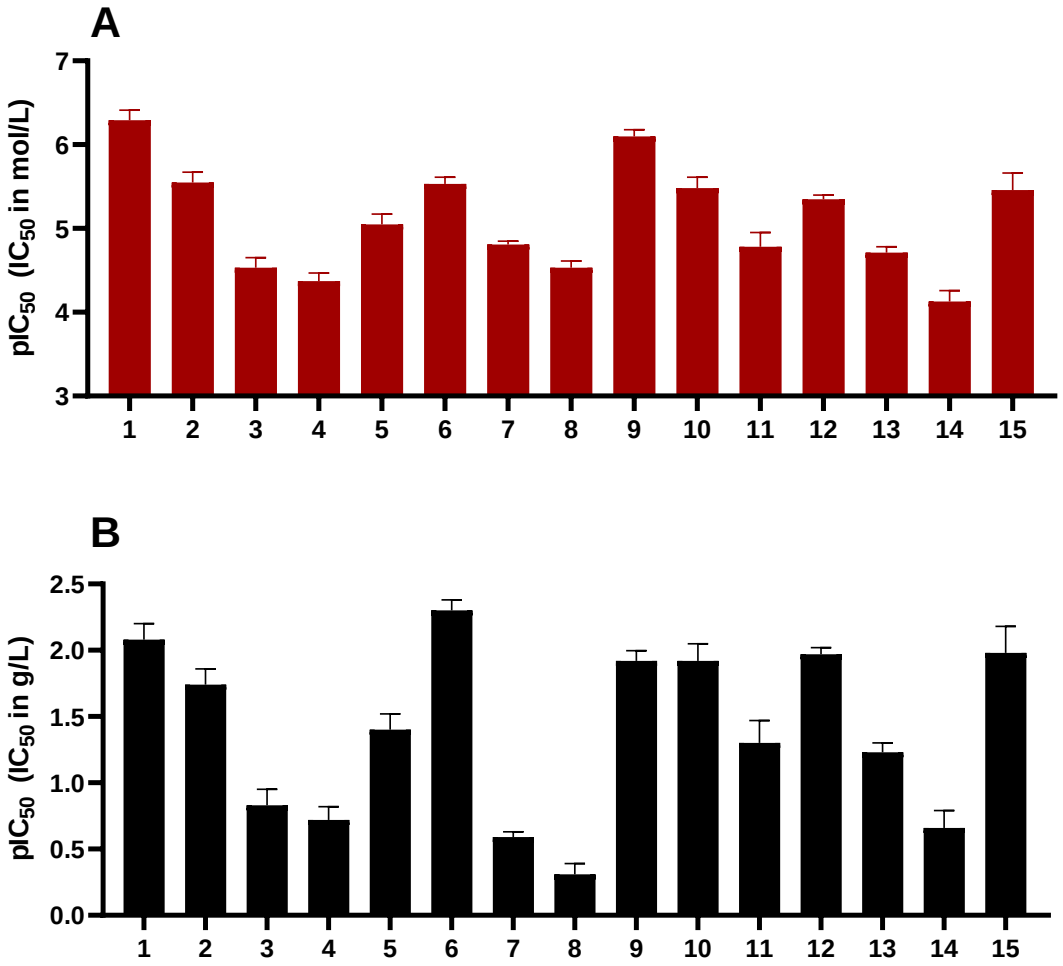

Figure 3. pIC_{50} values in mol/L (**A**) and g/L (**B**) of compounds **1-15** at the human ectonucleotidase NPP1 are shown. Error bars represent SD values. For IC_{50} values and details

see Table 1. ATP was used as a substrate. A CE-UV-assay was used for detection and quantification of the product AMP. For details see Experimental Section 3.1.

Selectivity versus other ectonucleotidases

Next, we studied the selectivity of selected heparins versus other members of the ectonucleotidase family. Heparin sodium (**1**) Fondaparinux (**6**) and G9694 (**7**) were selected as group representatives (**Figure 4**). These compounds showed high selectivity for NPP1 versus other NPP subtypes, NPP3, -4, and -5, versus NTPDases, NTPDase2, -3, and -8, and versus CD73. A concentration was selected by which full inhibition at NPP1 was observed. Compound **7** (G9694), tested at 800 µg/mL (48 µM), slightly inhibited NTPDase1 and -2 by about 35%, but no effect was observed on the other enzymes. Compound **6** (fondaparinux), tested at 20 µg/mL (12 µM), showed ~45 % inhibition of NTPDase2, but no effect on the other investigated enzymes, while compound **1** (heparin sodium), tested at 50 IU/mL (roughly 6 µM), inhibited only NTPDase1, blocking its activity by 50 %.

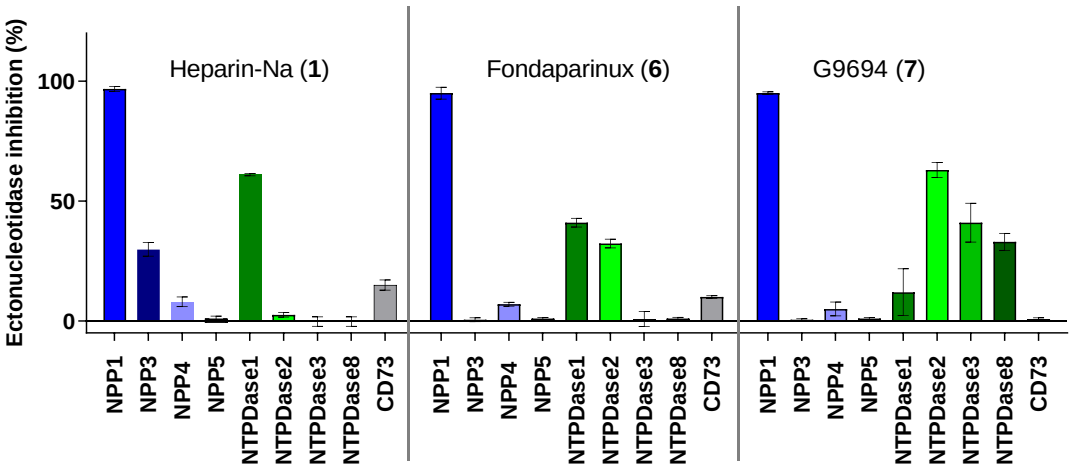

Figure 4. Selectivity studies of ectonucleotidase inhibition by three compounds: heparin sodium (**1**), Fondaparinux (**6**) and G9694 (**7**) selected as group representative of UFH, LMWH and non-commercial, respectively. A concentration was selected by which full inhibition at NPP1 was observed. Compound **1** was tested at 50 IU, compound **6** at 20 µg/mL (12 µM) and compound **7** was tested at a concentration of 800 µg/mL (48 µM). NPP1 and NTPDase1, 2, 3 and 8 activities

were analyzed using a CE-based assay employing ATP as a substrate; NPP3 was investigated using *p*-Nph-5′-TMP as a substrate; NPP4 was tested versus Ap_4A as a substrate using a luciferase assay; for CD73 activity a radio-ligand-based assay was performed. The data are normalized with respect to positive (100%) and negative (0%) controls of each enzyme, for details see Experimental Section.

Determination of inhibition type

Next, we investigated the mechanism of inhibition for compound **7** (G9694, not anticoagulative) and compound **6** (Fondaparinux) as group representatives. We studied the effect on ATP hydrolysis by NPP1 in the absence and in the presence of the inhibitors. Five different concentrations of the substrate ATP were employed (20, 50, 100, 200 and 500 µM), each tested in the presence of 0, 0.4 and 4 µM of Fondaparinux (**6**) or 0, 4 and 40 µM of G9694 (**7**). For the determination of the inhibition type, Lineweaver-Burk plots were obtained (**Figure 5 B** and **D**), and the kinetic parameters of ATP hydrolysis by NPP1, in the absence and presence of inhibitors **6** and **7** were calculated (**Figure 5A** and **C**). The results indicate a mixed-type of NPP1 inhibition by these heparin derivatives (**Figure 5**).

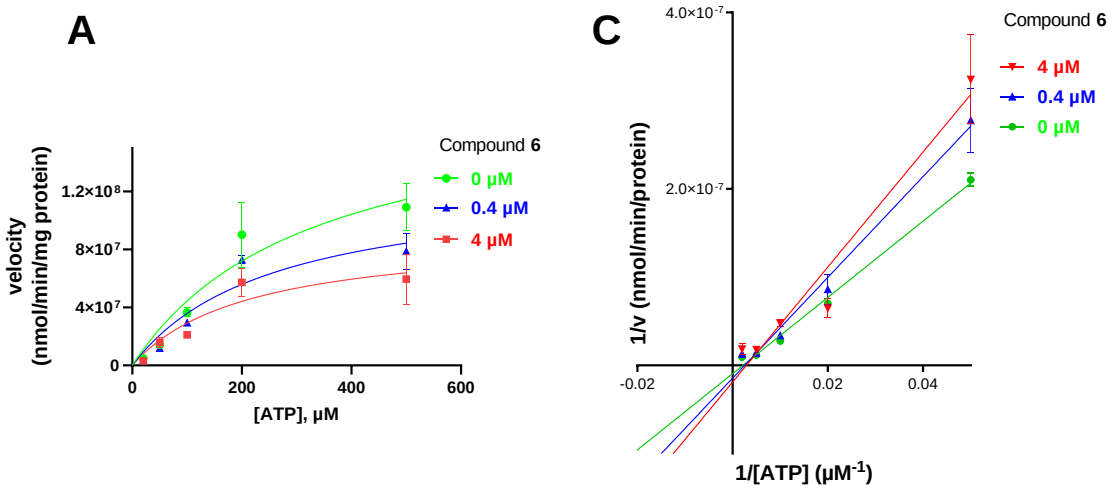

Compound **6** (μM)	**0**	**0.4**	**4**
K_m apparent (μM)	326	255	212
V_{max} (nmol/min/mg protein)	1.89×10^8	1.28×10^8	0.91×10^8

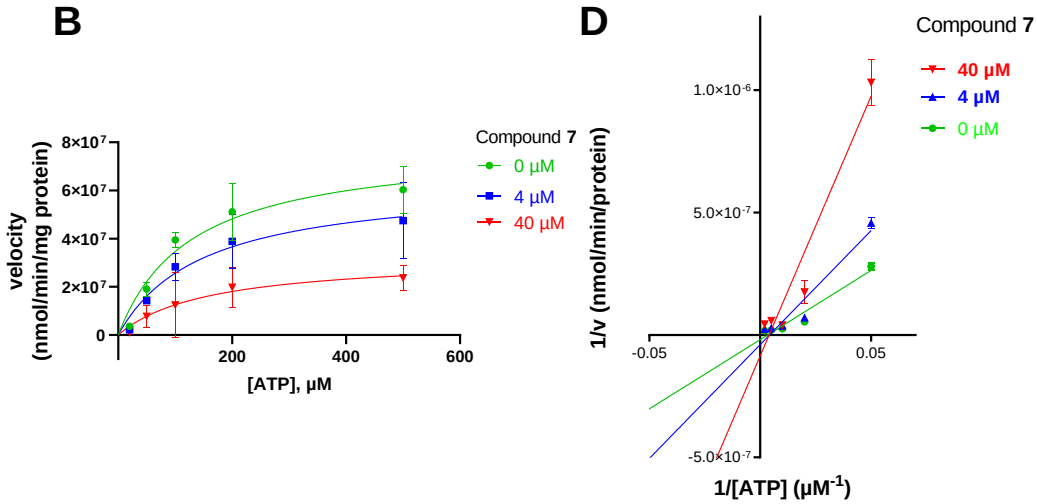

Compound **7** (μM)	**0**	**4**	**40**
K_m apparent (μM)	128	148	172
V_{max} (nmol/min/mg protein)	7.91×10^7	6.37×10^7	3.32×10^7

Figure 5. Investigation of the inhibition type of inhibitors **6** (Fondaparinux) and 7 (G9694) at human NPP1. In **A** and **B**, the Michaelis-Menten curves are shown without and in the presence of different concentrations of inhibitors. For the determination of the inhibition type, Lineweaver-Burk plots are shown in **C** and **D**. The kinetic parameters of ATP hydrolysis by NPP1, in the absence and presence of inhibitors **6** and **7** are provided in the table. The results indicate a mixed type of inhibition. Data obtained from three independent experiments, each performed in duplicate.

Identification of cancer cell lines with high NPP1 expression

To test the compounds in a more complex system, we searched for a native cell line with high NPP1 expression. Thus, mRNA expression analysis of ectonucleotidases in several tumor cell lines was carried out. Altogether 10 different cell lines were investigated with respect to 12 genes encoding members of the ectonucleotidase family. Expression of NPP1 was previously reported to be increased in human astrocytic brain tumors (glioblastoma), and NPP1 expression was observed to increase with tumor grade [18]. NPP1 was shown to be expressed in N2a mouse neuroblastoma cells, the expression level significantly decreasing upon differentiation into a neuronal-like phenotype [30]. Therefore, we studied the gene expression of adult human brain-derived neural progenitor cells (155Z and 167Z), primary human glioblastoma cell lines (106Z, 138Z, 46Z, 78Z) and established human glioblastoma cell lines (LN229, T98G, U138 and U87). NPPs expression (ENPP-1, 2 and 3) and NTPDases expression (ENTPD1, -2, -3 and -8) was studied. The gene NT5E encoding for CD73 protein was analyzed as well. In addition, we analyzed the expression of the genes encoding alkaline phosphatases, ALPI (alkaline phosphatase, intestinal), ALPL (alkaline phosphatase, biomineralization associated) ALPP (alkaline phosphatase, placental) and ALPPL2 (alkaline phosphatase, germ cell). These latter enzymes can also hydrolyze extracellular ATP, but show a much higher K_m value as compared to the other ectonucleotidases [7].

A

Cell lines	APs				NPPs			NTPDases				eN
	Cq ALPI	Cq ALPL	Cq ALPP	Cq ALPPL2	Cq ENPP1	Cq ENPP2	Cq ENPP3	Cq ENTPD1	Cq ENTPD2	Cq ENTPD3	Cq ENTPD8	Cq NT5E
155Z		33.88	34.79	≥35	26.68	26.81	≥35	32.93	≥35	≥35	≥35	21.71
167Z	≥35	32.53	≥35	≥35	26.15	26.09	≥35	31.38	≥35	≥35	≥35	22.53
LN229	≥35	≥35	≥35	≥35	29.62	25.99	≥35	≥35	≥35	≥35	≥35	27.00
T98G	≥35	≥35	≥35	≥35	33.82	31.58	≥35	≥35	≥35	≥35	≥35	31.06
U138	≥35	≥35	≥35	≥35	27.95	34.28	≥35	≥35	≥35	≥35	≥35	28.65
U87	≥35	31.53	≥35	≥35	27.07	25.53	≥35	≥35	≥35	≥35	≥35	23.76
106Z	≥35	33.03	≥35	≥35	28.68	36.28	≥35	33.00	31.93	30.01	≥35	28.06
138Z	≥35	≥35	≥35	≥35	27.78	28.53	≥35	≥35	≥35	≥35	≥35	25.28
46Z	≥35	≥35	≥35	≥35	27.45	29.15	≥35	≥35	30.94	31.60	≥35	25.04
78Z	≥35	≥35	≥35	≥35	27.93	30.10	≥35	≥35	≥35	≥35	≥35	25.54

Cq ≥35	no mRNA expression
Cq = 30-34	very low mRNA expression
Cq < 30	low mRNA expression
Cq ≤ 25	high mRNA expression

Cell lines:
adult human brain-derived neural progenitor cells
human glioblastoma cell line
primary human glioblastoma cells

B

Cell lines	NPPs		NTPDases		eN	Reference genes	
	Cq ENPP1	Cq ENTPD1	Cq ENTPD2	Cq ENTPD3	Cq NT5E	Cq ß-actin	Cq GAPDH
167Z	26.42 ± 0.27	30.68 ± 0.70	≥35	≥35	22.45 ± 0.09	18.19 ± 0.48	19.38 ± 0.10
LN229	29.51 ± 0.12	≥35	≥35	≥35	25.86 ± 1.15	19.71 ± 1.01	19.93 ± 0.44
U87	26.67 ± 0.40	≥35	≥35	≥35	23.06 ± 0.70	18.52 ± 0.81	19.92 ± 0.38
138Z	27.59 ± 0.19	≥35	≥35	≥35	25.19 ± 0.09	19.03 ± 0.15	19.50 ± 0.13
46Z	28.05 ± 0.60	≥35	31.15 ± 0.21	32.00 ± 0.39	25.00 ± 0.05	19.13 ± 0.23	19.66 ± 0.07

Figure 6. mRNA gene expression analysis of ectonucleotidases in human cell lines. **A**. Data from the first biological replicate (Cq, n=4) where the genes of interest were investigated in 10 different cell lines. **B**. (Cq ± SEM) second investigation with selected cell lines and ectonucleotidases (Cq, n=8) (for details see Experimental Section 2.7). APs: alkaline phosphatases; NPPs: nucleotide pyrophosphatase/phosphodiesterase; NTPDases: nucleoside triphosphate diphosphohydrolases; eN: ecto-nucleotidase; Cq: quantitation cycle; alkaline phosphatases genes, ALPI: alkaline phosphatase, intestinal; ALPL: alkaline phosphatase, biomineralization associated; ALPP: alkaline phosphatase, placental; ALPPL2: alkaline phosphatase, germ cell; ENPPs: ectonucleotide pyrophosphatase; ENTPDases: ectonucleoside triphosphate diphosphohydrolases; NT5E: ecto-5'-nucleotidase gene; GAPDH: glyceraldehyde-3-phosphate dehydrogenase.

In the first biological replicate (**Figure 6A**) of 10 different cell lines which were investigated with respect of 12 genes encoding members of the ectonucleotidase family, we observed very low or no mRNA expression for alkaline phosphatases and NTPDases, while relatively high mRNA expression for NPP1 was observed in all the cell lines, and very high mRNA expression for CD73 was detected. In the second biological replicate we specifically studied the expression

profile of ENPP1, ENTPD-1,2 and 3, and NT5E (encoding for CD73) in the cell lines which showed higher expression from the first replicate. Indeed, we observed that 167Z, LN229, U87, 138Z and 46Z have high mRNA expression of CD73 and NPP1, and very low or no expression for NTPDases. Based on the observed expression of the genes of interest in these cell lines, we selected the glioblastoma cell line U87 for further experiments. This cell line is an established human glioblastoma cell line that expresses NPP1 and NT5E (CD73), with no significant mRNA expression of any of the other investigated genes, thus making it suitable for our purpose (see **Figure 6**).

Studies on membrane preparations of the glioblastoma cell line U87

The selected cell line (U87) was biochemically characterized, and kinetic parameters using cell membrane preparations were determined. First, we investigated the enzymatic activity leading to the formation of adenosine upon incubation with ATP using cell membrane preparations (**Figure 7C**). Employing ATP and AMP as natural substrates (**Figure 7A** and **B**) we determined the K_m values, which were 83 µM for ATP and 38 µM for AMP. These data are in conformance with NPP1 and CD73, respectively [7]. Next, the inhibitory activity of compounds **7** (G9694) and **6** (Fondaparinux) on the formation of adenosine by U87 cell membrane preparations was investigated. Both heparin derivatives inhibited the formation of adenosine in a dose-dependent manner (see **Figure 7**).

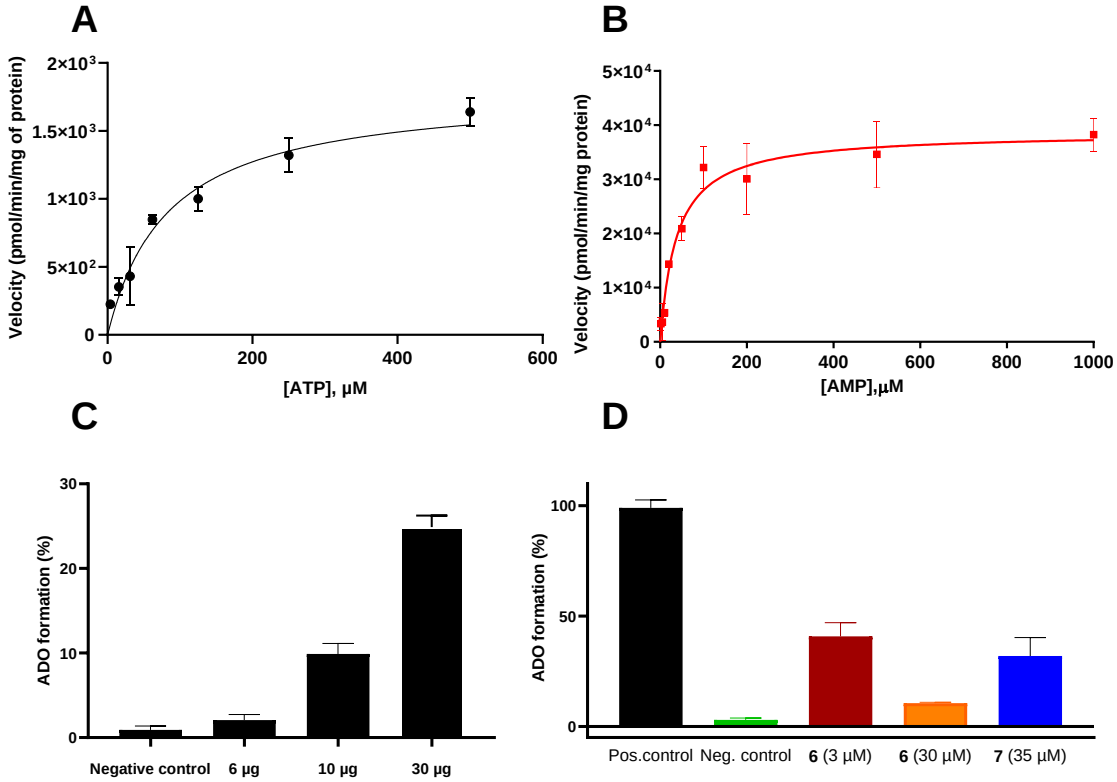

Figure 7. Enzyme kinetics for ATP (**A**) and AMP (**B**) as substrates of ectonucleotidases expressed in U87 cell membrane preparations. **C.** Enzymatic activity: three different amounts of U87 cell membrane preparations were incubated with 100 µM ATP at 37°C for 30 min, followed by heating to deactivate the enzymes. A control was included using the known NPP1 inhibitor PSB-POM141 (20 µM) [15]. **D.** Blockade of adenosine formation from ATP by compounds **6** (fondaparinux) and **7** (G9694) in human U87 glioblastoma cell membrane preparations. Negative (Neg.) control: the potent NPP1 inhibitor PSB-POM141 (20 µM) was added which led to a full blockade of NPP1 activity thereby preventing the formation of AMP and consequently its hydrolysis to adenosine. Positive (Pos.) control: cell membrane preparation without any test compounds. For the analysis and quantifications of the products in all experiments CE-based assays were employed (for details see Experimental Section 2.8).

Studies on living glioblastoma U87 cells

Finally, the inhibition of ATP degradation and adenosine formation by selected heparin derivatives was studied in intact cells. The compounds were employed at a range of different concentrations. Dose-dependent inhibition of adenosine formation by all investigated compounds was observed. To be able to relate the employed concentrations to the clinically used

concentrations of these anticoagulant compounds, we adapted the amounts to the therapeutic concentrations, given in I.U. for the heparins **1**, **2** and **3**, and in µg for fondaparinux (**6**). In order to use a comparable scale and select a mean therapeutic concentration, as well as a higher one slightly exceeding the typical therapeutic doses, we selected 1 I.U./mL and 5 I.U./mL, for heparin-Na (**1**), tinzaparin (**2**) and enoxaparin (**5**), and 2 µg/mL and 10 µg/mL for fondaparinux (**6**). The non-commercial heparin derivatives G9694 (**7**), G5645 (**8**), G6658 (**9**) were tested at 50 µM, compound **7** was additionally tested at 100 µM, compounds A3875-G6 (**10**), A3875-H6 (**11**) and A3875-I6 (**12**) were studied at 20 and 50 µM. All the heparin derivatives studied were able to inhibit adenosine formation from ATP in U87 cells (**Figure 8**). In fact, UFH (**1**), and LMWH **2** and **5** inhibited adenosine formation by 30-60% using 5 IU, while fondaparinux (**6**) inhibited up adenosine formation by 60% using 10 µg/mL (~6 µM). These results are comparable to the data previously obtained on the isolated soluble NPP1. The data obtained at intact U-87 cells were well in agreement with data observed at membrane preparations (**Figure 7D**) and at recombinant NPP1 (**Figure 3**).

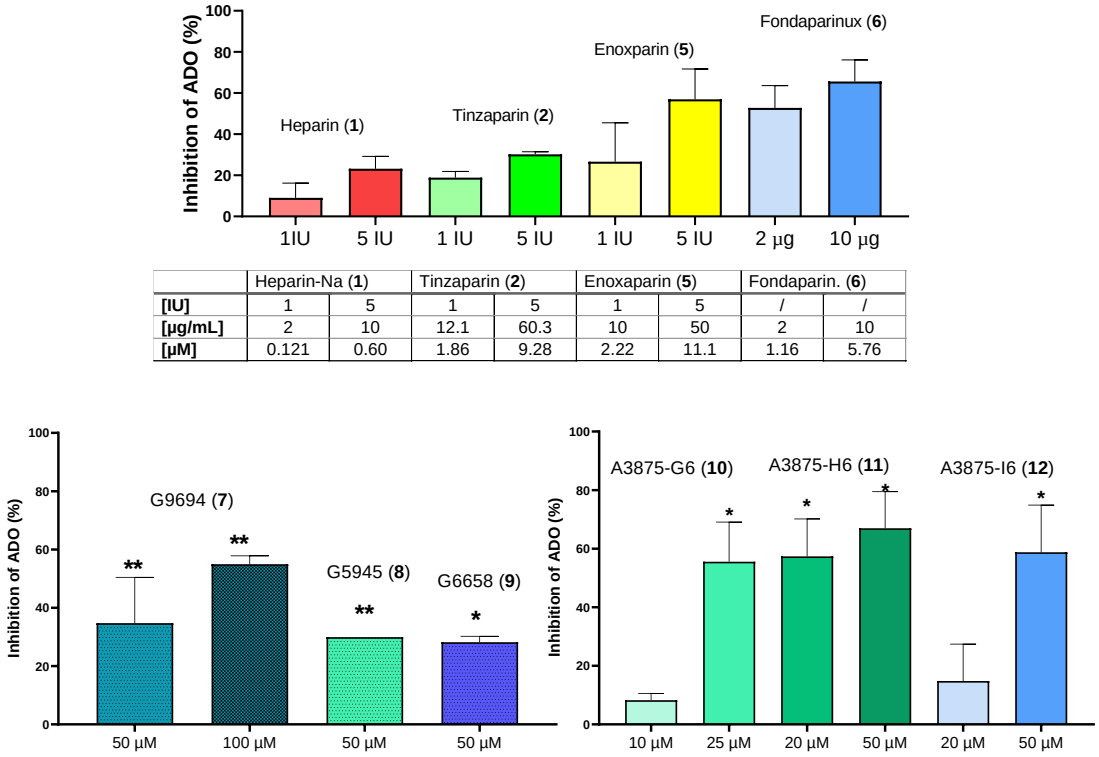

	Heparin-Na (1)		Tinzaparin (2)		Enoxaparin (5)		Fondaparin. (6)	
[IU]	1	5	1	5	1	5	/	/
[µg/mL]	2	10	12.1	60.3	10	50	2	10
[µM]	0.121	0.60	1.86	9.28	2.22	11.1	1.16	5.76

Figure 8. Blockade of extracellular adenosine formation from ATP by compound (**1**), (**2**), (**5**), (**6**) as representative of commercial heparin derivatives (**A**) and compounds (**7**), (**8**), (**9**), (**10**), (**11**), (**12**) as representative of non-commercial heparin derivatives (**B** and **C**) on human U87 glioblastoma cells. The cells were treated with ATP (ectonucleotidase substrate) and incubated for 3 h in the presence of dipyridamole to prevent cellular uptake of adenosine, and EHNA to prevent adenosine deamination. Adenosine was quantified by CE-UV (for details see Experimental Section 2.9. and Table 1). Statistical analysis: one-way ANOVA (normal vs treatment). * p-value ≤ 0.05, ** p-value ≤ 0.01.

Heparin and derivatives are well tolerated and safe drugs. UFH is used in a therapeutic range of 8,000-10,000 IU s.c. every 8 hours, or 15,000-20,000 IU s.c. every 12 hours with plasma concentrations reported to range from 0.2 IU/mL to 15 IU/mL on average [31,32] and a half-life ($T_{1/2}$) of 4-6 h [32]. Compound **1**, heparin-sodium (UFH), has an IC_{50} value at NPP1 of ~4 IU/mL which is in the range of the plasma concentration reached in patients at therapeutic doses. It is worth mentioning that the IC_{50} value of UFH at P-selectin is 24.5 µg/mL [33], while at NPP1 it is 3-fold lower (8.26 µg/mL). LMWHs (e.g., **2**, **3**, **4** and **5**), have a therapeutic range of 0.50-

1.00 IU/mL with twice-daily dosing, or 1.00-2.00 IU/mL with once-daily dosing (4,500 IU), reaching plasma levels of 0.25 and 0.87 IU/mL. The therapeutic dosage for fondaparinux (**6**) is typically 2.5 mg/daily and the plasma concentrations have been reported to range from 0.1 to 0.5 mg/L for adult patients on thromboprophylaxis and from 0.6 to 1.5 mg/L for adults on therapeutic doses, with a half-life of 17 h [34].

The non-commercial heparin derivatives showed potent inhibitory activity on the formation of adenosine in U87 tumor cells (**Figure 8B** and **C**). All the investigated compounds showed a reduction in adenosine formation of at least 50% when tested at 50 µM (**Figure 8** section **A** and **B**). Heparin derivatives and analogs exhibit a strong inhibitory activity on NPP1 demonstrated to be NPP1-specific, suggesting a potential for immuno-oncological treatments. Yet it is still debatable whether this is the main mechanism of action. NPP1 inhibition is likely contributing to the clinical observations in heparinized oncological patients.

CONCLUSIONS

In conclusion, we discovered that heparin and its derivatives are potent, mixed-type inhibitors of the ectonucleotidase NPP1 showing high selectivity versus other ectonucleotidases. This enzyme catalyzes the hydrolysis of proinflammatory, antiproliferative ATP to produce, in conjunction with the AMP-hydrolyzing ectoenzyme CD73, adenosine, which has immunosuppressive and tumor-promoting properties. Indeed, we observed decreased adenosine production by human glioma U87 cells treated with representative heparin derivatives. Heparin exhibits a significant effect on adenosine formation that was demonstrated to be NPP1-dependent, suggesting a role for immuno-oncological therapies. The presented structure-activity relationships provide a basis for optimization of the NPP1-inhibitory activity of heparins while reducing or abolishing the anticoagulant properties.

Author contributions: Christa Müller designed and supervised the study; Vittoria Lopez performed experiments on NPP1, NPP4 and U87 membrane preparation; Riham M. Idris, Christian Renn, Laura Schäkel, Salahuddin Mirza and Sang-Yong Lee performed selectivity experiments on ectonucleotidase; Maximilian Schuh and Michael S. Schmidt performed cell-based assays under the supervision of Gerd Bendas; Annamaria Naggi provided non-commercial synthetized heparins; Julie Pelletier and Jean Sévigny provided NTPDase preparations; Björn Scheffler provided cell lines; Katharine Sylvester performed qRT-PCR analysis experiments; VL and CEM wrote the manuscript with contribution from all coauthors.

Funding: This study was funded by the Federal Ministry of Education and Research (BMBF, BIGS DrugS project) and by the Deutsche Forschungsgemeinschaft (DFG, SFB1328).

Conflicts of Interest: The authors declare no conflict of interest. The funders had no role in the design of the study, in the collection, analyses, or interpretation of data, in writing the manuscript, or in the decision to publish the results.

References

1. Paluck, S.J.; Nguyen, T.H.; Maynard, H.D. Heparin-Mimicking Polymers: Synthesis and Biological Applications. *Biomacromolecules* **2016**, *17*, 3417–3440, doi:10.1021/acs.biomac.6b01147.
2. Ma, S.N.; Mao, Z.X.; Wu, Y.; Liang, M.X.; Wang, D.D.; Chen, X.; Chang, P. an; Zhang, W.; Tang, J.H. The anti-cancer properties of heparin and its derivatives: a review and prospect. *Cell Adhes. Migr.* **2020**, *14*, 118–128, doi:10.1080/19336918.2020.1767489.
3. Borsig, L. Antimetastatic activities of heparins and modified heparins. Experimental evidence. *Thromb. Res.* **2010**, *125*, S66–S71, doi:10.1016/S0049-3848(10)70017-7.
4. Bendas, G.; Borsig, L. Cancer cell adhesion and metastasis: Selectins, integrins, and the inhibitory potential of heparins. *Int. J. Cell Biol.* **2012**, *2012*, doi:10.1155/2012/676731.
5. Smorenburg, S.M.; Van Noorden, C.J.F. The complex effects of heparins on cancer progression and metastasis in experimental studies. *Pharmacol. Rev.* **2001**, *53*, 93–105.
6. Lopez, V.; Schäkel, L.; Schuh, H.J.M.; Schmidt, M.S.; Mirza, S.; Renn, C.; Pelletier, J.; Lee, S.-Y.; Sévigny, J.; Alban, S.; et al. Sulfated Polysaccharides from Macroalgae Are Potent Dual Inhibitors of Human ATP-Hydrolyzing Ectonucleotidases NPP1 and CD39. *Mar. Drugs* **2021**, *19*, 51, doi:10.3390/md19020051.
7. Zimmermann, H. History of ectonucleotidases and their role in purinergic signaling. *Biochem. Pharmacol.* **2021**, *187*, 114322, doi:10.1016/j.bcp.2020.114322.
8. Lee, S.-Y.; Müller, C.E. Nucleotide pyrophosphatase/phosphodiesterase 1 (NPP1) and its inhibitors. *Medchemcomm* **2017**, *8*, 823–840, doi:10.1039/C7MD00015D.
9. Yegutkin, G.G. Enzymes involved in metabolism of extracellular nucleotides and nucleosides: functional implications and measurement of activities. *Crit. Rev. Biochem. Mol. Biol. 49*, 473–97, doi:10.3109/10409238.2014.953627.
10. Namasivayam, V.; Lee, S.-Y.; Müller, C.E. The promiscuous ectonucleotidase NPP1: molecular insights into substrate binding and hydrolysis. *Biochim. Biophys. Acta - Gen. Subj.* **2017**, *1861*, 603–614, doi:10.1016/j.bbagen.2016.12.019.
11. Onyedibe, K.I.; Wang, M.; Sintim, H.O. ENPP1, an Old Enzyme with New Functions, and Small Molecule Inhibitors—A STING in the Tale of ENPP1. *Molecules* **2019**, *24*, 4192, doi:10.3390/molecules24224192.
12. Kato, K.; Nishimasu, H.; Oikawa, D.; Hirano, S.; Hirano, H.; Kasuya, G.; Ishitani, R.; Tokunaga, F.; Nureki, O. Structural insights into cGAMP degradation by Ecto-nucleotide pyrophosphatase phosphodiesterase 1. *Nat. Commun.* **2018**, *9*, 4424, doi:10.1038/s41467-018-06922-7.
13. Carozza, J.A.; Brown, J.A.; Böhnert, V.; Fernandez, D.; AlSaif, Y.; Mardjuki, R.E.; Smith, M.; Li, L. Structure-Aided Development of Small-Molecule Inhibitors of ENPP1, the Extracellular Phosphodiesterase of the Immunotransmitter cGAMP. *Cell Chem. Biol.* **2020**, *27*, 1347-1358.e5,

doi:10.1016/j.chembiol.2020.07.007.

14. Naggi, A.; Casu, B.; Perez, M.; Torri, G.; Cassinelli, G.; Penco, S.; Pisano, C.; Giannini, G.; Ishai-Michaeli, R.; Vlodavsky, I. Modulation of the heparanase-inhibiting activity of heparin through selective desulfation, graded N-acetylation, and glycol splitting. *J. Biol. Chem.* **2005**, *280*, 12103–12113, doi:10.1074/jbc.M414217200.
15. Lee, S.-Y.; Fiene, A.; Li, W.; Hanck, T.; Brylev, K.A.; Fedorov, V.E.; Lecka, J.; Haider, A.; Pietzsch, H.-J.; Zimmermann, H.; et al. Polyoxometalates--potent and selective ecto-nucleotidase inhibitors. *Biochem. Pharmacol.* **2015**, *93*, 171–81, doi:10.1016/j.bcp.2014.11.002.
16. Lee, S.-Y.; Sarkar, S.; Bhattarai, S.; Namasivayam, V.; De Jonghe, S.; Stephan, H.; Herdewijn, P.; El-Tayeb, A.; Müller, C.E. Substrate-Dependence of Competitive Nucleotide Pyrophosphatase/Phosphodiesterase1 (NPP1) Inhibitors. *Front. Pharmacol.* **2017**, *8*, doi:10.3389/fphar.2017.00054.
17. Gorelik, A.; Randriamihaja, A.; Illes, K.; Nagar, B. Structural basis for nucleotide recognition by the ectoenzyme CD203c. *FEBS J.* **2018**, *285*, 2481–2494, doi:10.1111/febs.14489.
18. Gorelik, A.; Randriamihaja, A.; Illes, K.; Nagar, B. A key tyrosine substitution restricts nucleotide hydrolysis by the ectoenzyme NPP5. **2017**, *5*, 1–9, doi:10.1111/febs.14266.
19. Lopez, V.; Lee, S.-Y.; Stephan, H.; Müller, C.E. Recombinant expression of ecto-nucleotide pyrophosphatase/phosphodiesterase 4 (NPP4) and development of a luminescence-based assay to identify inhibitors. *Anal. Biochem.* **2020**, *603*, 113774, doi:10.1016/j.ab.2020.113774.
20. Lévesque, S.A.; Lavoie, E.G.; Lecka, J.; Bigonnesse, F.; Sévigny, J. Specificity of the ecto-ATPase inhibitor ARL 67156 on human and mouse ectonucleotidases. *Br. J. Pharmacol.* **2007**, *152*, 141–50, doi:10.1038/sj.bjp.0707361.
21. Kukulski, F.; Lévesque, S.A.; Lavoie, E.G.; Lecka, J.; Bigonnesse, F.; Knowles, A.F.; Robson, S.C.; Kirley, T.L.; Sévigny, J. Comparative hydrolysis of P2 receptor agonists by NTPDases 1, 2, 3 and 8. *Purinergic Signal.* **2005**, *1*, 193–204, doi:10.1007/s11302-005-6217-x.
22. Freundlieb, M.; Zimmermann, H.; Müller, C.E. A new, sensitive ecto-5′-nucleotidase assay for compound screening. *Anal. Biochem.* **2014**, *446*, 53–58, doi:10.1016/j.ab.2013.10.012.
23. Junker, A.; Renn, C.; Dobelmann, C.; Namasivayam, V.; Jain, S.; Losenkova, K.; Irjala, H.; Duca, S.; Balasubramanian, R.; Chakraborty, S.; et al. Structure-Activity Relationship of Purine and Pyrimidine Nucleotides as Ecto-5’-Nucleotidase (CD73) Inhibitors. *J. Med. Chem.* **2019**, *62*, 3677–3695, doi:10.1021/acs.jmedchem.9b00164.
24. Bradford, M.M. A rapid and sensitive method for the quantitation of microgram quantities of protein utilizing the principle of protein-dye binding. *Anal. Biochem.* **1976**, *72*, 248–254, doi:10.1016/0003-2697(76)90527-3.
25. Iqbal, J.; Vollmayer, P.; Braun, N.; Zimmermann, H.; Müller, C.E. A capillary electrophoresis method for the characterization of ecto-nucleoside triphosphate diphosphohydrolases (NTPDases) and the analysis of inhibitors by in-capillary enzymatic microreaction. *Purinergic Signal.* **2005**, *1*, 349–58, doi:10.1007/s11302-005-8076-x.
26. Qurishi, R.; Kaulich, M.; Müller, C.E. Fast, efficient capillary electrophoresis method for measuring nucleotide degradation and metabolism. *J. Chromatogr. A* **2002**, *952*, 275–81, doi:10.1016/s0021-9673(02)00095-x.

27. Pastor-Anglada, M.; Pérez-Torras, S. Who Is Who in Adenosine Transport. *Front. Pharmacol.* **2018**, *9*, doi:10.3389/fphar.2018.00627.

28. Poppe, D.; Doerr, J.; Schneider, M.; Wilkens, R.; Steinbeck, J.A.; Ladewig, J.; Tam, A.; Paschon, D.E.; Gregory, P.D.; Reik, A.; et al. Genome Editing in Neuroepithelial Stem Cells to Generate Human Neurons with High Adenosine-Releasing Capacity. *Stem Cells Transl. Med.* **2018**, *7*, 477–486, doi:10.1002/sctm.16-0272.

29. Kaulich, M.; Qurishi, R.; Müller, C.E. Extracellular metabolism of nucleotides in neuroblastoma x glioma NG108-15 cells determined by capillary electrophoresis. *Cell. Mol. Neurobiol.* **2003**, *23*, 349–64, doi:10.1023/a:1023640721630.

30. Gómez-Villafuertes, R.; Pintor, J.; Miras-Portugal, M.T.; Gualix, J. Ectonucleotide pyrophosphatase/phosphodiesterase activity in Neuro-2a neuroblastoma cells: changes in expression associated with neuronal differentiation. *J. Neurochem.* **2014**, *131*, 290–302, doi:10.1111/jnc.12794.

31. Wahr, J.A.; Yun, J.H.; Yang, V.C.; Lai Ming Lee; Fu, B.; Meyerhoff, M.E. A new method of measuring heparin levels in whole blood by protamine titration using a heparin-responsive electrochemical sensor. *J. Cardiothorac. Vasc. Anesth.* **1996**, *10*, 447–450, doi:10.1016/S1053-0770(05)80002-3.

32. ENGELBERG, H. Plasma heparin levels in normal man. *Circulation* **1961**, *23*, 578–581, doi:10.1161/01.CIR.23.4.578.

33. Gomes, A.M.; Kozlowski, E.O.; Borsig, L.; Teixeira, F.C.O.B.; Vlodavsky, I.; Pavão, M.S.G. Antitumor properties of a new non-anticoagulant heparin analog from the mollusk Nodipecten nodosus: Effect on P-selectin, heparanase, metastasis and cellular recruitment. *Glycobiology* **2015**, *25*, 386–93, doi:10.1093/glycob/cwu119.

34. Depasse, F.; Gerotziafaz, G.T.; Busson, J.; Van Dreden, P.; Samama, M.M. Assessment of three chromogenic and one clotting assays for the measurement of synthetic pentasaccharide fondaparinux (Arixtra®) anti-Xa activity [1]. *J. Thromb. Haemost.* **2004**, *2*, 346–348, doi:10.1111/j.1538-7933.2004.0584a.x.

SUPPORTING INFORMATION

Heparin are potent inhibitors of ectonucleotide pyrophosphatase/phosphodiesterase-1 (NPP1)- a promising target for cancer immunotherapy

Vittoria Lopez, [a, b] H.J. Maximilian Schuh, [c] Salahuddin Mirza, [a, b] Laura Schäkel, [a, b] Michael S. Schmidt,[c] Katharina Sylvester , [a, b] Riham Mohammed Idris, [a, b] Christian Renn, [a, b] Julie Pelletier,[d, e] Jean Sévigny, [d, e] Annamaria Naggi, [f] Sang-Yong Lee, [a, b] Björn Scheffler,[g] Gerd Bendas,[c] and Christa E. Müller [a, b]*[1]

[1] The author sequence after the first author is provisional and may change in the final published version

[a] Pharmaceutical Institute, Pharmaceutical & Medicinal Chemistry, University of Bonn, Bonn, Germany

[b] PharmaCenter Bonn, University of Bonn, An der Immenburg 4, 53121 Bonn, Germany

[c] Pharmaceutical Institute, Pharmaceutical and Cell Biology Chemistry, University of Bonn, Bonn, Germany

[d] Centre de Recherche du CHU de Québec – Université Laval, Québec City, QC, Canada

[e] Départment de Microbiologie-Infectiologie et d'Immunologie, Faculté de Médecine, Université Laval, Quebec City, QC, Canada

[f] Institute for Chemical and Biochemical Research "G. Ronzoni", Milan, Italy

[g] Division of Translational Oncology / Neurooncology at the West German Cancer Canter (WTZ) University Hospital Essen, Germany.

*Address correspondence to:

Prof. Dr. Christa E. Müller
Pharmaceutical Institute, Pharmaceutical & Medicinal Chemistry
An der Immenburg 4, D-53121 Bonn, Germany
Phone: +49-228-73-2301
Fax: +49-228-73-2567
E-Mail : christa.mueller@uni-bonn.de

Table of content
Fig. S1 Initial screening of four commercial heparins on the most important ectonucleotidases
Fig. S2 IC_{50} curves of the investigated compounds in the study

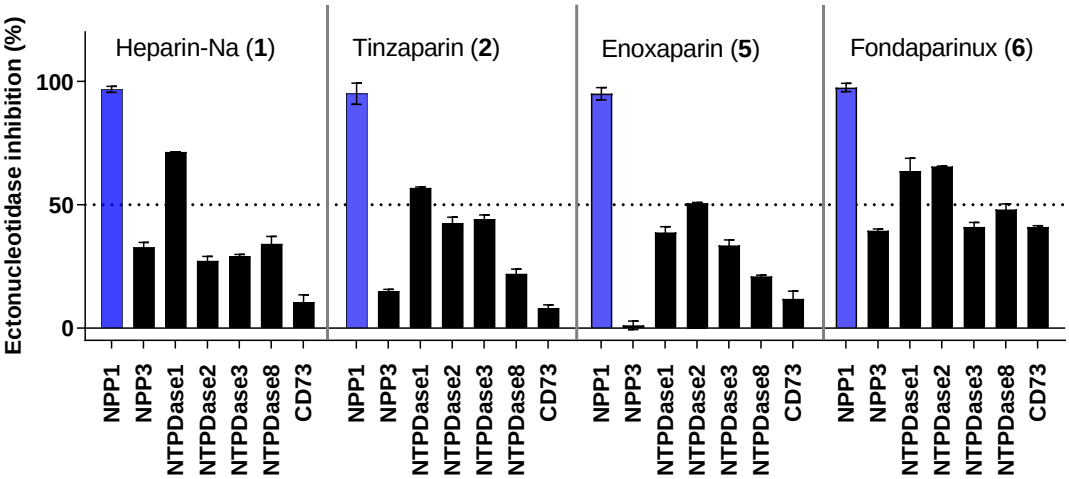

Figure S1. Initial screening of four commercial heparins on the most important ectonucleotidases. The compounds were tested at the following concentrations: compounds **1** and **2** at 63 IU/mL, compound **5** at 250 µg/mL (55 µM), compound **6** was tested at 50 µg/mL (30 µM). For detailed information about the assays, see section 2.0.

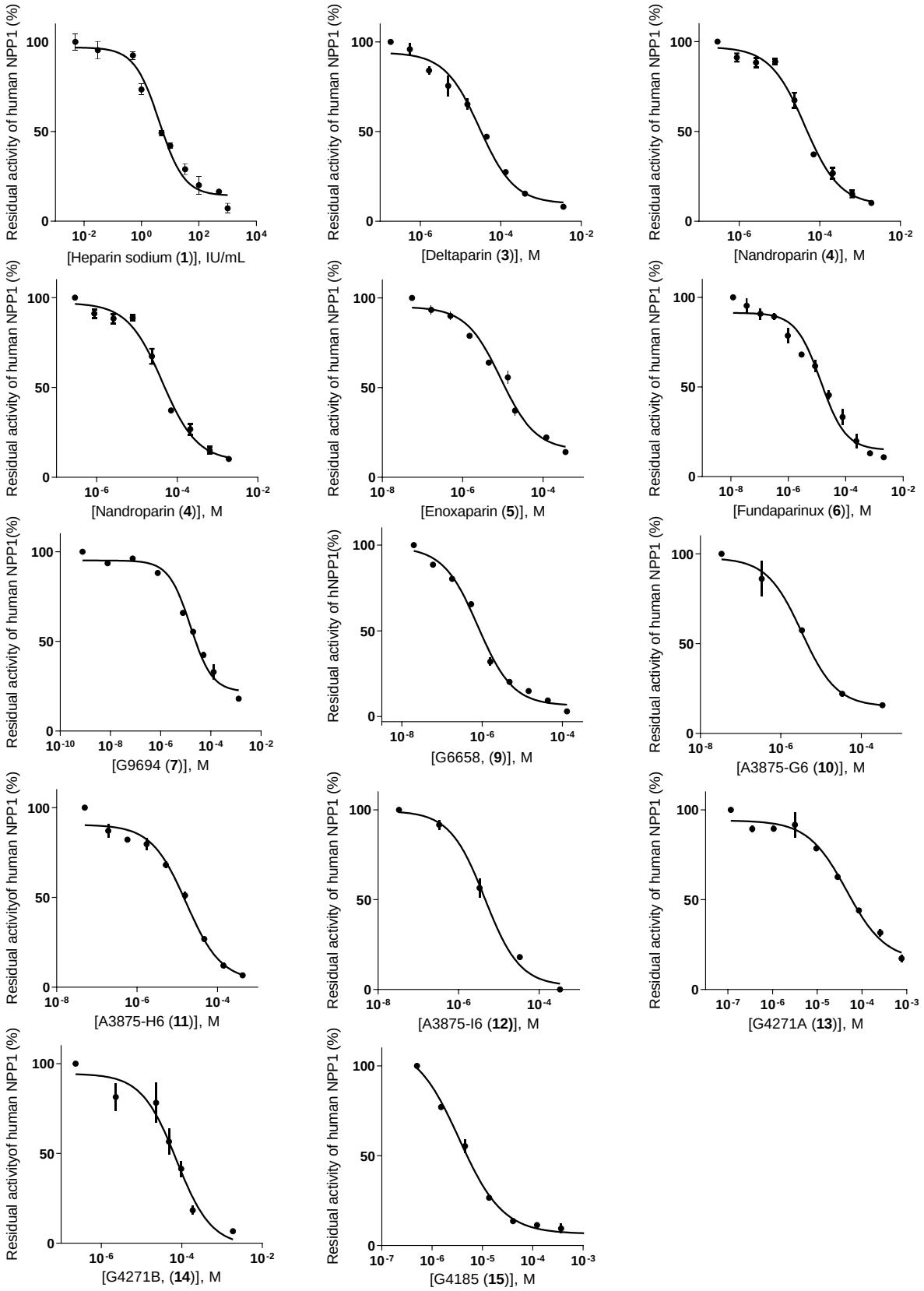

Figure S2. Concentration-inhibition curves of compound **1-15** at human NPP1 versus ATP. IC_{50} values of (**8**) and (**2**) were extrapolated from % inhibition. For details see section 2.1.

3.3 Summary and outlook

Several recent clinical studies suggest that heparin, particularly low-molecular-weight heparin, enhances cancer patient survival. Heparin's potential to inhibit metastasis has been demonstrated experimentally in a variety of animal models. Apart from its anticoagulant function, heparin possesses several biological activities that may influence cancer growth, including the inhibition of heparinase, the suppression of P- and L-selectin-mediated cell adhesion and the prevention of angiogenesis. Most likely more biological targets are still unknown and given the involvement of hNPP1 in the immune-oncology we sought to elucidate a possible correlation between hNPP1 inhibition and effects of heparin on cancer patients. Hence, we evaluated four commercially available heparins against the most essential members of the ectonucleotidase family and observed total inhibition of hNPP1 activity with high specificity. Subsequently, we investigated heparin derivatives that are either commercially available or have been produced with just modest chemical changes. All 13 compounds in the study were fully pharmacologically characterized (Fig. 3 and S2), followed by selectivity studies, among ectonucleotidase family, of the most interesting compounds: UFH (1), fondaparinux (6) and G9694 (7) (Fig. 4). Their IC_{50}, except for one derivative, were in the range of 0.41-30 μM and the selectivity studies showed high specificity for hNPP1. Additionally, their mechanism of action was examined utilizing G9694 and fondaparinux as representative compounds. The results indicate that these heparin derivatives inhibit hNPP1 with mixed-type inhibition (Fig. 5). Following that, we sought to identify a cell line expressing hNPP1 in order to evaluate our molecules in a more complex system than the isolated enzyme. The mRNA gene expression of ectonucleotidases was investigated in a variety of cell tumor lines. We searched primarily glioblastoma cell lines and identified a cell line for further analysis that expressed hNPP1 in addition to a very high level of CD73 (Fig. 6). The selected cell line U87 was biochemically characterized. We initially determined the membrane preparation's enzymatic activity and then determined its kinetic parameters. Following

that, we tested the inhibitory impact of G9694 and Fondaparinux on a membrane preparation of U87 cells and discovered that both drugs suppressed adenosine production. Finally, using a cell-based assay system we aimed to observe if the most active heparin derivatives have an inhibitory effect on the suppression of the degradation of proinflammatory ATP resulting in reduction of adenosine, which has immunosuppressive and tumor-promoting activities. We observed a dose-dependent inhibitory activity of those heparin derivatives, in accordance with our results obtained from the isolated hNPP1 enzyme. Heparin has an unexpected effect on ENs that is NPP1-dependent, indicating a role for immunological oncological treatments. It is unknown, however, whether this is significant or only contributes to the insufficient understanding of clinical data from heparinized oncological patients. The data presented represent a solid base for further future research.

4. Recombinant expression of ecto-nucleotide pyrophosphatase/ phosphodiesterase 4 (NPP4) and development of a luminescence-based assay to identify inhibitors

4.1 Introduction

In the last two decades, the interest in modulating the purinergic system and the ectonucleotidase family as therapeutic targets has grown. Among the NPP family, the function, and characteristics of human isoform 4 had so far not been fully studied. Recently, it was proposed that inhibiting NPP4 might have antithrombotic effects due to its involvement in hydrolyzing Ap_3A to ADP at the site of thrombus formation [1,2]. To elucidate the enzyme's physiological and pathological functions, it is critical to have tool substances capable of modulating the enzyme's activity. Therefore, we successfully expressed the protein using a host organism and we established and optimized a high-throughput screening assay for monitoring NPP4 activity in the presence of test compounds in order to find potential inhibitors, since none are known in the literature so far. In the following publication we present the results of our study.

References

1. Albright, R. A.; Chang, W. C.; Robert, D.; Ornstein, D. L.; Cao, W.; Liu, L.; Redick, M. E.; Young, J. I.; De La Cruz, E. M.; Braddock, D. T. NPP4 is a procoagulant enzyme on the surface of vascular endothelium. *Blood* **2012**, *120*, 4432–4440.

2. Albright, R.A.; Ornstein, D.L.; Cao, W.; Chang, W.C.; Robert, D.; Tehan, M.; Hoyer, D.; Liu, L.; Stabach, P.; Yang, G.; et al. Molecular basis of purinergic signal metabolism by ectonucleotide pyrophosphatase/phosphodiesterases 4 and 1 and implications in stroke. *J. Biol. Chem.* **2014**, *289*, 3294–3306, doi:10.1074/jbc.M113.505867.

4.2 Publication

Analytical Biochemistry 603 (2020) 113774

Contents lists available at ScienceDirect

Analytical Biochemistry

journal homepage: www.elsevier.com/locate/yabio

Recombinant expression of ecto-nucleotide pyrophosphatase/phosphodiesterase 4 (NPP4) and development of a luminescence-based assay to identify inhibitors

Vittoria Lopez[a,b], Sang-Yong Lee[a,b], Holger Stephan[c], Christa E. Müller[a,b,*]

[a] Pharmaceutical Institute, Pharmaceutical & Medicinal Chemistry, University of Bonn, An der Immenburg 4, 53121, Bonn, Germany
[b] PharmaCenter Bonn, University of Bonn, An der Immenburg 4, 53121, Bonn, Germany
[c] Institute of Radiopharmaceutical Cancer Research, Helmholtz-Zentrum Dresden-Rossendorf, Bautzner Landstraße 400, 01328, Dresden, Germany

ARTICLE INFO

Keywords:
Antithrombotic drug
Assay development
Ectonucleotidase
Recombinant enzyme expression
High-throughput screening
Luminescence detection
NPP4 inhibitors

ABSTRACT

Nucleotide pyrophosphatase/phosphodiesterase 4 (NPP4) is a membrane-bound enzyme that hydrolyzes extracellular diadenosine polyphosphates such as diadenosine triphosphate (Ap_3A) and diadenosine tetraphosphate (Ap_4A) yielding mononucleotides. NPP4 on the surface of endothelial cells was reported to promote platelet aggregation by hydrolyzing Ap_3A to ADP, which activates pro-thrombotic G protein-coupled $P2Y_1$ and $P2Y_{12}$ receptors. Thus, NPP4 inhibitors have potential as novel antithrombotic drugs. In the present study we expressed soluble human NPP4 in Sf9 insect cells and established an enzyme assay using diadenosine tetraphosphate (Ap_4A) as a substrate. The reaction product ATP was quantified by luciferin-luciferase reaction in a 96-well plate format. The sensitive method displayed a limit of detection (LOD) of 14.6 nM, and a Z′-factor of 0.68 indicating its suitability for high-throughput screening. The new assay was applied for studying enzyme kinetics and led to the identification of the first NPP4 inhibitors.

1. Introduction

Extracellular nucleotides are signaling molecules which regulate short- and long-term cellular functions including platelet aggregation, smooth muscle contraction, secretion of hormones, control of cell proliferation and differentiation, modulation of immune responses and apoptosis by activation of purinergic P2X and P2Y receptors on cell membranes [1–5]. Nucleotide-activated signaling is regulated by the extracellular hydrolysis of nucleotides through membrane-bound ecto-nucleotidases, such as ecto-nucleoside triphosphate diphosphohydrolases (NTPDases, including NTPDase1/CD39), ecto-nucleotide pyrophosphatases/phosphodiesterases (NPPs) and the non-specific alkaline phosphatases (APs) [2]. Nucleoside monophosphates, e.g. AMP, are further hydrolyzed by ecto-5′-nucleotidase (CD73) or by APs to adenosine, which activates membrane-bound adenosine receptors (P1 receptors) [2,6]. The enzyme family of NPPs consists of seven members (NPP1-7), four of which are known to hydrolyze extracellular nucleotides: NPP1 (PC-1), NPP3, NPP4 and NPP5 [1–3,7]. While NPP1 and 3 can hydrolyze a variety of nucleotides including nucleoside triphosphates (e.g. ATP, UTP), dinucleotide polyphosphates (e.g. Ap_3A, Ap_4A), cyclic dinucleotides (e.g. 2′,3″-cGAMP) and nucleotide sugars (e.g. UDP-glucose, ADP-ribose) [7–10], NPP4 was reported to hydrolyze the physiological dinucleotides Ap_3A and Ap_4A. The artificial substrate *p*-nitrophenyl thymidine 5′-monophosphate (*p*NP-TMP) is also cleaved by NPP4, while ATP hydrolysis by this enzyme is negligible [2,4,9,11]. NPP5 has recently been reported to hydrolyze nicotinamide adenine dinucleotide (NAD^+) [12]. Other members of the NPP family, i.e. NPP2 (autotaxin), NPP6 and NPP7 (alkaline sphingomyelinase) act as phospholipases catalyzing the hydrolysis of phospholipids [2]. The NPP family is implicated in a variety of physiologic and pathologic processes including tumor invasion and metastasis, inflammation, lung fibrosis and angiogenesis (NPP2), tissue calcification, bone development (NPP1), and platelet aggregation (NPP4) [2,5,7,11,13,14]. NPP4 is widely and highly expressed in many organs, tissues and cells in the brain as well as in the periphery, e.g. on brain vascular endothelial cells and on platelets. The nucleotide ADP activates the membrane-bound purinergic G protein-coupled receptor subtypes $P2Y_1$ and $P2Y_{12}$ expressed on thrombocytes resulting in platelet aggregation. However, ADP is rapidly degraded to AMP by membrane-associated NTPDase1 (CD39) thereby limiting thrombus formation. NPP4 has been reported to hydrolyze diadenosine triphosphate (Ap_3A) to ADP and AMP (see Fig. 1), thus inducing an extended platelet aggregation [11], possibly together with NPP1 [9]. Moreover, Ap_4A

* Corresponding author. Pharmaceutical Institute, Pharmaceutical and Medicinal Chemistry, An der Immenburg 4, D-53121, Bonn, Germany.
E-mail address: christa.mueller@uni-bonn.de (C.E. Müller).

https://doi.org/10.1016/j.ab.2020.113774
Received 5 January 2020; Received in revised form 24 April 2020; Accepted 10 May 2020
Available online 20 May 2020
0003-2697/ © 2020 Elsevier Inc. All rights reserved.

List of abbreviations

Ap_4A	diadenosine tetraphosphate
Ap_3A	diadenosine triphosphate
CHES	(2-(*N*-cyclohexylamino)ethanesulfonic acid)
FDA	Food and Drug Administration
HEPES	4-(2-hydroxyethyl)piperazine-1-ethanesulfonic acid
HTS	high-throughput screening
ICH	International Council for Harmonisation
LOD	limit of detection
LOQ	limit of quantification
NPP	ecto-nucleotide pyrophosphatase/phosphodiesterase
NTPDase	nucleoside triphosphate diphosphohydrolase
*p*NP-TMP	*p*-nitrophenyl thymidine 5′-monophosphate
PSB-POM145	$Na_6[H_2W_{12}O_{40}]\cdot 21H_2O$
PSB-POM146	$K_7[Ti_2W_{10}PO_{40}]\cdot 8H_2O$
RLU	relative light unit
RSD	relative standard deviation
TRIS	tris(hydroxymethyl)aminomethane

accumulation due to NPP4 inhibition may lead to a blockade of the prothrombotic $P2Y_1$ and $P2Y_{12}$ receptors thereby exerting anti-thrombotic effects, in addition to indirect inhibitory effects on P2X1 receptor activation, another platelet-activating receptor [15–17]. Thus, NPP4 inhibitors may be useful as antithrombotic drugs.

So far, no inhibitors of NPP4 have been described in literature. However, such compounds are required as pharmacological tools for investigating the (patho)physiological roles of NPP4 and its potential as a novel drug target. In order to identify and characterize inhibitors of NPP4 a high-throughput screening assay is required. In this study, we expressed human NPP4 and developed a novel luminescence-based assay for monitoring NPP4 enzymatic reactions. The new assay was validated according to the International Council of Harmonisation (ICH) and the United States Food and Drug Administration (FDA) guidelines for bioanalytical method validation. Finally, it was applied for investigating enzyme kinetics and for the screening of compound libraries to identify NPP4 inhibitors and the mechanism of inhibition on the enzyme.

2. Experimental section

2.1. Materials

ATP, calcium chloride, 2-(*N*-cyclohexylamino)ethanesulfonic acid (CHES), 4-(2-hydroxyethyl)piperazine-1-ethanesulfonic acid (HEPES), luciferase, D-luciferin, CoA, magnesium chloride and tris(hydroxymethyl)aminomethane (TRIS) were obtained from Sigma (Steinheim, Germany). Ap_4A and Ap_3A were obtained from Jena Bioscience (Jena, Germany). PSB-POM145 ($Na_6[H_2W_{12}O_{40}]\cdot 21H_2O$) and PSB-POM146 ($K_7[Ti_2W_{10}PO_{40}]\cdot 8H_2O$) were provided byHolger Stephan (Dresden, Germany) [18]. The pAcGP67-A baculovirus expression vector was purchased from BD BaculoGold (Becton, Dickinson and Company (BD) New Jersey, USA). Greiner 96-well plates (white and half area) were obtained from Merck KGaA (Darmstadt, Germany).

2.2. Recombinant expression of human NPP4

Human NPP4 is a type I transmembrane protein, with a single catalytic domain consisting of 453 amino acid residues. Soluble NPP4 was obtained by C-terminal and N-terminal truncation to eliminate the cytoplasmic and transmembrane domains. The full length human cDNA of NPP4 (Genbank accersion no. NM_014936) was obtained from Origene (Rockville, USA). In order to obtain soluble enzyme, only the extracellular domain of NPP4, was cloned. To amplify the cDNA, polymerase chain reactions (PCR) were performed by using two primers (forward: fhNPP4-45-XbaI 5′-gatc-tctaga-a-tttagaagtgactcttcctcta-3′, and reverse rhNPP4-1212-NotI 5′-gatc-gcggccgc-tta-gtggtggtggtggtgatggtggtggtg-ggcttctgggagattaatgc-3′) obtained from Thermo Scientific Inc. (Waltham, USA). A 9xHisTag was added for purification. Amplification was started by an incubation of 2 min at 95 °C which was followed by 35 cycles of 20 s denaturation at 95 °C, 20 s annealing at 56 °C and 1 min primer extension at 70 °C, ending with 10 min incubation at 70 °C. The PCR products were purified on agarose gel using the Zymo Gel DNA Recovery Kit (Freiburg, Germany). The DNA fragment of NPP4 was then digested with NotI and XbaI and ligated into a baculovirus expression vector pAcGP67-A previously digested with NotI and XbaI, possessing a gp67 secretion signal (essential for the entry of baculovirus particles into susceptible insect cells) followed on the C-terminus by a 9xHisTag. The protein was expressed using a baculovirus system, yielding soluble recombinant protein which was secreted into the extracellular fluid [14,18]. The recombinant cDNAs were stably transfected into *Spodoptera frugiperda* (Sf9) insect cells. Sf9 insect cells were grown at 27 °C in Insect Xpress media containing 0.1 mg/mL of gentamicin. After initial transfection, recombinant baculoviruses were produced, which were subsequently used for infecting Sf9 cells. NPP4 plasmid (ca. 500 ng) was mixed with Insect Xpress medium without antibiotics and the baculovirus genomic vector DNA BaculoGold™ (Becton, Dickinson and Company (BD) New Jersey, USA), and the mixture was then added to a solution of Cellfectin™ obtained from Thermo Scientific Inc. (Waltham, USA) and Insect Xpress medium and incubated for 20 min at room temperature. The transfection mixture was added drop-wise to the Sf9 cells, which were left at 25 °C for 30 min, and then incubated overnight at 27 °C. Then, the transfection mixture was replaced by Insect Xpress medium containing gentamicin, and the cells were cultured at 27 °C until signs of viral infection were observed, usually for 4–5 days. The supernatant, containing the P1 virus generation, was used to produce a high virus titer stock, which was then used to infect cells for protein production. After multiple infections of the insect cells (at least 5 amplification rounds), the supernatant of the Sf9 cells containing the recombinant enzyme was collected and concentrated by centrifugation through a dialysis filter (Amicon® Ultra, 10 kDa cutoff, 5000×*g*, 40 min, Merck, Darmstadt, Germany). Subsequently, the collected protein was purified on a HisPur™ Ni-NTA Spin Purification Kit (ThermoFisher® Cat. Num: 88229). Finally, the proteins were kept at −80 °C in enzyme buffer (10 mM HEPES, 2 mM $CaCl_2$, 1 mM $MgCl_2$, 5% glycerol, pH 8.0) until use. Western blots were performed to confirm the presence of the expressed NPP4. A bis-Tris-SDS-Page gel was run, and the separated

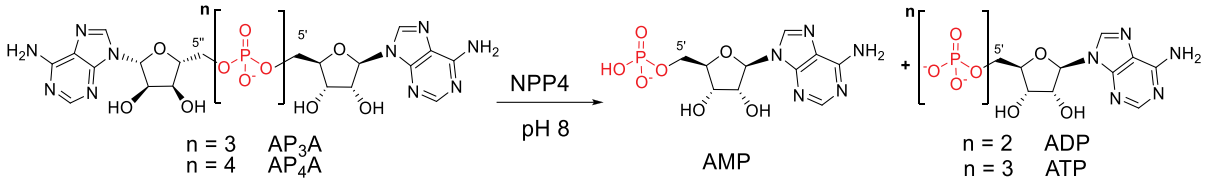

Fig. 1. Reactions catalyzed by NPP4.

proteins were then blotted onto a matrix (nitrocellulose membrane), where they were stained with antibodies (first antibody: mouse Anti-His, cat. No. MAB050R; second antibody: anti-mouse, HRP cat. No. HAF007 obtained from R&D system, Wiesbaden, Germany). After adding the second antibody the immune reaction was measured using horseradish peroxidase (HRP) substrate for enhanced chemiluminescence.

2.3. Instrumentation

All luminiscence measurements were carried out on a BMG PheraStar FS plate reader (BMG Labtech GmbH, Ortenberg, Germany).

2.4. Development and optimization of a luminescence-based NPP4 assay

A luminiscence-based NPP4 assay with Ap_4A as a substrate, resulting in the formation of ATP, was established. The formed ATP was quantified by a luciferase reaction leading to an ATP concentration-dependent luminiscence signal. The following parameters were optimized: the amount of firefly luciferase, the addition of coenzyme A in buffer B, and the buffer pH value (enzyme reaction buffer A). In order to find the optimal firefly luciferase concentration to work with, three different amounts of firefly luciferase were employed, 25, 50 and 100 ng in H_2O for the preparation of buffer C. Furthermore, the effect of CoA was investigated by comparing the signal emitted by a solution of 2 μM ATP in the presence or absence of CoA. The luciferase substrate D-luciferin in buffer B (300 mM Tris-HCl, 15 mM $MgCl_2$, 450 μg/ml D-luciferin, pH 7.8) [19] was added to the ATP solution with or without CoA (750 μM) [20], and subsequently buffer C (50 ng luciferase) was added leading to the emission of a bioluminescence signal. In order to verify the robustness of the luminescence method and with the aim to select the optimal pH value for the NPP4 enzyme assay, different pH values for buffer A were studied (pH 7.4, 8.0 and 9.0). The reaction buffer A contained 10 mM HEPES, 1 mM $MgCl_2$ and 2 mM $CaCl_2$ except for the pH 9.0 buffer, for which CHES (10 mM) instead of HEPES was used. All NPP4 and Ap_4A solutions for the NPP4 assays were prepared in reaction buffer A. A high-throughput screening (HTS) assay was established by further optimizing the substrate concentration and the amount of NPP4 by titration. The optimized assay was used for monitoring NPP4 activity and for the screening of a compound library to identify inhibitors. Solutions of substrate and enzyme were prepared in reaction buffer A (10 mM HEPES, 1 mM $MgCl_2$ and 2 mM $CaCl_2$, pH 8.0). The substrate Ap_4A was tested at three different concentrations (10, 12.5 and 20 μM). The reaction was initiated by adding 20 μl of a solution of human NPP4 (0.28, 0.70, or 1.40 μg, respectively). The mixture was incubated at 37 °C for 60 min, and then stopped by heating at 90 °C for 5 min. After the incubation, 50 μl of buffer B (300 mM Tris-HCl, 15 mM $MgCl_2$, 100 ng D-luciferin, pH 7.8) and 50 μl of buffer C (50 ng of luciferase in H_2O) were added to each well. Negative controls were performed in the presence of inactivated NPP4 enzyme, which was achieved by previous heating of the enzyme at 90 °C for 5 min.

2.5. Method validation

The NPP4 enzyme assay was validated according to the ICH and the FDA guidelines for bioanalytical method validation [21]. An eight-point calibration curve (0.01–2 μM of ATP) dissolved in reaction buffer A (10 mM HEPES, 1 mM $MgCl_2$ and 2 mM $CaCl_2$, pH 8.0) was determined. Each concentration was measured twice, each in triplicates. To each well, 50 μl of the ATP solution, and subsequently 50 μl of buffer B and 50 μl of buffer C were added. Luminescence was then measured on a BMG PheraStar FS plate reader (BMG Labtech GmbH, Ortenberg, Germany). Calibration curves were obtained by correlating the measured Relative Light Units (RLU) with the employed concentrations of ATP. Precision and recovery were evaluated in a concentration range of 0.044–1 μM, tested in six replicates. The limit of detection (LOD) and the limit of quantification (LOQ) were calculated from the calibration curve using the values of standard deviation of the y-intercept (σ) and the slope (S) (LOD = 3.3 x σ/S, LOQ = 10 x σ/S). The Z′-factor was calculated with the formula of Zhang et al. [22] by using 16 positive controls with NPP4 and 16 negative controls with inactivated NPP4 (previously denatured by heating at 95 °C for 5 min). The robustness was calculated using three different buffer pH values as described in paragraph 2.4. Four repetitions for each buffer were tested and the relative standard deviation (RSD) in % was calculated. For determination of precision and accuracy, RSD (%) was calculated at different ATP concentrations.

2.6. Biochemical characterization of NPP4

Solutions containing different concentrations of Ap_4A ranging from 2.5 to 600 μM were prepared in enzyme reaction buffer A (1 $MgCl_2$ mM, 2 $CaCl_2$ mM, 10 HEPES mM, pH 8.0). The enzymatic reactions were initiated by the addition of 20 μl of human NPP4 (0.28 μg/well) while keeping the plates on ice, followed by an incubation at 37 °C for 60 min and 5 min at 95 °C to stop the enzymatic reaction. The further procedure for the determination of ATP as a product of NPP4 activity was performed as described above. Each analysis was carried out in three separate experiments, each performed in triplicates. The kinetic parameters of NPP4 were calculated using Prism 7.0 (GraphPad software, San Diego, CA, USA).

2.7. NPP4 inhibition assays

The newly developed assay was used for the screening of a compound library (1120 compounds) to search for inhibitors of human NPP4. The conditions of the assay were the same as described in the previous section. The test compounds were dissolved in 10% aqueous DMSO solution and tested at a final concentration of 10 μM in the presence of 2% DMSO. Two hit compounds were selected for determination of full concentration-response curves, PSB-POM145 and PSB-POM146. The inhibitors were tested versus 20 μM of the substrate Ap_4A (K_m ca. 400 μM). Solutions of inhibitors in concentrations ranging from 0.0001 to −300 μM were prepared. The further procedure was the same as described above. The IC_{50} values were determined by nonlinear curve fitting using Graphpad Prism 7.0. The mechanism of inhibition at human NPP4 was determined employing four different concentrations of the investigated inhibitor (PSB-POM145) ranging from 0 to 10 μM, vs. five different substrate concentrations ranging from 10 to 200 μM of Ap_4A. The assay procedure and operation conditions were the same as described in chapter 2.6. The experiment was conducted twice, each in duplicates. Lineweaver-Burk, was calculated using GraphPad Prism for predicting the inhibition type of the compound.

2.8. Capillary electrophoresis-based assay

For kinetic characterization of NPP4, several Ap_4A concentrations (from 15 to 1000 μM) were incubated with ~1 ng of NPP4 at 37 °C for 90 min. The reaction was stopped by heating for 5 min at 90 °C. Capillary electrophoresis (CE) coupled to UV detection was used for analysis and quantification of the products (injection: −6 kV for 30 s, 40 cm [30 cm eff.] polyacrylamide-coated capillary, 100 mM phosphate pH 6.5 as a running buffer, −10 kV of separation voltage, detection at 260 nm). The same CE procedure was used for inhibitor characterization using 100 μM of Ap_4A as a substrate; all other conditions were as described above.

2.9. Capillary electrophoresis assay to study CoA as a potential NPP4 substrate

CoA solution in water was freshly prepared before performing the experiments. CoA was incubated with NPP4 for 90 min at 37 °C and the

reaction was stopped by heating for 5 min at 95 °C. Three concentrations of CoA (50, 100 and 200 μM) and two enzyme amounts (1 and 2 ng) were used. Two independent experiments, each in triplicate, along with positive and negative controls were performed. The CE was used for analysis and quantification of the products (injection: −6 kV for 30 s, 40 cm [30 cm eff.] polyacrylamide-coated capillary, 50 mM phosphate pH 6.5 as a running buffer, −90 μA of separation current, detection at 260 nm). No cleavage of CoA by NPP4 was observed.

3. Results and discussion

3.1. Recombinant expression of human NPP4

The soluble form of human NPP4 bearing a His-tag was successfully cloned, recombinantly expressed in Sf9 insect cells and released into the supernatant [11] (see Fig. 2). In order to confirm stable transfection of the soluble recombinant protein, a Western Blot was carried out using an anti-His tag antibody. The results confirmed the presence of the recombinant protein with a molecular weight of around 50 kDa (Fig. 2C). As a next step, the enzymatic activity of the expressed NPP4 was confirmed. The ectonucleotidase can hydrolyze diadenosine triphosphate (Ap_3A) yielding ADP and AMP, and diadenosine tetraphosphate (Ap_4A) producing ATP and AMP. To monitor NPP4 reactions, we initially utilized CE (capillary electrophoresis) for analysis and quantification of the products. The crude enzyme was incubated with the substrate Ap_3A at 37 °C for 60 min and the reaction was subsequently stopped by heating for 5 min at 90 °C. A denatured enzyme preparation (heated at 90 °C for 3 min) was tested as a negative control, and the cell medium of uninfected insect cells was measured to exclude background activity of the cells (Fig. 2B). The results clearly showed enzymatic NPP4 activity. As a next step the His-tagged enzyme was purified using nickel affinity column chromatography. The purified protein (Fig. 2A) was tested under the same conditions as described above, the purified enzyme displaying a higher enzymatic activity than the crude enzyme as expected, using the same conditions (Fig. 2D).

3.2. Luciferase assay to monitor NPP4

Monitoring NPP4 activity by a CE assay does not allow for high-throughput screening (HTS). Therefore, we developed a novel strategy for assaying NPP4 activity by determining the produced ATP by subsequent luciferase reaction (see Fig. 3) [23]. The amount of ATP formed from the substrate Ap_4A, which is hydrolyzed to ATP and AMP, correlates with the detected luminescence. Firefly luciferase from *Photinus pyralis* (firefly beetle) whose enzymatic activity is dependent on ATP, was employed [24]. The reaction could easily be performed in a 96-well plate format, and luminescence was determined on a microplate reader.

3.2.1. Development and optimization of a luminescence-based NPP4 assay

Initially, the optimal amount of luciferase was investigated employing three different amounts: 25, 50 and 100 ng. As expected, an increase in the amount of luciferase led to an increased signal. An amount of 50 ng of luciferase was chosen for further experiments which provided a suitably high luminescence signal for quantification (see Fig. S1). When luciferase was added to the luciferin sample, there was an immediate flash of light which reached its peak within few seconds before it decayed rapidly. It was previously reported that CoA initially added to the assay buffer should prevent the fast decay extending the

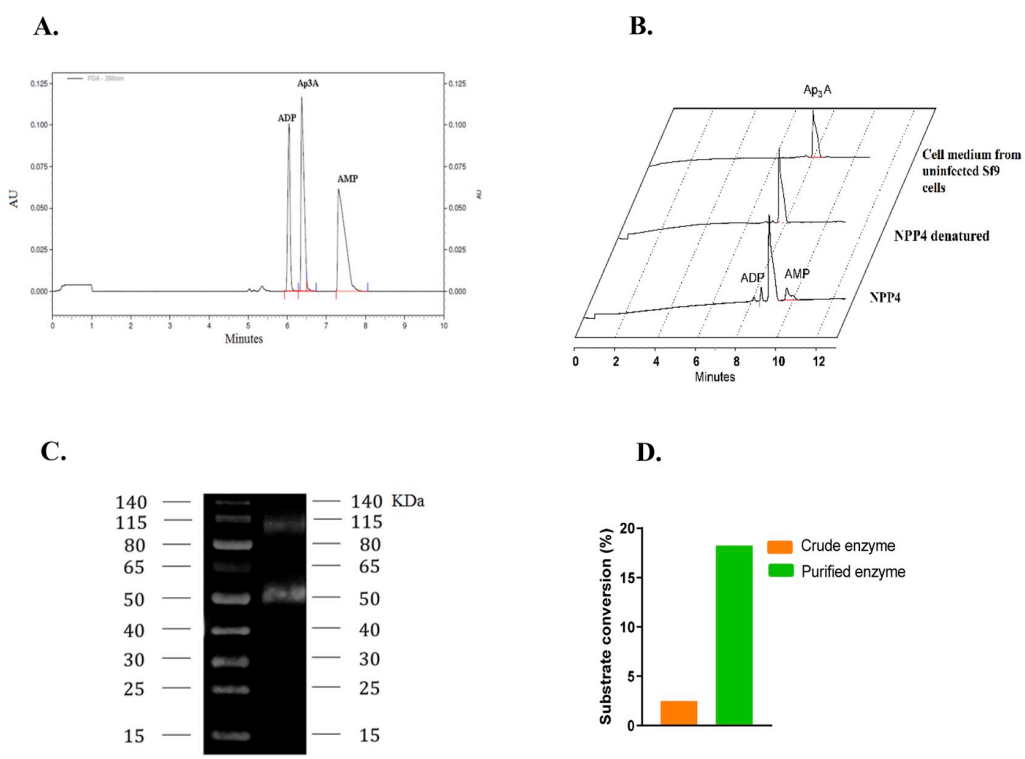

Fig. 2. A. Example of electropherogram obtained from CE after enzymatic reaction of purified NPP4 (1.5 μg) with Ap_3A (400 μM) as a substrate. The mixture was incubated at 37 °C for 60 min and then stopped by heating for 5 min at 90 °C. Capillary electrophoresis (CE) was used for analysis and quantification of the products (injection: −6 kV for 30 s, 40 cm [30 cm eff.] polyacrylamide-coated capillary, 100 mM phosphate pH 6.5 as a running buffer, −10 kV of separation voltage, detection at 260 nm). **B.** Enzyme activity test with crude enzyme using Ap_3A as a substrate compared with denatured enzyme (5 min at 90 °C) and cell medium of uninfected Sf9 cells. Enzymatic activity assay and CE analysis was performed as described for Fig. 2A. **C.** Western blot of the expressed soluble human NPP4 using an anti-His-tag antibody; the band around 50 kDa corresponds to NPP4, while the second band is due to unspecific binding. **D.** Comparison of enzyme activities between crude and purified enzyme. Ap_3A (400 μM) was used as a substrate, and 20 μl of crude or purified enzyme (each containing 1 μg of protein) were added. The mixture was incubated at 37 °C for 60 min and then stopped by heating for 5 min at 90 °C. The CE separation conditions are the same as described in Fig. 2A.

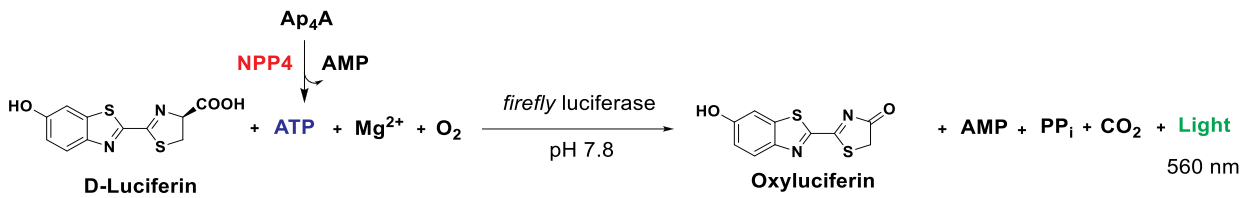

Fig. 3. Detection of ATP formed as a product of NPP4 activity from Ap_4A as a substrate by the D-luciferin-luciferase reaction.

Table 1
Validation parameters of the NPP4 luminescence assay.

Parameters	Results	Acceptable range
Linearity (R^2)	0.9973	
LOD	14.6 nM	
LOQ	44.3 nM	
Recovery (%)		
0.044 μM	100%	40–120%
0.1 μM	116%	40–120%
0.5 μM	98%	40–120%
1 μM	114%	40–120%
Robustness (RSD %)	5.5%	
Precision (RSD %)		
0.044 μM	8.4%	< 30%
0.1 μM	8.5%	
0.5 μM	3.4%	
1 μM	3.4%	
Z′-factor	0.68	0.5–1.0

Table 2
Determined kinetic parameters for Ap_4A as a substrate of NPP4.

Parameter	Determined values Luminescence assay	Literature values [11]	Determined values CE assay
K_m (μM ± SD)	417 ± 25	209 ± 3	220 ± 49
k_{cat} (s^{-1} ± SD)	0.53 ± 0.02	0.78 ± 0.01	0.46 ± 0.04
k_{cat}/K_m	1.26×10^3	3.73×10^3	2.08×10^3

half-life of the observed signal [24]. We investigated whether CoA was cleaved by NPP4 using a CE-UV method, but no enzymatic cleavage was observed (see SI Fig. S4). Thus, to study the effect of CoA addition and with the aim to detect the best time window, the signal was measured every 2 min, with and without CoA, until a significant reduction of luminescence was observed. We observed that the signal was drastically decreased within the first 6 min reaching linearity after about 10 min (see Fig. S1). Thus, the time between 10 and 14 min, after the addition of luciferase was chosen for detection. In the presence of CoA, an about

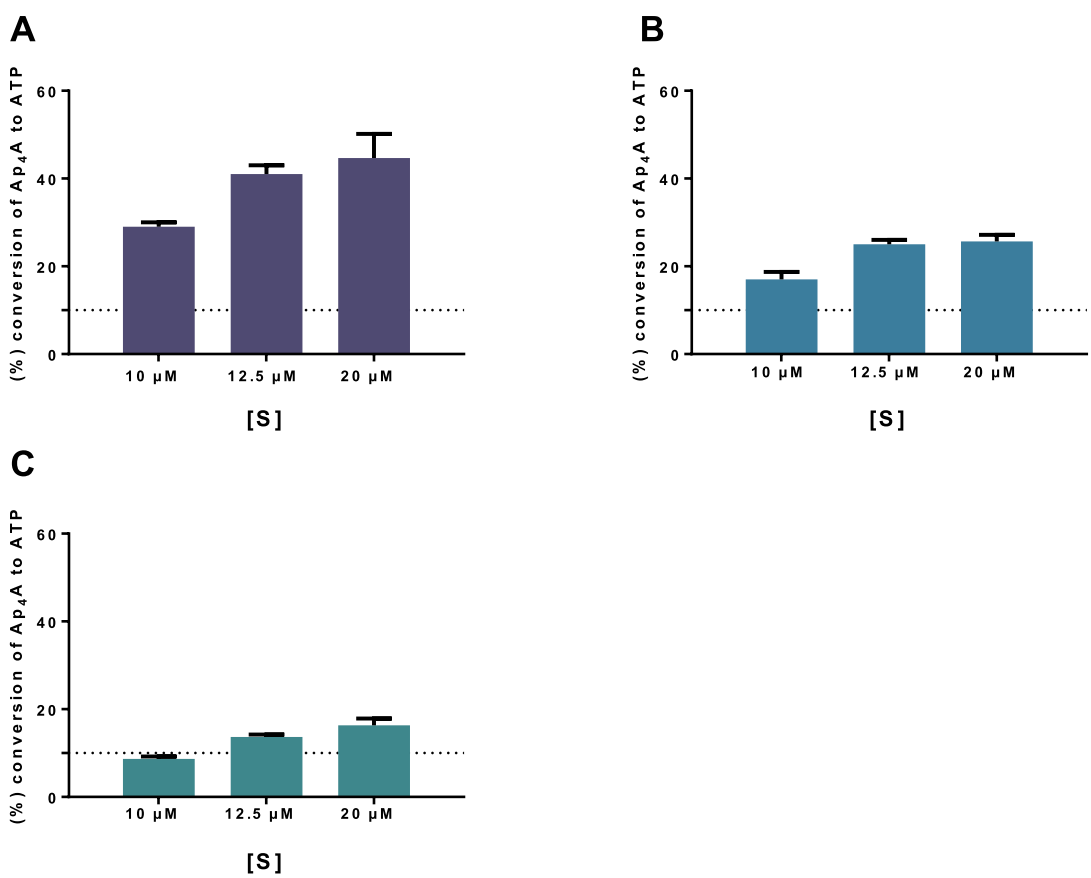

Fig. 4. Enzyme titration using three different amounts of NPP4 and three different Ap_4A concentrations employed as a substrate. **A**. 1.40 μg of NPP4; **B**. 0.,7 μg of NPP4 and **C**. 0.28 μg of NPP4. The dotted line indicates 10% substrate conversion, [S], substrate concentration.

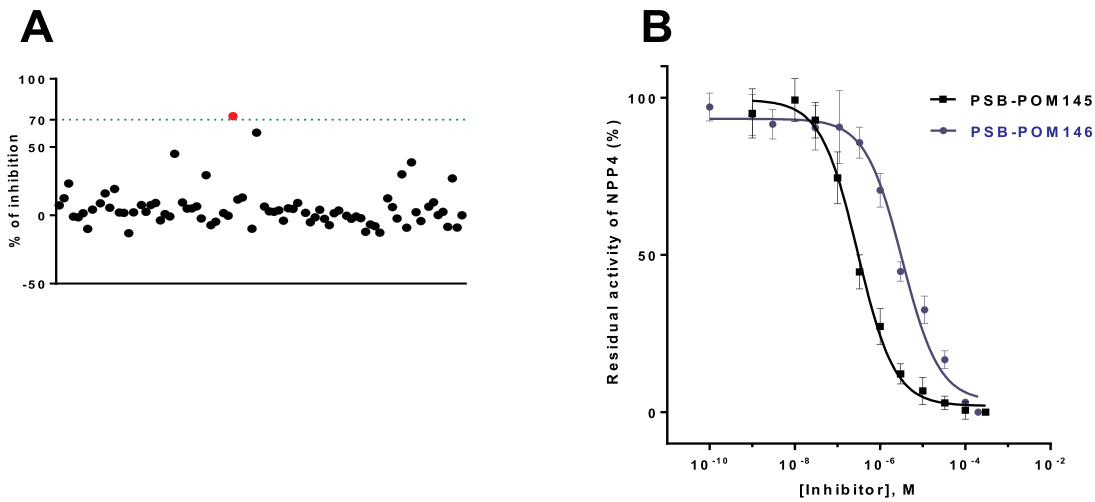

Fig. 5. A. Example of compound library screening. The best hit showed > 70% inhibition of NPP4 activity at **10** μM concentration. **B.** Concentration–inhibition curves of NPP4 inhibitors PSB-POM145 (IC_{50} = 0.298 ± 0.052 μM) and PSB-POM146 (IC_{50} = 3.36 ± 0.46 μM) discovered by HTS at human NPP4 using 20 μM Ap_4A as a substrate (K_m: 417 μM). The enzyme reaction product ATP was detected by luciferin-luciferase reaction.

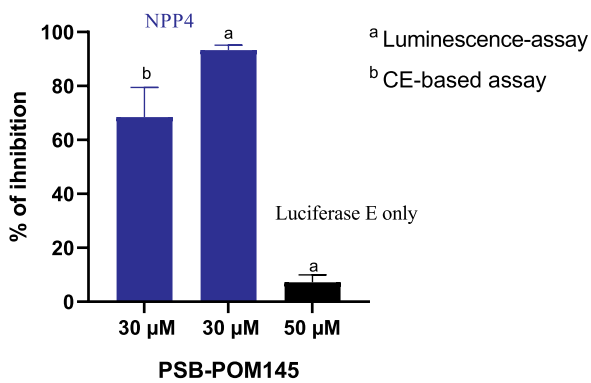

Fig. 6. Comparison of inhibitory activity of PSB-POM145 (30 μM) on NPP4 using two different assay systems. A control experiments to determine direct inhibition of luciferase by a high concentration of PSB-POM145 showed that this was negligible.

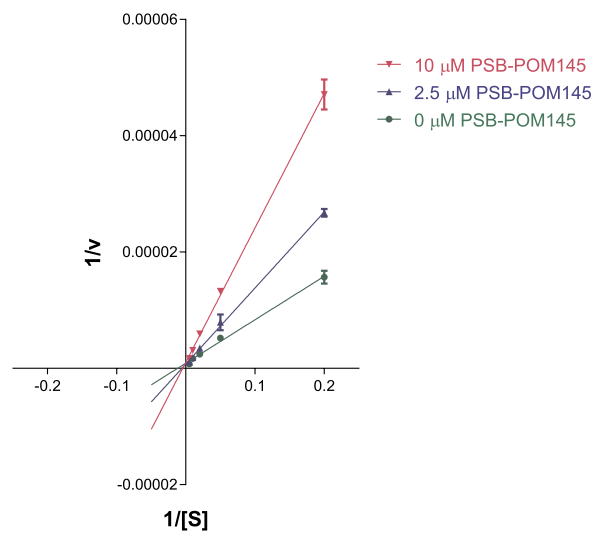

Fig. 7. Prediction of the type of inhibition mechanism by Linear weaver-Burk plot using 0, 2.5 and 10 μM of PSB-POM145 and five substrate concentrations, 5, 20, 50, 100 and 200 μM of Ap_4A determined by the luciferase-based NPP4 assay.

2-fold enhanced luminescence signal was observed. However, in contrast to the literature report, the decrease in luminescence observed within the first 10 min of the reaction was neither stopped nor reduced [24]. Furthermore, in the presence of CoA, the standard deviations were larger.

Therefore, we decided not to add CoA in further experiments. With the aim to select the optimal pH value for the NPP4 enzyme assay, different pH values for buffer A were studied (pH 7.4, 8.0 and 9.0). The experiments showed that no significant differences were observed with different pH values (Fig. S2). We selected pH 8.0 because it had been proposed as an optimal pH value for NPP4 activity [11], and this pH value had also been recommended for the luciferin-luciferase reaction [24]. The data obtained from the experiments were used to calculate the robustness of the assay discussed in the method validation section (see Table 1). After fixing the conditions for the luciferase reaction, the parameters for the NPP4 reactions were optimized by enzyme titration experiments. Three different amounts of NPP4 and three substrate concentrations were studied (Fig. 4). Employing 0.28 μg of NPP4 and 12.5 μM of Ap_4A as a substrate was found to be suitable. Under these conditions, 10–15% substrate conversion was observed, which can be regarded as an optimal conversion rate for inhibition assays, and a suitable window for detection was obtained. The established assay for monitoring NPP4-catalyzed enzymatic reaction was finally utilized for the screening of a compound library.

3.2.2. Method validation

The NPP4 assay was validated according to the ICH and FDA guidelines [21]. An overview of the quantitative parameters of the method validation is provided in Table 1.

The concentration of the reaction product ATP was set between 0.0125 and 1.25 μM (0.0125 μM: 99% inhibition of NPP4 activity and 1.25 μM: 0% inhibition of NPP4 activity). The calibration curve for ATP showed strict linearity in a concentration range of 0.01–2 μM (R^2 = 0.9973, see Fig. S3). The calculated limit of detection (LOD) and limit of quantification (LOQ) were 14.6 nM and 44.3 nM, respectively. The recovery rate (%) was calculated at four different concentrations of ATP resulting in a range of 98–116%, which is within the acceptable range of 40–120%. The RSD (%) of the calculated precision was in a range of 3.4–8.4% which is well below the acceptable range of 30%. The calculated RSD (%) of the method's robustness, determined by using different pH values, was 5.5%. The Z'-factor

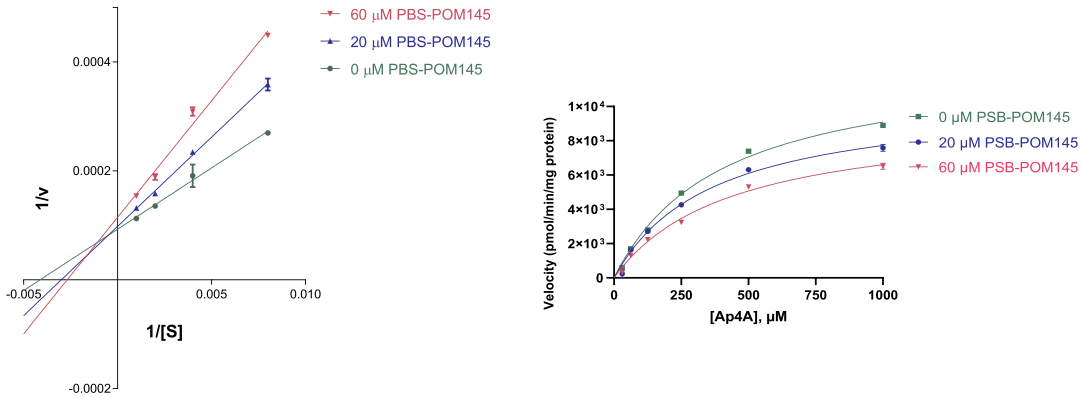

Fig. 8. Confirmation of the mechanism of NPP4 inhibition by a capillary electrophoresis-based assay.

was 0.68, which indicates that the developed assay is suitable for HTS (acceptable range: 0.5–1.0) [22].

3.3. Biochemical characterization of NPP4

The newly developed assay was subsequently applied for the biochemical characterization of the expressed NPP4 enzyme. The Michaelis-Menten constant (K_m), the turnover number (k_{cat}), and the substrate specificity parameter (k_{cat}/K_m) were determined for the NPP4 substrate Ap_4A. A K_m value of 417 ± 25 μM, a k_{cat} value of 0.53 ± 0.02 s^{-1} and a k_{cat}/K_m value of 1.26 × 10^3 were determined (see Table 2). The K_m value was consonant with the previously published value (417 *vs.* 209 μM) determined by a different assay method [11]. The k_{cat} value and k_{cat}/K_m were also in the same range as the published values (k_{cat}: 0.53 *vs.* 0.78 s^{-1} and k_{cat}/K_m: 1.26 × 10^3 *vs.* 3.73 × 10^3). We additionally characterized the enzyme preparation by a previously developed CE-UV method, which led to similar values (see Table 2). The slight differences may be due to different assay conditions such as incubation time and buffer, different amounts and preparations of enzyme used, and different methods for the monitoring of NPP4 activity and for product quantification (i.e. luminescence *vs.* HPLC/UV spectroscopy) [11].

3.4. NPP4 inhibition assays

The newly developed NPP4 assay is fast, economic, and displays high precision and sensitivity. We subsequently utilized it for HTS of a compound library of 1120 compounds, which were tested at a screening concentration of 10 μM versus 20 μM of Ap_4A as a substrate. Several hit compounds were identified that inhibited NPP4 activity, the most potent inhibitor displaying > 70% inhibition of NPP4 activity (red dot in Fig. 5A), the polyoxometalates PSB-POM145 ($Na_6[H_2W_{12}O_{40}]\cdot 21H_2O$) and the related PSB-POM146 ($K_7[Ti_2W_{10}PO_{40}]\cdot 8H_2O$) were selected for determining concentration inhibition curves (see Fig. 5B). The determined IC_{50} values were 0.298 ± 0.052 μM (PSB-POM145) and 3.36 ± 0.45 μM (PSB-POM146). These polyoxometalates had previously been characterized as potent and selective inhibitors of NPP1 but do not inhibit NPP2 and NPP3 [18].

To confirm this result and to exclude potential inhibition of luciferase instead of NPP4, we additionally studied NPP4 inhibition by the most potent compound, PSB-POM145, in an orthogonal, CE-UV-based assay using 100 μM of Ap_4A as a substrate due to the lower sensitivity of this method. In addition, a control experiment was performed without the addition of NPP4 to examine the possibility of a direct inhibitory effect of the compound on luciferase. PSB-POM145 inhibited NPP4 in both assays, but showed only a negligible direct effect on luciferase confirming that the new assay successfully detected the first NPP4 inhibitors (see Fig. 6).

The mechanism of inhibition at human NPP4 was determined employing different concentrations of the most potent inhibitor PSB-POM145 with concentrations ranging from 0 to 10 μM, vs. different substrate concentrations ranging from 10 to 200 μM of Ap_4A. The assay procedure and operation conditions for the enzyme assay were same as described in chapter 2.6. The experiment was conducted twice, each in duplicates. The Lineweaver-Burk plot [25], was calculated using GraphPad Prism for predicting the inhibition type of the compound.

The Lineweaver-Burk plot determined at concentrations of 0, 2.5 and 10 μM of PSB-POM145 in the presence of 5, 20, 50, 100 and 200 μM of the substrate Ap_4A, showed a typical pattern for competitive antagonists, where the lines meet on the y-axis (see Fig. 7). This was confirmed by an orthogonal, CE-based assay (see Fig. 8). Thus, we conclude that the PSB-POM145 is a competitive inhibitor of human NPP4.

4. Conclusions

In conclusion, a simple, sensitive and efficient luminescence-based assay has been developed for investigating NPP4 activity. The soluble form of human NPP4 was successfully expressed, and the kinetic parameters for Ap_4A used as a substrate were determined. The newly developed assay can be performed in a 96-well plate format and is suitable for high-throughput screening of compound libraries. This sensitive analytical method (LOD for the enzymatic product ATP formed from Ap_4A: 14.6 nM) allows studying enzymatic reactions with low enzyme and substrate concentrations. We expect that the technique can be easily adapted to a 384-well plate format using a fully automated robotic system. Upon screening of a compound library, hit compounds were identified, and their IC_{50} values and the mechanism of inhibition were determined leading to the discovery of the first inhibitors for NPP4. The developed assay will be useful for the identification and characterization of alternative substrates and modulators for this pharmacologically relevant class of enzymes.

Funding

This study was funded by the Federal Ministry of Education and Research (BMBF, BIGS DrugS project) and by the Deutsche Forschungsgemeinschaft (DFG, SFB1328).

Author contributions

V.L. and S-Y.L. performed the experiments and analyzed the data, C.E.M supervised the study, which was designed by C.E.M, S.-Y.L. and V.L. H.S. provided PSB-POM145 and PSB-POM146. V.L. and C.E.M. wrote the manuscript with contributions by S.-Y.L. and H.S.

Declaration of competing interest

The authors declare no conflict of interest.

Appendix A. Supplementary data

Supplementary data to this article can be found online at https://doi.org/10.1016/j.ab.2020.113774.

References

[1] G. Burnstock, Pathophysiology and therapeutic potential of purinergic signalling, Pharmacol. Rev. 58 (2006) 58–86, https://doi.org/10.1124/pr.58.1.5.

[2] H. Zimmermann, M. Zebisch, N. Sträter, Cellular function and molecular structure of ecto-nucleotidases, Purinergic Signal. 8 (2012) 437–502, https://doi.org/10.1007/s11302-012-9309-4.

[3] M.P. Abbracchio, G. Burnstock, J.-M. Boeynaems, E.A. Barnard, J.L. Boyer, C. Kennedy, G.E. Knight, M. Fumagalli, C. Gachet, K.A. Jacobson, G.A. Weisman, International Union of Pharmacology LVIII: update on the P2Y G protein-coupled nucleotide receptors: from molecular mechanisms and pathophysiology to therapy, Pharmacol. Rev. 58 (2006) 281–341, https://doi.org/10.1124/pr.58.3.3.

[4] C. Coddou, Z. Yan, T. Obsil, J.P. Huidobro-Toro, S.S. Stojilkovic, Activation and regulation of purinergic P2X receptor channels, Pharmacol. Rev. 63 (2011) 641–683, https://doi.org/10.1124/pr.110.003129.

[5] L. Antonioli, C. Blandizzi, P. Pacher, G. Haskó, The purinergic system as a pharmacological target for the treatment of immune-mediated inflammatory diseases, Pharmacol. Rev. 71 (2019) 345–382, https://doi.org/10.1124/pr.117.014878.

[6] B.B. Fredholm, A.P. IJzerman, K.A. Jacobson, J. Linden, C.E. Müller, International Union of Basic and Clinic Pharmacology . LXXXI. Nomenclature and classification of adenosine receptors—an update, Pharmacol. Rev. 63 (2011) 1–34, https://doi.org/10.1124/pr.110.003285.

[7] S.-Y. Lee, C.E. Müller, Nucleotide pyrophosphatase/phosphodiesterase 1 (NPP1) and its inhibitors, MedChemComm 8 (2017) 823–840, https://doi.org/10.1039/C7MD00015D.

[8] V. Namasivayam, S.Y. Lee, C.E. Müller, The promiscuous ectonucleotidase NPP1: molecular insights into substrate binding and hydrolysis, Biochim. Biophys. Acta Gen. Subj. 1861 (2017) 603–614, https://doi.org/10.1016/j.bbagen.2016.12.019.

[9] R.A. Albright, D.L. Ornstein, W. Cao, W.C. Chang, D. Robert, M. Tehan, D. Hoyer, L. Liu, P. Stabach, G. Yang, E.M. De La Cruz, D.T. Braddock, Molecular basis of purinergic signal metabolism by ectonucleotide pyrophosphatase/phosphodiesterases 4 and 1 and implications in stroke, J. Biol. Chem. 289 (2014) 3294–3306, https://doi.org/10.1074/jbc.M113.505867.

[10] K. Kato, H. Nishimasu, D. Oikawa, S. Hirano, H. Hirano, G. Kasuya, R. Ishitani, F. Tokunaga, O. Nureki, Structural insights into cGAMP degradation by ecto-nucleotide pyrophosphatase phosphodiesterase 1, Nat. Commun. 9 (2018) 4424, https://doi.org/10.1038/s41467-018-06922-7.

[11] R.A. Albright, W.C. Chang, D. Robert, D.L. Ornstein, W. Cao, L. Liu, M.E. Redick, J.I. Young, E.M. De La Cruz, D.T. Braddock, NPP4 is a procoagulant enzyme on the surface of vascular endothelium, Blood 120 (2012) 4432–4440, https://doi.org/10.1182/blood-2012-04-425215.

[12] A. Gorelik, A. Randriamihaja, K. Illes, B. Nagar, A key tyrosine substitution restricts nucleotde hydrolysis by the ectoenzyme NPP5 5 (2017), pp. 1–9, https://doi.org/10.1111/febs.14266.

[13] E.E. Shayhidin, E. Forcellini, M.C. Boulanger, A. Mahmut, S. Dautrey, X. Barbeau, P. Lagüe, J. Sévigny, J.F. Paquin, P. Mathieu, Quinazoline-4-piperidine sulfamides are specific inhibitors of human NPP1 and prevent pathological mineralization of valve interstitial cells, Br. J. Pharmacol. 172 (2015) 4189–4199, https://doi.org/10.1111/bph.13204.

[14] M. Nassir, U. Arad, S.-Y. Lee, S. Journo, S. Mirza, C. Renn, H. Zimmermann, J. Pelletier, J. Sévigny, C.E. Müller, B. Fischer, Identification of adenine-N9-(methoxy)ethyl-β-bisphosphonate as NPP1 inhibitor attenuates NPPase activity in human osteoarthritic chondrocytes, Purinergic Signal. 15 (2019) 247–263, https://doi.org/10.1007/s11302-019-09649-2.

[15] H. Chang, I.B. Yanachkov, E.J. Dix, Y.F. Li, M.R. Barnard, G.E. Wright, A.D. Michelson, A.L. Frelinger, Modified diadenosine tetraphosphates with dual specificity for $P2Y_1$ and $P2Y_{12}$ are potent antagonists of ADP-induced platelet activation, J. Thromb. Haemostasis 10 (2012) 2573–2580, https://doi.org/10.1111/jth.12035.

[16] H. Chang, I.B. Yanachkov, A.D. Michelson, Y. Li, M.R. Barnard, G.E. Wright, A.L. Frelinger, Agonist and antagonist effects of diadenosine tetraphosphate, a platelet dense granule constituent, on platelet $P2Y_1$, $P2Y_{12}$ and P2X1 receptors, Thromb. Res. 125 (2010) 159–165, https://doi.org/10.1016/j.thromres.2009.11.006.

[17] I.B. Yanachkov, H. Chang, M.I. Yanachkova, E.J. Dix, M.A. Berny-Lang, T. Gremmel, A.D. Michelson, G.E. Wright, A.L. Frelinger, New highly active antiplatelet agents with dual specificity for platelet $P2Y_1$ and $P2Y_{12}$ adenosine diphosphate receptors, Eur. J. Med. Chem. 107 (2016) 204–218, https://doi.org/10.1016/j.ejmech.2015.10.055.

[18] S.Y. Lee, A. Fiene, W. Li, T. Hanck, K.A. Brylev, V.E. Fedorov, J. Lecka, A. Haider, H.J. Pietzsch, H. Zimmermann, J. Sévigny, U. Kortz, H. Stephan, C.E. Müller, Polyoxometalates - potent and selective ecto-nucleotidase inhibitors, Biochem. Pharmacol. 93 (2015) 171–181, https://doi.org/10.1016/j.bcp.2014.11.002.

[19] Y. Oba, M. Ojika, S. Inouye, Firefly luciferase is a bifunctional enzyme: ATP-dependent monooxygenase and a long chain fatty acyl-CoA synthetase, FEBS Lett. 540 (2003) 251–254, https://doi.org/10.1016/S0014-5793(03)00272-2.

[20] H. Fraga, D. Fernandes, R. Fontes, J.C.G. Esteves Da Silva, Coenzyme A affects firefly luciferase luminescence because it acts as a substrate and not as an allosteric effector, FEBS J. 272 (2005) 5206–5216, https://doi.org/10.1111/j.1742-4658.2005.04895.x.

[21] I. Taverniers, M. De Loose, E. Van Bockstaele, Trends in quality in the analytical laboratory. II. Analytical method validation and quality assurance, TrAC Trends Anal. Chem. 23 (2004) 535–552, https://doi.org/10.1016/j.trac.2004.04.001.

[22] J.H. Zhang, T.D.Y. Chung, K.R. Oldenburg, A simple statistical parameter for use in evaluation and validation of high throughput screening assays, J. Biomol. Screen 4 (1999) 67–73, https://doi.org/10.1177/108705719900400206.

[23] G.G. Yegutkin, Enzymes involved in metabolism of extracellular nucleotides and nucleosides: functional implications and measurement of activities, Crit. Rev. Biochem. Mol. Biol. 49 (2014) 473–497, https://doi.org/10.3109/10409238.2014.953627.

[24] H. Fraga, Firefly luminescence: a historical perspective and recent developments, Photochem. Photobiol. Sci. 7 (2008) 146, https://doi.org/10.1039/b719181b.

[25] H. Lineweaver, D. Burk, The determination of enzyme dissociation constants, J. Am. Chem. Soc. 56 (1934) 658–666, https://doi.org/10.1021/ja01318a036.

SUPPORTING INFORMATION

Recombinant expression of ecto-nucleotide pyrophosphatase/phosphodiesterase 4 (NPP4) and development of a luminescence-based assay to identify inhibitors

Vittoria Lopez, [a, b] Sang-Yong Lee, [a, b] Holger Stephan [c] and Christa E. Müller [a, b]*

[a]*Pharmaceutical Institute, Pharmaceutical and Medicinal Chemistry, University of Bonn, An der Immenburg 4, 53121 Bonn, Germany*

[b]*PharmaCenter Bonn, University of Bonn, An der Immenburg 4, 53121 Bonn, Germany*

[c]Institute of Radiopharmaceutical Cancer Research, Helmholtz-Zentrum Dresden-Rossendorf, Bautzner Landstraße 400, 01328 Dresden, Germany

*Address correspondence to:

Prof. Dr. Christa E. Müller

Pharmaceutical Institute, Pharmaceutical and Medicinal Chemistry

An der Immenburg 4, D-53121 Bonn, Germany

Phone: +49-228-73-2301

Fax: +49-228-73-2567

E-Mail: christa.mueller@uni-bonn.de

Table of Contents:

Fig. S1 ATP and time dependence of luminescence signal page. 2

Fig. S2 Different buffers to study method robustness page. 3

Fig. S3 Calibration curve page. 4

Fig. S4 CE-UV chromatogram of CoA as potential NPP4 substrate page. 5

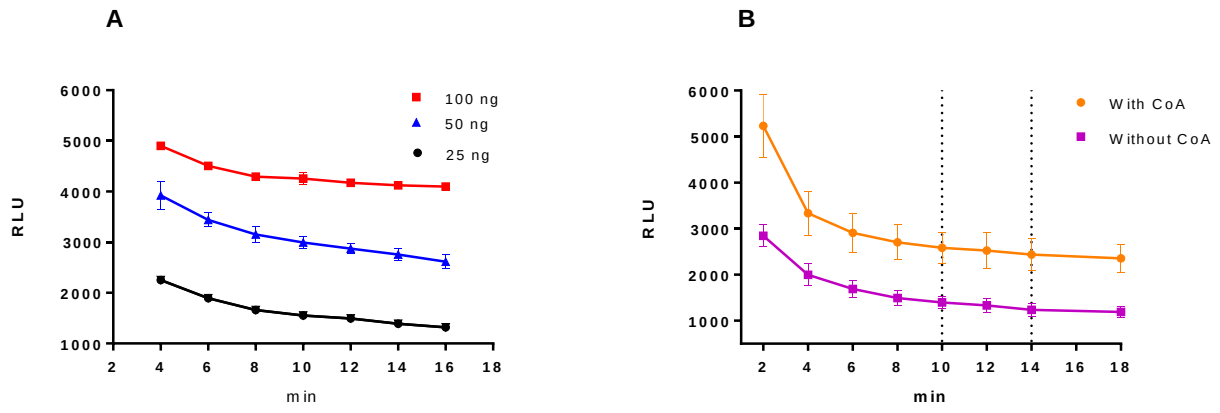

Fig. S1 A. ATP- dependent luciferase reaction with three different luciferase concentrations. To 1 µM of ATP solution, 50 µl of buffer B (300 mM Tris-HCl, 15 mM $MgCl_2$, 100 ng D-luciferin, 750 µM of CoA, pH 7.8) and 50 µl of buffer C (25, 50 or 100 ng of luciferase in H_2O) were added to each well, the luminescence was measured using BMG PheraStar FS plate reader; **S1 B.** Time-dependence of detected luminescence signal in the presence or absence of CoA. To a solution of 1 µM ATP, 50 µl of buffer B (300 mM Tris-HCl, 15 mM $MgCl_2$, 100 ng D-luciferin, pH 7.8 with or without 750 µM of Co-A) and 50 µl of buffer C (50 ng of luciferase in H_2O) were added, then the luminescence was measured using BMG PheraStar FS plate reader.

RLU= Relative Luminescence Units; data points represent means ± SD of two/three independent experiments performed in triplicate.

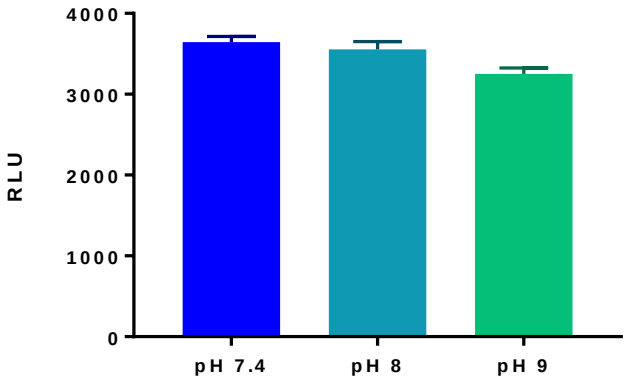

Fig S2 Experiments conducted using buffers at different pH to validate method robustness. Assays were performed at pH 7.4, pH 8.00 and pH 9.0 respectively, all in 10 mM HEPES, 1 mM $MgCl_2$ and 2 mM $CaCl_2$, except for pH 9.0 where 10 mM CHES instead of 10 mM HEPES was used. The substrate Ap_4A (20 µM) and the NPP4 enzyme (0.5 µg) were prepared using the three different buffers. After 60 min of incubation time the NPP4 enzymatic reaction was stopped at 90° for 5 min. For the detection of the product formed (ATP) 50 µl of buffer B (300 mM Tris-HCl, 15 mM $MgCl_2$, and D-luciferin 100 ng, pH 7.8) and 50 µl of buffer C (50 ng luciferase in H_2O) were added. Luminescence was then measured on a BMG PheraStar FS plate reader.

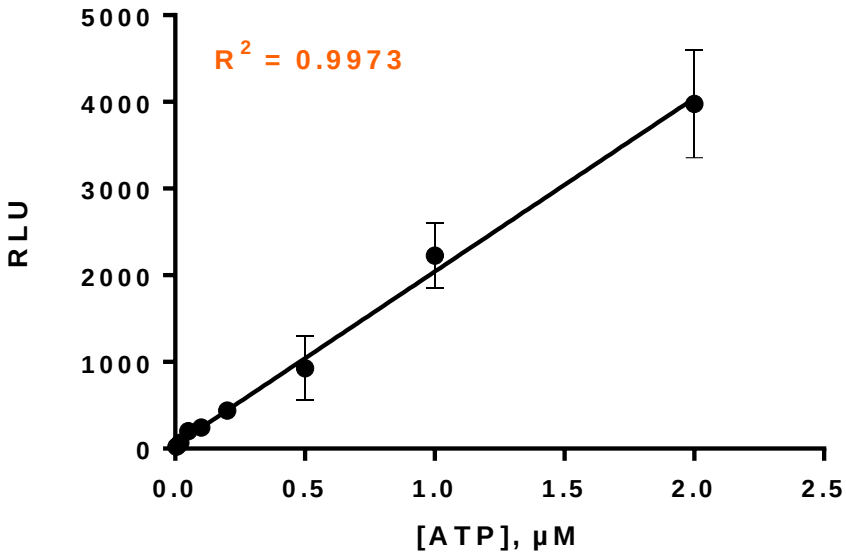

Fig. S3 Calibration curve using ATP as substrate (R^2 = 0.9973).

An eight-point calibration curve (0.01 - 2 µM), dissolved in assay buffer (10 mM HEPES, 1 mM $MgCl_2$ and 2 mM $CaCl_2$, pH 8.0) was determined for ATP. Each concentration was measured twice, each in triplicate. To each well, 50 µl of the ATP solution, and subsequently, 50 µl buffer B (final conc. 300 mM Tris-HCl, 15 mM $MgCl_2$, and D-luciferin 100 ng, pH 7.8) and 50 µl of buffer C (50 ng of luciferase in H_2O) were added. Luminescence was then measured on a BMG PheraStar FS plate reader. Calibration curves were obtained by correlating the measured RLUs (relative light units) with the employed concentrations of ATP.

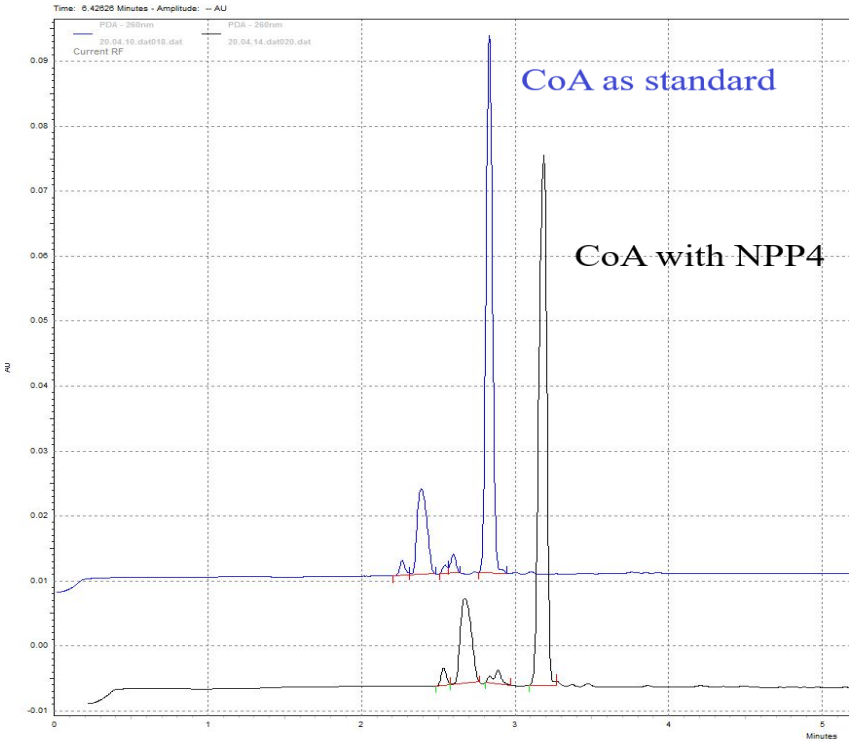

Fig. S4 CE-UV chromatogram of experiments, in which CoA was investigated as a potential substrate of NPP4. Conditions: injection: -6 kV for 30 s, 40 cm [30 cm eff.] polyacrylamide-coated capillary, 50 mM phosphate pH 6.5 as a running buffer, -90 µA of separation current, detection at 260 nm. Blue: CoA standard sample; black: analysis after incubation of CoA with human NPP4 at 37 °C for 90 min. The declared purity for the product (Sigma, article number C4282) was 85% (UV, HPLC).

4.3 Summary and outlook

The heterologous expression of hNPP4 in Sf9 insect cells, using baculovirus for transfection, was successful. The isolated and purified soluble enzyme was used for the optimization and validation of the HTS using bioluminescence detection. The assay was validated following FDA guidelines with an LOD of 14.6 nM, and a Z-factor of 0.68 indicating its suitability for high-throughput screening. The assay is fast, economic, and displays high precision and sensitivity, it was used for the biochemical characterization of the enzyme with the known substrates, Ap_3A and Ap_4A, and for the screening of a compound library. The first hNPP4 inhibitors have been identified and fully characterized pharmacologically, PSB-POM145 and PSB-POM146, having IC_{50} value of 0.298 and 3.36 μM, respectively. To confirm these results and to exclude potential artifacts, we additionally studied NPP4 inhibition by the most potent compound, PSB-POM145, in an orthogonal CE-UV-based assay. Furthermore, PSB-POM145 was studied with regard to its mechanism of inhibition using both assays, revealing a competitive mode of inhibition. These discoveries are of great importance since such tool compounds are essential for further advancements in basic research on hNPP4 and for target validation studies. Extensive characterization of NPP4 and its substrates, including the discovery of new physiological substrates, is described in the following chapters.

"This article was published in *Anal. Biochem.*, *603*, Lopez, V.; Lee, S.-Y.; Stephan, H.; Müller, C.E., Recombinant expression of ecto-nucleotide pyrophosphatase/phosphodiesterase 4 (NPP4) and development of a luminescence-based assay to identify inhibitors, 113774, Copyrigh Elsevier (2020)."

5. Search for novel NPP4 inhibitors by high-throughput screening

Introduction

Initial phases in drug development are identifying and validating prospective therapeutic targets associated with human disease. Typically, these targets are specific proteins or nucleic acids. These targets include: receptors, enzymes, hormones, nuclear receptors, ion channels and DNA, if a target has been selected, screening assays are developed. These tests are used to determine which compounds exhibit the desired activity against the therapeutic target. These are known as "hit" molecules. During the initial phase of hit compound identification, by high-throughput screening (HTS), a compound library containing numerous possible hit molecules is screened for any compounds exhibiting the desired activity against the target. Additional assays are required to re-evaluate the activity of the hit molecule and its derivatives at the target. Finally, cell-based assays and *in vivo* studies on animals are utilized to determine further properties, e.g., toxicity, safety, and efficacy of the potential clinical candidate. The creation of high-quality assays is critical for drug discovery and development. The more robust the developed assays are, the fewer possible issues will arise. Appropriate assay creation takes into consideration a variety of parameters, including relevance, repeatability, quality, interference, and cost. In Chapter 4 of the present thesis an HTS-assay development using bioluminescence detection is described, which led to the only NPP4 inhibitors know so far. With the aim of finding new hit compounds, we proceeded with the screening of different compound libraries, including a broad spectrum of natural and synthetized chemical scaffolds, as well drugs available on the market. The hits have been validated with a second assay system leading to the discovery of new scaffolds that will allow subsequent drug discovery of hNPP4 inhibitors.

5.1 Compound library screening to identify novel NPP4 inhibitors

In total 2656 compounds have been tested as potential hNPP4 inhibitors, of which 60 compounds were tested in a second phase as analogues or derivatives of the hit compounds identified in the initial screening. Full concentration-inhibition curves were determined for selected hit compounds. The hit rate was 0.77%. However, not all hit compounds could be confirmed. In Fig. 1-8 the results of the HTS using Ap_4A as substrate in the luminescence-based assay system are presented. Each dot or bar chart represents a compound depicting its percent of inhibition or activation of hNPP4 activity in comparison with a control. Assay conditions are as published [1] (for detailed information see Chapter 4). In short, 20 µl of Ap_4A, final concentration of 20 µM, 20 µl of hNPP4 at a concentration adapted after enzyme titration in order to work in a range of 10-15 % of substrate conversion, and 10 µl of test compound (final concentration of 10 µM containing 2% DMSO) was used. Negative and positive controls were run in parallel. The enzymatic assay was carried out in a 96-well plate, for 90 min at 37°C, followed by enzymatic denaturation at 95 °C for 5-7 min and cooling down on ice. In order to measure the enzymatic activity and detect one of the released products, ATP, the luciferin–luciferase reaction was used. The firefly luciferase reacts with D-luciferin in the presence of the formed ATP and Mg^{2+} which act as cofactors. The resulting luminescence correlates to the hNPP4 activity. Measurement was performed at 560 nm using a microplate reader (BMG PheraStar, Labtech GmbH, Ortenberg, Baden-Württemberg, Germany).

The screened libraires comprise:

- TOCRIS® (~1200 compounds)
- InterBioScreen® (400 compounds)
- Commercially available drugs (560 compounds)

- Prof. Dr. Holger Stark, Institute for Pharmaceutical and Medicinal Chemistry, University of Düsseldorf (320 compounds for initial screening plus ~ 30 analogues)
- MolPort® library (36 compounds)
- Indole scaffolds library from PharmaCenter Bonn (80 compounds)
- Uridine scaffolds library from PharmaCenter Bonn (31 compounds)

Table 1. Assay conditions for monitoring NPP4 activity in HTS

	Component	**Volume**	**Final concentration**
1.	**Substrate Ap_4A**, 50 µM	20 µl	**20 µM**
2.	**Test compound**, 50 µM in 10% DMSO	10 µl	**10 µM**
3.	**Enzyme** diluted to 14 ng/µl	20 µl	**0.28 µg**
	Total	50 µl	

Reaction in white 96 well plates (half area)

1. Incubate the mixture for 90 min at 37 °C and 500 rpm.

2. Inactive the enzyme at 90° for 5 min

3. Add 50 µl Luciferase reaction buffer I (firefly luciferase 2 µg/ml)

4. Add 50 µl Luciferin reaction buffer II (Tris-HCl 300 mM, $MgCl_2$ 15 mM, D-luciferin 450 µg/µl in H_2O

5. Read the luminescence immediately (within 15 min)

6. Measure the luminescence value using PheraStar

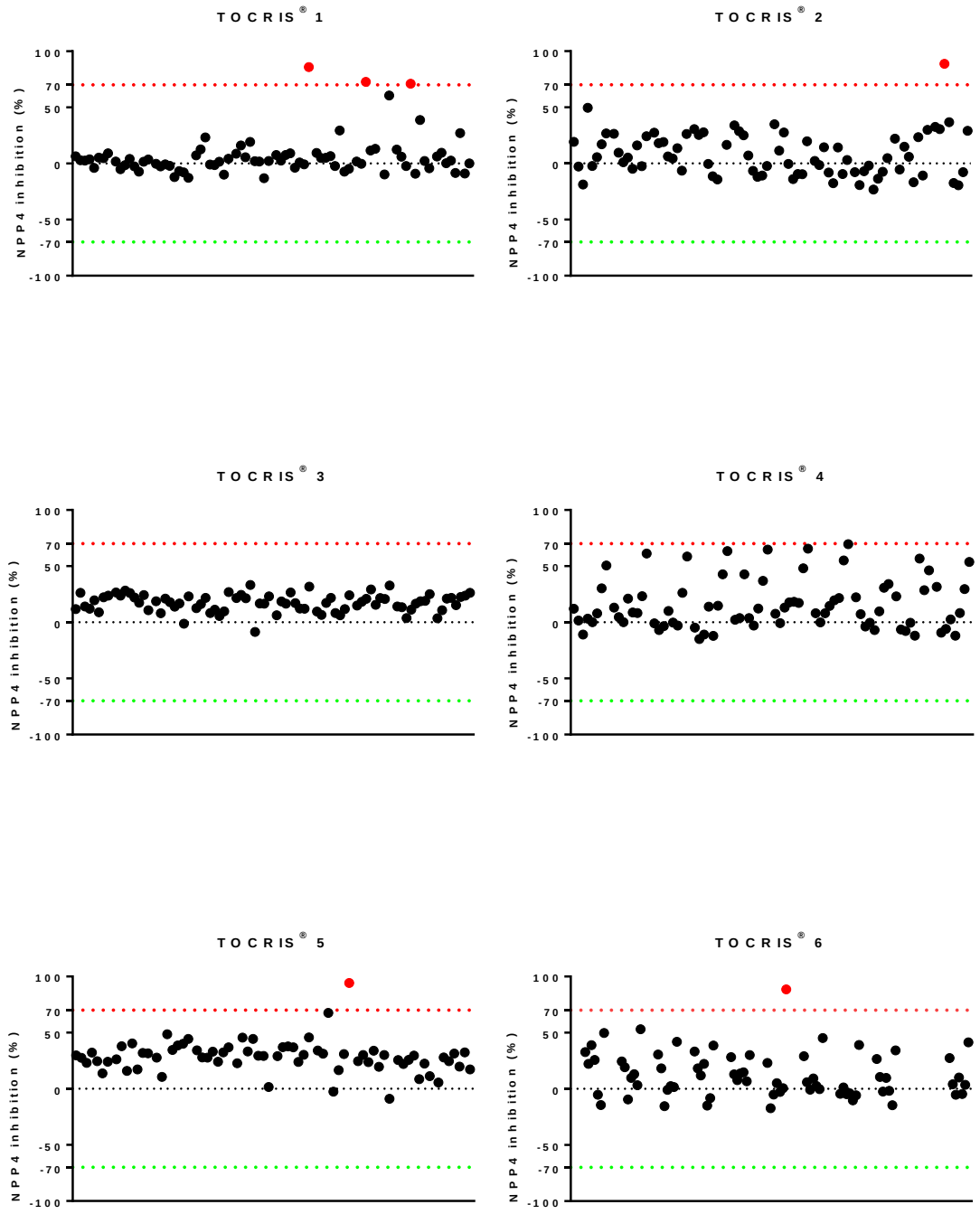

Fig. 1. Screening results from HTS where NPP4 activity was investigated in the presence of test compounds, using Ap_4A as substrate and bioluminescence detection. Each dot represents a test compound, from TOCRIS® plate 1-6, compounds were tested at a final concentration of 10 µM. Each plate contains ~80 compounds.

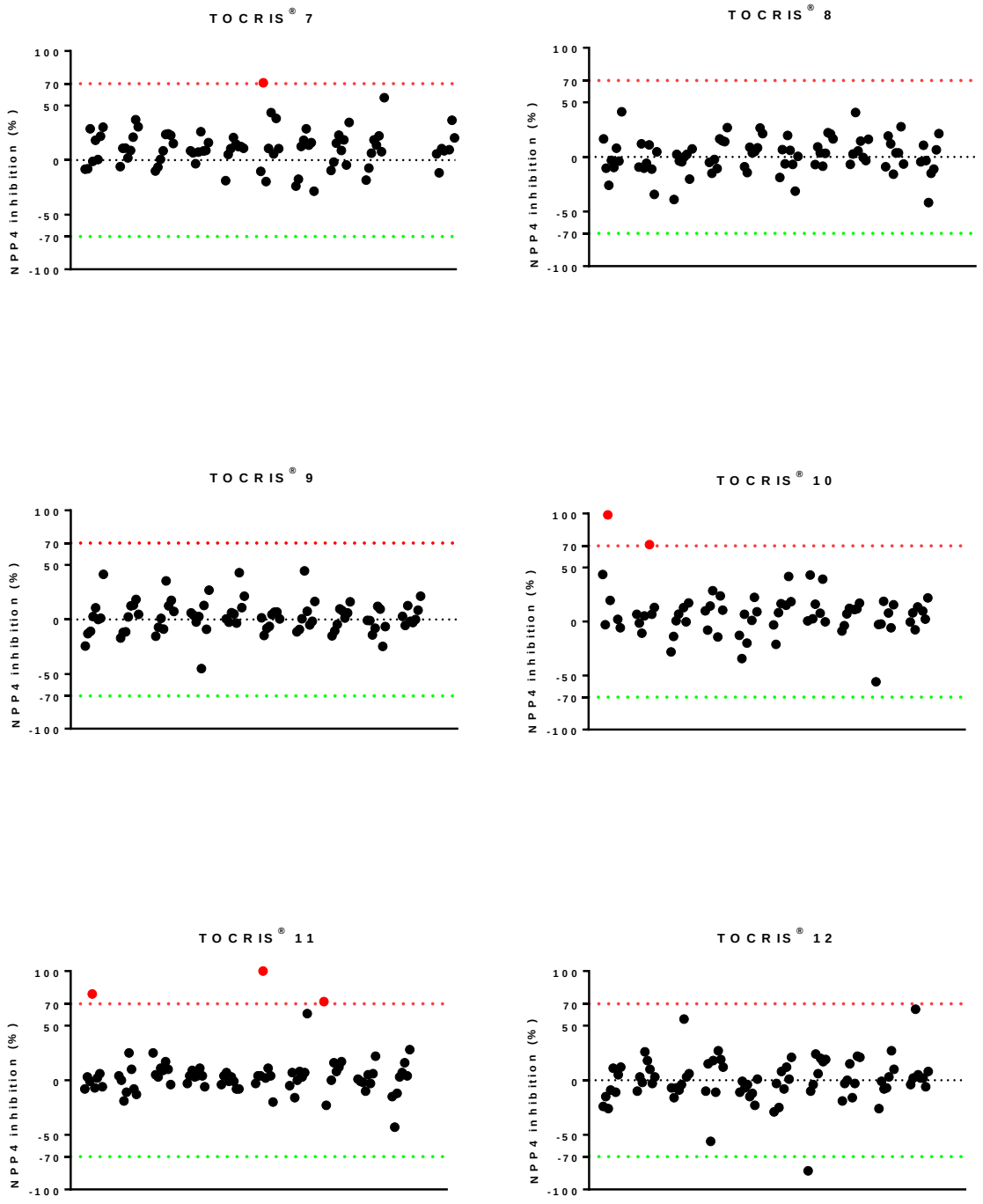

Fig. 2. Screening results from HTS where NPP4 activity was investigated in the presence of test compounds, using Ap_4A as substrate and bioluminescence detection. Each dot represents a test compound, from TOCRIS® plate 7-12, compounds were tested at a final concentration of 10 µM. Each plate contains ~80 compounds.

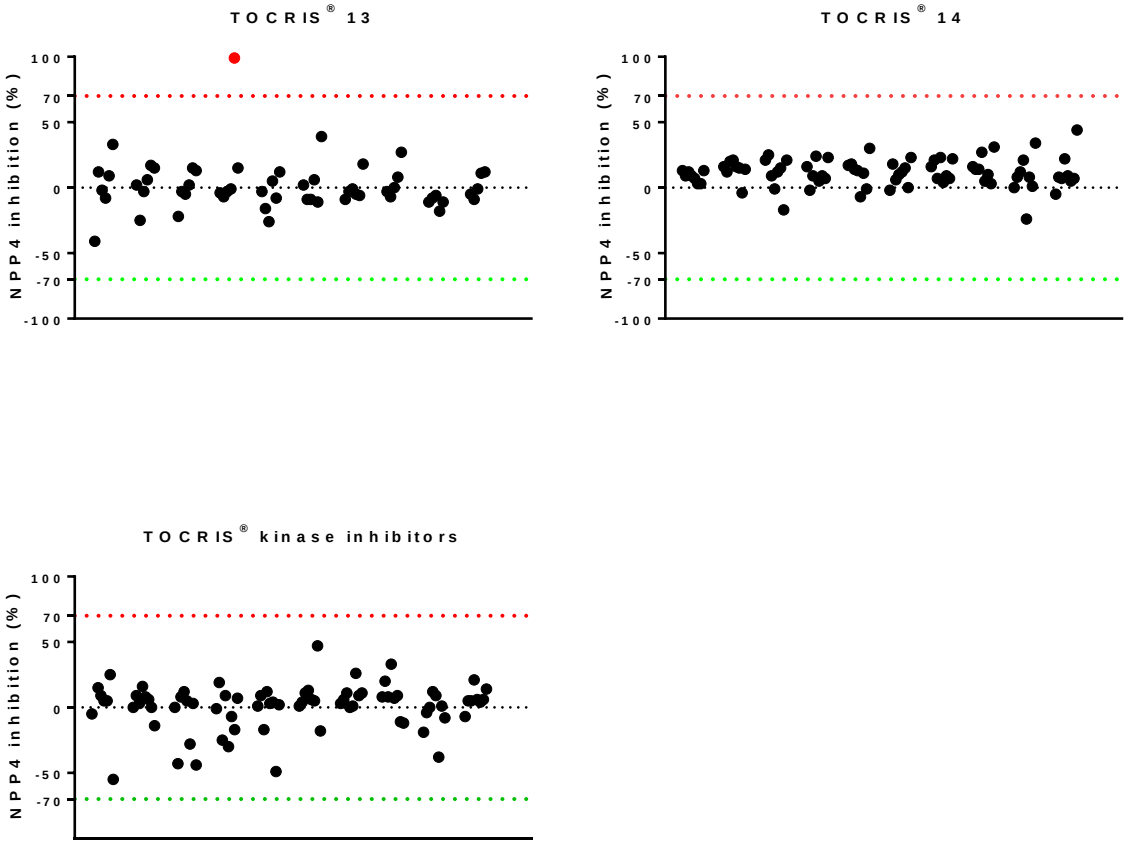

Fig. 3. Screening results from HTS where NPP4 activity was investigated in the presence of test compounds, using Ap_4A as substrate and bioluminescence detection. Each dot represents a test compound, from TOCRIS® 13, 14 and kinase library, compounds were tested at a final concentration of 10 μM. Each plate contains ~80 compounds.

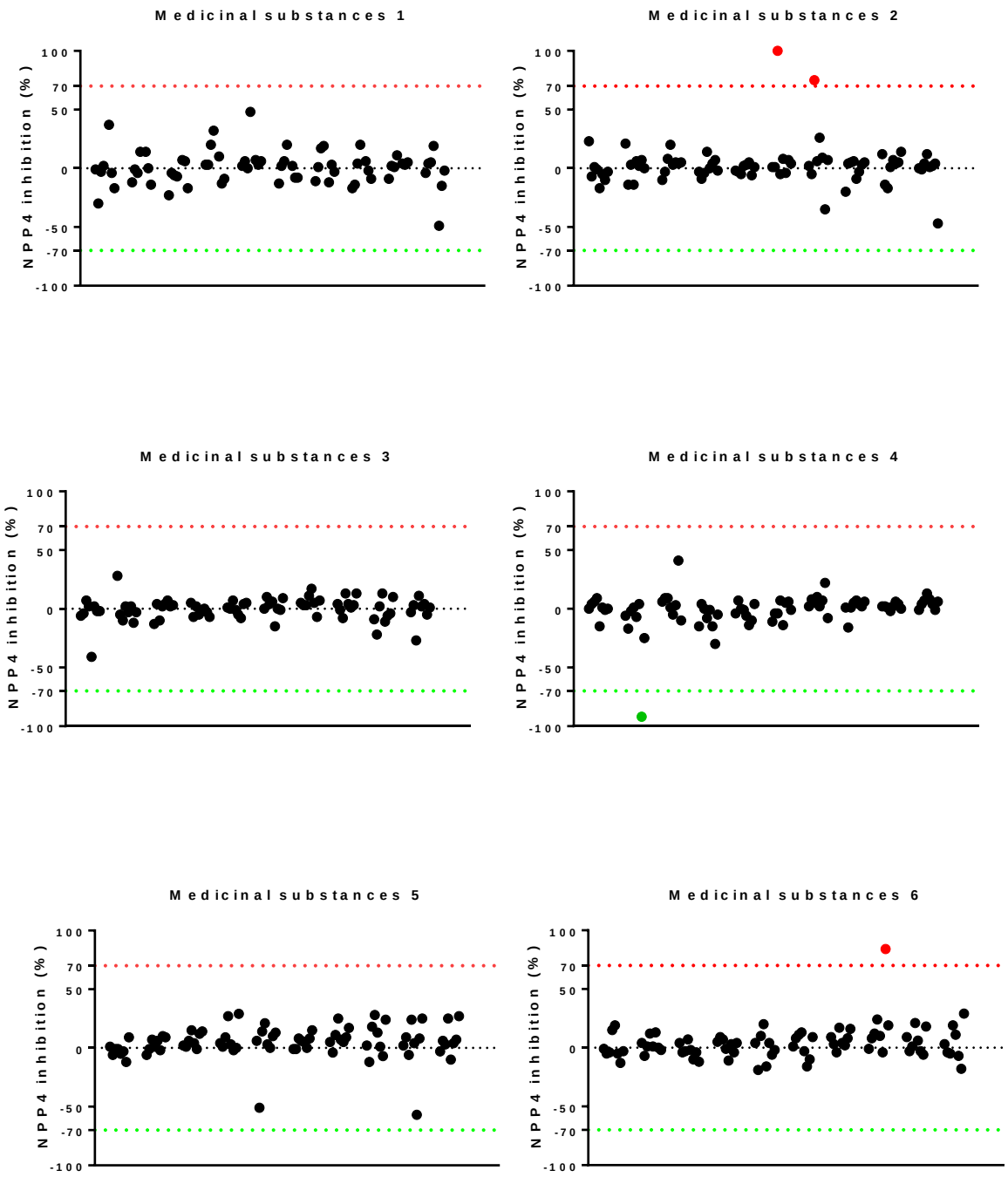

Fig. 4. Screening results from HTS where NPP4 activity was investigated in the presence of test compounds, using Ap_4A as substrate and bioluminescence detection. Each dot represents a test compound, commercial drug plate 1-6, compounds were tested at a final concentration of 10 μM. Each plate contains ~80 compounds.

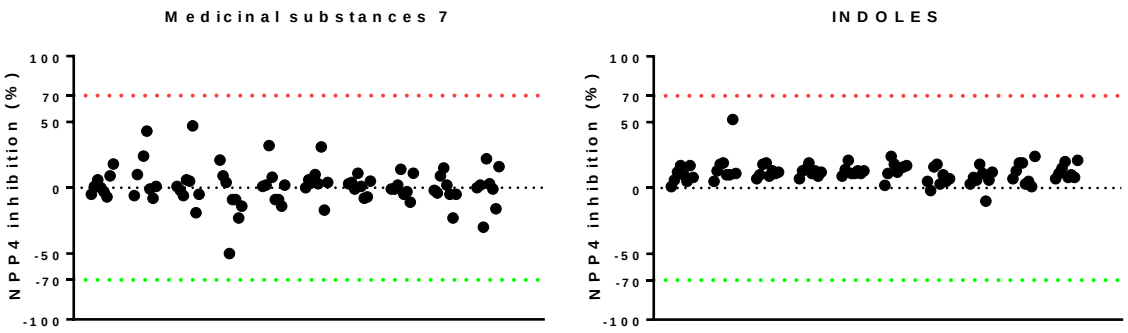

Fig. 5. Screening results from the HTS where NPP4 activity was investigated with the presence of test compounds, using Ap_4A as substrate and bioluminescence detection. Each dot represents a test compound, from commercial drug plate 7 and indoles library, which was tested at the final concentration of 10 μM against hNPP4. Each plate contains ~80 compounds

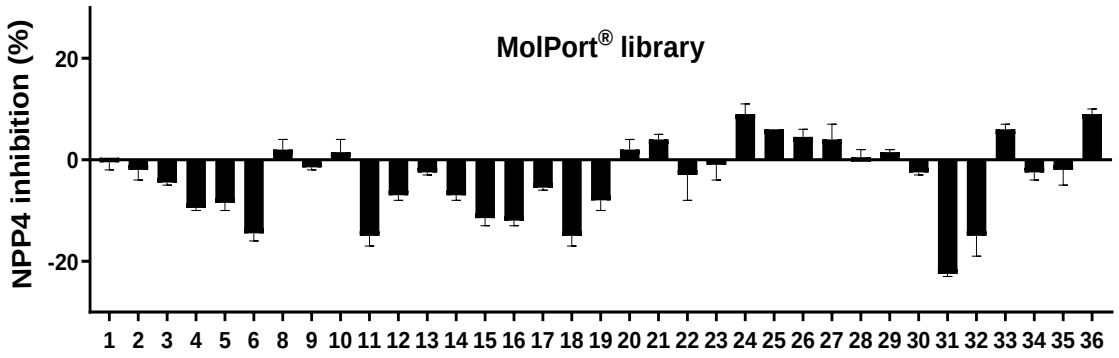

Fig. 6. Results from the HTS where NPP4 activity was investigated with the presence of test compounds, using Ap_4A as substrate and bioluminescence detection. Each bar represents a test compound, from the MolPort® library, which was tested at the final concentration of 10 μM against hNPP4. Error bar represent SD.

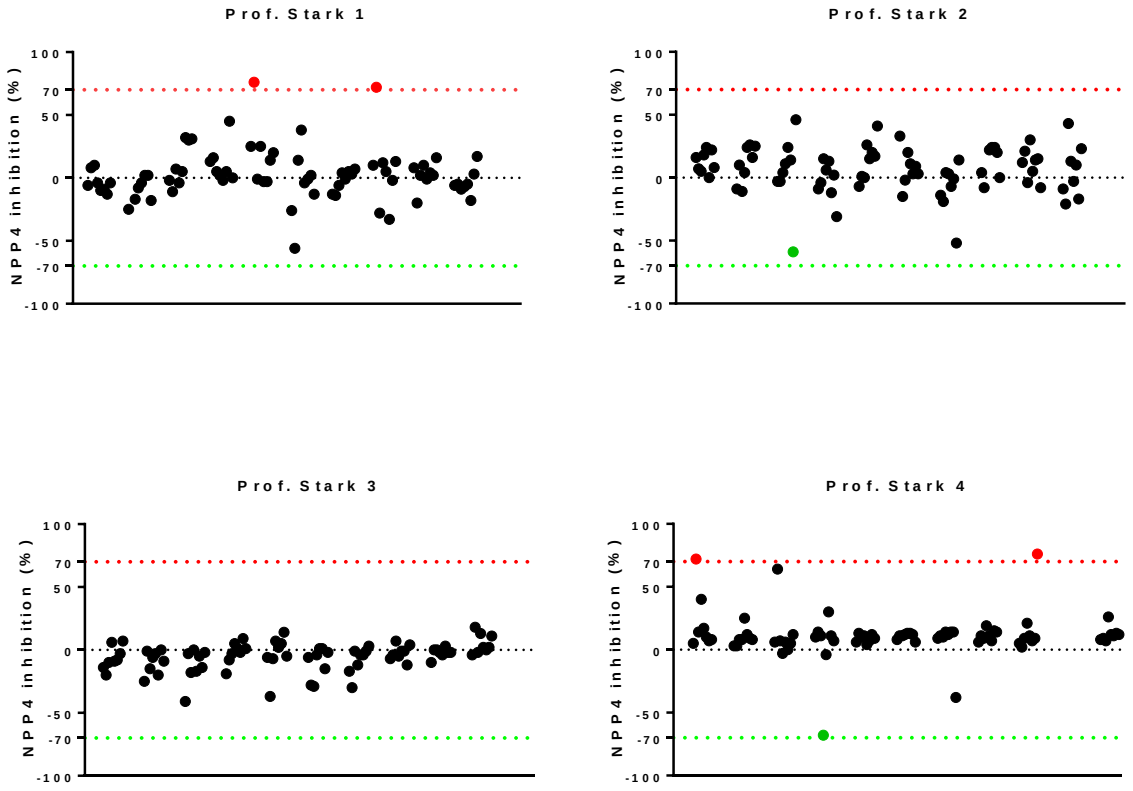

Fig. 7. Results from the HTS where NPP4 activity was investigated with the presence of test compounds, using Ap_4A as substrate and bioluminescence detection. Each dot represents a test compound, from Prof. Stark library, which was tested at the final concentration of 10 μM against hNPP4. Each plate contains ~80 compounds.

In the primary screen, our strategy aimed to test whether a compound has effects strong enough to reach a pre-set level of 70% inhibition or activation of hNPP4 activity. From the initial screening several compounds were identified as modulators of hNPP4 activity, few of them were false positives as revealed in the following replications. The hits compounds identified had to be validated using an orthogonal assay system. In Table 2 the hit compounds are listed with respect to their activity using a second assay system, capillary electrophoresis (CE) coupled to UV detection for analysis and quantification of the products (injection: −6 kV for 30 s, 40 cm [30 cm eff.]

polyacrylamide-coated capillary, 100 mM phosphate pH 6.5 as a running buffer, −10 kV of separation voltage, detection at 260 nm). Then, the compounds were fully characterized and their IC_{50} value were calculated. Their selectivity versus other enzymes of the ectonucleotidase family was studied and considered. Two of the identified inhibitors, PSB-POM145 and PSB-POM146, are described also with their respect to the inhibition type in Chapter 4 of this thesis and they are so far the only hNPP4 inhibitors described in the literature.

Table 2. Potency of compounds discovered by HTS and confirmed with an orthogonal assay, as inhibitors or activators of NPP4

	Internal code	**Effect on hNPP4 activity**	**Luminescence-based assay** [a] (hNPP4 activity ± SD)%, n=3	**CE- based assay** [b] (hNPP4 activity ± SD)%, n=3
I	**PZB11321005**	activator	+(50 ± 3) %	+(30 ± 4)%
II	**PZB20709064**	inhibitor	-(87 ± 5) %	-(40 ± 1) %
III	**PZB20308204**	activator	+(50 ± 1) %	+21 %
IV	**PZB10914066A**	inhibitor	-(83 ± 1) %	- (40 ± 4) %
V	**PZB10914178A**	inhibitor	-(70 ± 0) %	- (32 ± 1) %
VI	**PZB10914018A**	activators	+(63 ± 10) %	-(20 ± 3)%
VII	**PSB-POM145**	inhibitor	-(93 ± 2) %	- (70 ± 10) %
VIII	**PSB-POM146**	inhibitor	-(75 ± 3) %	not determined

a. Luminescence-based assay: **Ap_4A** (f.c. 20 μM), enzyme (f.c. 70 ng/μL), test compounds (f.c. 10 μM in 2% DMSO, except for PSB-POM145 tested at 30 μM)

b. CE-based assay: **Ap_3A** (f.c. 100 μM), enzyme (f.c. 70 ng/μL), test compounds (f.c. 10 μM in 2% DMSO except for PSB-POM145 tested at 30 μM)

Table 3. Compounds identified by HTS as modulators of hNPP4 activity

No.	PZB code; name; molecular weight	Structure	Information IC_{50}/EC_{50} determinate by HTS assay
I	**PZB11321005** (Dilazep dihydrochloride) 677.6 g/mol	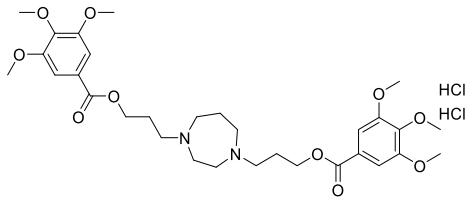	• **Activator** ⇧ (50 ± 3) % of hNPP4 activity with 10 μM of test compound
II	**PZB20709064** (Hamamelitannin) 484.36 g/mol	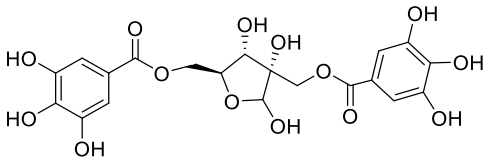	• **Inhibitor** Isolated from *Canastea sativa* **IC_{50}** ± SD **3.68** ± 0.47 **μM**
III	**PZB20308204** (Nystatin) 926.09 g/mol	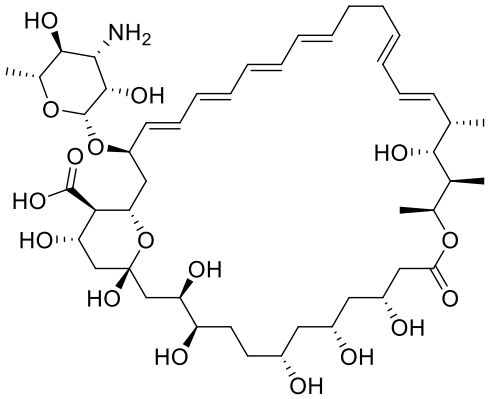	• **Activator** Antifungal agents Topic or ~500,000 unit of oral suspension 4 times a day **EC_{50}** ± SD **5.10** ± 0.14 **μM**
IV	**PZB10914066A** (ST 1366) 463.59 g/mol	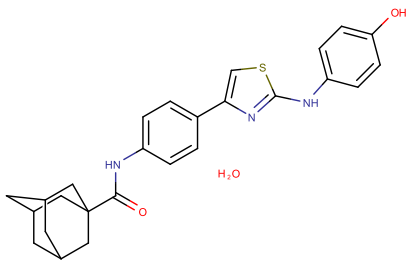	• **Inhibitor** **IC_{50}** ± SD **5.25** ± 1.13 **μM**

V	**PZB10914178A** (ST 1389) 224.26 g/mol	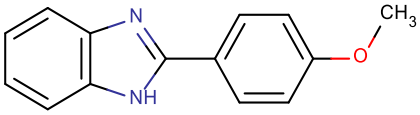	• **Inhibitor** **IC$_{50}$** ± SD **18.5** ± 1.14 **μM**
VI	**PZB10914018A** (ST 1699) 321 g/mol	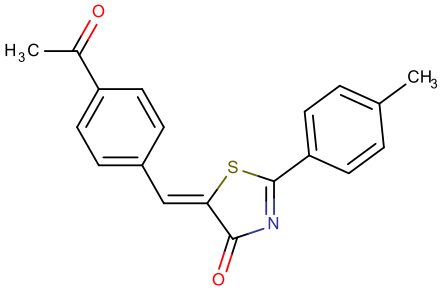	• **Activator** ⇧(63 ± 10) % of hNPP4 activity with 10 μM of test compound (Unconfirmed in CE assay)
VII	**PSB-POM145** 3366 g/mol	 $Na_6[H_2W_{12}O_{40}]\cdot 21H_2O$	• **Inhibitor** **IC$_{50}$** ± SD **0.298** ± 0.052 **μM**
VIII	**PSB-POM146** 3023 g/mol	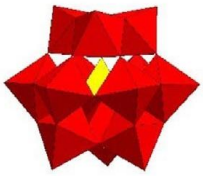 $K_6H_2[TiW_{11}CoO_{40}]\cdot 13H_2O$	• **Inhibitor** **IC$_{50}$** ± SD **3.36** ± 0.45 **μM**

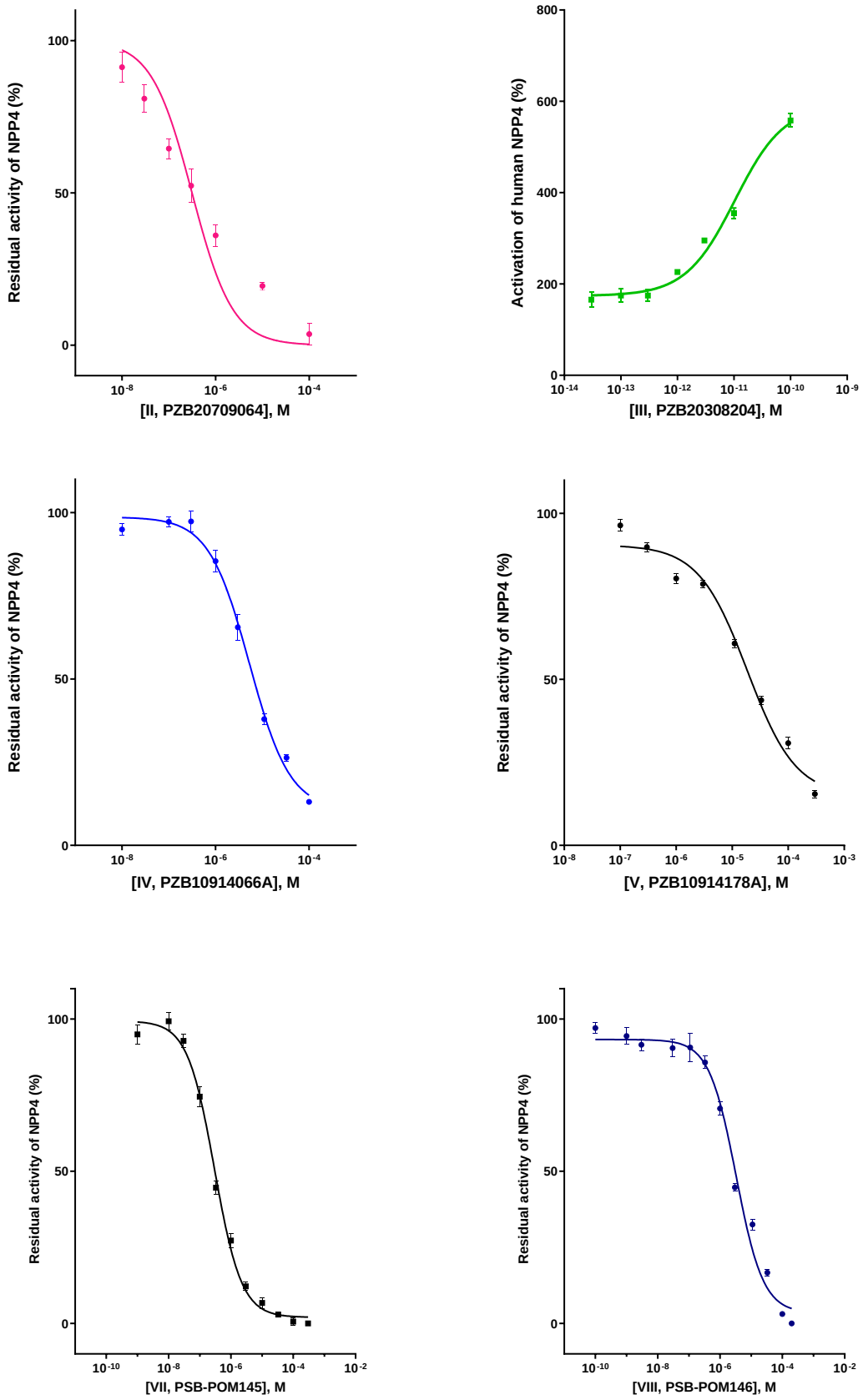

Fig. 8. *IC_{50}/EC_{50}* of hit compounds at hNPP4 determined in luciferase assay.

5.2 Selectivity studies of NPP4 inhibitors

In order to evaluate the NPP4 inhibitors, discovered by the HTS screening campaign, four of the test compounds were selected for testing on other members of the ectonucleotidase family. Fig. 9 shows, in a bar chart graph, the selectivity profiles of the investigated compounds tested at a final concentration of 10 μM. All compounds showed highest inhibition of NPP4, which was inhibited by more than 75% at the tested concentration, combined with high selectivity versus the other NPP subtypes, except for compound PZB10914066A (**IV**) which is somehow equipotent in inhibiting CD73 activity and its IC_{50} value was calculated to be 1.48 ± 0.47 μM, thus making the compound as dual inhibitor of hNPP4 and hCD73 activity. The second highest inhibition was observed at NPP1 for compounds (**II**), (**III**), (**V**), while inhibition of all other enzymes was below 25%. The test compound PZB10914178A (**V**) showed the best selectivity profile, with a slight inhibition of around 30% on NPP1 activity only. The natural substance hamamelitannin PZB20709064 (**II,** Fig.9A) appears to inhibit only NPP1 and NPP4 activity, with ~60% and 87% respectively. The compound PZB20308204 (**III,** Fig.9B) which appeared to positively modulates the activity of NPP4, was found to positively modulate the enzymatic activity of CD73 by ~70% as well, with no influence on the activity of the other ectonucleotidase family members.

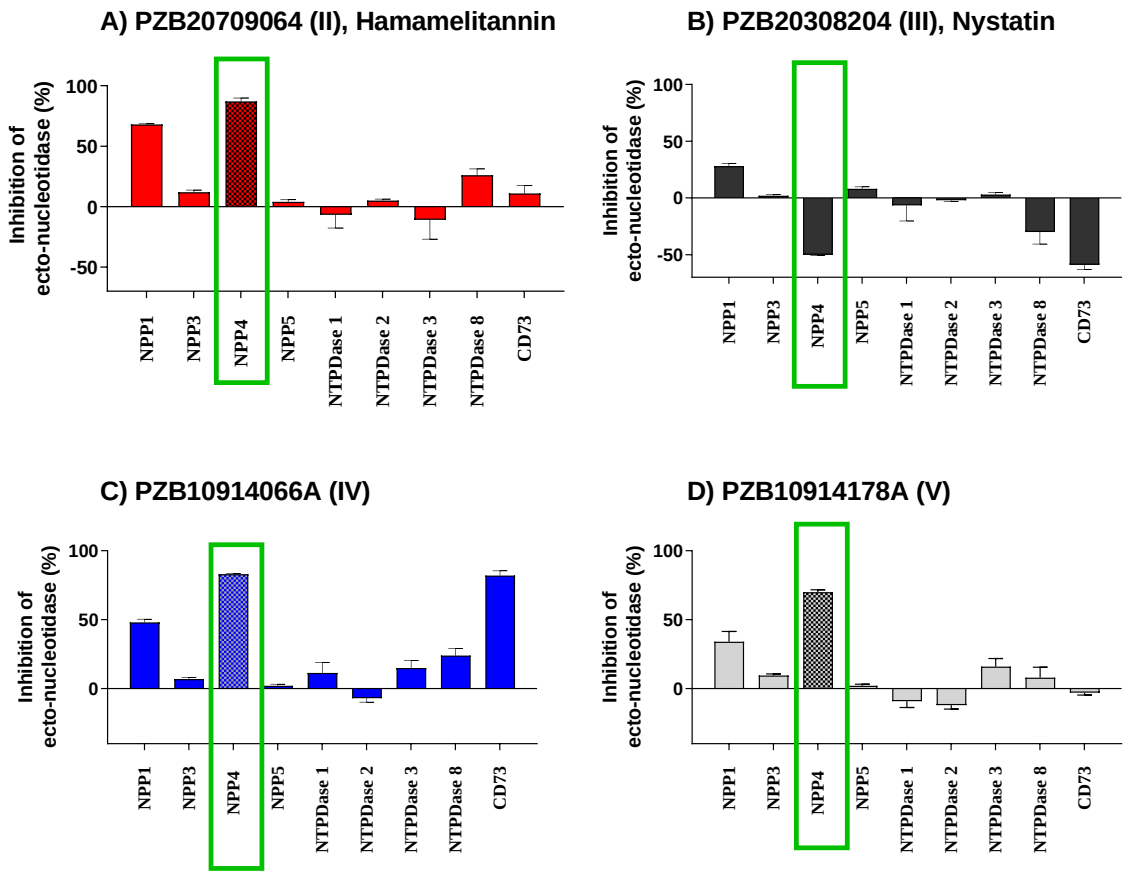

Fig. 9. Selectivity of NPP4 inhibitor on ectonucleotidase family members. Compounds were tested at a concentration of 10 µM. NTPDase1, 2, 3 and 8 activities were analyzed using a CE-based assay employing ATP or ADP as a substrate; NPP1, NPP3 and NPP5 were investigated using *p*-Nph-5´-TMP as a substrate; NPP4 was tested with Ap_4A as a substrate using a luciferase assay; CD73 was analyzed using a radio assay; experiments on NTPDases 1, 2, 3 and 8 were conducted from Laura Schäkel, experiments on CD73 were conducted by Riham Idris, while experiments on NPP3 and NPP5 were performed by Salahuddin Mirza.

Experimental details

Screening on NTPDases by a CE-assay based

One experiment was performed in triplicate (n=3). The selected substrate concentration (ATP) was 100 μM. The inhibitors were investigated at 10 μM. The enzyme concentration was chosen after an enzyme titration and adjusted to ensure 10 – 20 % conversion rates. The reaction buffer was 10 mM HEPES, 2 mM $CaCl_2$, 1 mM $MgCl_2$, pH 7.4. The mixtures for enzyme reaction were incubated at 37 °C for 30 min and terminated by heating at 95 °C for 10 min. The nucleotides were separated by capillary electrophoresis and detected at 260 nm with a DAD-detector. The inhibition was calculated by the quantitation of AMP for hNTPDases1, -3 and -8 and ADP for hNTPDase2.

The % inhibition was calculated as described below:

$$\%\ inhibition = \frac{(B - T)}{B} * 100$$

B: **μM AMP/ADP of blank**

T: **μM AMP/ADP of test compound**

Table 4. Instrument and method of CE-UV assay

Instrument	Capillary electrophoresis with DAD-detection system; Sciex P/ACE™ MDQ *plus*
Software	32 Karat software
Capillary	FS-polyacrylamide coated (ID 50 μm; AD 360 μm), 20 cm effective length
Buffer	50 mM Phosphate, pH 5.5
Method	
Rinse	30 psi, 2.0 min
Injection	-6.0 kV, 30 sec.
Separation	0.17 ramp, reverse polarity, -100 μA, 0.2 psi, 5 min
Detection	260 nm

Radioassay of ecto-5′-nucleotidase (CD73)

The inhibition of hCD73, prepared as previously described [2] was investigated at 10 μM of test compounds using a radioassay [3]. Compounds were diluted in assay reaction buffer (25 mM Tris, 140 mM sodium chloride, 25 mM 50 mM sodium dihydrogen phosphate, pH 7.4). After addition of 10 μl of the compound solution to 80 μl of assay reaction buffer and 10 μl of 1.23 μg/ml of hCD73, the reaction was initiated by the addition of 10 μl of [2,8-H^3]AMP (specific activity 3,7x109 Bq/mmol (100 mCi/mmol)), American Radio-labeled Chemicals, MO, USA, distributed by Hartman Analytic, Braunschweig, Germany) resulting in a final substrate concentration of 5 μM. After the reaction, which was performed for 25 min at 37 °C in a shaking water bath, 500 μl of cold precipitation buffer (100 mM lanthanum chloride, 100 mM sodium acetate, pH 4.0) were added to stop the reaction and to facilitate precipitation of free phosphate and unconverted [2,8-3H]AMP. After the precipitation was completed (after at least 30 min on ice) the mixture was separated by filtration through GF/B glass fiber filters using a cell harvester (M-48, Brandel, Gaitherburg, MD, USA). After washing each reaction vial three times with 500 μl of cold (4°C) Milli-Q water, 5 ml of the scintillation cocktail ULTIMA Gold XR (PerkinElmer) was added and radioactivity was measured by scintillation counting (TRICARB 2900 TR, Packard/PerkinElmer; counting efficacy: 49-52%). Experiments were performed in triplicate.

Absorbance-based assay for monitoring NPP1, NPP3 and NPP5

The selected substrate concentration (*p*-Nph-5′-TMP) was 400 μM. The inhibitors were investigated at 10 μM. The enzyme concentration was chosen after an enzyme titration and adjusted to ensure 10 – 20 % conversion rates, in details: 100 ng for NPP1, 90 ng for NPP3 and 400 ng for NPP5, the enzyme preparation as in the publish procedure [4]. The reaction buffer was 10 mM CHES, 2 mM $CaCl_2$, 1 mM $MgCl_2$, pH 9.00. The mixtures for enzyme reaction were incubated at 37 °C for 30 min for NPP1 and NPP3 and 100 min for NPP5, the enzymatic reaction was then terminated by adding 20 μl of NaOH. The

enzymatic ester hydrolysis of *p*-nitrophenyl-5′-TMP (*p*-Nph-5′-TMP) results in the formation of *p*-nitrophenolate anion, which shows an absorption maximum of 400 nm and it is detected using BMG PheraStar FS plate reader.

5.3 Screening of hit analogues and an additional tailored library

After the screening campaign of a broad spectrum of different chemical scaffolds, using the newly developed and optimized biochemical assay for the monitoring of NPP4 activity, and after their pharmacological characterization, we were looking for analogues to improve the inhibitory activity. During the screening campaign at human NPP4, three compounds (listed in Table 1) provided by Prof. Dr. Holger Stark, Institute for Pharmaceutical and Medicinal Chemistry, University of Düsseldorf, were found to modulate NPP4 activity. PZB10914018A (ST1699) appeared to increase the activity of NPP4, but its EC_{50} value was not determined since a plateau was not reached within the range of the tested concentrations. To exclude artifacts, the compound was additionally tested in a different assay system, however the second assay system did not confirm the potential positive modulation. In contrast, compound ST1699 is a weak inhibitor. Compounds PZB10914066A (ST1366) and PZB10914178A (ST1389) were found to be inhibitors of human NPP4 with low to moderate potency. Using an orthogonal assay (see section 5.4 for details), we examined a series of derivatives of the two lead compounds. The results indicated that all of the derivatives were moderately potent inhibitors of hNPP4 activity (see Table 5 and Fig. 10), but the inhibitory potency was not significantly improved compared to the hit compounds.

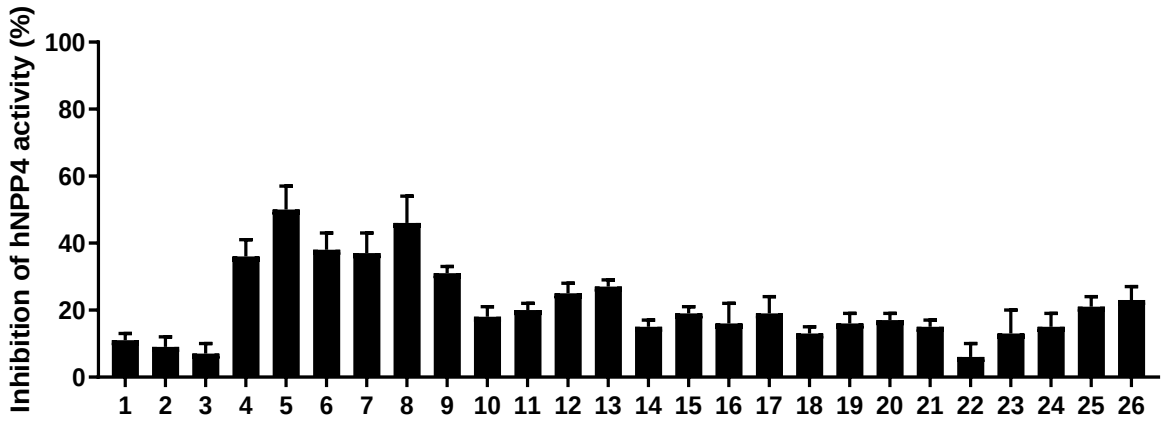

Fig. 10. Analogues of PZB10914066A and PZB10914178A tested at 50 μM, in a CE-based assay using 400 μM of Ap_4A as a substrate (5.4 for details on the detection method and assay condition)

Furthermore, based on information collected from a parallel project on the substrate preferences of hNPP4 (Chapter 6 for details), we identified uridine derivatives as possible modulators of NPP4 activity. In order to test our hypothesis, we studied the enzymatic activity in the presence of compounds from our library at Pharma-Zentrum Bonn, containing a uridine moiety. We collected a total of 96 compounds with a uridine moiety (Table 6), and after a careful selection, 31 of these compounds were studied as potential modulators of NPP4 activity. The experimental conditions were as described in Table 1, using bioluminescence detection of the enzyme products. The investigated compounds, tested at concentration of 10 μM, were found to moderately inhibit the NPP4 activity in a range of 31-67% with a mean value of 45% (Table 6 and Fig. 11), corroborating our hypothesis. Due to their moderate inhibition, full pharmacological characterization was not performed, instead it would be useful to design and synthetize new derivatives in the future.

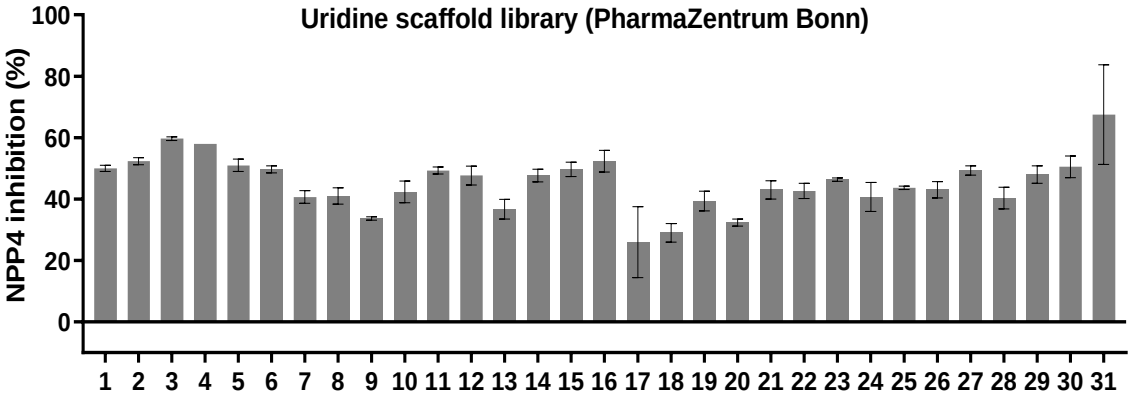

Fig. 11. Compounds with a uridine scaffold tested at 10 μM on hNPP4 using Ap_4A as substrate and the luminescence -based assay for the detection of the products (see Table 1 for details on assay condition and detection of the product)

Table 5. List of the PZB10914066A and PZB10914178A derivatives tested as potential inhibitors of hNPP4 activity with CE-based assay

	Code	Structure	Molecular Weight Inhibition at 50 μM (% ± SD); n=6
1	**ST-1448**	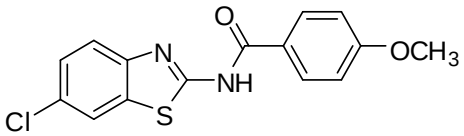	318.8 g/mol 11 ± 4
2	**ST-1500**	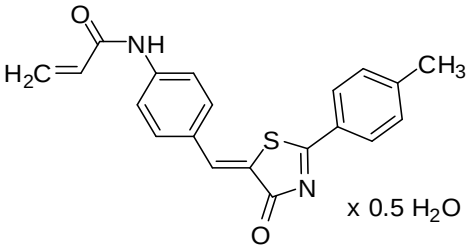	357.1 g/mol 9 ± 3

3	**ST-1407**	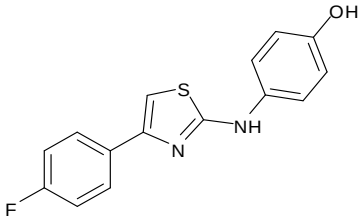	286.3 g/mol 7 ± 3
4	**ST-1253**	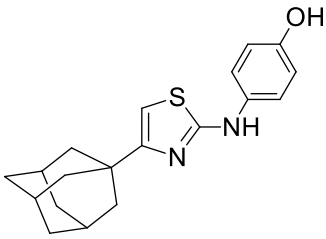	326.5 g/mol 36 ± 5
5	**ST-1392**	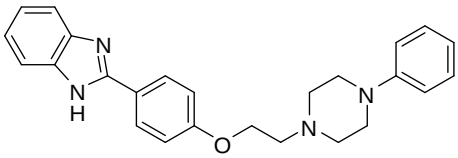	398.5 g/mol 50 ± 7
6	**ST-1367**	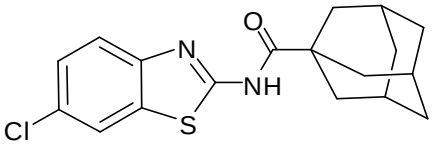	346.9 g/mol 38 ± 5
7	**ST-1378**	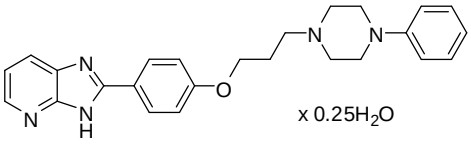	418.0 g/mol 37 ± 6
8	**ST-1379**	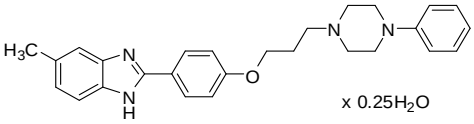	431.1 g/mol 46 ± 8

9	**ST-1416**	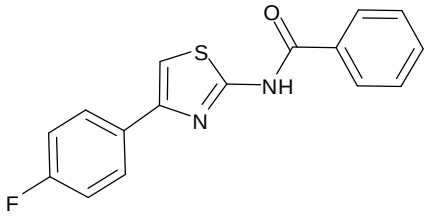	298.3 g/mol 31 ± 2
10	**ST-1469**	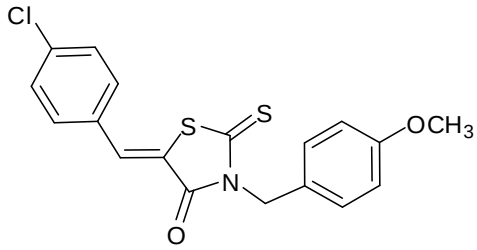	375.9 g/mol 18 ± 3
11	**ST-1476**	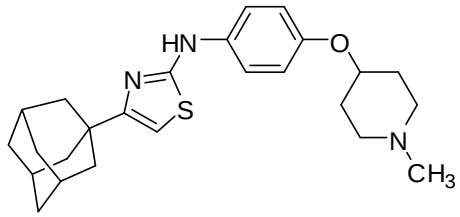	423.6 g/mol 20 ± 2
12	**ST-1493**	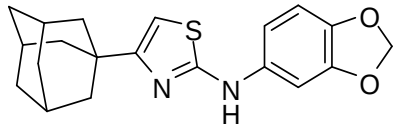	354.7 g/mol 25 ± 3
13	**ST-1495**	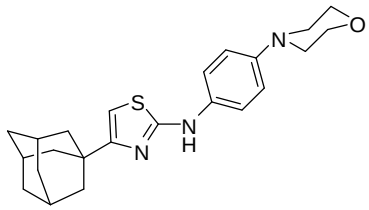	395.6 g/mol 27 ± 2

14	**JNJ7777120**	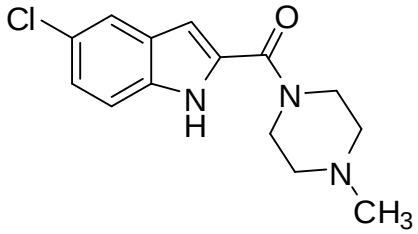	277.70 g/mol 15 ± 2
15	**ST-1565**	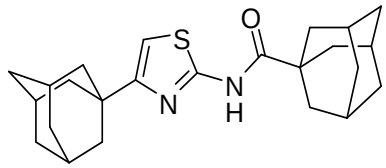	396.6 g/mol 19 ± 2
16	**ST-1605**	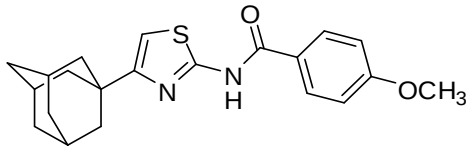	368.5 g/mol 16 ± 6
17	**ST-1629**	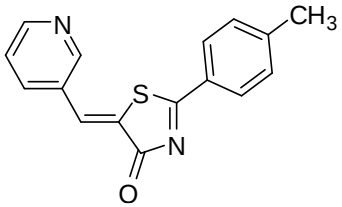	280.3 g/mol 19 ± 5
18	**ST-1630**	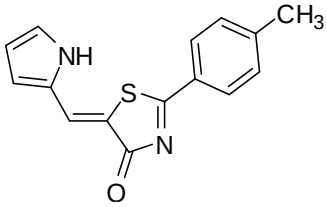	268.3 g/mol 13 ± 2

19	**ST-1631**	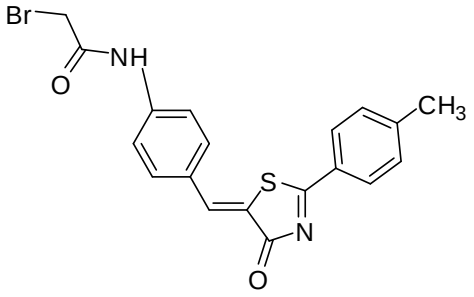	415.1 g/mol 16 ± 3
20	**ST-1634**	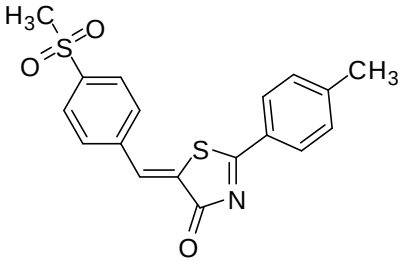	357.4 g/mol 17 ± 2
21	**ST-1684**	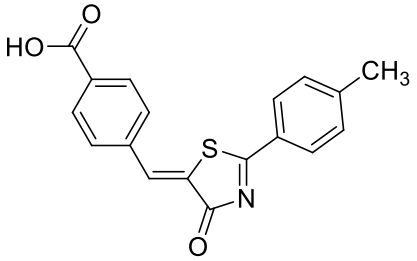	323.4 g/mol 15 ± 2
22	**ST-1685**	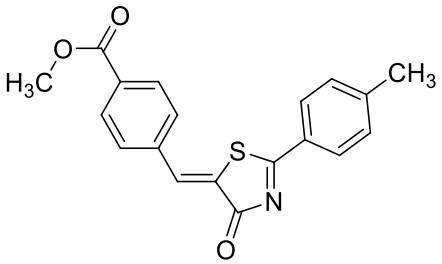	337.4 g/mol 6 ± 4

23	**ST-1689**	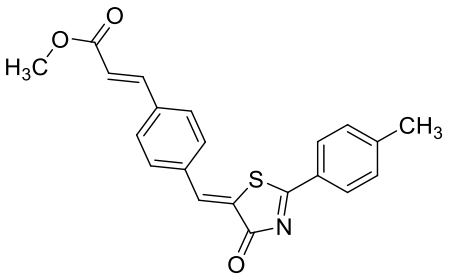	363.4 g/mol 13 ± 7
24	**ST-1694**	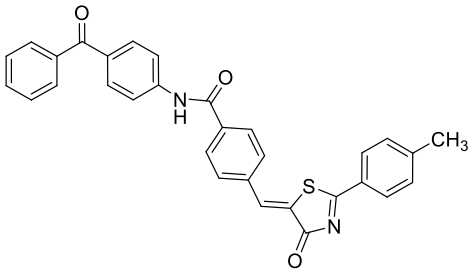	502.6 g/mol 15 ± 4
25	**ST-1760**	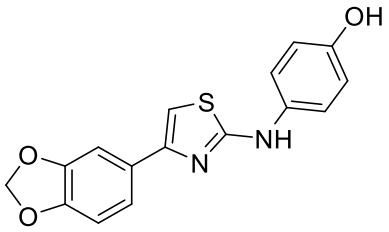	312.3 g/mol 21 ± 3
26	**ST-1810**	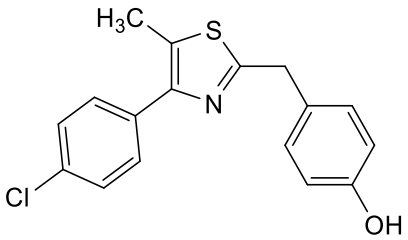	315.8 g/mol 23 ± 4

Table 6. Selected compounds with a uridine scaffold (PharmaCenter Bonn)

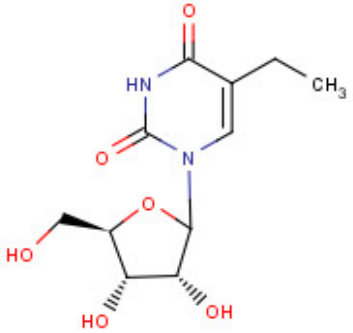

PZB00113018

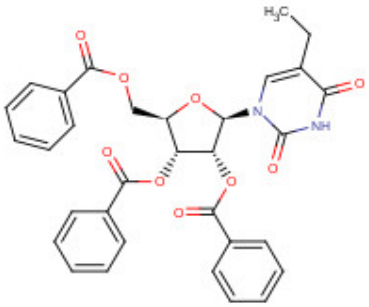

PZB00113091

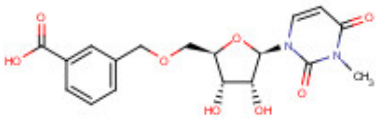

PZB00909261

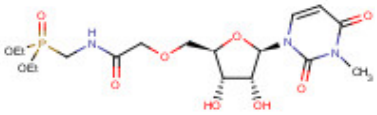

PZB00909262

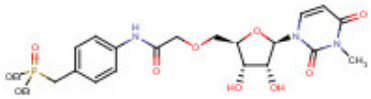

PZB00909263

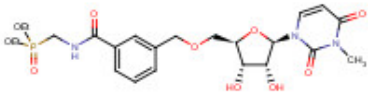

PZB00909264

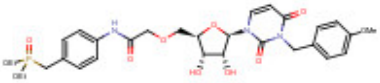

PZB00909265

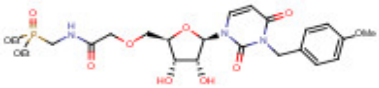

PZB00909266

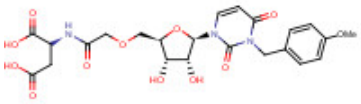

PZB00909282

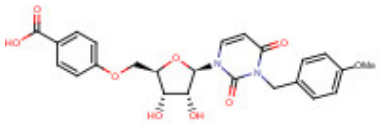

PZB00909283

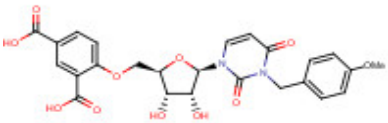

PZB00909284

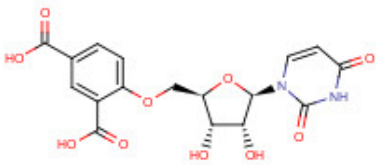

PZB00909285

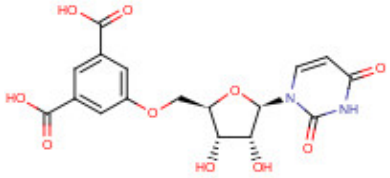

PZB00909286

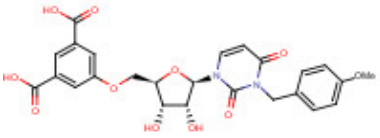

PZB00909287

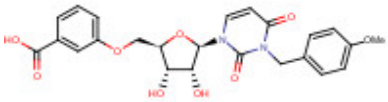

PZB00909288

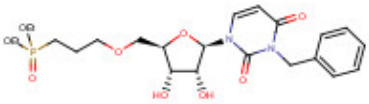

PZB00909289

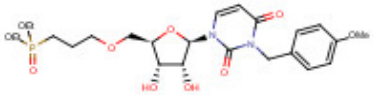

PZB00909290

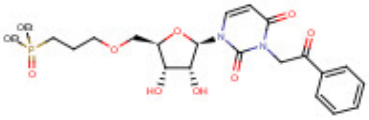

PZB00909291

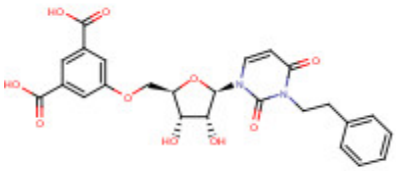

PZB00909292

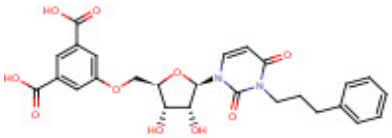

PZB00909293

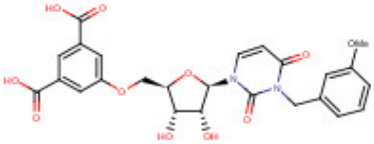

PZB00909294

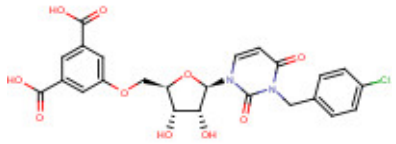

PZB00909295

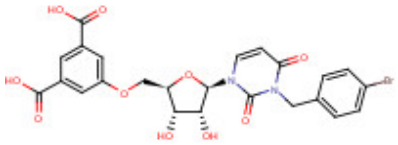

PZB00909296

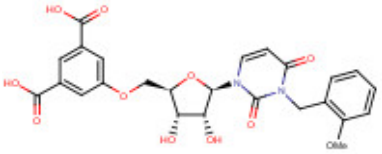

PZB00909297

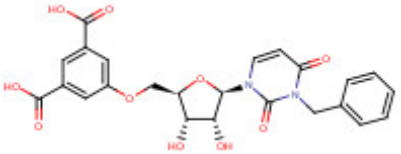

PZB00909298

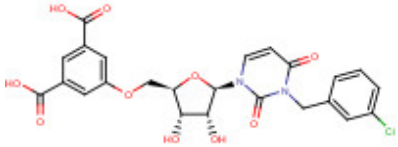

PZB00909300

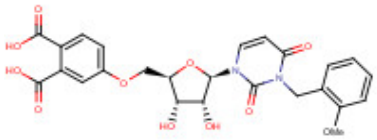

PZB00909301

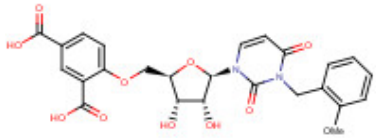

PZB00909302

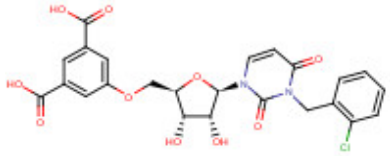

PZB00909303

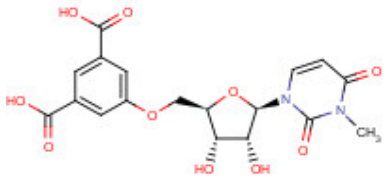

PZB00909304

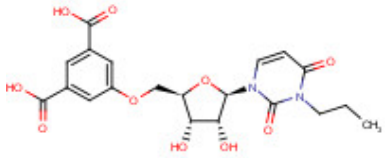

PZB00909305

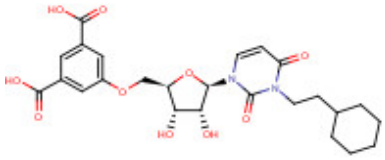

PZB00909306

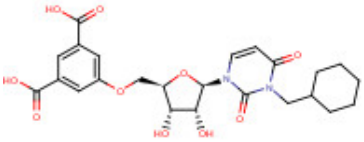

PZB00909307

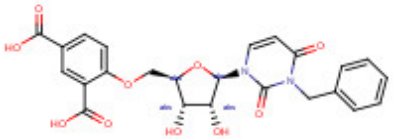

PZB00909338

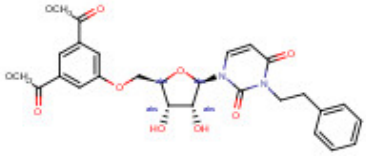

PZB00909339

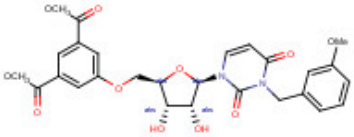

PZB00909340

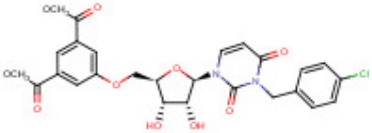

PZB00909341

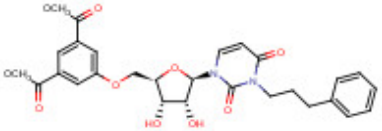

PZB00909342

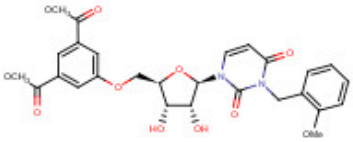

PZB00909343

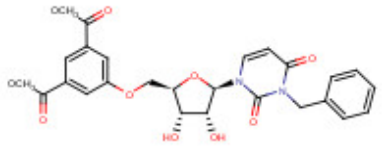

PZB00909344

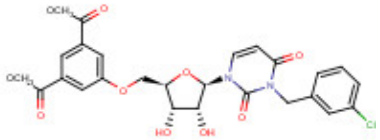

PZB00909345

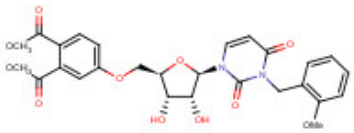

PZB00909346

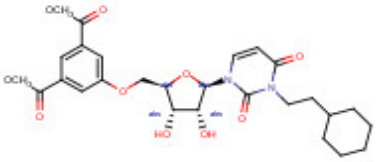

PZB00909347

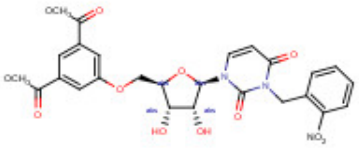

PZB00909348

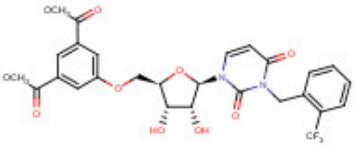

PZB00909349

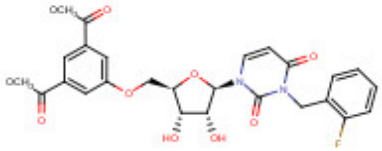

PZB00909350

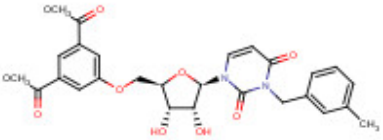

PZB00909351

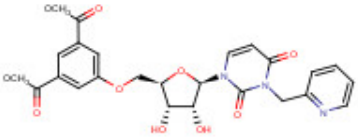

PZB00909352

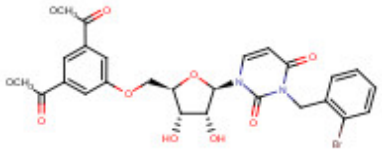

PZB00909353

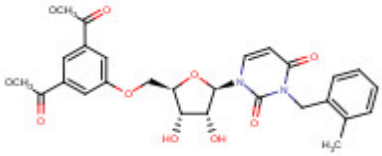

PZB00909354

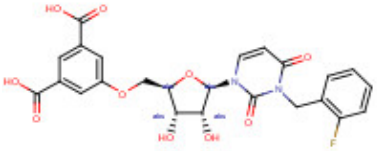

PZB00909355

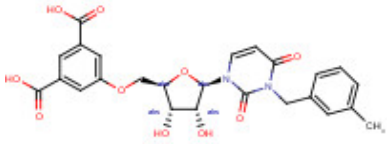

PZB00909356

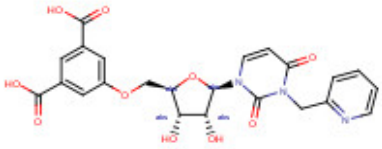

PZB00909357

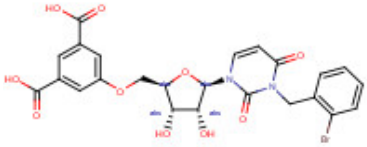

PZB00909358

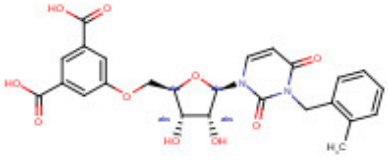

PZB00909359

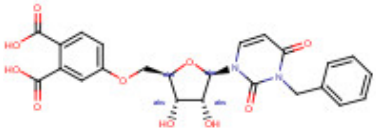

PZB00909364

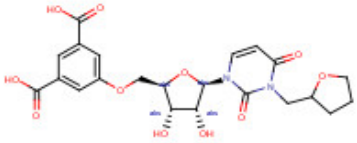

PZB00909365

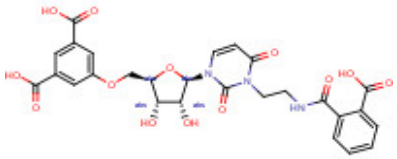

PZB00909366

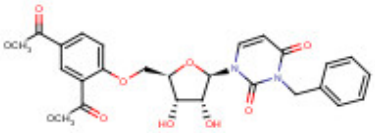

PZB00909367

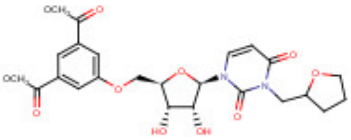

PZB00909368

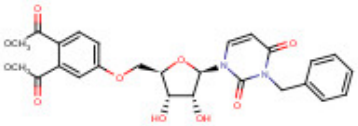

PZB00909370

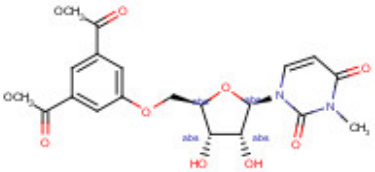

PZB00909372

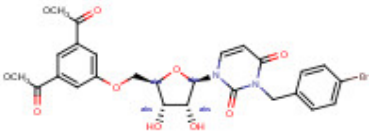

PZB00909373

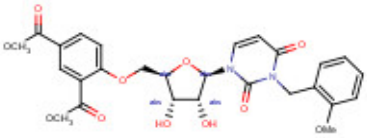

PZB00909374

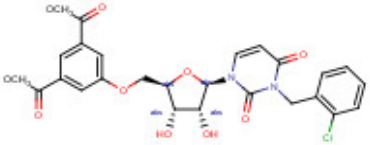

PZB00909375

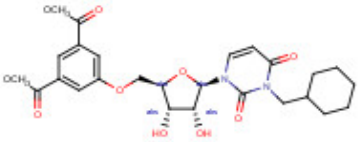

PZB00909376

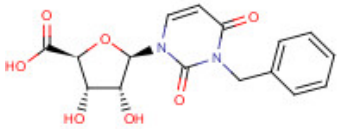

PZB00909454

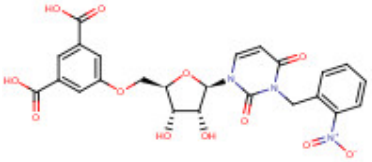

PZB00911030

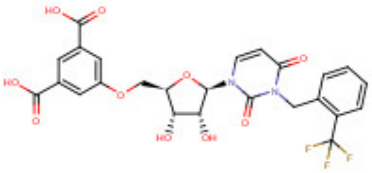

PZB00911031

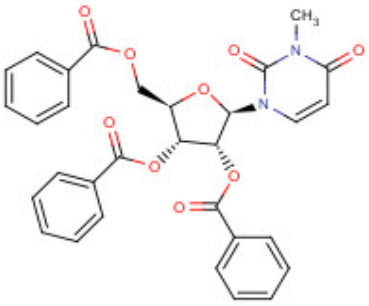

PZB01410007

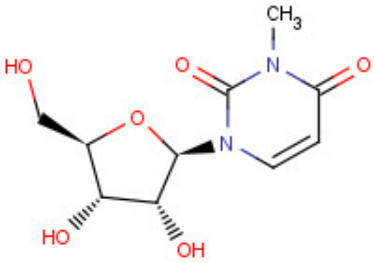

PZB01410015

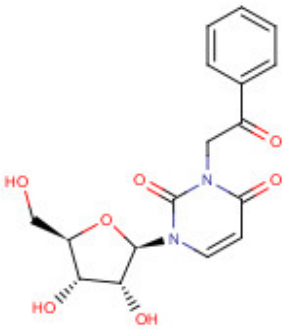

PZB01410016

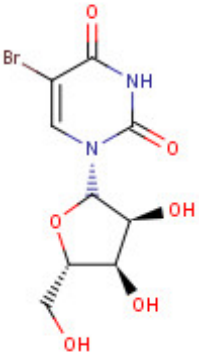

PZB01410028

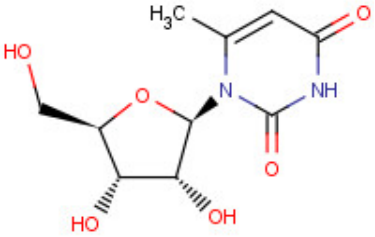

PZB01410029

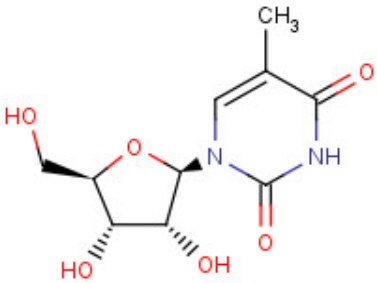

PZB01410031

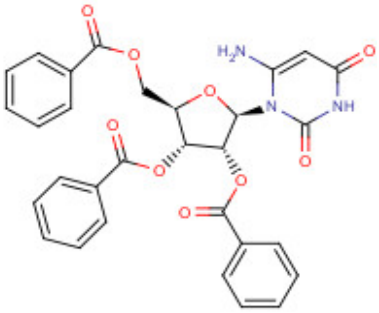

PZB01410035

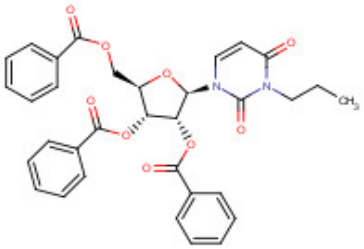

PZB01410036

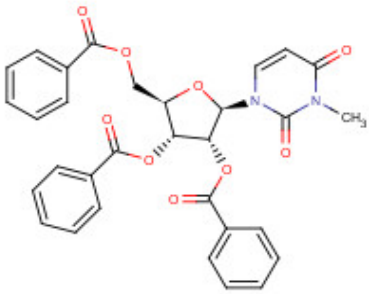

PZB01410039

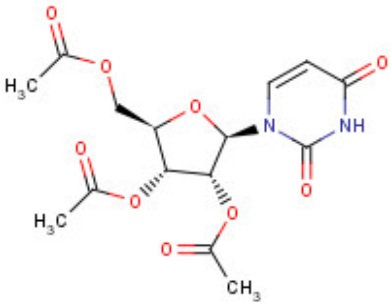

PZB01410045

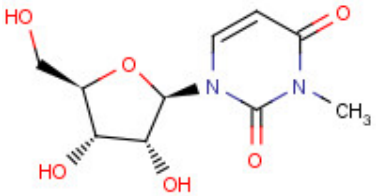

PZB01410048

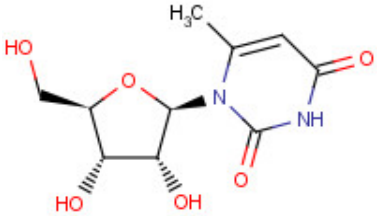

PZB01410049

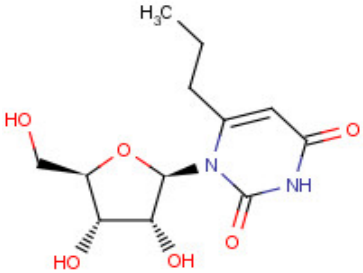

PZB01410050

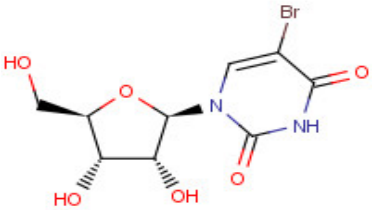

PZB01410052

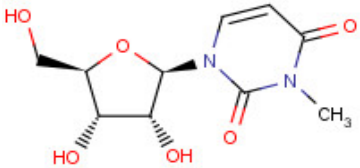

PZB01410054

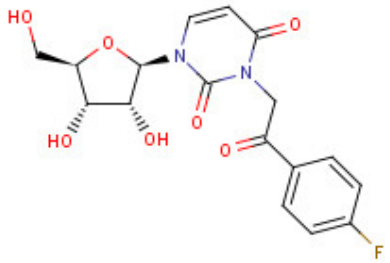

PZB01410056

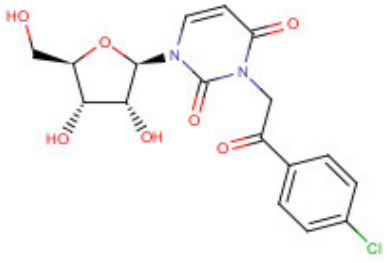

PZB01410057

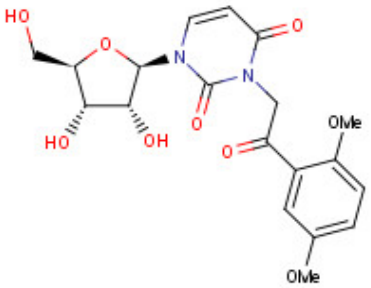

PZB01410058

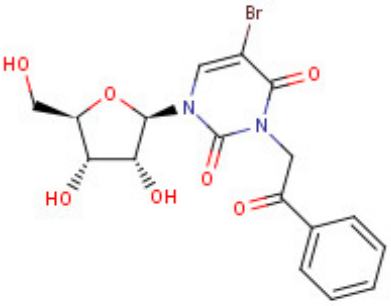

PZB01410059

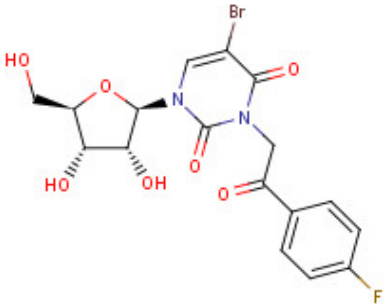

PZB01410060

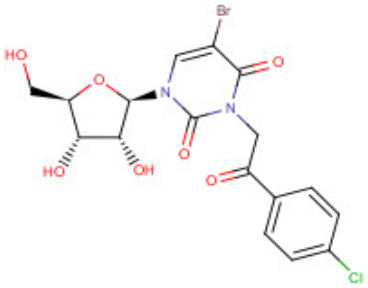

PZB01410061

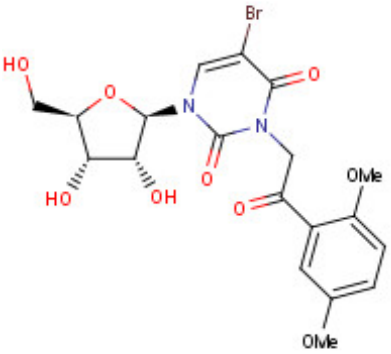

PZB01410062

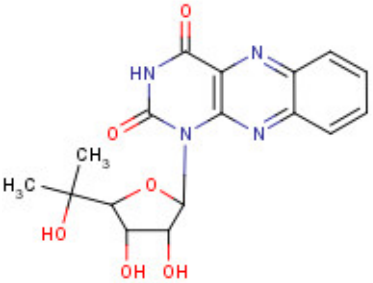

PZB06811018

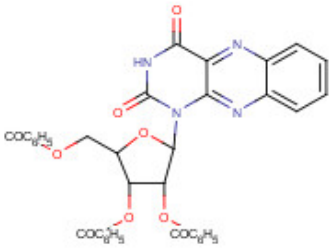

PZB06811030

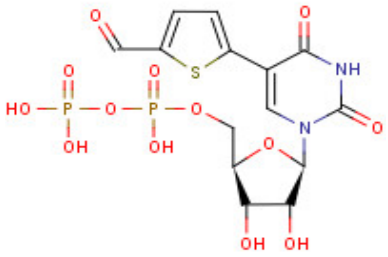

PZB12414001

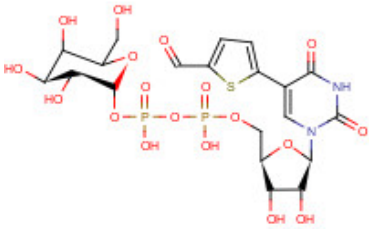

PZB12414002

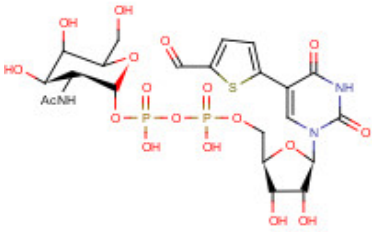

PZB12414003

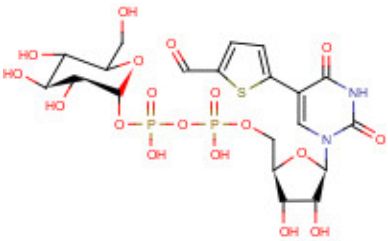

PZB12414004

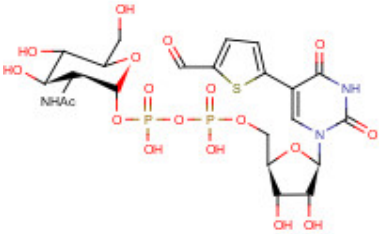

PZB12414005

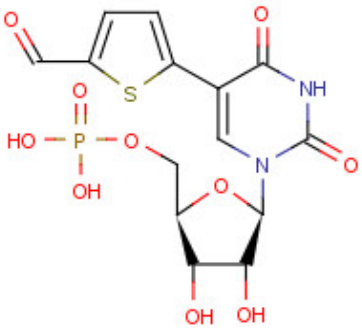

PZB12414006

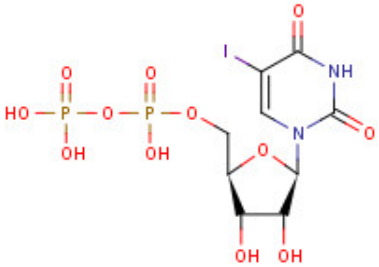

PZB12414007

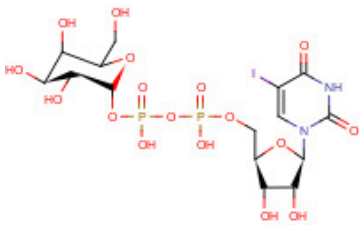

PZB12414008

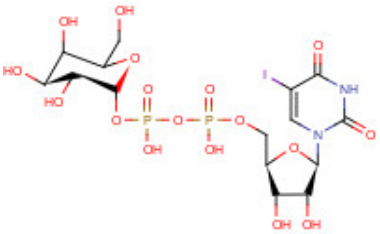

PZB12414009

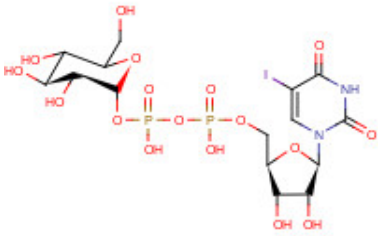

PZB12414010

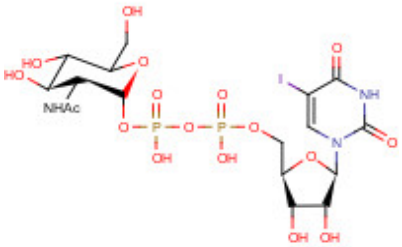

PZB12414011

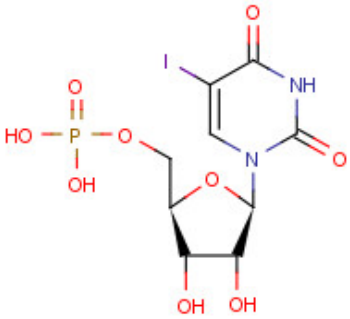

PZB12414012

Table 7. Compounds with uridine scaffold from Bonn PharmaCenter library tested as potential inhibitors of hNPP4 activity

Nr.	Markush structure	Internal ID	(Inhibition at 10 µM ± SD) %; n=6	M.W. in g/mol
1	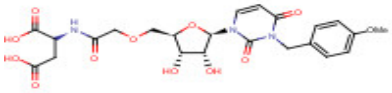	PZB00909282	50 ± 1	537,47
2	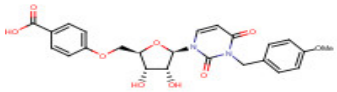	PZB00909283	53 ± 1	484,46
3	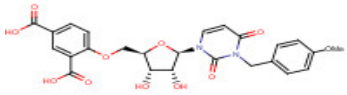	PZB00909284	60 ± 1	528,46
4	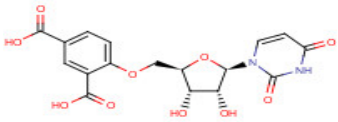	PZB00909285	58 ± 0	408,32
5	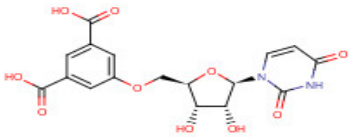	PZB00909286	51 ± 2	408,32
6	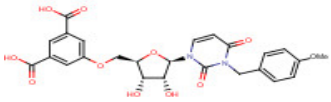	PZB00909287	50 ± 1	528,46
7	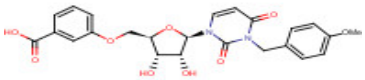	PZB00909288	41 ± 2	484,46
8	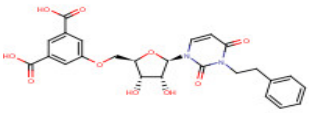	PZB00909292	41 ± 2	512,47

9	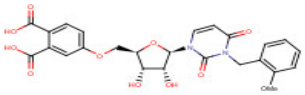	PZB00909301	50 ± 2	528,46
10	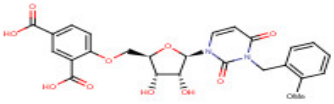	PZB00909302	52 ± 3	528,46
11	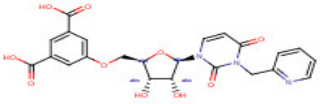	PZB00909357	41 ± 5	499,43
12	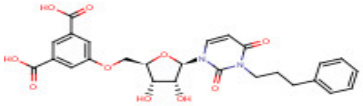	PZB00909293	34 ± 0	526,49
13	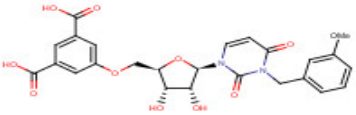	PZB00909294	42 ± 4	528,46
14	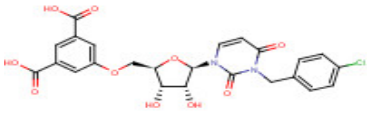	PZB00909295	49 ±1	532,88
15	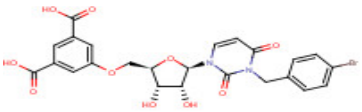	PZB00909296	47 ± 3	577,34
16	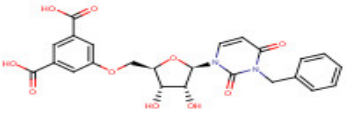	PZB00909298	37 ± 3	489,44
17	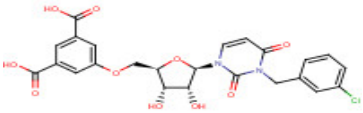	PZB00909300	48 ± 2	532,88
18	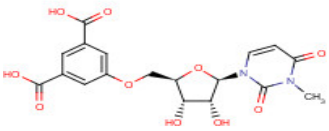	PZB00909304	36 ± 29	422,34

19	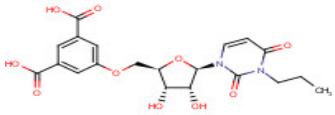	PZB00909305	29 ± 3	450,40
20	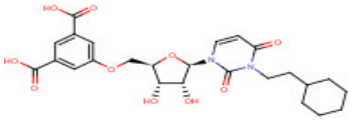	PZB00909306	39 ± 3	518,51
21	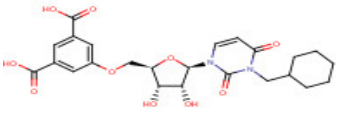	PZB00909307	32 ± 1	504,49
22	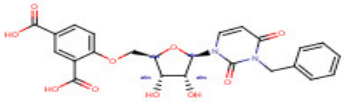	PZB00909338	43 ± 3	498,44
23	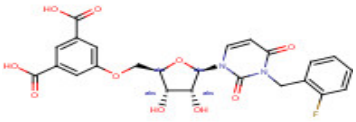	PZB00909355	42 ± 2	516,43
24	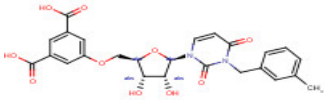	PZB00909356	47 ± 1	512,47
25	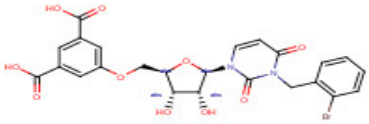	PZB00909358	44 ± 1	577,34
26	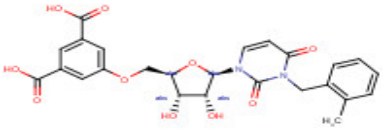	PZB00909359	43 ± 3	512,47
27	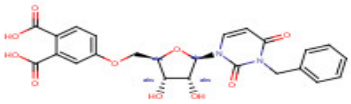	PZB00909364	49 ± 1	498,44

28	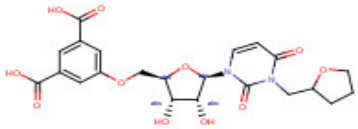	PZB00909365	40 ± 3	492,43
29	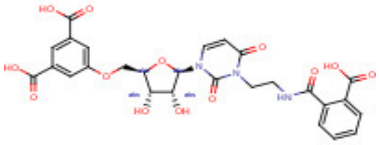	PZB00909366	48 ± 3	599,50
30	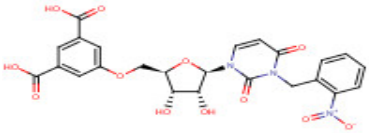	PZB00911030	51 ± 3	543,44
31	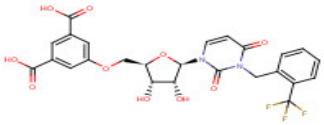	PZB00911031	67 ± 16	566,44

5.4 Orthogonal assay system for monitoring NPP4 activity

As already discussed, it is very crucial to validate results with a second assay system. For this purpose, a CE-based assay was developed for monitoring the enzymatic activity. The mixture of substrate (400 µM of Ap_3A or Ap_4A), hNPP4 at a concentration to ensure 10-15% of substrate formation (Fig. 13), and test compound or control instead, was incubated at 37 °C for 90 min and then stopped by heating for 5 min at 90 °C, and placed on ice. Substrate and enzyme are diluted in the buffer: 10 mM HEPES (4-(2-hydroxyethyl)-1-piperazineethanesulfonic acid), 1 mM $MgCl_2$ and 2 mM $CaCl_2$, pH 8.0. Capillary electrophoresis (CE) was used for analysis and quantification of the products (injection: -6 kV for 30 s, 40 cm [30 cm eff.] polyacrylamide-coated capillary, 100 mM phosphate pH 6.5 as a running buffer, -10 kV of separation voltage, detection at 260 nm) allowing separation of the products and quantification within 4 min (Fig. 12). The assay itself had to be validated and LOD (limit of detection) and LOQ (Limit of quantification) for AMP were ~0.5 µM and ~1.5 µM, respectively.

A

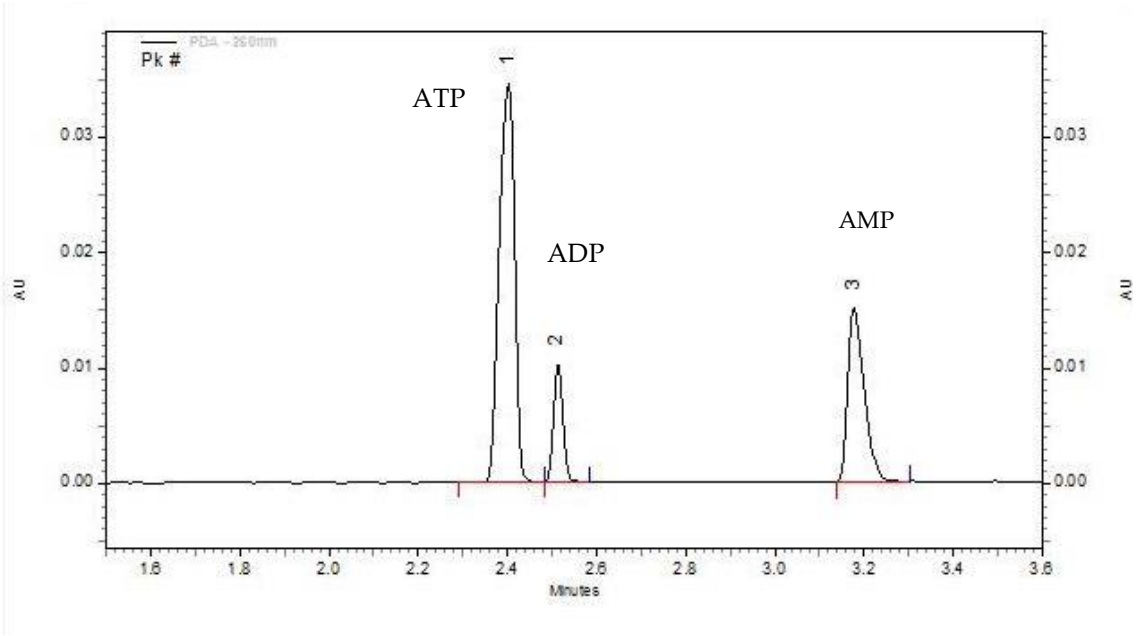

B

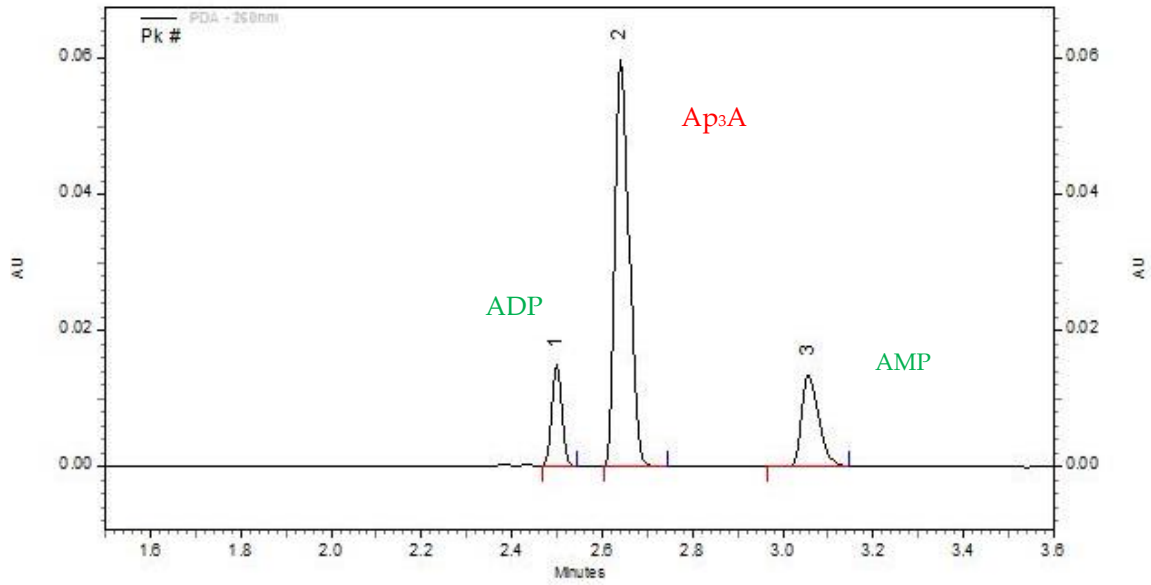

Fig. 12. Examples of CE electropherograms.

A. the separation and quantification of standards used for the validation of the method

B. an example of the analysis of NPP4 products, ADP, and AMP, formed from enzymatic activity of hNPP4 with Ap_3A used as substrate

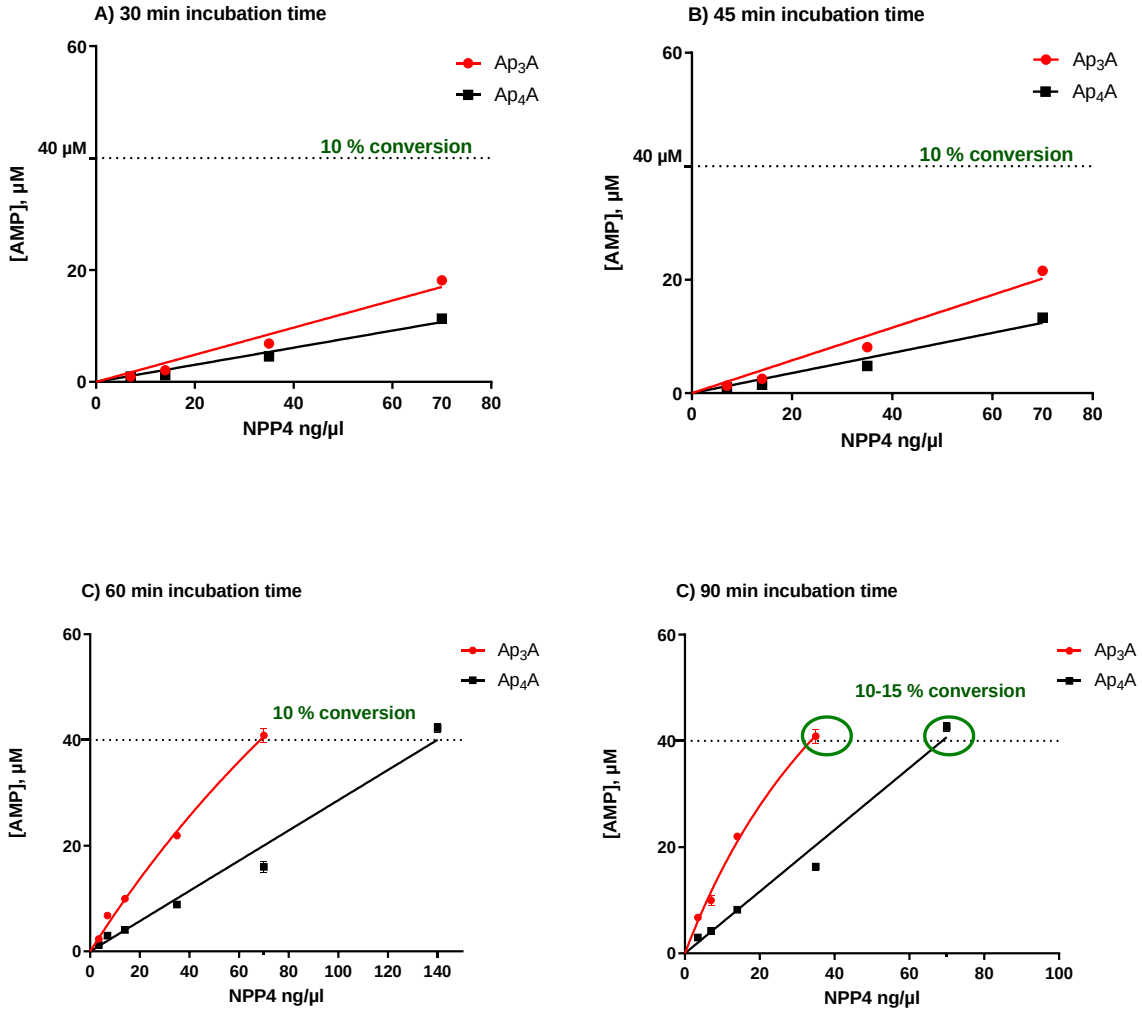

Fig. 13. Enzyme titration with different NPP4 concentration and different incubation time, the experiments have been made in triplicate.

5.5 Summary and outlook

The project on the identification of compounds able to modulate the activity of hNPP4 has resulted in few qualified hits. Using the newly developed HTS, 2656 compounds were screened and their effects on hNPP4 activity studied. A total of 8 hit compounds were identified from the first screening campaign (Table 2); compounds PSB-POM145 and PSB-POM146 were described and characterized in Chapter 4 of this thesis. Four of the hit compounds, namely PZB20709064, PZB20308204, PZB1091066A and PZB10914178A, were additionally validated by an orthogonal assay system, and their selectivity within members of the ecto-family was studied (Fig. 8 and Fig. 9). Test compound PZB20709064 has an IC_{50} value of 3.68 μM and displays high selectivity. PZB20308204, which is a positive modulator of the activity of hNPP4, has an EC_{50} value of 5.10 μM and it appears to additionally effect only CD73 activity within the ectonucleotidase family. PZB1091066A showed an IC_{50} value 5.25 μM at hNPP1 and IC_{50} value of 1.48 μM at hCD73, thus making the compound a dual inhibitor of NPP4 and CD73, with high selectivity among the other members of ectonucleotidase family. The best compound in term of potency and selectivity is PZB10914178A with IC_{50} value of 18.5 μM at hNPP4. Further tailored libraries of derivatives based on the chemical scaffolds of the hit series were studied, and based on information collected from our kinetic study, we investigated the inhibitory effect of a series of compounds with a uridine moiety. Unfortunately, although they inhibited hNPP4 activity, none of the derivatives showed higher potency than the original hit.

In conclusion, we were able to identify hNPP4 inhibitors (PSB-POM145 and PSB-POM146, IC_{50} values of 0.298 and 3.36 μM, respectively) which may serve as tool compounds for the investigation of the patho-physiological roles of the enzyme. In addition, we discovered new chemical scaffolds (PZB1091066A and PZB10914178A IC_{50} values 5.25 and 18.5 μM, respectively), which may serve as lead compounds for a series of new compounds to be synthetized, aiming at improving their potency at hNPP4.

6. Characterization of NPP4: Substrate preferences and enzyme kinetics

Introduction

To add more knowledge at the current state of the art about the (patho)-physiological role of poorly investigated hNPP4, reported to be a prothrombotic intravascular enzyme that stimulates platelet aggregation, it is essential to study and determine if hNPP4 is involved in the hydrolysis of substrates other than Ap_3A and Ap_4A. We extensively studied the kinetic characteristics of this enzyme. We screened several potential natural substrates on hNPP4 and we observed the rate of product conversion using different analytical methods including CE-based assay. Full biochemical characterization was performed for some of them leading to the discovery of novel hNPP4 substrates.

6.1 Screening of nucleotides as potential NPP4 substrates

So far, only Ap_3A and Ap_4A have been identified and reported in the literature as substrates of hNPP4. In the present project, we investigated a broad range of different potential substrates that are involved in purinergic signaling. A total of 30 potential natural nucleotides with different chemical properties were investigated (see **Table 8** and **Fig. 15**, **Fig. 16,** and **Fig. 17**). At first, the enzymatic assay and the detection methods had to be validated. The commercial nucleotides were checked for impurity, and only compounds with a purity greater than 95 % were used. An amount of 1.4 μg of the soluble enzyme, expressed as previously described [1], was utilized in each experiment. This apparently high quantity of enzyme was required in order to increase the chances of activity detection. The substrates utilized were employed at a final concentration of 400 μM. Substrate and enzyme were diluted in the buffer: 10 mM HEPES, 1 mM $MgCl_2$ and 2 mM $CaCl_2$, pH 8.0. and performed in a 96 well plate. The incubation time was 60 min at 37 °C followed by denaturation at 90 °C for 5 min, and by placement on ice. Positive and negative controls as well standards were run in parallel. For analysis and

qualification of the products with the CE-based assay different conditions were used (see paragraph 6.3 and **Table 11** for details) and the standards were always run in parallel. In **Fig. 14**, an overview of the tested substrates shows their percent hydrolysis yielding the respective products, while in **Fig. 18** the substrates are presented in separate categories, according to structure, namely, nucleoside monophosphates (NMP), e.g., AMP and UMP; nucleoside diphosphates (NDP) and their sugar derivatives, e.g., GDP, UDP-glucose; nucleoside triphosphates (NTP), e.g., ATP, CTP; cyclic nucleotides e.g., cGAMP, cUMP, 2′,3′-cAMP; and di-nucleotides such as Ap_6A, Up_4U. Chemical structures of substrates and their quantified products after enzymatic assay are presented in **Fig. 15-17**.

The screening of the potential substrates clearly showed the ability of hNPP4 to hydrolyze Ap_3A and Ap_4A (as already known). Surprisingly, the enzyme showed a high hydrolysis rate of UTP and CTP, which was even greater than the one observed for Ap_3A and Ap_4A, using the same assay conditions and detection method (**Fig. 14**). Furthermore, it is interesting to notice that among the NTPs, the enzyme hydrolyzes specifically UTP and CTP, low to moderate hydrolysis of GTP was detected, whereas for other nucleoside trisphosphates the conversion was negligible (**Fig. 18 C**). The investigated cyclic nucleotides (**Fig. 18 E**), NMPs (**Fig. 18 A**), NDPs and related sugars (**Fig. 18 B**) are not suitable substrates of hNPP4 catalytic activity.

To better elucidate the substrates specificity among NTPs, we observed the conversion rate from substrates to products using four different amounts of hNPP4. These further studies validated the high conversion rate of UTP to UMP and CTP to CMP, as well as the moderate conversion of GTP to GMP by hNPP4. It is also very clear that hNPP4 does not convert ATP, in contrast to the other members of this ecto-enzyme family, nor 5-methyl-UTP (**Fig.19**). UTP and CTP have a similar structure, they differ in position 4 of the base where in the case of UTP a carbonyl group is present, while in CTP this is replaced by an amino group, which changed the overall hydrogen-bond donor-acceptor motifs. Considering the structural similarity between UTP, CTP and 5-methyl-UTP, it is

evident that the enzyme has a high degree of selectivity and we hypothesized that also the latter would be hydrolyzed similarly. To better elucidate the potential activity of hNPP4 with 5-methyl-UTP (5-mUTP) we additionally observed its hydrolysis using combination of different concentrations of 5-mUTP and hNPP4 (**Fig. 20** for details) and increasing the incubation time up to 90 min. However, despite the different conditions used, the hydrolysis of hNPP4 on 5-mUTP was always below 5 %, thus making it negligible.

Table 8. List of substrates tested on hNPP4

NMP$^{\alpha}$	**NDP and NDP-sugar derivatives** $^{\beta,\gamma}$	**NTP** $^{\beta,\gamma}$	**Cyclic nucleotides** $^{\delta}$	**di-nucleotides** $^{\beta,\gamma}$
AMP	ADP	ATP	2′-3′-cAMP	Ap_3A
GMP	GDP	GTP	3′-5′-cAMP	Ap_4A
UMP	UDP	UTP	cGAMP$^{\alpha,\delta}$	Ap_5A
TMP	UDP-glucose	TTP	cUMP	Ap_6A
CMP	UDP-galactose	CTP	cGMP	Up_4U
	UDP-glucosamine	ITP	cIMP	NAD^+
		5′-methyl-UTP		

α,β,γ and δ are different CE methods, for details see Table 11.

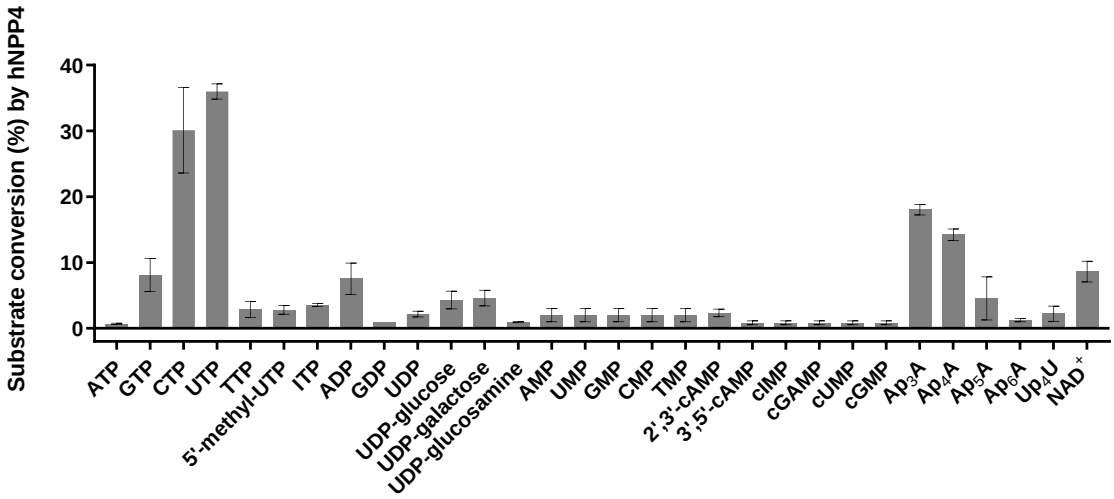

Fig. 14 Overview of the substrates tested at the concentration of 400 μM using 1.4 μg of hNPP4 and incubating for 60 min at 37 °C, following 5 min of heating at 90 °C for stopping the reaction. Separation and quantification of the products using the CE with DAD detector. Different separation conditions were applied. Positive controls, negative controls and standards were run in parallel.

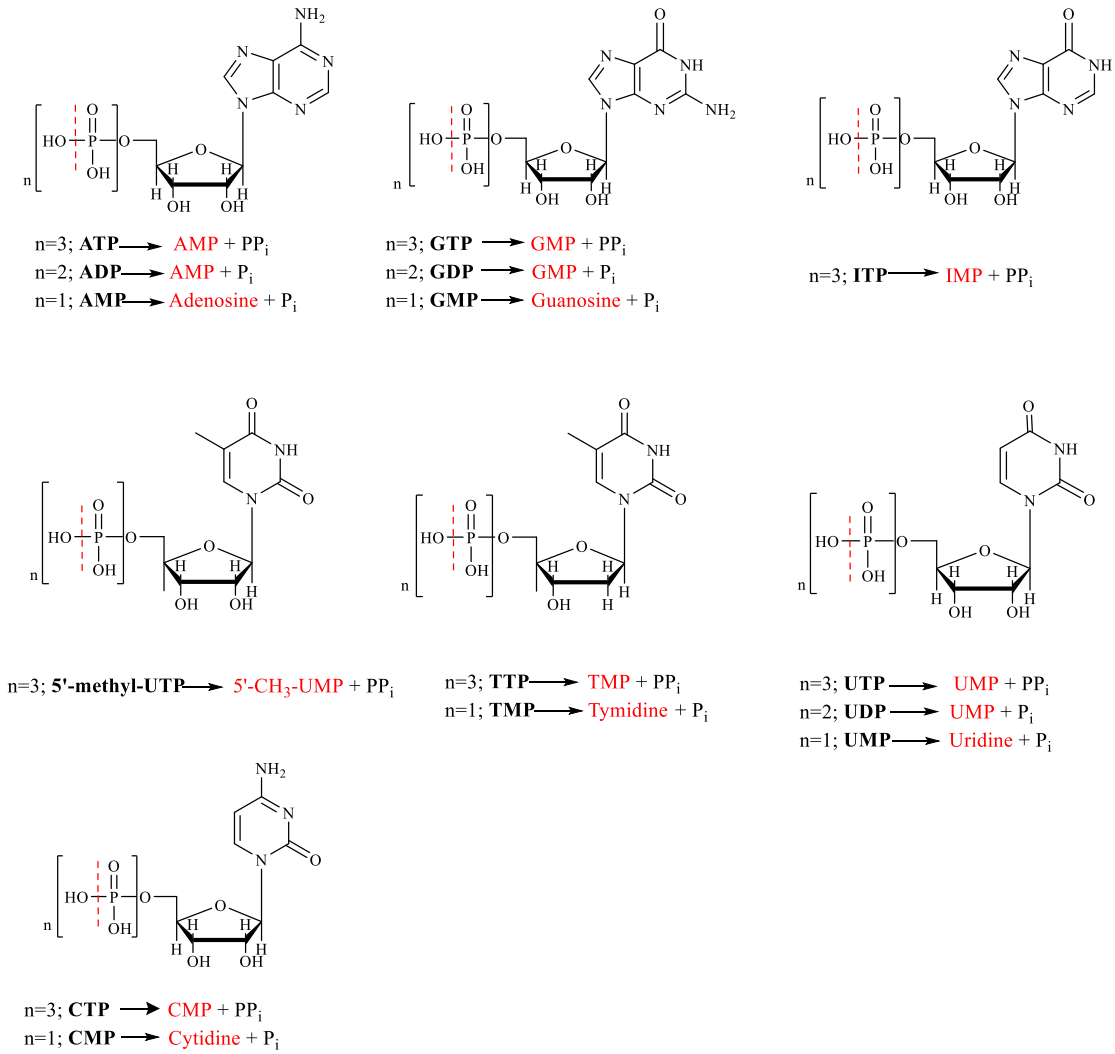

Fig. 15 Structures of potential natural substrates investigated with hNPP4. In red the quantified products separated and analyzed using CE-based assay (Table 8 and 11 for details). The site of hydrolysis is marked with a dashed red line.

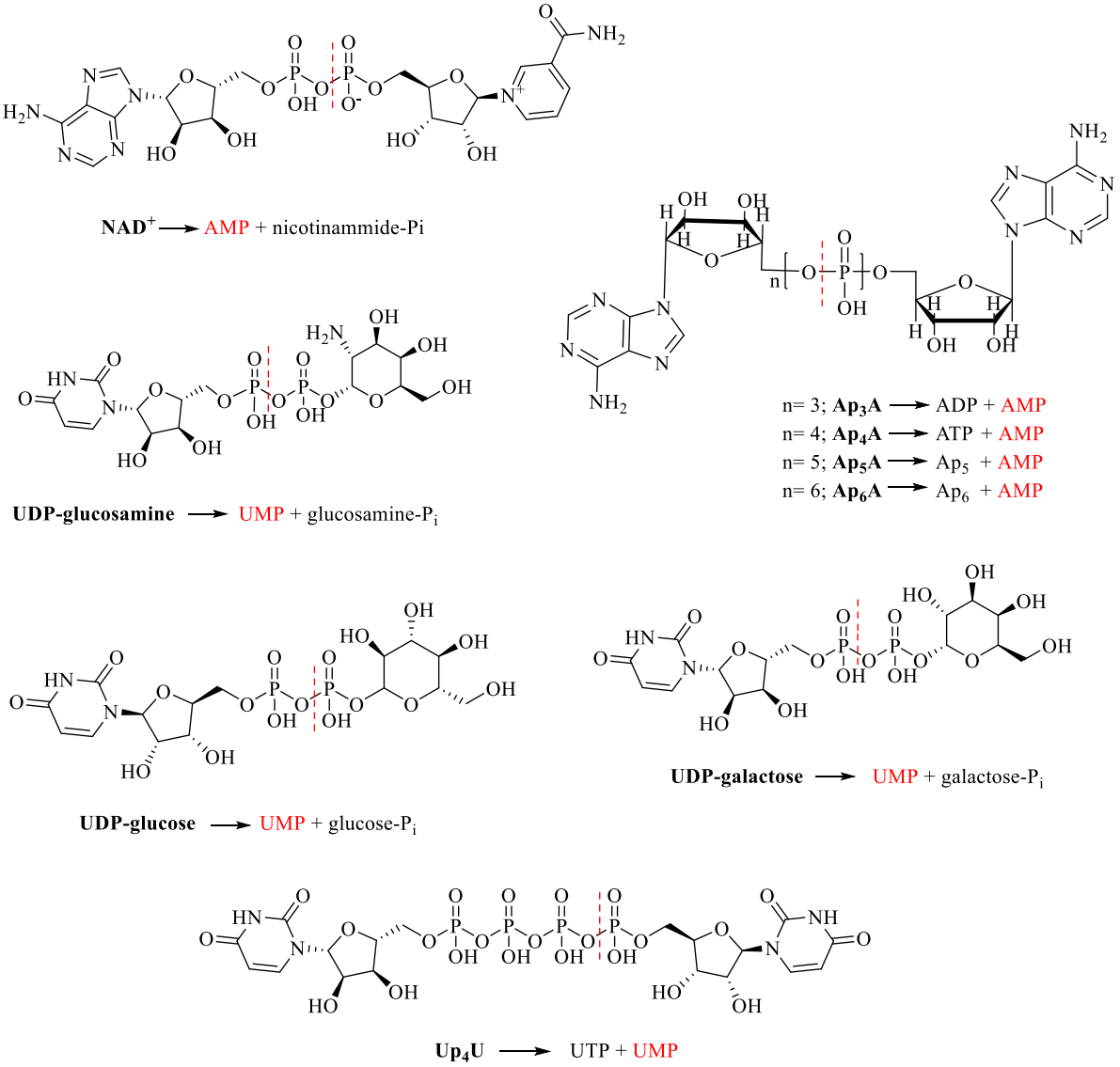

Fig. 16 Structures of potential natural substrates investigated with hNPP4. In red the quantified products separated and analyzed using CE-based assay (Table 8 and 11 for details). The site of hydrolysis is marked with a dashed red line.

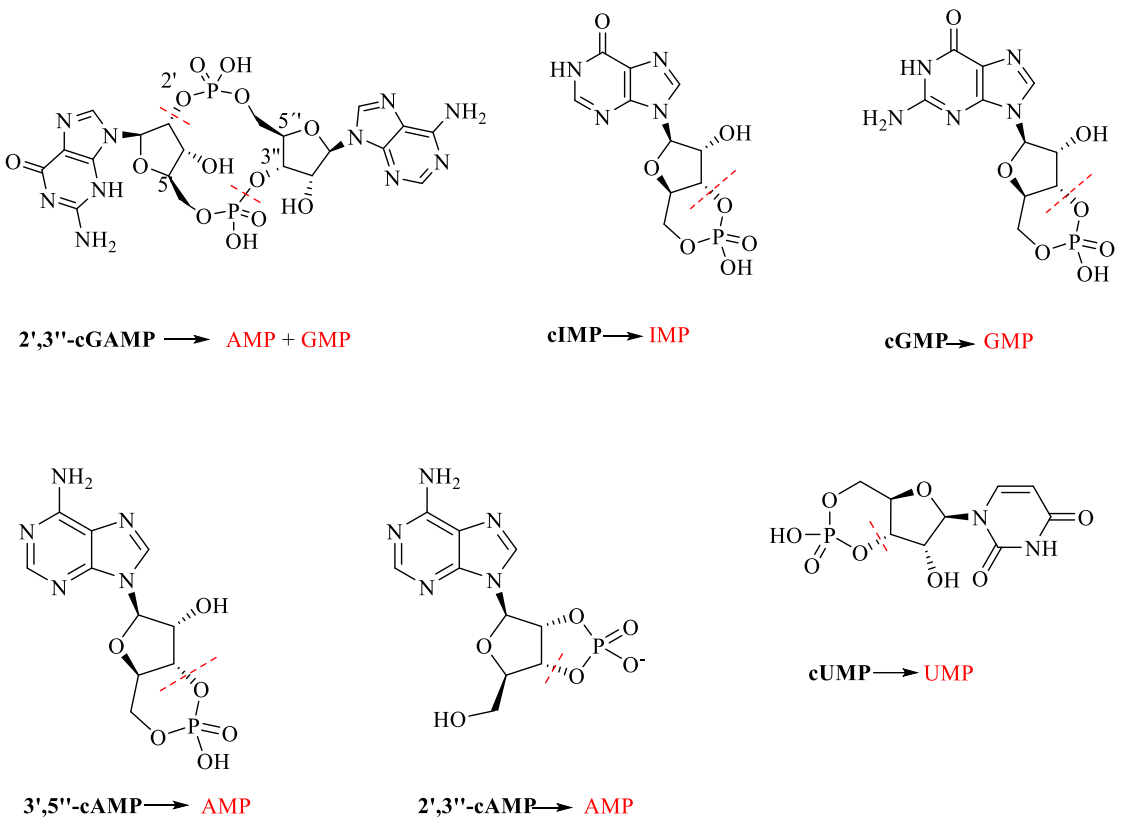

Fig. 17 Structures of potential natural substrates investigated with hNPP4. In red the quantified products separated and analyzed using CE-based assay (Table 8 and 11 for details). The site of hydrolysis is marked with a dashed red line.

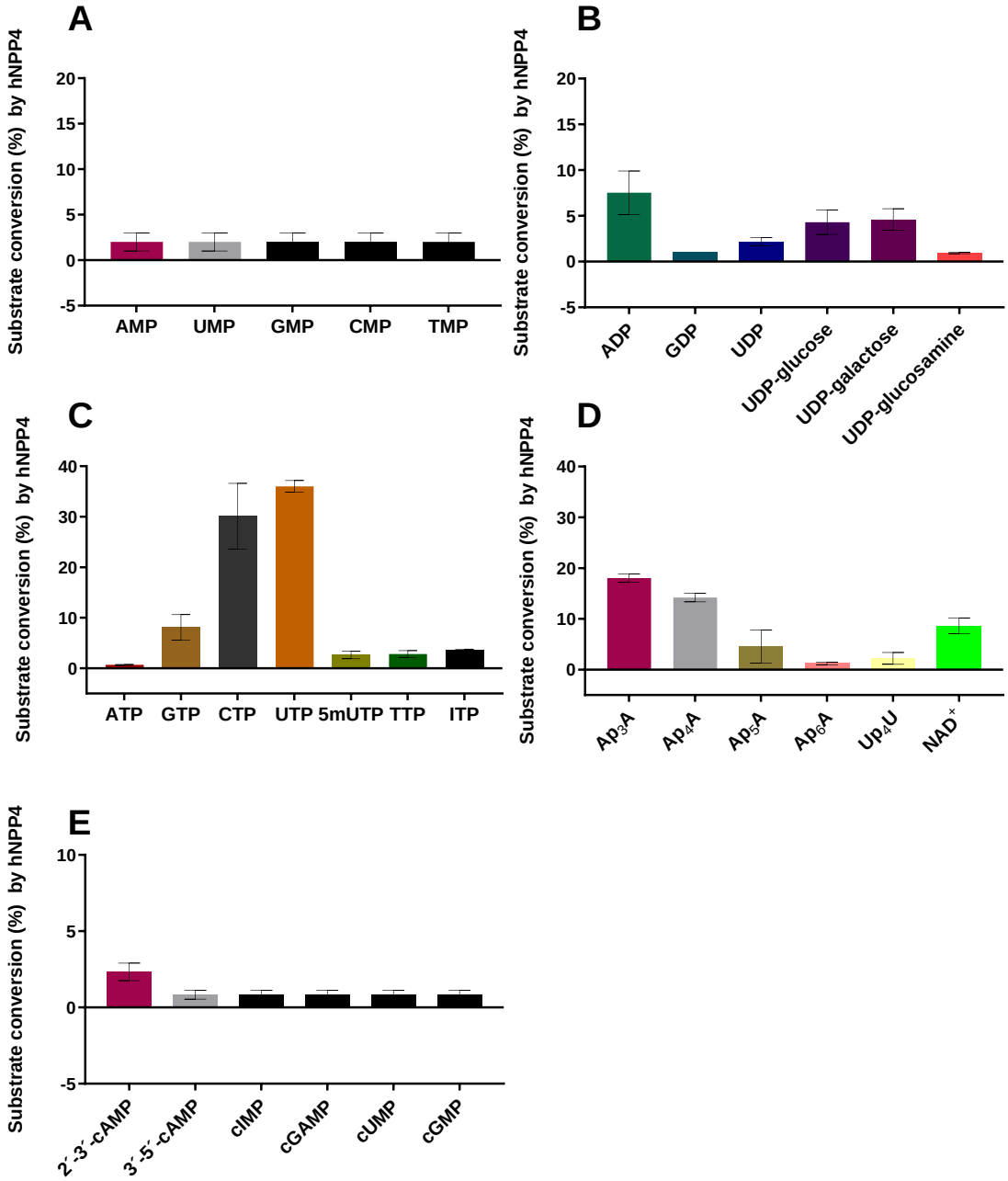

Fig. 18 Overview of the substrates tested on hNPP4 and their percent conversion to the respective products. Direct comparison within structural classes.

A. nucleotide monophosphates (NMP), **B.** NDP, **C.** NTP, **D.** dinucleotides, **E.** cyclic nucleotides. Substrates were tested in the same conditions using 400 µM of each and 1.4 µg of hNPP4. CE-based assay for analysis of the products (see Table 8 and 11 for details).

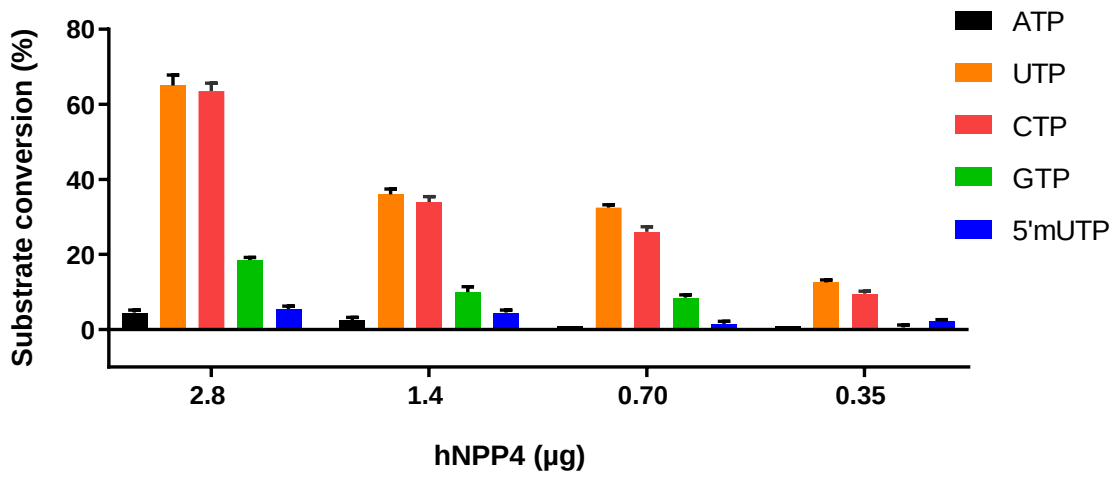

Fig. 19 Hydrolysis of nucleoside triphosphates by hNPP4. Substrates were tested at 400 µM concentration using different amounts of hNPP4, for 60 min at 37°C, followed by 5 min at 90 °C. Analysis of the products with CE-DAD using method β (see Table 11 for detailed conditions).

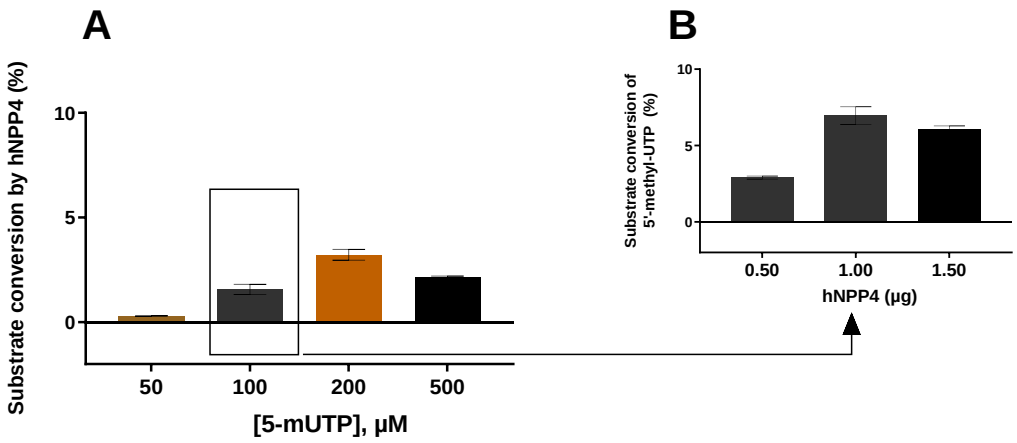

Fig. 20 Study of the potential hydrolysis of 5′ methyl-UTP by hNPP4. **A.** Fixed concentration of hNPP4 (0.35 µg) was tested with four different 5-mUTP concentrations. **B.** 100 µM of 5-mUTP and different amount of hNPP4 were used. Incubation time of 90 min at 37°C, followed by 5 min 95°C. CE-DAD for detection and analysis of the products using method γ (see Table 11 for conditions). Positive, negative controls and standards were run in parallel.

6.2 Biochemical characterization of NPP4 kinetics

Enzyme kinetics is the study of the rates of chemical reactions that are catalyzed by enzymes. The study of the enzyme's kinetics provides insights into the catalytic mechanism of the enzyme, its role in metabolism, how its activity is controlled in the cell and how drugs can inhibit its activity. During the substrates screening the enzyme activity clearly showed a novel preference in the hydrolysis of specific substrates namely UTP and CTP, in addition to Ap_3A and Ap_4A whose hydrolysis was already known. Subsequently, a full biochemical characterization was performed for these substrates that showed the highest rates of conversion. Enzyme reactions with the substrates are characterized by kinetic parameters like K_m, K_{cat} and K_{cat}/K_m. K_m is the Michaelis-Menten constant that indicates substrate concentration at which half of the maximum velocity of the enzyme reaction is performed. If V is the rate of enzyme reaction, V_{max} is the maximum rate achieved by the reaction and [S] is the substrate concentration, then K_m can be determined using the following Michaelis-Menten equation:

$$V = V_{max}[S]/(K_m + [S])$$

One enzyme can have different K_m value for different substrates and it varies with the change of temperature and pH. K_m may differ from species to species and varied on the types of enzyme preparations. The size of K_m value can revel several information about a particular enzyme [7]. A small K_m indicates that the enzyme requires only a small amount of substrate to become saturated. Hence, the maximum velocity is reached at relatively low substrate concentrations. A large K_m indicates the need for high substrate concentrations to achieve maximum reaction velocity. The substrate with the lowest K_m upon which the enzyme acts as a catalyst is frequently assumed to be enzyme's natural substrate, though this is not true for all enzymes. K_{cat} (turn-over number) is the number of substrate molecules turned over per enzyme molecule per second. The following equation is used to determine K_{cat} value of an enzymatic reaction:

$K_{cat} = V_{max} / [E_T]$

E_T= concentration of enzyme catalytic sites. Unit: concentration per time.

In enzyme characterization, K_m is often associated with the binding affinity of the enzyme for the substrates, but it is not enough to express the enzyme kinetics, since it describes only the ground state of enzyme reactions. In contrast, K_{cat} express the velocity of product release from the enzyme-substrate complex, which is often slow and therefore indicates the rate-limiting step of enzyme reactions. Since K_{cat} value describes the transition state of enzyme reactions, it is a better parameter to characterize the enzyme kinetics than K_m value. The ratio between K_{cat} and K_m (K_{cat}/K_m) indicates the catalytic efficiency of the enzyme. This ratio regards both K_{cat} and K_m parameters and it is therefore the best parameter to characterize the enzyme kinetics. K_m and V_{max} are determined by incubating the enzyme with varying concentrations of substrate, the results can be plotted as a graph of rate of reaction (v) against concentration of substrate [S], and will normally yield a hyperbolic curve. A series of different concentrations of substrates Ap_3A and Ap_4A, CTP and UTP were prepared. Three replicates in three independent experiments were performed for each of the concentrations. The enzyme amount which was used was selected after enzyme titration. The reaction mixture was carried out for incubation at 37 °C for 60 minutes and blocked at 90 °C for 5 minutes, following cooling down on ice. The separation and quantification of the products was achieved using CE-based detection (for details see Table 11 method β). In **Fig. 21** and **22** the Michaelis-Mentes plots of UTP, CTP, Ap_3A and Ap_4A are displayed, and in **Table 9** their calculated K_m, K_{cat} and K_m/K_{cat} values are presented.

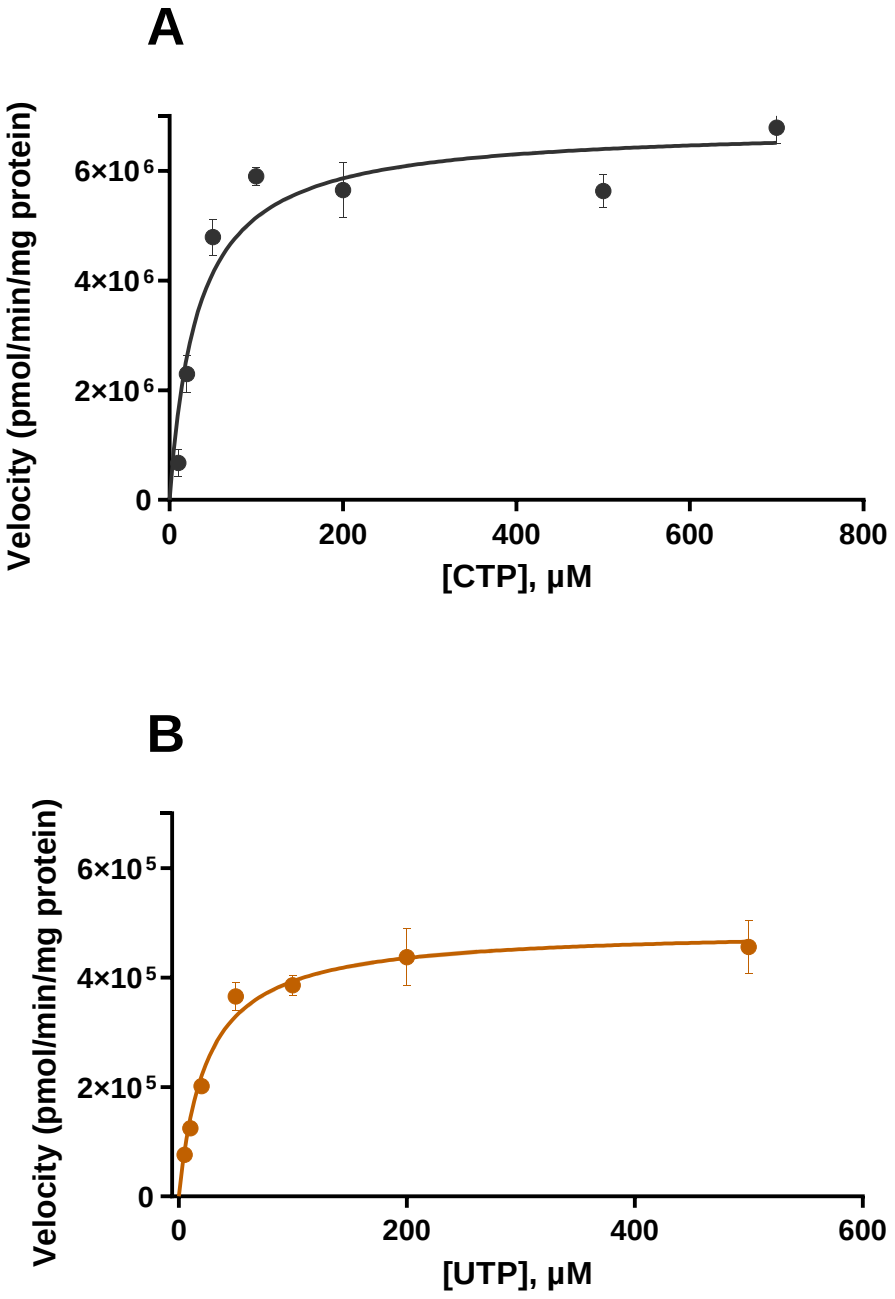

Fig. 21 Michaelis-Menten Plots (v *vs*. [S]) of the hydrolysis of CTP (A) and UTP (B) by human NPP4. Data points represent means ± SD from three separate experiments each performed in triplicates. For the determined K_m, k_{cat} and k_{cat}/K_m values, see Table 9.

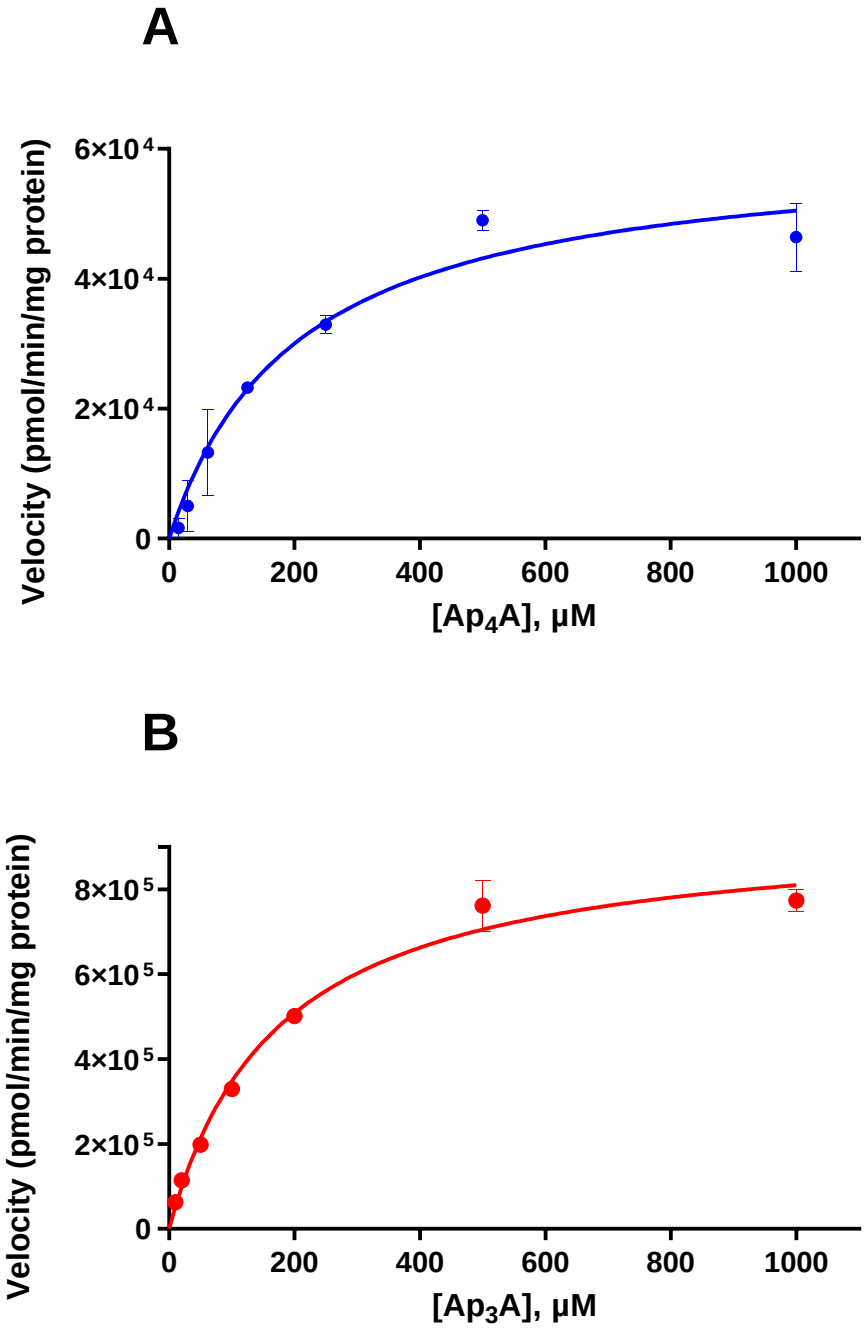

Fig. 22 Michaelis-Menten Plots (v *vs*. [S]) of the hydrolysis of Ap_4A (A) and Ap_3A (B) by human NPP4. Data points represent means ± SD from three separate experiments each performed in triplicates. For the determined K_m, K_{cat} and K_{cat}/K_m values, see Table 9.

Table 9. Kinetic parameters of hNPP4 reactions for different substrates

	K_m ± SD (μM)	K_{cat} ± SD (s^{-1})	K_{cat}/K_m
Ap_4A [a]	220 ± 49	0.46 ± 0.03	2.08×10^3
Ap_3A [a]	228 ± 15	0.165 ± 0.005	0.72×10^3
CTP	32.4 ± 5.8	0.051 ± 0.002	1.57×10^3
UTP	19.2 ± 3.9	0.073 ± 0.004	3.38×10^3

[a] consistent with literature values. Albright, R. *et al.*, *Blood* **2012**, *120*, 4432-4440

From our kinetic study we observed and confirmed the high hydrolysis rate of hNPP4 on UTP and CTP. UTP, having a K_m value of ~20 μM (for Ap_3A it is 10-fold higher), is likely to be a natural substrate of hNPP4 and, if further confirmed, this might lead to a better understanding of the physiological role of the enzyme. In fact, UTP is a known physiological substrate for purinergic receptors, $P2Y_2$ and $P2Y_4$ (Table 10. for details). In some tissue P2Yr and hNPP4 are co-expressed (mRNA and protein level). Ectoenzyme regulate the homeostasis of the nucleotides-activating purine receptors and considering the novel data of hNPP4 in hydrolase UTP, this suggest further potential physiological role of hNPP4 in the purinergic signaling, which must be studied in the future.

Table 10. Overview of human uracil nucleotide-activated P2Yr

	UniProt ID	Physiological substrate	Therapeutic potential	Tissue co-expression with NPP4[a]
$P2Y_2$	P41231	ATP; UTP	**Agonists:** Neurodegenerative disorders, dry eyes, ocular hypertension, retinal degeneration, cystic fibrosis **Antagonist**: atherosclerosis, osteoporosis, inflammation	Endocrine tissue (thyroid) GI tract (small intestine) Cardiac muscle
$P2Y_4$	P51582	ATP; UTP	**Agonists**: Neurodegenerative disorders, cystic fibrosis **Antagonist**: Neurodegenerative disorders, myocardial infarction, constipation	GI tract (small intestine)

[a] The Human protein Atlas at protein and mRNA level, created by combining the data from the three transcriptomics datasets (HPA, GTEx and FANTOM5)

6.3 Qualitative and quantitative substrate analysis CE-UV

Capillary electrophoresis (CE) has been used most frequently for monitoring enzymatic reactions, especially for monitoring biological activities of ecto-nucleotidases [5]. Enzyme assays based on CE are rapid and automatic, and they provide high resolution of separation [5]. Basic components of CE include: high voltage, injection system, capillary, and detection system [5].

High voltage

The high voltage is usually in the range from 2 to 30 kV the voltage or current can be constant. Normal polarity means that the cathode is on the side of the detector, while reverse polarity, means that the anode is on the side of the detector [6].

Injection system

In CE, there are two different types of injection systems: hydrodynamic and electrokinetic injections. The electrokinetic system is an injection by applying voltage, and only charged molecules, for example nucleotides, can be injected. In the hydrodynamic injection system, charged and uncharged molecules (such as nucleosides having no charge) can be injected because the injection is achieved by applying pressure [6].

Capillary

Many materials have been suggested and tested for the construction of capillaries for CE. These include fused silica, borosilicate glass, and polytetrafluoroethylene (Teflon®). Fused silica is now the preferred material for the construction of capillaries. The silica used is of very high purity like that used to produce silicon chips for electronic components. Two types of capillaries are important: normal and coated capillaries. In plain capillaries there is the presence of an EOF (electroosmotic flow); in fact, the total mobility of the molecules results from the EOF and the electrophoretic mobility; moreover, a simultaneous separation of charge and uncharged molecules is possible,

but the migration time is usually not constant. For the coated capillaries there is no EOF and the separation of the nucleosides due to their electrophoretic mobility, it has a better reproducibility and it's easy to handle. The disadvantages are the cost and the neutral compounds are not detectable [6].

Detection system

There are three type of detection systems [6]. A UV detector (**DAD**) is usually applied for proteins and nucleic acids. The detector limit is 10^{-4} ~ 10^{-7} M. A laser fluorescence detector (**LIF**) is usually applied for DNA fragments and has a detector limit is 10^{-7} ~ 10^{-13} M. Mass spectrometry detector (**MS**) is usually applied for proteins and peptides and the detector limits is 10^{-6} ~ 10^{-8} M.

Separation principle

In CE, analytes are mainly separated by charge and molecular weight, e.g., for polyacrylamide-coated capillary with reverse polarity, the four-fold negatively charged ATP can move faster than three-fold negatively charged ADP and the two-fold negatively charged AMP, because ATP has a higher electrophoretic mobility than ADP and AMP. In another case, e.g., between UTP (uridine 5'-triphosphate) and ATP, UTP can move faster than ATP because UTP has a lower molecular weight than ATP. Coated capillaries can be applied for separation of the charged molecules. Contrary to nucleotides, nucleosides like adenosine have no charge and therefore, an electro-osmotic flow (EOF) is required to move such neutral species to the detector. For this, a fused-silica capillary is used to get the EOF, e.g., for the fused-silica capillary with normal polarity, neutral adenosine can move faster than two-fold negatively charged AMP because the sum of the EOF and the electrophoretic mobility is much higher for adenosine than the AMP.

Based on the chemical characteristics of the analytes to be detected, separated, identified, and quantified, different methods had to be improved and validated with

respect of these differences. Four different methods have been used in the present project related to the substrate's preference of hNPP4. .

Table 11. Different methods used with CE for detection and separation

α	30 cm of uncoated capillary, which was conditioned before each injection as follows: 2 min NaOH at 10 mM, 2 min H_2O, 2 min with 100 mM SDS, injected with pressure, running buffer used was 10 mM phosphate at pH 8.00.
β	30 cm coated capillary which was conditioned before each injection as follows: 1 min buffer, 1 min H_2O, 1 min buffer, injected with electrokinetic injection (-6.0 kV, 30 sec.), running buffer used for separation was 50 mM phosphate at pH 6.5, -90 μA.
γ	Same as β except for buffer (100 mM phosphate, pH 9.2) and separation condition: 15 kV applied.
δ	Same as β but longer capillary length: 50 cm.

A

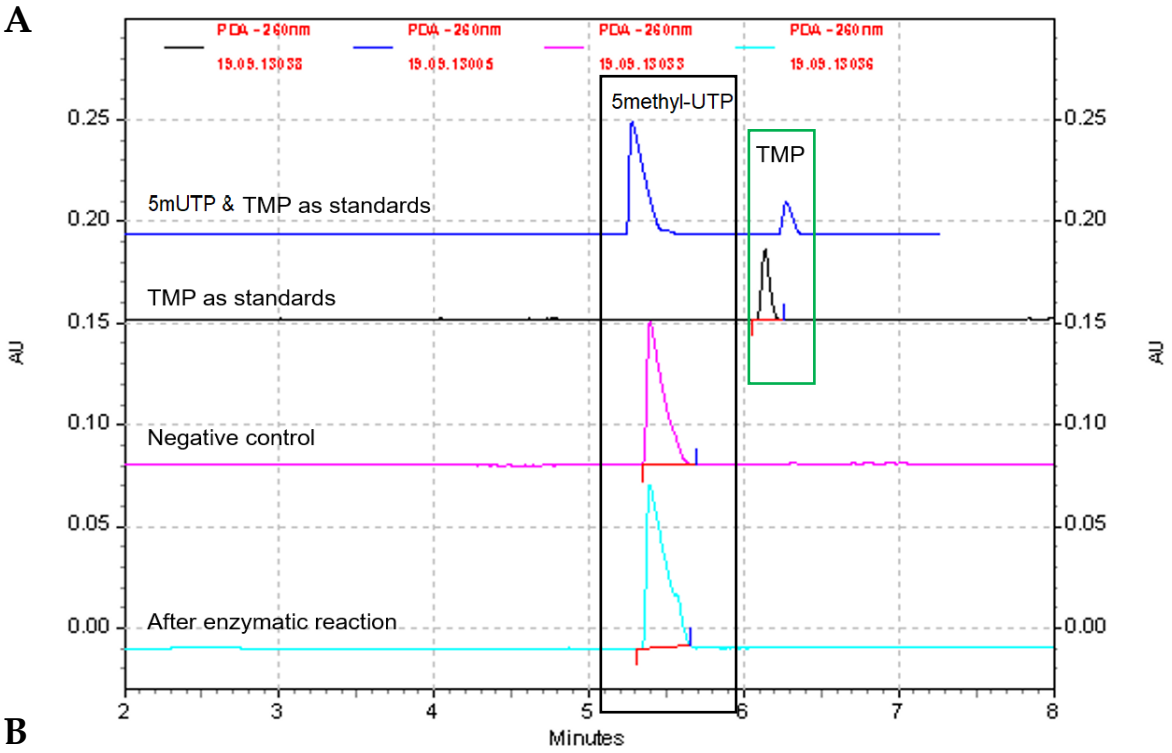
PDA - 260nm
19.05.13038
PDA - 260nm
19.05.13005
PDA - 260nm
19.05.13033
PDA - 260nm
19.05.13036
5methyl-UTP
TMP
5mUTP & TMP as standards
TMP as standards
Negative control
After enzymatic reaction
AU
Minutes

B

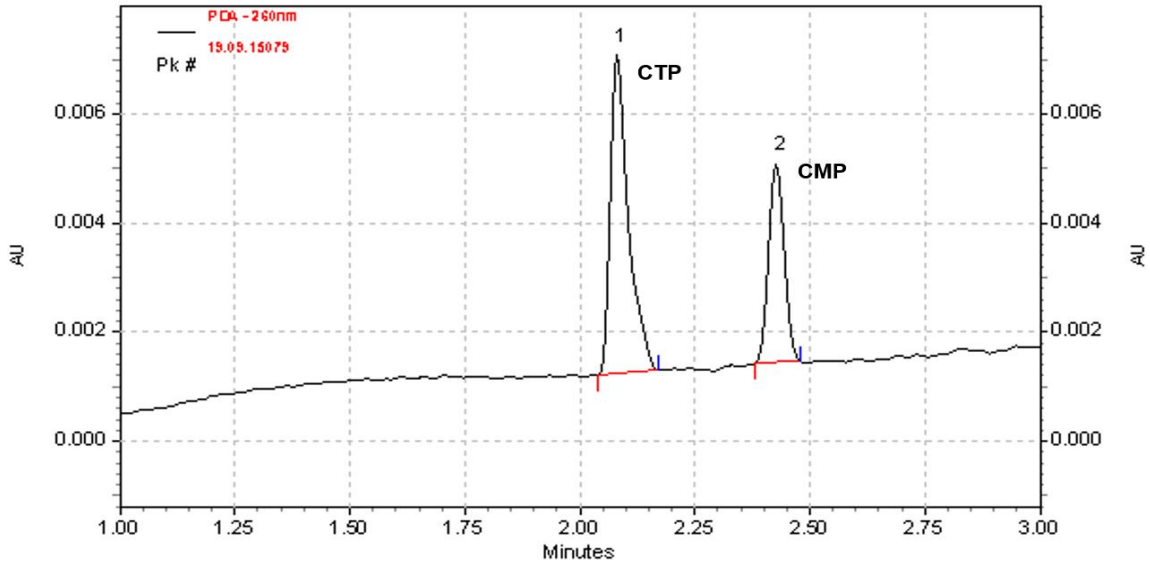
PDA - 260nm
19.05.15075
Pk #
1
CTP
2
CMP
AU
Minutes

C

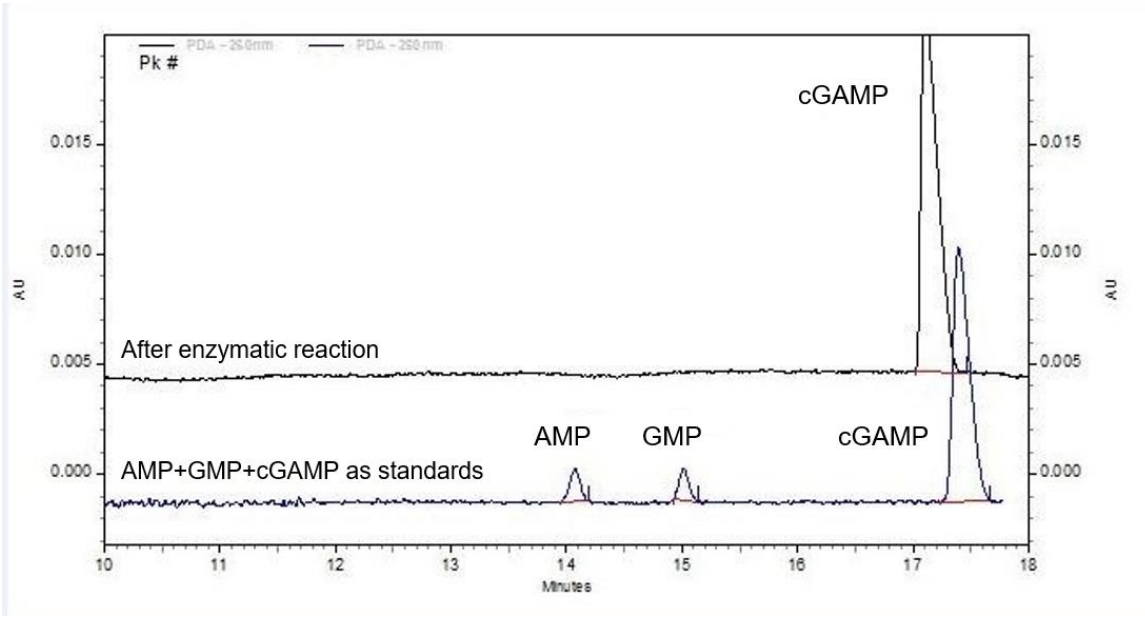

Fig. 23 CE electropherograms shown as representative examples. A. method β was used; comparison is showed between the standards and the sample after enzymatic reaction, where no 5-methyl-UTP is detected. B. The example shows CTP and CMP run as standards, 400 and 40 μM respectively, using method γ. C. comparison of standards AMP, GMP and cGAMP, at 10, 10 and 100 μM is shown with the samples analyzed after enzymatic reaction.

References

1. Lopez, V.; Lee, S.-Y.; Stephan, H.; Müller, C.E. Recombinant expression of ecto-nucleotide pyrophosphatase/phosphodiesterase 4 (NPP4) and development of a luminescence-based assay to identify inhibitors. *Anal. Biochem.* **2020**, *603*, 113774, doi:10.1016/j.ab.2020.113774.

2. Junker, A.; Renn, C.; Dobelmann, C.; Namasivayam, V.; Jain, S.; Losenkova, K.; Irjala, H.; Duca, S.; Balasubramanian, R.; Chakraborty, S.; et al. Structure–Activity Relationship of purine and pyrimidine nucleotides as ecto-5′-nucleotidase (CD73) Inhibitors. *J. Med. Chem.* **2019**, *62*, 3677–

3695, doi:10.1021/acs.jmedchem.9b00164.

3. Freundlieb, M.; Zimmermann, H.; Müller, C.E. A new, sensitive ecto-5′-nucleotidase assay for compound screening. *Anal. Biochem.* **2014**, *446*, 53–58, doi:10.1016/j.ab.2013.10.012.

4. Lee, S.-Y.; Fiene, A.; Li, W.; Hanck, T.; Brylev, K.A.; Fedorov, V.E.; Lecka, J.; Haider, A.; Pietzsch, H.-J.; Zimmermann, H.; et al. Polyoxometalates-potent and selective ecto-nucleotidase inhibitors. *Biochem. Pharmacol.* **2015**, *93*, 171–81, doi:10.1016/j.bcp.2014.11.002.

5. Geiger, M.; Hogerton, A.L.; Bowser, M.T. Capillary electrophoresis. *Anal. Chem.* **2012**, *84*, 577–596, doi:10.1021/ac203205a.

6. Landers, J.P. *Capillary and microchip electrophoresis and associated microtechniques*; Third edit.; CRC Press Taylor & Francis Group, **2008**;

7. Copeland, R. Enzymes: A Practical Introduction to Structure, Mechanism, and Data Analysis, 2nd ed.; **2004**.

6.4 Summary and outlook

Besides the interest in finding new lead compounds, we aimed to elucidate, in a parallel project, the kinetics of the enzyme against a broad spectrum of different substrates. We first optimized, validated, and implemented analytical methods for the analysis and quantification of the substrates and their products. Using the same assay conditions, 30 substrates were tested at hNPP4 and the products were detected and quantified. A broad spectrum of substrates was investigated: nucleoside monophosphates (NMP), e.g., AMP and UMP; nucleoside diphosphates (NDP) and their sugar derivatives, e.g., GDP, UDP-glucose; nucleoside triphosphates (NTP), e.g., ATP, CTP; cyclic nucleotides e.g., cGAMP, cUMP, 2′,3′-cAMP; and di-nucleotides such as Ap_6A, Up_4U.

The substrates showing a high rate of product formation were fully characterized biochemically. Our findings show that hNPP4 can hydrolyze, among NTP, specifically UTP and CTP. Moderate hydrolysis was observed for GTP, and none or negligible product formation was observed when ATP, TTP and 5'methyl-UTP were used as substrates. UTP and CTP showed K_m/K_{cat} values of 3.8×10^3 μM/s^{-1} and 1.57×10^3 μM/s^{-1}, respectively. UTP and CTP are better substrates for hNPP4, since they are more efficiently cleaved, then Ap_3A/Ap_4A, which are the only two natural substrates known so far.

In conclusion, essential new knowledge on the kinetic properties of hNPP4 were obtained; in fact, we discovered that pyrimidines nucleotides are preferred hNPP4 substrates, and uridine derivatives can act as moderately potent inhibitors of hNPP4 activity. Due to their great potential, based on this novel data further investigations should utilize computational method, e.g., a ligand-based virtual screening approach, for improving their potency and docking studies should be applied to explain the preference of hNPP4 for hydrolyzing UTP and CTP.

7. Summary and conclusions

The purpose of this PhD project was to advance the development of ligands, tools, and drugs for the ectonucleotidase family with a focus on hNPP1 and hNPP4. Both enzymes are involved in purinergic and non-purinergic pathways and may represent novel molecular targets for development of new drugs, such as antithrombotic agents hNPP4, or medications for CPPD (calcium pyrophosphate dihydrate deposition) disease, and drugs for cancer immune-therapy that act on hNPP1. The present dissertation is composed of six chapters. The first section is an introduction, in which a literature review of ecto-nucleotide pyrophosphatase/phosphodiesterase-1 and -4 is presented. The main content is a comprehensive discussion of the inhibitors, drugs, drug candidates, and pharmacological tools available to date and a comprehensive description of their pathophysiological roles, as well as tissue localization and enzyme structures and kinetics.

Sulfonated polysaccharides as ectonucleotidase inhibitors (Chapter 2)

We investigated the potential of sulfonated polysaccharides isolated from brown and red sea algae as ectonucleotidase inhibitors. All candidates inhibited NPP1 and CD39 with higher potency than the other ectonucleotidases. These sulfonated polysaccharides from marine algae are the most potent NPP1 inhibitors known to date, with nano- to sub-nanomolar potencies. Ancillary CD39 inhibition (K_i 1.72 nM) and strong selectivity for NPP1 (K_i 0.0517 nM) characterize compound **5** (isolated from *Delesseria sanguinea*). Sulfated polysaccharide **6** (from *Saccharina latissima*) is a dual inhibitor of NPP1 and CD39, and due to the enzymes' involvement in ATP hydrolysis, this dual activity may be beneficial for cancer immunotherapy. We explored the mechanism by which compound **7** (from *Fucus vesiculosus*) inhibits hNPP1 and hCD39. The data suggest a non-competitive/mixed inhibition type. Finally, we investigated compound **7** in a more dynamic cellular setting using a human glioma cell line (U-87) to find out how extracellular ATP, which shows proliferative and antiangiogenic effects, is hydrolyzed

in cancer cells producing adenosine which displays pro-angiogenic, proliferation-enhancing, metastasis-promoting and immunosuppressive effects when released into the tumor microenvironment. We observed that adenosine generation was decreased in a concentration-dependent manner by the sulfonated polysaccharide in U87 glioma cells, which is thought to be due to inhibition of NPP1 activity. In conclusion, we found that sulfated polysaccharides from marine algae are extremely potent non-competitive inhibitors of NPP1 and CD39, with significantly stronger activity against NPP1. Together with the AMP-hydrolyzing ectoenzyme CD73, these enzymes generate adenosine, an immunosuppressive and tumor-promoting signaling molecule, and the reported reduction of its formation using the investigated polysaccharide may explain or at least contribute to the previously reported anti-cancer effects of this nontoxic and well tolerated sulfated algal polysaccharides from seaweeds. These results provide innovative and promising insights laying the foundation for future research on natural anticancer medicines.

Heparins as potent ectonucleotidase inhibitors (Chapter 3)

Previous studies indicated that heparin and derivatives may improve cancer patient survival and their ability to suppress metastasis has been tested in several animal models. Since ectonucleotidases have been reported to play a role in immunotherapy of cancer, and heparins are anionic compounds, like polyoxometalates previously discovered as ectonucleotidase inhibitors, we therefore decided to study effects of heparin and derivatives on ectonucleotidase activity. We observed high potency (with IC_{50} values in the range of 0.41-73 μM) and hNPP1-selectivity for the investigated compounds. Their mechanism of action was further studied using G9694 and Fondaparinux as models compounds which showed a mixed-type inhibition of hNPP1. Next, we looked for a cell line expressing hNPP1 to test our inhibitors in a more complex system than an isolated enzyme, and identified U87 (human glioblastoma) as a suitable cell line, which was biochemically characterized. The cell line displays high expression of hNPP1 and CD73 based on mRNA expression analysis. Finally, we used a cell-based

test system to study the best heparin derivatives characterized in the present study on intact tumor cells. They inhibited the breakdown of proinflammatory ATP and reduced adenosine levels, an immunosuppressive and tumor-promoting signaling molecule. The heparin derivatives showed dose-dependent inhibitory activities, similar as observed for the isolated hNPP1 enzyme. Heparin and derivatives were found to be potent and selective hNPP1 inhibitors, thus potentially modulating the innate immune system. These findings warrant further investigations.

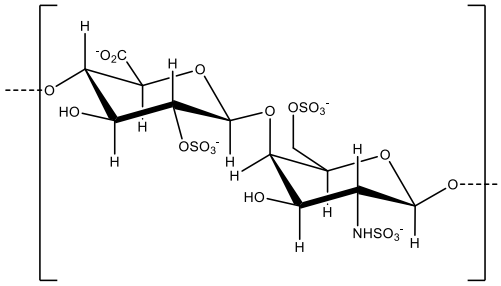

Fig. 1 Example of a scaffold studied as heparin derivatives.

Heterologous expression of NPP4 and development and validation of high-throughput screening assay (Chapter 4)

The heterologous expression of hNPP4 in insect cells was achieved utilizing baculovirus for transfection. An HTS, using bioluminescence detection utilizing the isolated and purified soluble enzyme, was developed, optimized, and validated. With an LOD of 14.6 nM and a Z-factor of 0.68, the assay was validated according to FDA requirements, confirming its suitability for high-throughput screening. The enzymatic assay was utilized for biochemical characterization of the enzyme with known substrates, Ap_3A and Ap_4A, as well as the screening of a compound library. It is rapid, inexpensive, and has high precision and sensitivity. PSB-POM145 and PSB-POM146, are the first hNPP4 inhibitors discovered and thoroughly characterized pharmacologically, with IC_{50} of 0.298 and 3.36 μM, respectively. We investigated NPP4 suppression by the most potent inhibitor, PSB-POM145, in an orthogonal CE-UV-based experiment to corroborate this

result and rule out any artifacts. Furthermore, the mechanism of inhibition of PSB-POM145 was investigated utilizing both assay system, resulting in a competitive mode of inhibition. These findings are significant, since molecular tools like these are required for future progress in the investigation of hNPP4 as a potential therapeutic target.

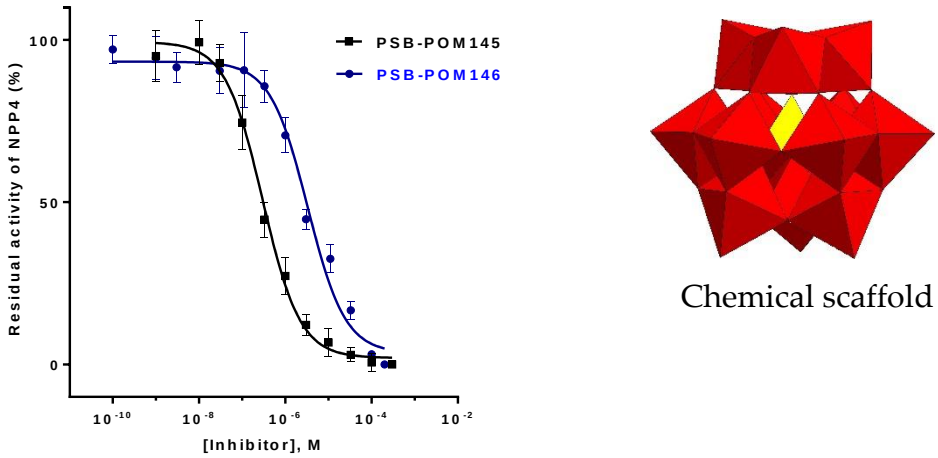

Fig. 2 The polyoxometalates PSB-POM145 ($Na_6[H_2W_{12}O_{40}]\cdot 21H_2O$) and the related PSB-POM146 ($K_7[Ti_2W_{10}PO_{40}]\cdot 8H_2O$) identified as the first hNPP4 inhibitors with IC_{50} values of 0.298 μM and 3.36 μM, respectively.

High-throughput screening to discover NPP4 modulators (Chapter 5)

Using the novel HTS assay, we identified hit compounds, which were validated by an orthogonal assay and pharmacologically characterized. Furthermore, these compounds were studied with respect to their selectivity profile. We reported IC_{50} values of 3 μM for compound PZB20709064 and value of 18.5 μM for PZB10914178A. PZB20308204 was identified as a positive modulator of hNPP4 activity and CD73, while the two aforementioned hit compounds showed selectivity for hNPP4 and ancillary inhibition of hNPP1. We further explored the inhibitory effects of a range of drugs having a uridine moiety based on information acquired from our investigations on hNPP4

substrates preferences. Despite being inhibitors of hNPP4, none of the derivatives outperformed the lead compounds, discovered by HTS.

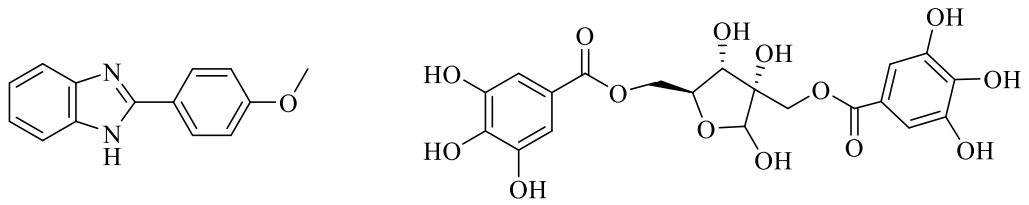

Fig. 3 Chemical structure of selected hit compounds discovered by HTS: PZB10914178A and PZB20709064.

Substrate preferences of NPP4 (Chapter 6)

Parallel to the search for new lead compounds, we investigated the enzyme's substrate preferences by studying a wide range of nucleosides as potential substrates. We initially optimized, validated, and applied analytical methods for the qualitative and quantitative analysis of the substrates and their products, and utilized these assay conditions for the measurement of various substrates and their products. Selected substrates with high conversion rates were further biochemically characterized. Our results reveal that hNPP4 can hydrolyze UTP and CTP, and less effectively GTP, but not ATP, 5′-methyl-UTP or TTP. UTP and CTP have K_m/K_{cat} of 3.8 x 10^3 μM/s^{-1} and 1.57 x 10^3 μM/s^{-1}, respectively. This value is the best measure of substrates specificity and catalytic efficiency of an enzyme, and UTP and CTP were characterized as better substrates of hNPP4 compared to Ap_3A/Ap_4A, which are the only two natural substrates known so far.

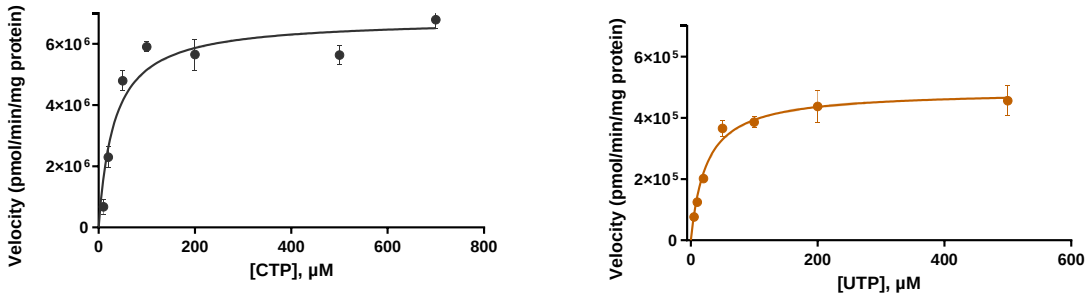

Fig. 4 Michaelis-Menten plots for CTP and UTP as substrates for hNPP4 hydrolysis.

In conclusion, we identified hNPP4 inhibitors (PSB-POM145 and PSB-POM146 described in Chapter 4) that may be used as pharmacological tools to investigate the enzyme's pathophysiological role, as well as new chemical scaffolds that may be used as lead compounds to design and synthesize new compounds for further SAR studies with the aim to improve their potency. Particular attention should be given to the uridine moiety. We discovered UTP to be a preferential hNPP4 substrate, and its analogs acted as inhibitors. A ligand-based virtual screening approach to increase potency, and docking studies to explain the preference of hNPP4 in hydrolyzing UTP/CTP could be the next steps based on these promising results.

8. Acknowledgment

I would like to thank Prof. Dr. C.E. Müller for the opportunity of doing my PhD in her working group. I am deeply grateful for the help and guidance I have received during my studies at the University of Bonn from April 2017 until June 2022. Thank you for the useful discussions that allowed me to grow as a scientist and as woman.

I am grateful to Prof. von Kügelgen, Prof. Bendas and Prof. Manthey to have accepted to be part of my doctoral committee. Special thank to Prof. Bendas for his kind support in the projects we have worked together.

I would like to thank all the members of AK Müller for the support, the nice and challenging atmosphere in the labs and in the group. Furthermore, I would like to thank the colleagues from the 4th semester for the help received while I was teaching assistant.

I am grateful to my family and amazing friends, my parents, my sisters Francesca and Ilaria, my brother-in-law Gianvito and my husband for their never-ending support and unconditional love through this long and tough path. I feel blessed and glad to have all of you in my life.

9. Publications

1. **Lopez, V**.; Lee, S.-Y.; Stephan, H.; Müller, C.E. Recombinant expression of ecto-nucleotide pyrophosphatase/phosphodiesterase 4 (NPP4) and development of a luminescence-based assay to identify inhibitors. *Anal. Biochem.* **2020**, *603*, 113774, doi:10.1016/j.ab.2020.113774.

2. Schäkel, L.; Schmies, C.C.; Idris, R.M.; Luo, X.; Lee, S.-Y.; **Lopez, V**.; Mirza, S.; Vu, T.H.; Pelletier, J.; Sévigny, J.; Namasivayam, V.; Müller, C.E.; Nucleotide Analog ARL67156 as a Lead Structure for the Development of CD39 and Dual CD39/CD73 Ectonucleotidase Inhibitors. Front. Pharmacol. **2020**, 11, doi:10.3389/fphar.2020.01294.

3. **Lopez, V**.; Schäkel, L.; Schuh, H.J.M.; Schmidt, M.S.; Mirza, S.; Renn, C.; Pelletier, J.; Lee, S.-Y.; Sévigny, J.; Alban, S.; Bendas, G.; Müller, C.E.; Sulfated Polysaccharides from Macroalgae Are Potent Dual Inhibitors of Human ATP-Hydrolyzing Ectonucleotidases NPP1 and CD39. *Mar. Drugs* **2021**, 19, 51, doi:10.3390/md19020051.

4. Breidenbach, J.; Lemke, C.; Pillaiyar. T.; Schäkel, L.; Al Hamwi, G.; Diett, M.; Gedschold, R.; Geiger, N.; **Lopez, V**.; Mirza, S.; Namasivayam, V.; Schiedel, AC.; Sylvester, K.; Thimm, D.; Vielmuth, C.; Phuong, Vu L.; Zyulina, M.; Bodem, J.; Gütschow, M.; Müller, C.E.; Targeting the Main Protease of SARS-CoV-2: From the Establishment of High Throughput Screening to the Design of Tailored Inhibitors. *Angew Chem Int Ed Engl*. 2021 Apr 26;60(18):10423-10429. doi: 10.1002/anie.202016961. Epub **2021** Mar 24. PMID: 33655614; PMCID: PMC8014119.

5. Schäkel L., Mirza S., Winzer R., **Lopez V.**, Idris R., Al-Hroub H., Pelletier J., Sévigny J., Tolosa E., Müller C.E.; Protein Kinase Inhibitor Ceritinib Blocks Ectonucleotidase CD39, a Promising Target for Cancer Immunotherapy. *Journal for ImmunoTherapy of Cancer* **2022**; 0: e004660. doi:10.1136/jitc-2022-004660.

6. **Lopez, V**.; Schuh, H.J.M.; Mirza, S.; Schmidt, M.S.; Sylvester, K.; Schäkel, L.; Renn, C.; Idris, R.M; Pelletier, J.; Lee, S.-Y.; Sévigny, J.; Naggi, A.; Björn, S.; Bendas, G.; Müller, C.E; Heparins are potent inhibitors of ectonucleotide pyrophosphatase/phosphodiesterase-1 (NPP1) – a promising target for the immunotherapy of cancer and infections (manuscript will be submitted).

10. Declaration

In lieu of oath, I affirm that the work submitted - apart from what expressly stated – it was made personally, independently and without use aids other than those specified; data and concepts taken directly or indirectly from other sources are explicitly identified. I affirm that the submitted work or similar work is not or has not been submitted as a dissertation and nor an earlier doctoral attempt has been made for the content-material creation, furthermore no outside help for the submitted work was received, in particular no paid help from placement or advisory services (doctoral advisors or other people) was received and no claims have been made to any third party, the doctoral candidate has not directly or have indirectly received monetary benefits for activities related with the content of the submitted thesis. The submitted dissertation has been published in extracts from the locations listed below:

1. **Lopez, V**.; Lee, S.-Y.; Stephan, H.; Müller, C.E. Recombinant expression of ecto-nucleotide pyrophosphatase/phosphodiesterase 4 (NPP4) and development of a luminescence-based assay to identify inhibitors. *Anal. Biochem.* **2020**, *603*, 113774, doi:10.1016/j.ab.2020.113774.

2. **Lopez, V**.; Schäkel, L.; Schuh, H.J.M.; Schmidt, M.S.; Mirza, S.; Renn, C.; Pelletier, J.; Lee, S.-Y.; Sévigny, J.; Alban, S.; Bendas, G.; Müller, C.E.; Sulfated Polysaccharides from Macroalgae Are Potent Dual Inhibitors of Human ATP-Hydrolyzing Ectonucleotidases NPP1 and CD39. Mar. Drugs **2021**, 19, 51, doi:10.3390/md19020051.